Section 5:
Session 4: Crack Growth Rate Studies for the Disposition of Flaws

US REGULATORY EXPERIENCE AND PROGNOSIS WITH RPV HEAD DEGRADATION AND VHP NOZZLE CRACKING

Presented by

Allen L. Hiser, Jr.
Materials and Chemical Engineering Branch
Office of Nuclear Reactor Regulation

Conference on Vessel Penetration Inspection, Cracking & Repairs

October 1, 2003

OUTLINE

- Background
- Order EA-03-009 (issued February 11, 2003)
  - Inspection requirements
  - Relaxation requests
  - Possible Modifications to Order EA-03-009
- Outlook
- Bulletin 2003-02

638

BACKGROUND

- Fall 2000
  - Oconee Unit 1 identifies deposits - axial leak

- Spring 2001
  - Oconee Unit 2 and 3 identify circumferential cracks
  - ANO Unit 1 identifies a leaking nozzle

- **NRC issues Bulletin 2001-01 - August 2001**
  - Focus is safety issue (circumferential cracks) for high susceptibility plants
  - Visual examinations considered acceptable

- Fall 2001
  - Circumferential cracks identified - Crystal River 3 and Oconee 3
  - Leaks and repairs at Surry 1, North Anna 2 and TMI

639

BACKGROUND (cont.)

- Spring 2002
  - Davis-Besse identifies RPV head wastage & circumferential cracking

- **NRC issues Bulletin 2002-01 - March 2002**
  - Focus is safety issue is RPV wastage for all plants

- Spring 2002
  - Millstone identifies part through-wall cracks (moderate plant)

- **NRC issues Bulletin 2002-02 - August 2002**
  - Focus is adequacy of inspection programs - methods (non-visual NDE for high susceptibility) and frequency
  - Licensee responses generally vague on future program, many cite MRP-75 program

640

BACKGROUND (cont.)

- Fall 2002
  - North Anna 2 identifies
    - ✓ Prevalent weld cracking, & leak from a repaired nozzle
    - ✓ Circumferential cracking at weld root without boron deposits
  - ANO Unit 1 identifies leak from a repaired nozzle
  - Oconee Unit 2 identifies possible through-wall cracking without boron deposits on the RPV head
  - Head corrosion at Sequoyah Unit 2 - above head boron source

- **NRC issues Order EA-03-009 - February 2003**
  - Mandates inspections for all PWRs

- Spring 2003
  - South Texas Project Unit 1 - boron deposits on the lower head

- **NRC issues Bulletin 2003-02 - August 2003**
  - Focus is inspections of bottom head Alloy 600 nozzles of PWRs

- Fall 2003
  - Oconee Unit 1 - Leak from a plugged thermocouple nozzle
  - (Alloy 690 plug and 152 weld)

641

OVERVIEW OF ORDERS

- Issued February 11, 2003
- Issued to all PWRs
- Adequate protection basis
  - ASME Code inspections are inadequate
  - Revisions to inspection requirements are not imminent
  - RPV head degradation and nozzle cracking pose safety risks if not promptly identified and corrected
- Provides a clear regulatory framework pending the incorporation of revised inspection requirements into 10 CFR 50.55a

642

ORDER REQUIREMENTS

- Evaluate susceptibility - effective degradation years (EDY), based on operating temperature and time
- High plants - bare metal visual AND non-visual NDE at EVERY RFO
- Moderate plants - BMV and non-visual NDE at alternating RFOs
- Low plants - BMV by next 2 RFOs (repeat every 3rd RFO or 5 years), non-visual by 2008 (repeat every 4th RFO or 7 years)
- Non-visual NDE is EITHER:
  - Ultrasonic with evaluation of interference fit leakage, OR
  - Wetted-surface examination

643

Order EA-03-009
Required Inspection Surfaces

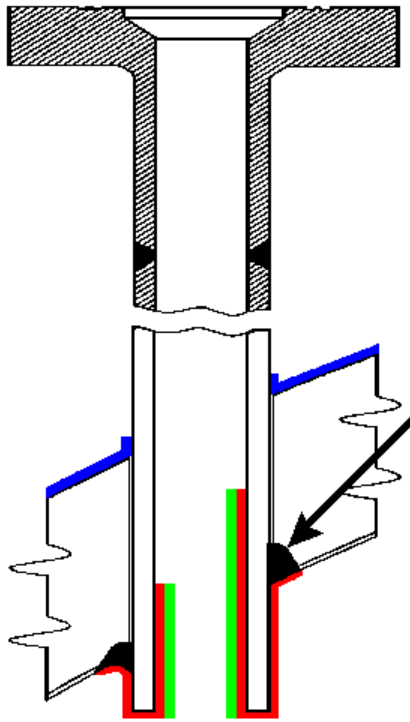

Bare Metal Visual
Inspection Area

J-groove Weld

Ultrasonic
Inspection Area

Wetted Surface
Inspection Area

644

ORDER REQUIREMENTS

- Explicit requirements and criteria to inspect repaired nozzles/welds
- Each RFO, must perform visual inspections to identify boric acid leaks from components above the RPV head - follow-up actions include inspections of potentially-affected RPV head areas and nozzles
- Flaw evaluation per NRC guidance (Strosnider letter fall 2001, revised guidance in Barrett letter April 2003)
- Orders also apply to new RPV heads, either Alloy 600 (Davis-Besse) or Alloy 690 (North Anna 2 and many others)
- Post-outage report 60 days after restart

645

LICENSEE OPTIONS

- Request Director of NRR to relax or rescind requirements of the order based on “good cause”

- Requests for relaxation for specific VHP nozzles will be evaluated using procedures for proposed alternatives to the ASME Code in accordance with 10 CFR 50.55a(a)(3)
  - The proposed alternative will provide an acceptable level of quality and safety
  - Compliance would result in hardship or unusual difficulty without a compensating increase in the level of quality and safety

646

NEED FOR ORDERS

- Past process of issuing Bulletins unwieldy, inconsistent, not stable, and has no regulatory weight (licensee commitments only)
- Rulemaking would take at least 1 or 2 years
- Orders can be revised or rescinded as necessary
- Although inspection plans for the next RFOs were generally acceptable, NRC wanted to provide licensees with planning time to meet order requirements
- Concerns that above RPV head leakage could result in undetected RPV head degradation

RELAXATION REQUESTS

- Limitations above the J-groove weld
  - Centering tabs & step on nozzle ID
  - Stress in non-inspected area below 28 ksi
  - Hardship - would have required guide sleeve removal and re-welding of a guide funnel onto nozzle

- Limitations below the J-groove weld
  - Guide funnel threads (ID & OD) and tapers on end of nozzles
  - Transducer coupling for time-of-flight-diffraction

- Bare metal visual examinations
  - Localized insulation and support shroud interferences
  - Insulation prevents total access to RPV head surface
    - ✓ Low frequency eddy current to demonstrate head integrity
    - ✓ Enhanced UT to detect “triple-point” cracking

Calvert Cliffs
Order Inspection Limitations

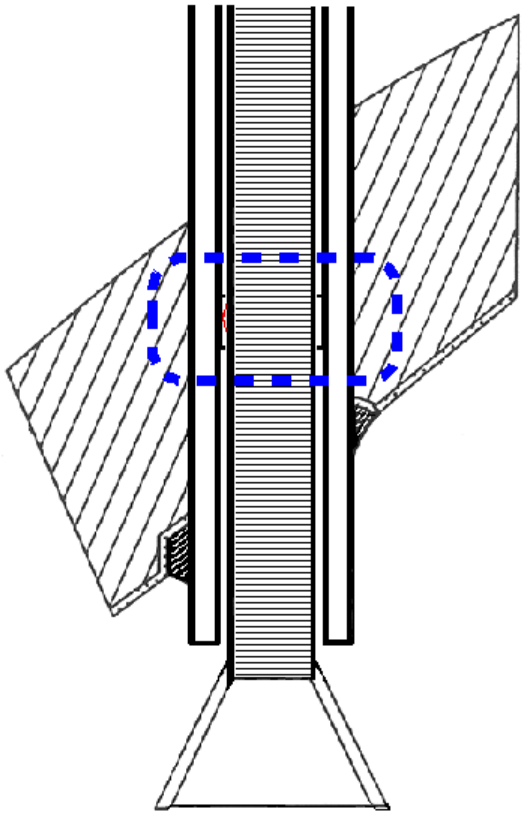

Thermal/Guide Sleeve

Sleeve Expansion Points

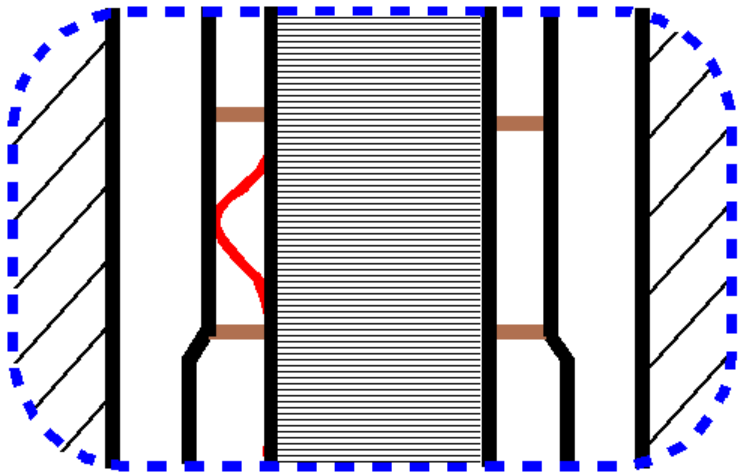

Farley Funnel Thread Inspection Limitation

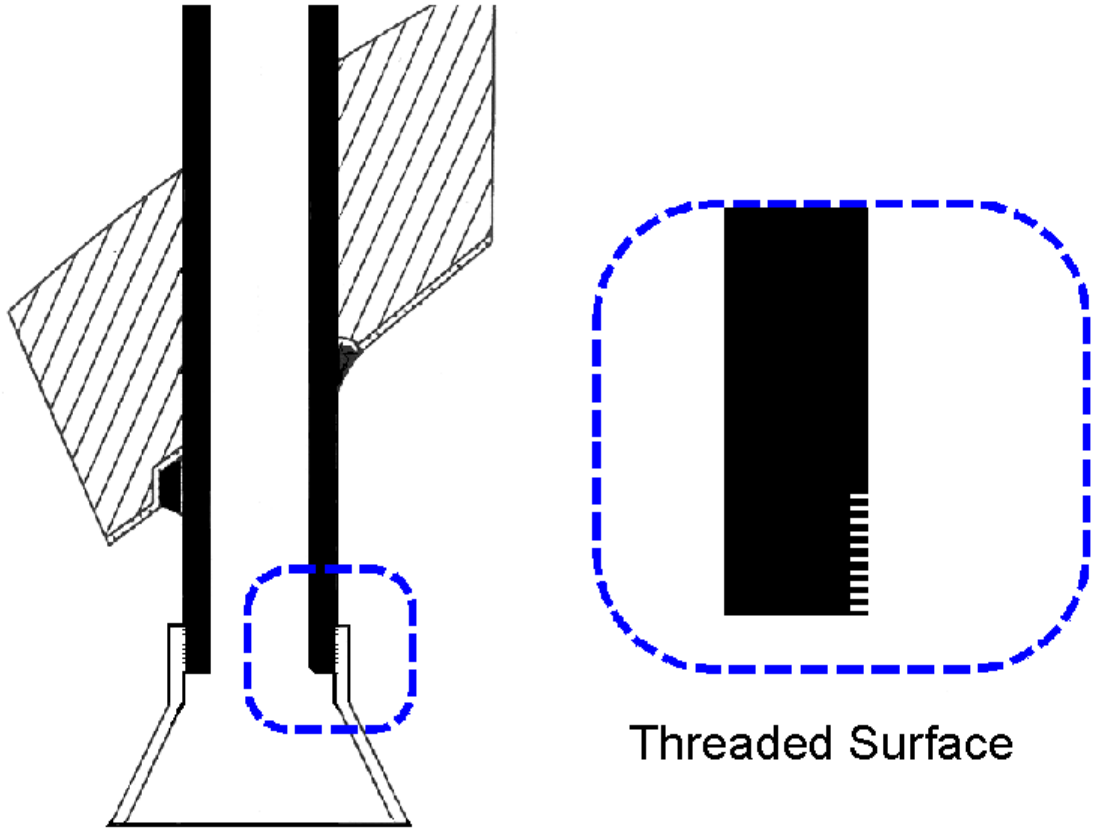

650

St. Lucie Unit 2
Typical RPV Nozzle With Threaded Guide Funnel

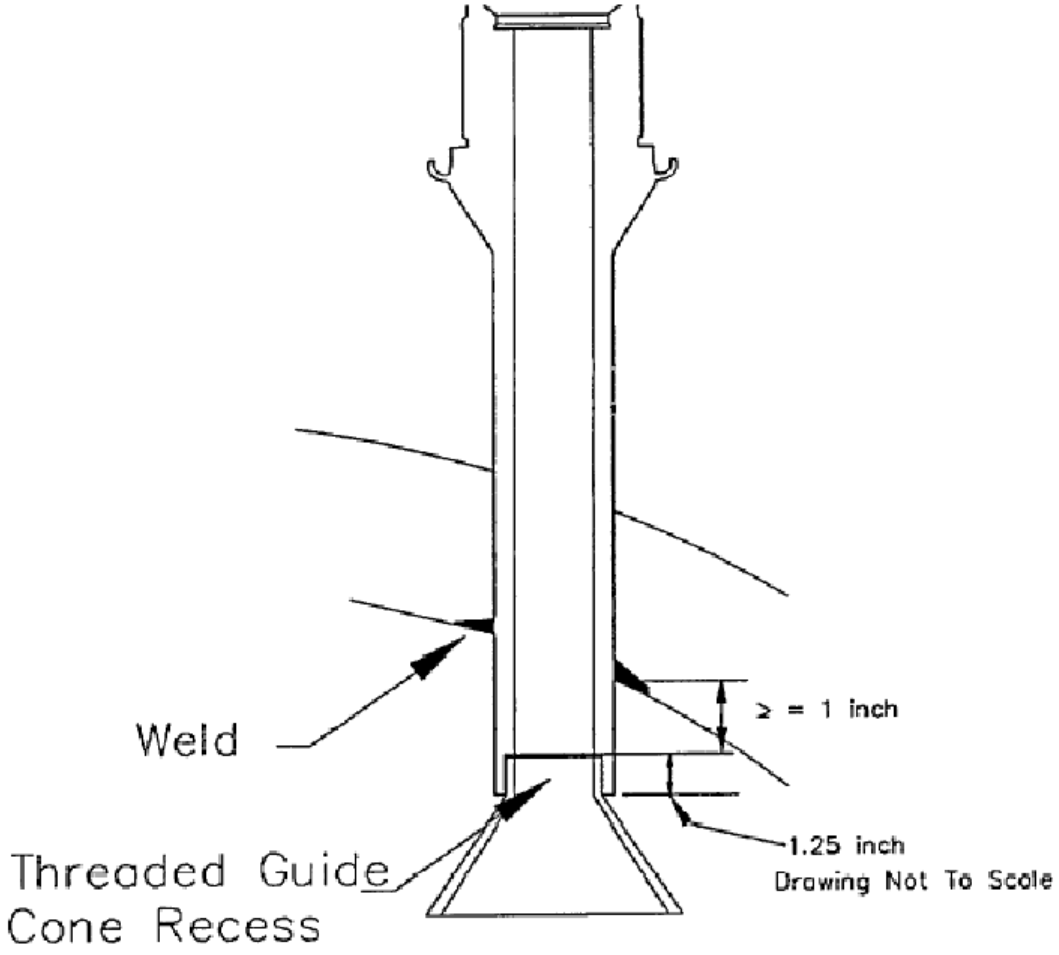

651

TOFD Transducer Coupling Limitations

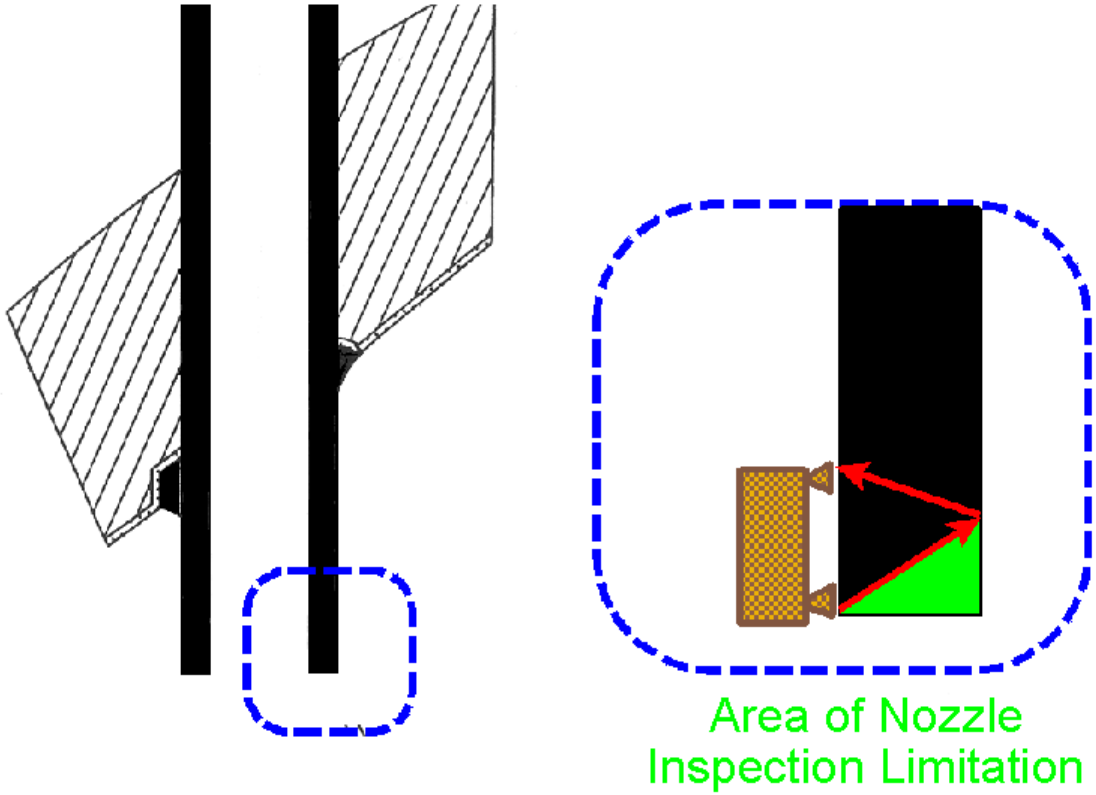

652

Millstone Power Station
Bare Metal Visual Inspection Restraints

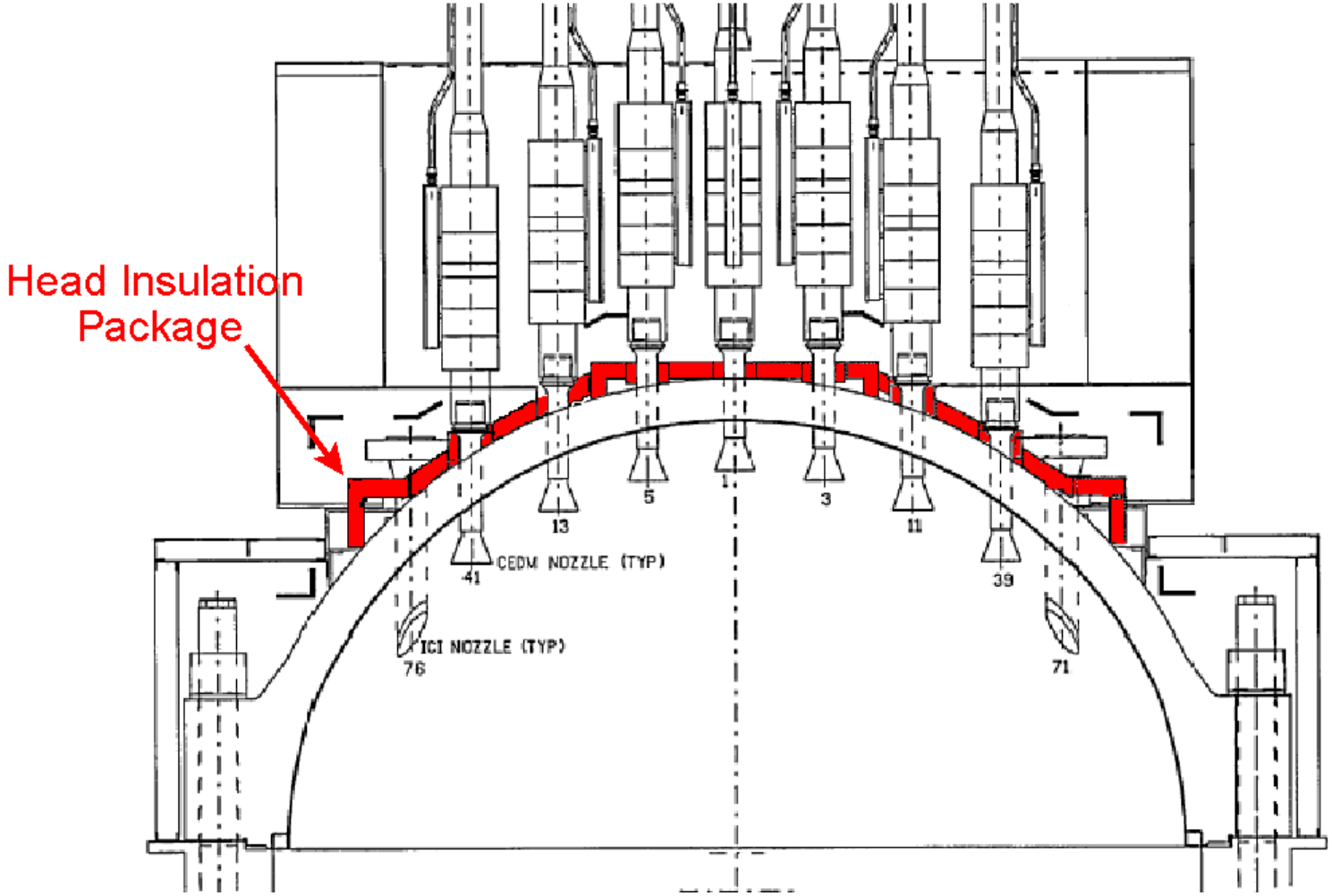

653

OUTLOOK

- Goal is “permanent” requirements for inspections to ensure structural integrity of the RPV head and VHP nozzles

- ASME Code is working to develop inspection requirements
  - Has been based upon industry report (MRP-75)
  - NRC staff has provided comments - report is not acceptable as submitted, acceptability is not certain
  - NRC has suspended review pending revisions by the industry based on fall 2002 findings
  - ASME Code adoption of requirements may not be complete until 2004 or later

- Inspection requirements will be implemented in 10 CFR 50.55a
  - Endorse the new ASME Code requirements (if acceptable) under expedited implementation, OR
  - Codify alternative inspection requirements
  - Will take 1-2 years once acceptable requirements are identified

654

POSSIBLE MODIFICATIONS TO ORDER EA-03-009

- Initially mentioned with industry on June 12
- Staff highlighted a high volume of similar relaxation requests for non-safety significant portions of the VHP nozzles and a potential for the industry to provide a generic analysis that could provide a technical basis for modifications to the Order - **report received September 26**
- The modification would result in a significant reduction in the burden on both the industry and the staff by reducing the number of repetitive evaluations, without impacting the level of safety provided by the Order

655

POSSIBLE MODIFICATIONS TO ORDER EA-03-009

- Allow combinations of non-visual NDE (UT and surface examinations) to be used on a RPV head to obtain full coverage for the head
  - Order currently specifies UT **or** surface examinations of **"each"** VHP nozzle or weld
- Modify scope of bare metal visual examination for support structure interferences (outside of VHP nozzle area) - examine above and below support structure
- Refine scope of coverage for each VHP nozzle to some elevation above the bottom of the nozzle, or some established stress level
  - Limitations due to internal or external threads (for guide cones or funnels) and bottom end chamfers restrict access and usefulness of examination data - this was not anticipated prior to Order issuance
  - Possible modification would eliminate need to examine areas with low stress and limited crack growth potential

656

RECENT INDUSTRY PROPOSAL

- Reduce frequency of UT or eddy current examinations for high susceptibility plants with a prior CLEAN examination (no leaks or cracks)
  - Proposed during teleconference July 8 - licensee submittal August 17
  - Small number of affected plants (4-5?), beginning this fall
  - Basis would be deterministic and/or probabilistic
  - May be a generic approach or plant-specific
- Considerations
  - A high threshold for the acceptability of prior inspections - must be consistent with the inspection criteria of the Order with current state-of-the-art techniques
  - Are two clean Order inspections necessary?

OTHER CONSIDERATIONS

- Use of Bulletins and early inspections for emergent issues intended to establish prevalence of issue - avoid significant events
  - Role of continuing “permanent” ISI activities is to re-establish defense-in-depth considerations
  - Tech. Spec requirements for no pressure boundary leakage
  - GDC 14 - “extremely low probability of abnormal leakage”

- Cause for leakage from plugged thermocouple nozzle (Alloy 690 plug and 152 weld) at Oconee Unit 1

658

BULLETIN 2003-02: INFORMATION REQUEST

- RPV lower head penetration inspections performed to date and findings
- Description of inspection program during next and **SUBSEQUENT** refueling outages
- If unable to perform BMV inspection of each penetration during next refueling outage, describe inspections able to perform and actions to be taken to permit inspection of each penetration during subsequent refueling outages
- If do not intend to perform either BMV or volumetric exam, provide basis for concluding requirements are and will continue to be met

659

BULLETIN 2003-02 (continued)

- Within 30 days after plant restart following next lower head inspection, summary of the inspections performed, conditions found, and any actions taken

- Provide response within 30 days if entering refueling outage before end of 2003

- All other addressees, provide response within 90 days

660

LOCKHEED MARTIN

Stress Corrosion Crack Growth Rates (SCCGRs) for Alloy 182 and 82 Welds

Steven A. Attanasio, John V. Mullen, John W. Wuthrich,
Weldon W. Wilkening, and David S. Morton

Lockheed Martin Corporation
Schenectady, NY

Alloy 600 SCC Workshop
Gaithersburg, MD
September 2003

661

Outline

- Background
- Data Overview
- Description of Compliant Self-Loaded Compact Tension Specimens
- Context - EPRI Materials Reliability Program (MRP)
- Use of Average Crack Growth Rate and Maximum-to-Average Ratio
- Alloy 182 and Alloy 82 SCCGR Data
  - Comparison to data from other investigators
  - Comparison of the two alloys
  - Modeling approaches
- Aqueous Hydrogen Effects on SCC of Ni-base alloys, including Alloy 82

662

Background

- Both Alloys 182 and 82 are susceptible to primary water SCC
  - VC Summer hot leg (*http://www.nrc.gov/NRC/REACTOR/SUMMER/index.htm)*

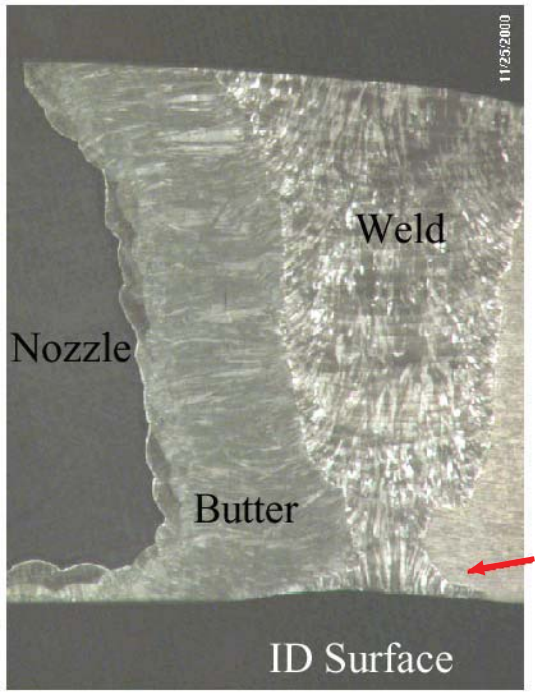

Weld repair

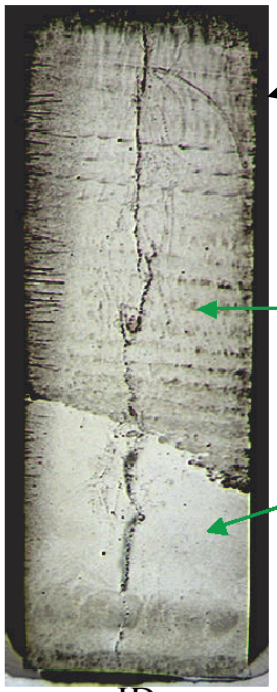

Cross-Section of Weld

Main Crack

Alloy 82

Alloy 182 butter

663

LOCKHEED MARTIN

Data Overview

- SCCGR data - compact tension (CT) specimens (most side-grooved)
  - Active load, bolt load, compliant self-loaded (CSLCTs) - precracked
- Alloy 182 and 82 welds
  - Yield strengths of 454 to 530 (182) and 439 to 465 (82)
  - Carbon levels ~ 0.02 and 0.03 wt% (182) and ~ 0.045 wt% (82)
- High temperature hydrogenated water (pH_T ~ 6.6)
  - Single hydrogen concentration in each test (20, 30, 35, or 40 scc/kg)
- Single temperature tests - 316 to 360°C
- Average K_I of 33 to 46 MPa$\sqrt{m}$ (182) and 23 to 55 MPa$\sqrt{m}$ (82)
- All T-S Orientation (growth from root to crown; parallel to dendrites)
- 11 Alloy 182 data points - 2 heats
- 20 Alloy 82 data points - 3 heats
  - Subjected to screening criteria similar to that used by EPRI-MRP group

664

Compliant Self-Loaded Compact Tension Specimens

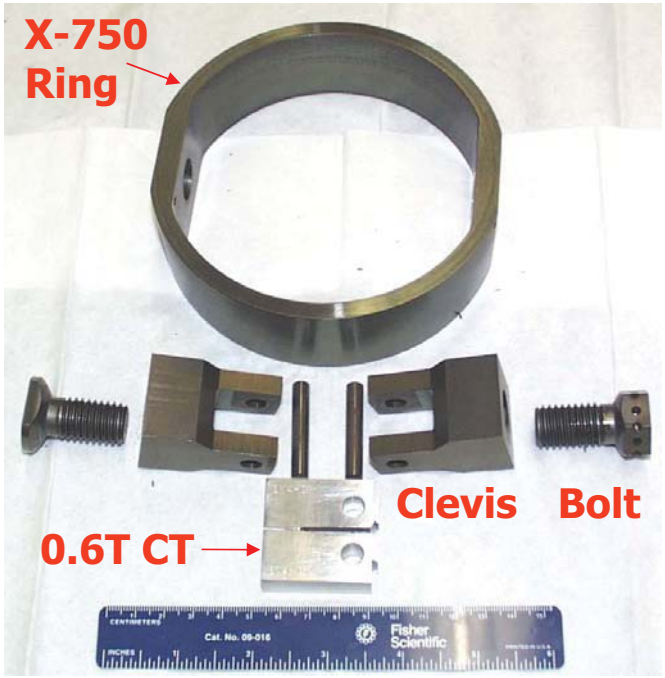

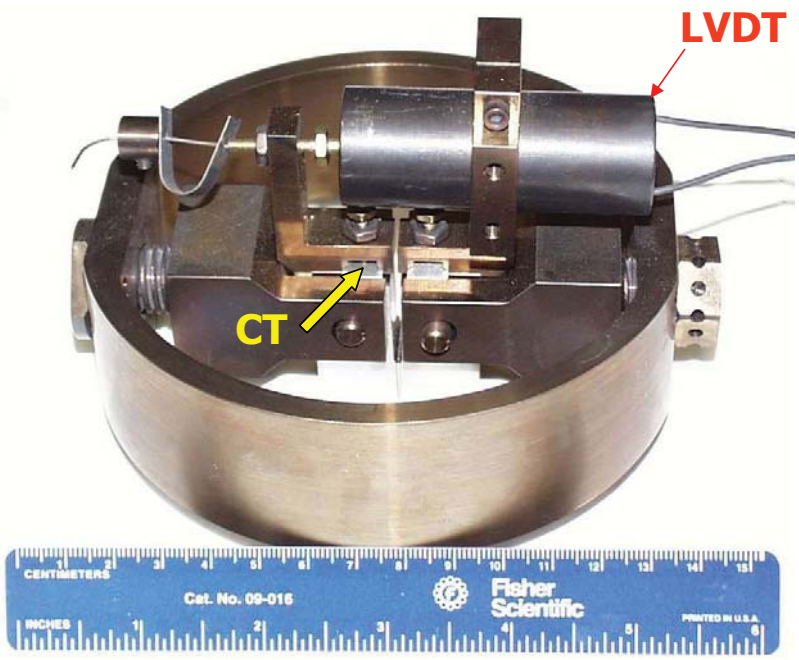

Loading Method:

- Compress ring using Instron machine, rotate bolt to apply 'setup' load to CT specimen
- Release Instron load slowly - CT specimen is loaded as ring expands
- Exact load is determined *via* measurement of ring spring constant and ring displacement
- Account for modulus changes due to heatup by increasing room temperature load

CSLCT Specimen Qualification

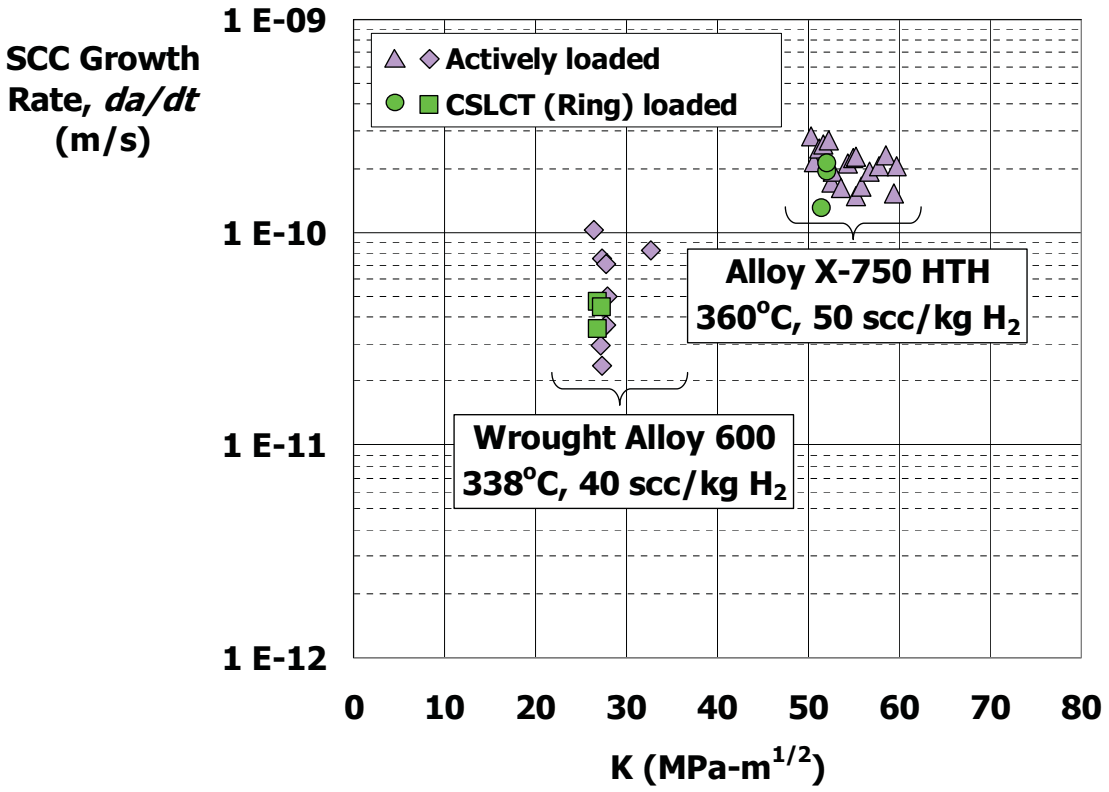

- Due to the compliance of the ring, load relaxation is minimal - even as SCC crack grows
- Can test up to 10 CSLCTs in a single 60 liter flowing autoclave (with LVDTs) - efficient

LOCKHEED MARTIN

999

Specimen Fabrication

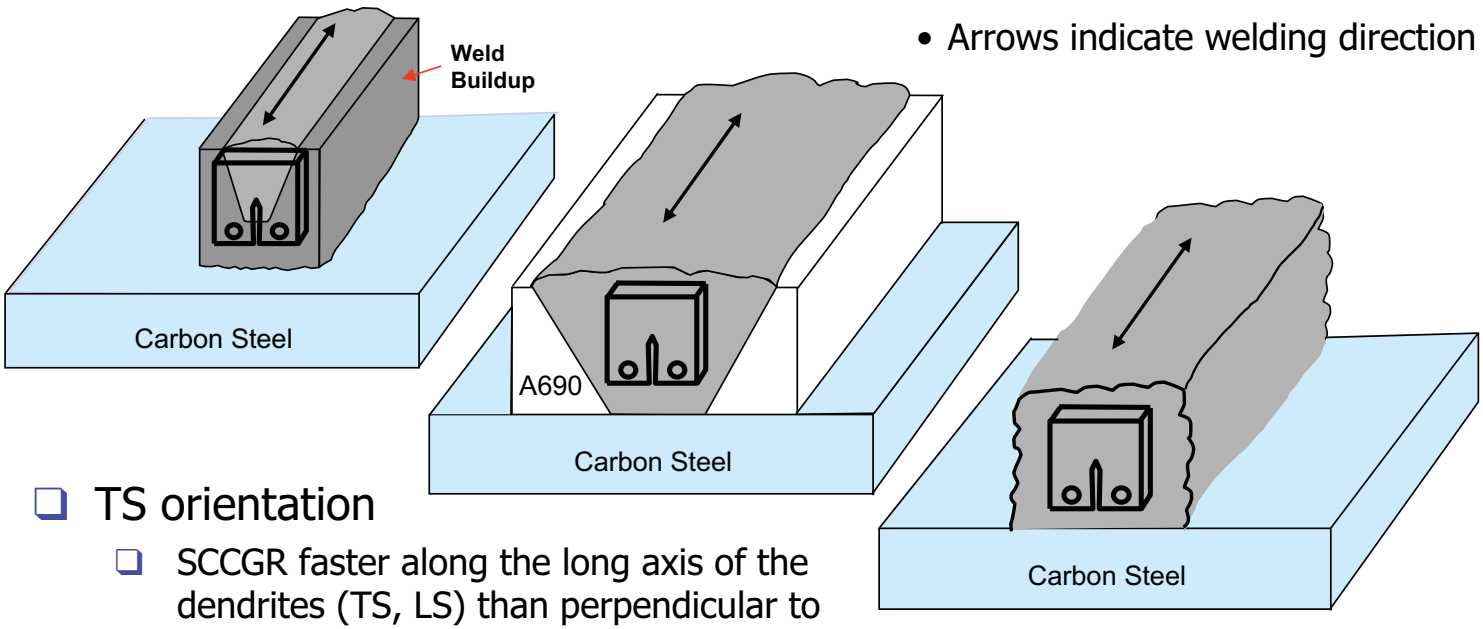

- Arrows indicate welding direction

- TS orientation
  - SCCGR faster along the long axis of the dendrites (TS, LS) than perpendicular to dendrites (e.g., TL)
    - Proven by Bamford *et al.* and others
- Weld process:
  - 182: Manual shielded metal arc welding
  - 82: Automatic gas tungsten arc welding

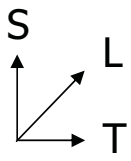

667

LOCKHEED MARTIN

EPRI Materials Reliability Program (MRP) Work

- MRP: Develop a SCCGR Model for Alloy 182 and 82 Weld Metals
  - Similar to the work performed for Wrought Alloy 600
- EPRI MRP-55 - Wrought Alloy 600 SCCGR Model (2002)
  - View/analyze present weld data *in part* using methods from MRP-55
  - Scott model - uses threshold K_I of 9 MPa$\sqrt{m}$
  - Thermal activation energy (Q_{SCCGR}) = 130 kJ/mole (31 kcal/mole)

$$\frac{da}{dt} = \alpha \cdot (K_I - 9)^{1.16} \cdot exp\left[-\frac{130{,}000}{8.314}\left(\frac{1}{T} - \frac{1}{598.15}\right)\right]$$

(*da/dt* in m/s, K_I in MPa$\sqrt{m}$, *T* in Kelvin)

  - Each heat described by its value of α
  - Data from different temperatures normalized to 325°C
    - Le Hong *et al.* - Alloy 182 Q_{SCCGR} is ~ 130 kJ/mole (EDF, ETH, CEA data)
    - Mills and Brown - Alloy 82 Q_{SCCGR} = 130 to 150 kJ/mole (31-35 kcal/mole)
      - In the present work, Alloy 82 and 182 data normalized using 130 kJ/mole

LOCKHEED MARTIN

668

Data Screening Criteria

- Single condition test
- ASTM E647 Size Criteria (flow strength at temperature)
- Minimum average crack extension = 0.2 mm
- Data based on post-test destructive examination (DE)
- Periodic unload-reload only if hold time > 60 minutes
- Careful autoclave chemistry control (including H_2)
- Minimum 'engagement' of fatigue precrack = 50%
  - Quantifies the percentage of precrack length with SCC
- All Lockheed Martin (LM) SCCGR data herein pass these screening criteria

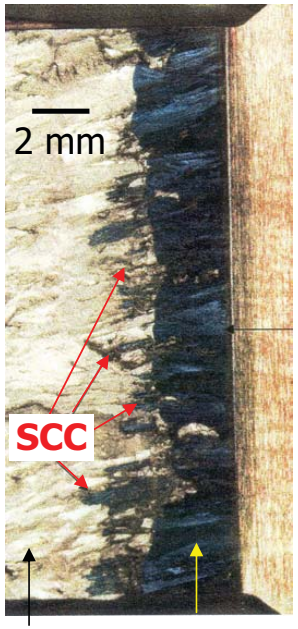

- LM Data reported as $SCCGR_{ave}$, rather than as $SCCGR_{max}$
  - Also report maximum-to-average SCC extension ratio (RATIO)
  - RATIO used by Lockheed Martin (LM) and by Mills (Bechtel)

699

LOCKHEED MARTIN

Max./Ave. Ratio Decreases as the Crack Grows

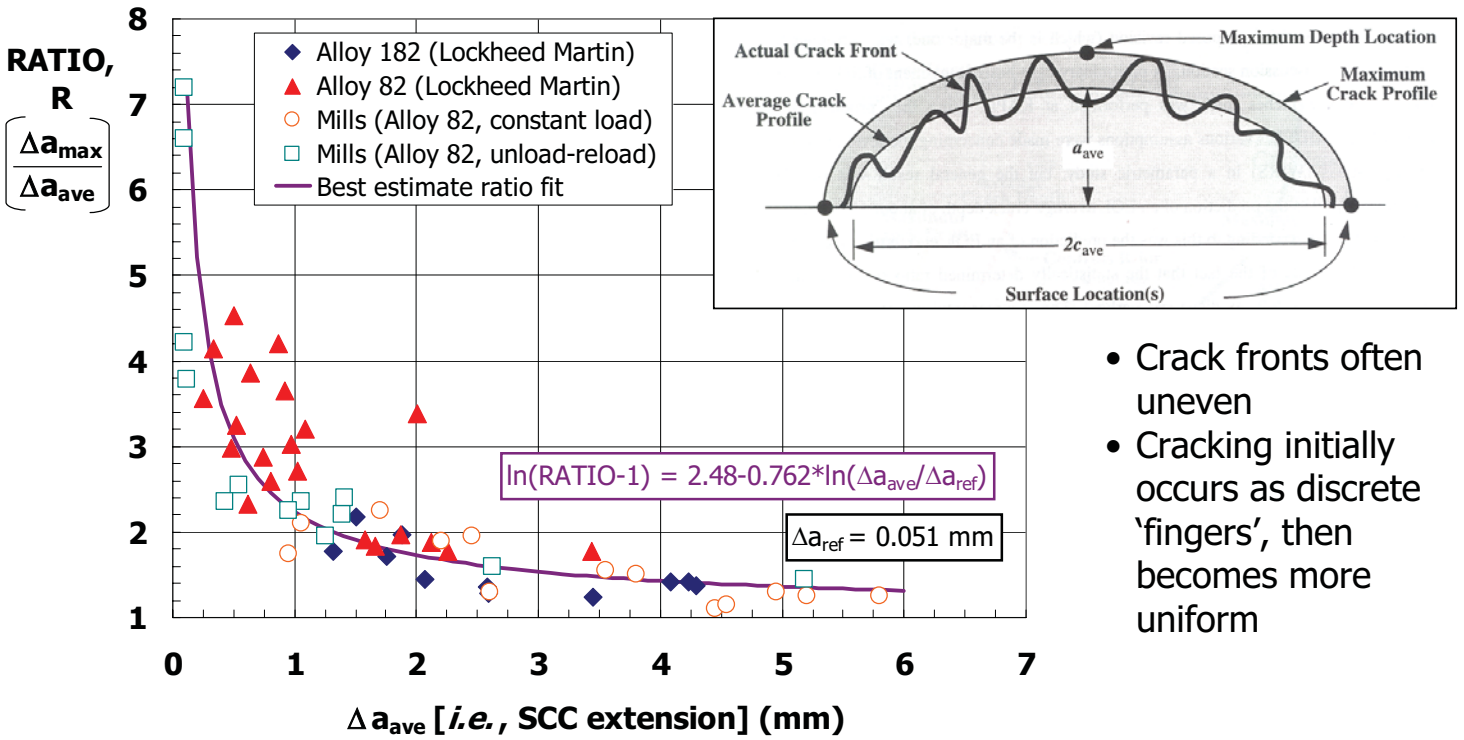

- Crack fronts often uneven
- Cracking initially occurs as discrete 'fingers', then becomes more uniform

- To broaden the ratio data set, some data were used that do not pass the screening criteria
- LM: Δa_{max} is maximum SCC depth at any location along the crack front
- Mills: Δa_{max} is maximum SCC depth at the DE measurement locations (ASTM E813)

Maximum SCCGR Depends on Test Duration

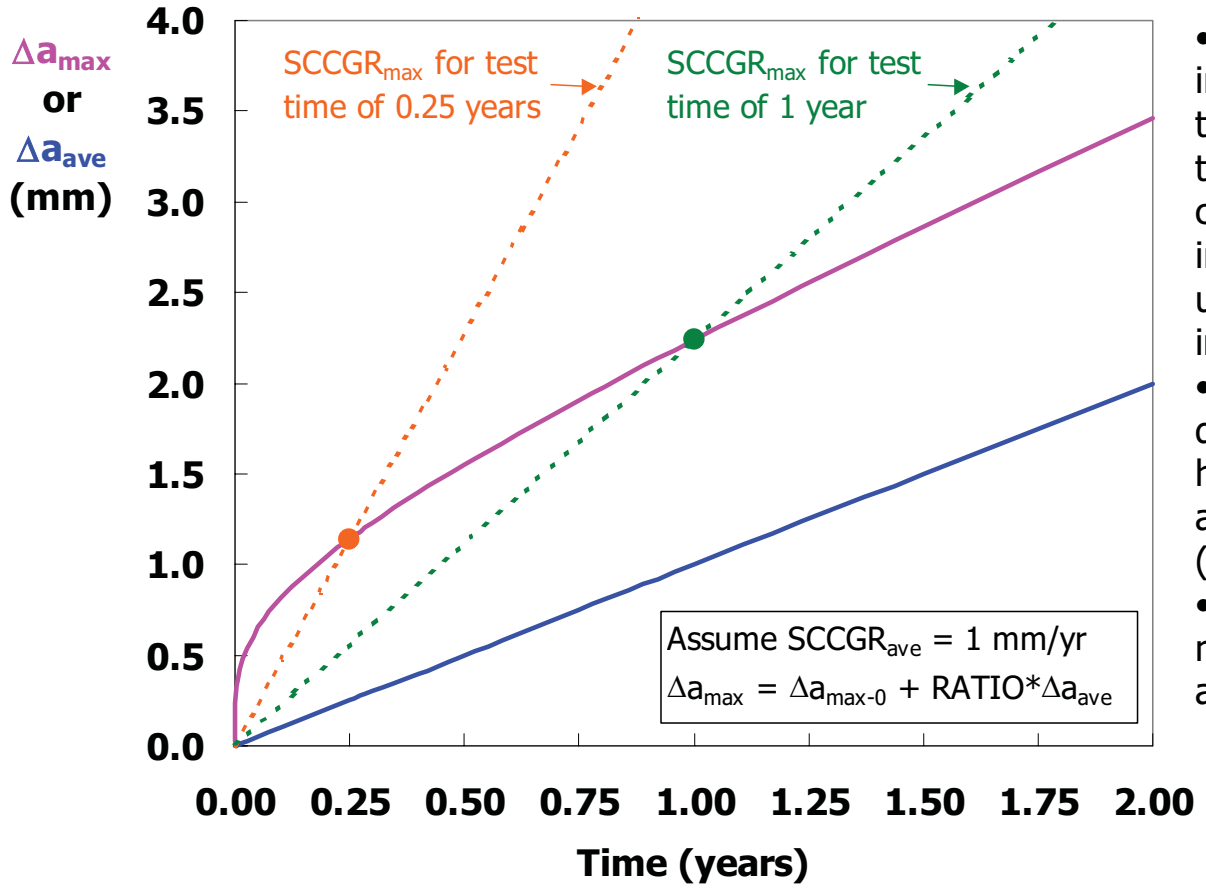

- Assumes no incubation time, or that the data are corrected for incubation time using *in-situ* instrumentation
- All SCCGR data reported herein are average rates (SCCGR$_{ave}$)
- Also report the maximum-to-average ratio

671

LOCKHEED MARTIN

Use RATIO to Infer % Engagement

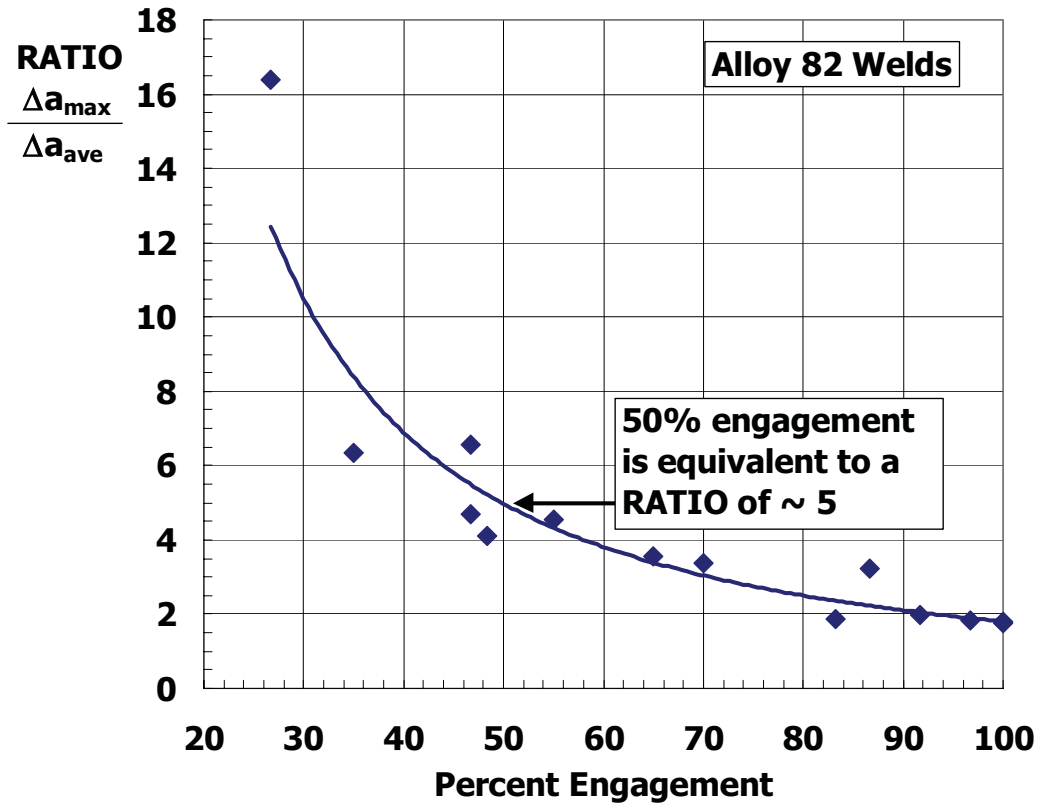

- Some of the data shown in this plot did not meet the screening criteria

672

LOCKHEED MARTIN

Use SCC Extent to Infer % Engagement

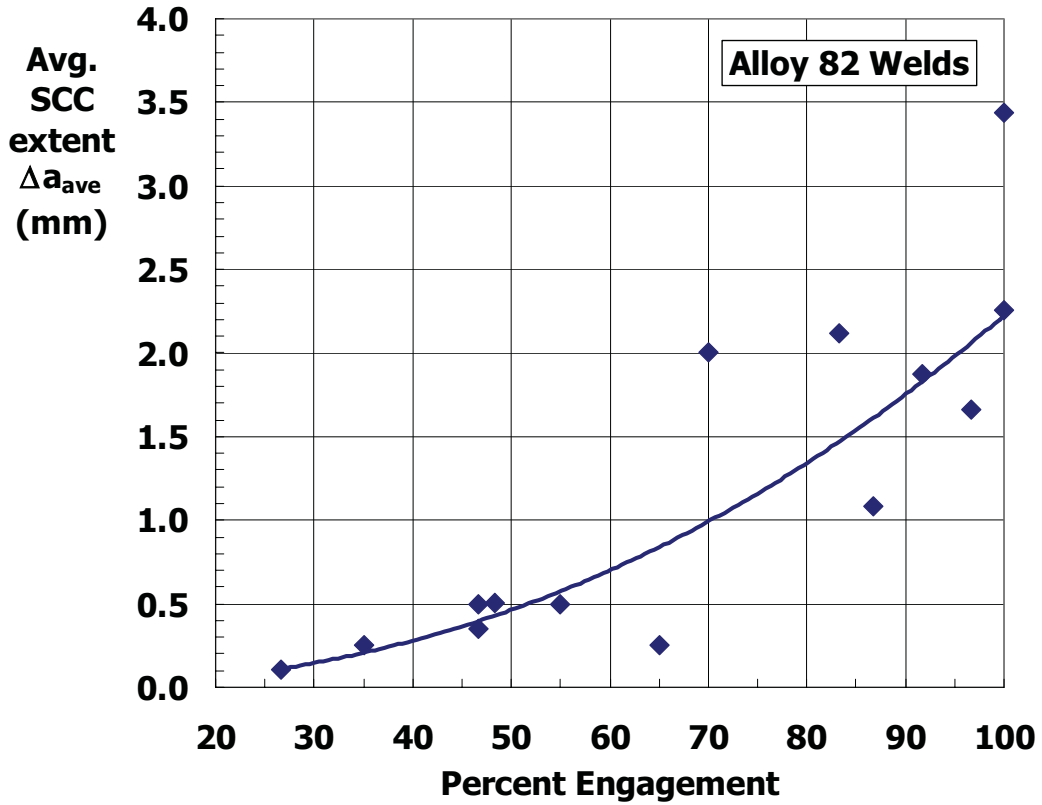

- Some of the data shown in this plot did not meet the screening criteria

673

LOCKHEED MARTIN

Alloy 182 SCCGRs and Comparison to Other Data

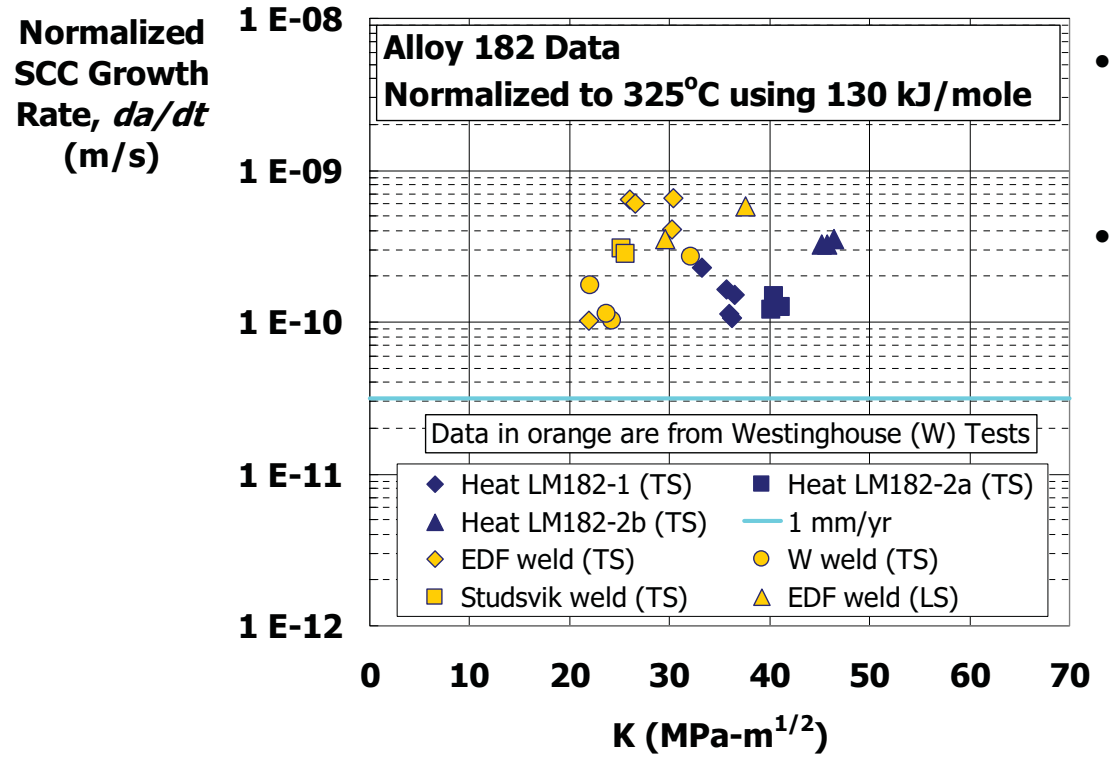

- 3 Westinghouse data points screened due to $\Delta a_{ave} < 0.2$ mm
- LM refers to Lockheed Martin

- Compare to published data where *average* SCCGR was reported (fairest comparison)
- Westinghouse data - 3 welds (W, EDF, Studsvik); carbon 0.025 to 0.053 wt%
- All root-to-crown growth; LM - 35 or 40 scc/kg H_2, Westinghouse (W) - 25 scc/kg H_2

Alloy 82 SCCGRs and Comparison to Other Data

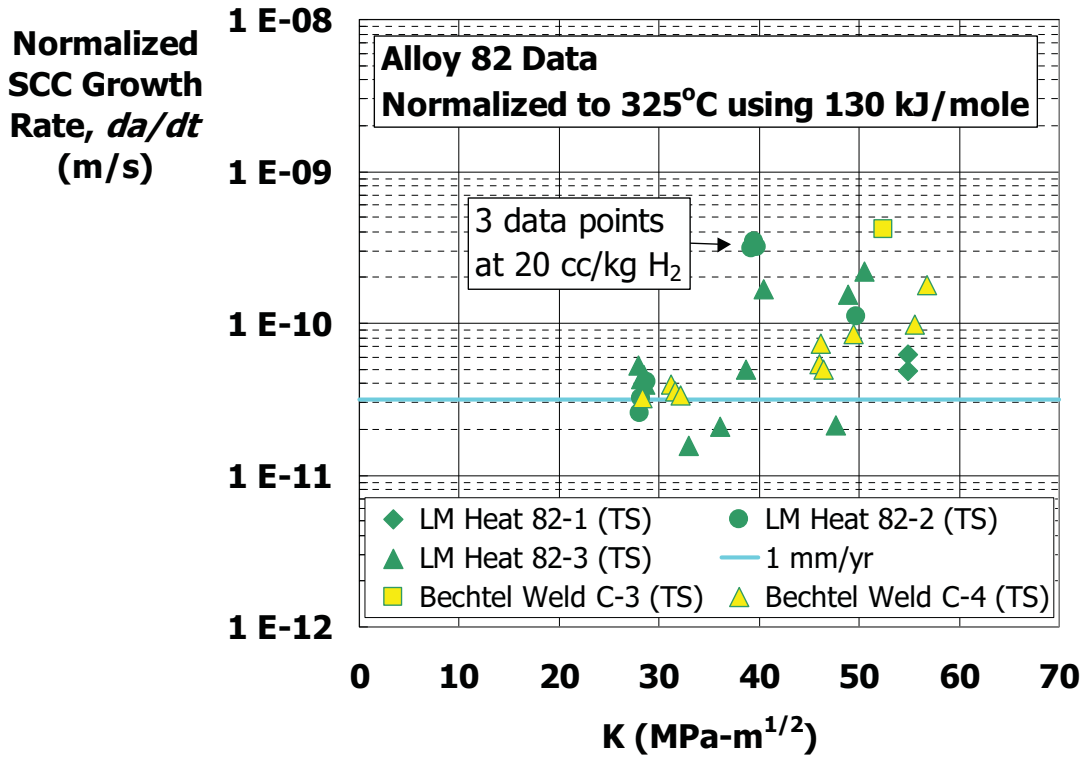

- Compare to published data where *average* SCCGR was reported (fairest comparison)
- All root-to-crown growth; LM data 20 or 40 scc/kg H_2; Bechtel data 40 to 60 scc/kg H_2
- Some of the variability in heat LM82-2 caused by H_2 (highest SCCGRs at 20 scc/kg H_2)

675

LOCKHEED MARTIN

Comparison of Alloy 182 and Alloy 82 - SCCGRs

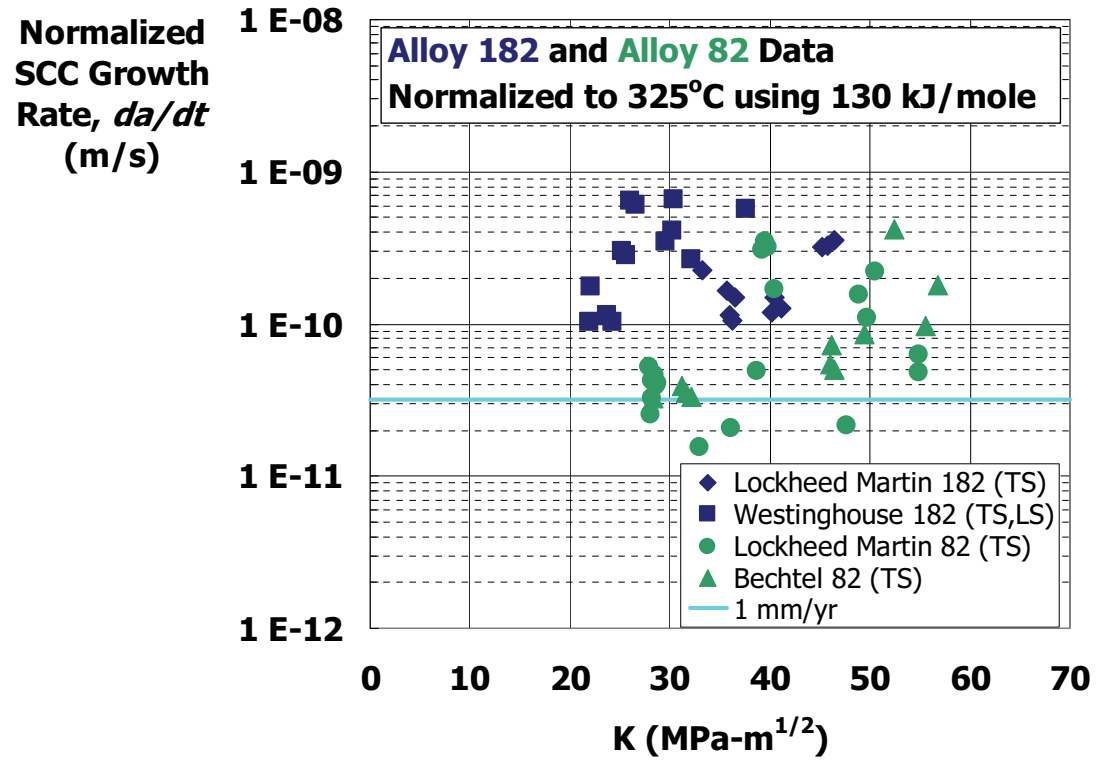

- Alloy 182 SCCGRs are faster on average (~15 *vs*. 20 %Cr, weld process, carbon levels)
  - May be appropriate to model 182 and 82 using an offset
- Insufficient data to identify and/or quantify an SCCGR threshold

676

LOCKHEED MARTIN

Empirical Modeling - Evaluate Three Model Forms

- All three forms are exponential in temperature, power law in K_I
- Use data from both 182 and 82 to determine K_I, 1/T dependencies
  - Not enough data to determine independently (most of 182 data at ~ 325°C)
  - Treat with an offset since the two weld metals appear to have different rates
- General model form:

$$\frac{da}{dt} = A \cdot B_{material} \cdot \left(\frac{K_I - K_{th}}{K_o} \right)^{\beta} \cdot exp\left[- \frac{Q}{R \cdot T} \right]$$

- Model 1: $K_{th} = 0$
- Model 2: $K_{th} = 9$
- Model 3: $K_{th} = 9$, β fixed at 1.16 (Scott form)
  - K_o is a normalizing value (1 MPa$\sqrt{m}$)

677

Model 1: No Threshold, K Dependence not Fixed

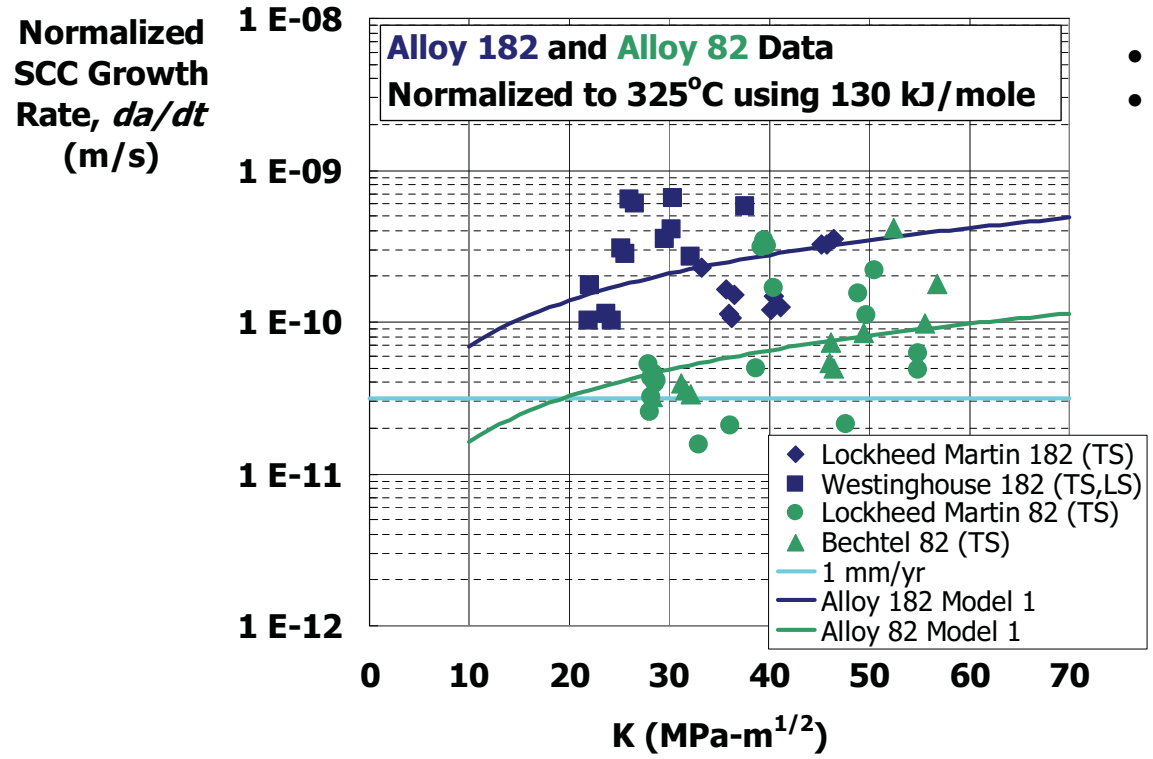

- R^2 = 0.550
- Std. Dev. = 0.760

$$\frac{da}{dt} = 14.76 \cdot \left\langle \begin{matrix} 4.272 & 182 \\ 1.000 & 82 \end{matrix} \right\rangle \cdot \left(\frac{K_I}{1} \right)^{0.999} \cdot exp\left[-\frac{148{,}300}{8.314 \cdot T} \right]$$

678

LOCKHEED MARTIN

Model 2: Threshold (K_{th} = 9), K Dependence not Fixed

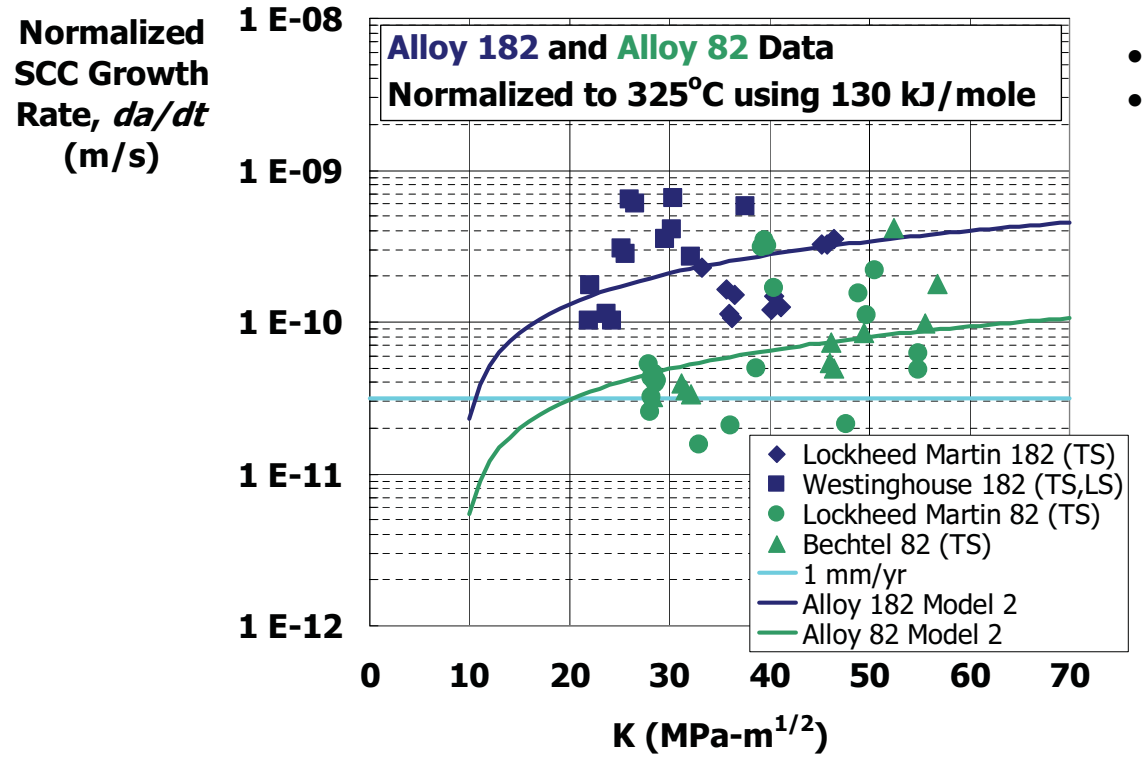

- R^2 = 0.549
- Std. Dev. = 0.760

$$\frac{da}{dt} = 71.24 \cdot \left\langle \begin{matrix} 4.267 & 182 \\ 1.000 & 82 \end{matrix} \right\rangle \cdot \left(\frac{K_I - 9}{1} \right)^{0.723} \cdot exp\left[-\frac{150{,}200}{8.314 \cdot T} \right]$$

679

LOCKHEED MARTIN

Model 3: Threshold (K_{th} = 9), K Dependence = 1.16

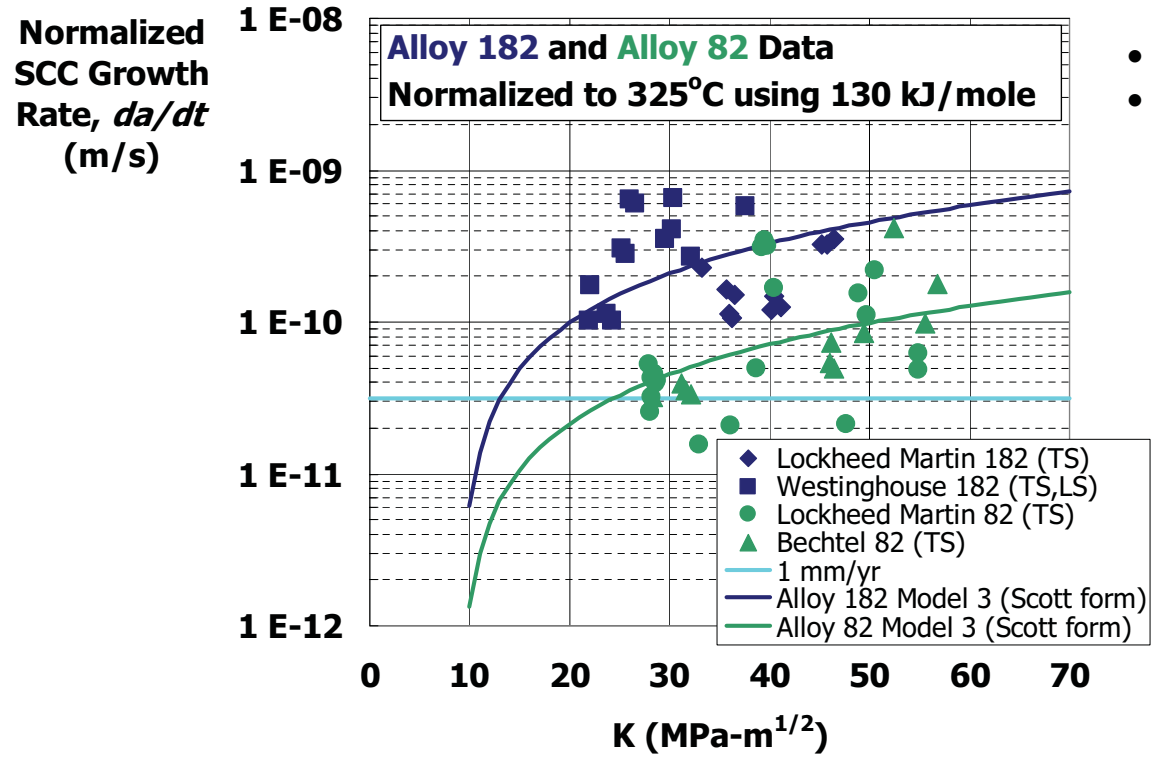

- R^2 = 0.520
- Std. Dev. = 0.764

$$\frac{da}{dt} = 5.028 \cdot \left\langle \begin{matrix} 4.618 & 182 \\ 1.000 & 82 \end{matrix} \right\rangle \cdot \left(\frac{K_I - 9}{1} \right)^{1.16} \cdot exp\left[-\frac{127{,}900}{8.314 \cdot T} \right]$$

680

LOCKHEED MARTIN

Comparison of Models 1, 2, and 3

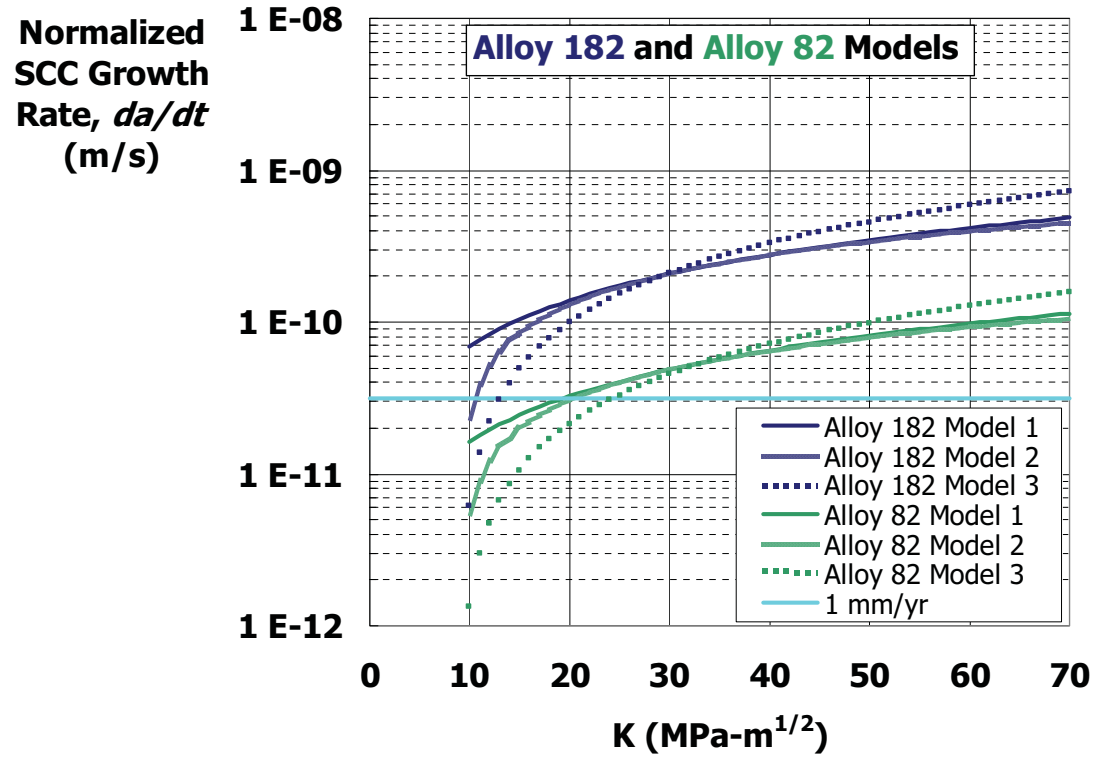

- Models 1 & 2 very similar for $K_I \geq 20$ MPa$\sqrt{m}$ (important region for flaw disposition)
- Model 3 (Scott form) within $\leq$ 1.5X of other models for 20 MPa$\sqrt{m} \leq K_I \leq$ 70 MPa$\sqrt{m}$

Model Summary

- Models 1 and 2 provide a viable approach for correlating the data
  - Model 3 is also reasonable
- Q_{SCCGR} values are 128 to 150 kJ/mol
- K dependencies are ~ 0.7 to 1.0 (when not forced to 1.16)
  - Somewhat lower than Scott model, but not very different than 1.16
  - K dependence of Alloy 182 may be lower than that of Alloy 82
    - EDF/ETH/CEA $SCCGR_{max}$ data for Alloy 182 suggest a low K-dependence ($K^{0.1}$)
- Weld variability is an issue for all three models (R^2 values ~ 0.55)
  - Attempted to collapse the data using a K-1/T interaction:

$$\frac{da}{dt} = A \cdot B_{material} \cdot \left(\frac{K_I - K_{th}}{K_o} \right)^{\beta} \cdot exp\left[-\frac{Q}{R \cdot T} \right] \cdot exp\left[\frac{C \cdot \left(\left(K - K_{th} \right) / K_o \right)}{R \cdot T} \right]$$

    - No measureable improvement in either R^2 or standard deviation
    - Not the only possible equation form to describe K-1/T interactions
  - Normalizing the data for aqueous hydrogen may help reduce scatter

682

Effect of Aqueous H_2 Concentration - Prior Work

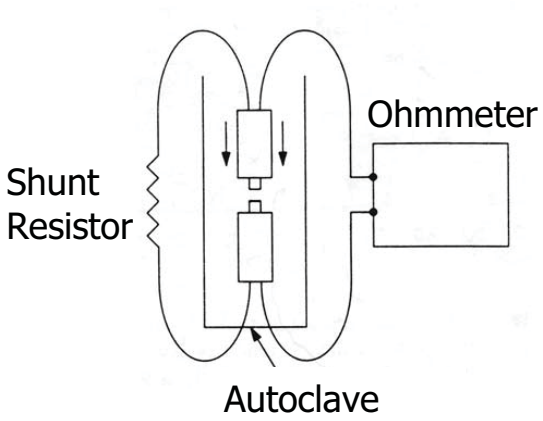

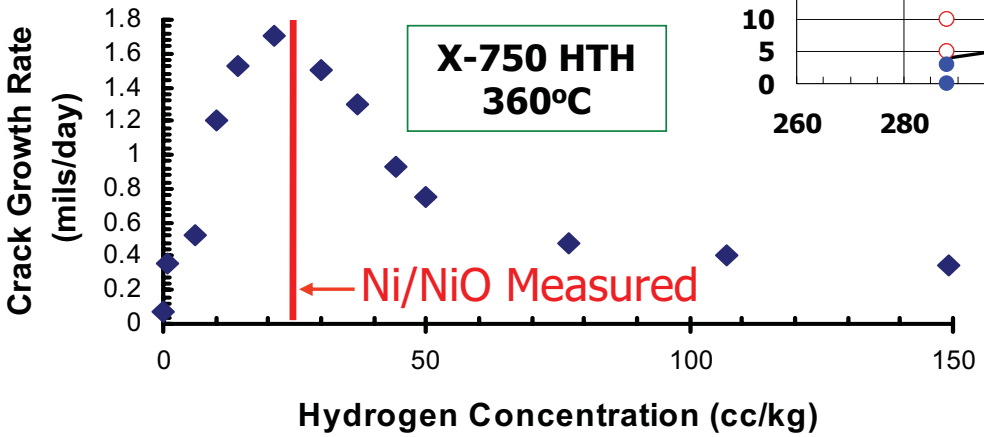

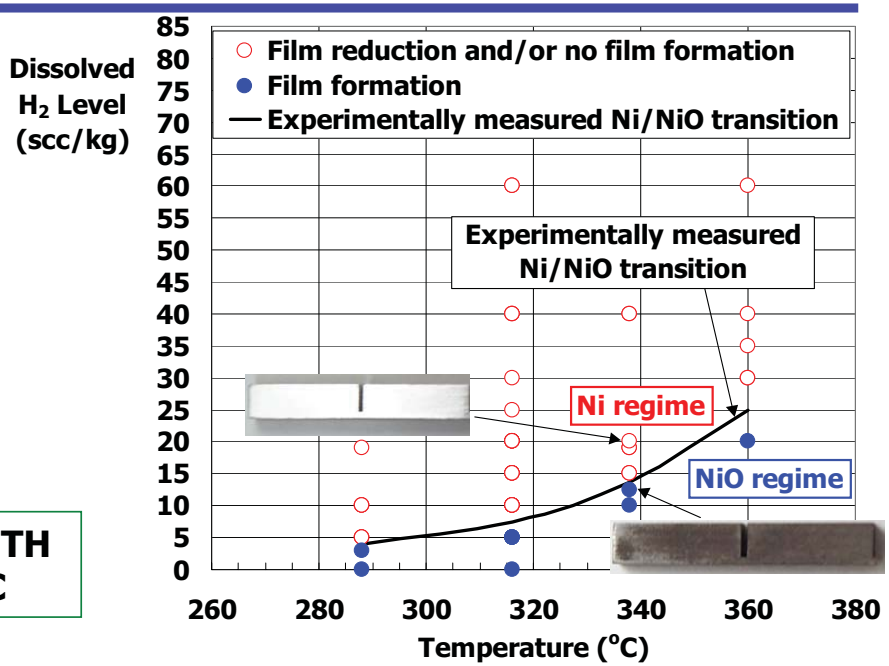

- Similar behavior noted for A600, X-750 AH (Morton, Attanasio)
- Also studied by Scott, Cassagne, Economy, Totsuka, Andresen, *etc.*

LOCKHEED MARTIN

Effect of Aqueous H_2 Concentration - Prior Work

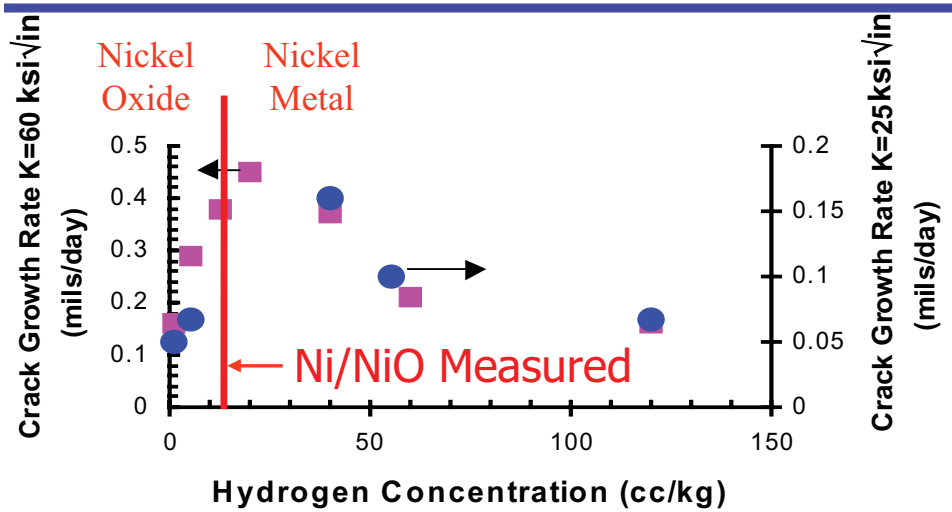

Wrought Alloy 600
K=66 & 27 MPa√m
(K=60 & 25 ksi√in)
338°C

- Correlations for H_2 effects on SCCGR have been presented for A600, X-750 AH, X-750 AH (Morton)
  - Use EcP *vs.* $EcP_{Ni/NiO}$ as correlating parameter
  - Measure EcP via Pt or YSZ/Fe-Fe_3O_4 electrode

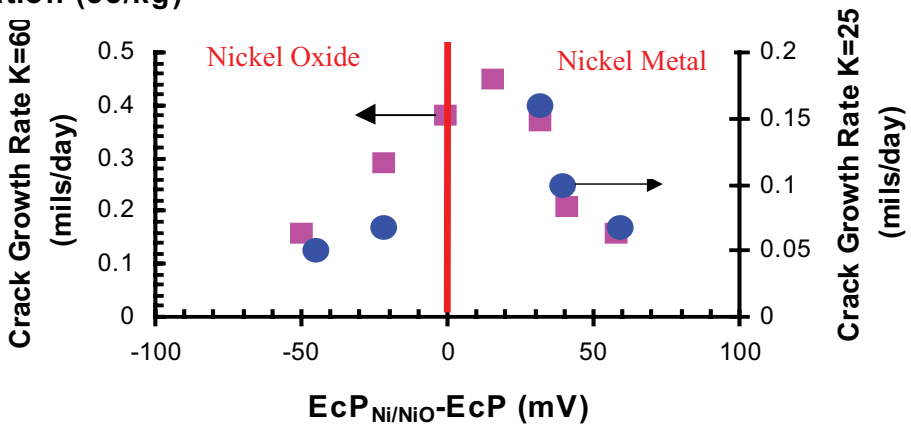

LOCKHEED MARTIN

Effect of Aqueous H_2 Concentration - Alloy 82

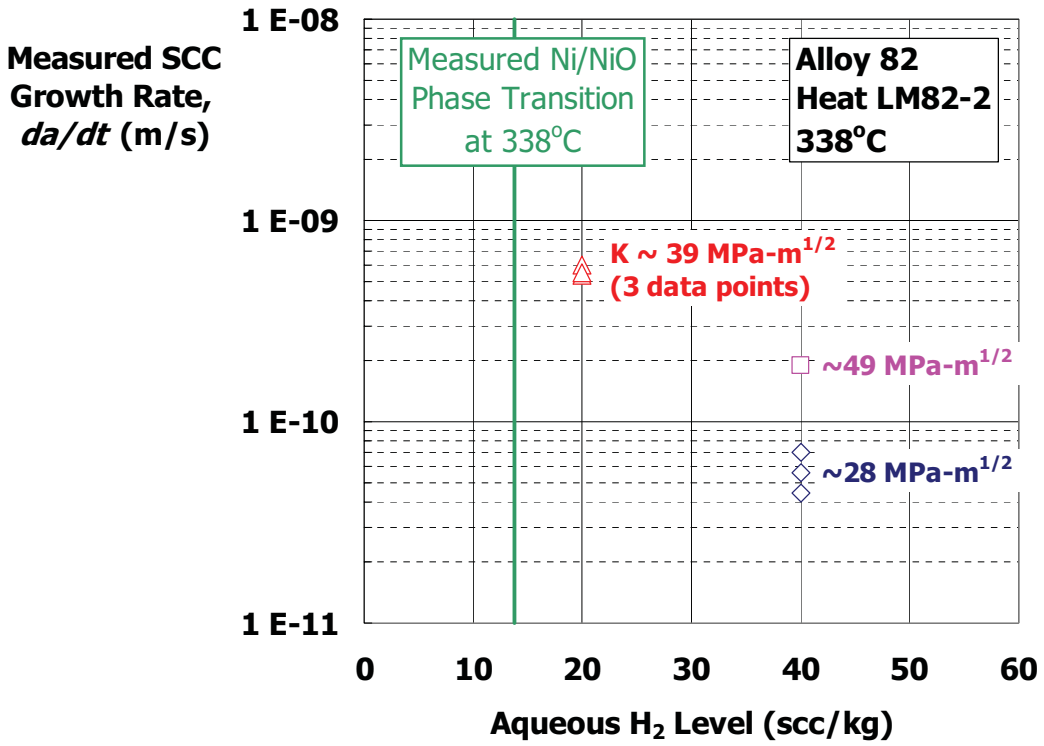

- SCCGRs increase as measured Ni/NiO phase transition is approached
- 20 cc/kg H_2 specimens are bolt loaded - H_2 effect confirmed using active load specimens
- Developing a weld metal correlation so that data can be normalized for H_2 effects

685

LOCKHEED MARTIN

Conclusions

- Ring-loaded specimens can generate efficient, viable SCCGR data
- Crack shape evolution well-described by the maximum/average ratio
- SCCGR data can be reasonably reported using $SCCGR_{ave}$ + RATIO
- LM data are consistent with $SCCGR_{ave}$ data from other researchers
- Three empirical model forms were evaluated - all seem reasonable
  - Data scatter leads to an appreciable standard deviation in all 3 cases
- Aqueous H_2 level influences SCCGR - more quantification is desirable

Acknowledgements

- Maureen Schurman, Brian Gain, John Schisano
- Norm Perazzo Kerry Cotterell, Bruce Furbeck (CSLCT specimens)
- Bill Mills (Bechtel)
- Glenn White (DEI) and John Hickling (EPRI)

687

References

- G White, EPRI Report MRP-55, August 12, 2002.
- N Totsuka, S Sakai, N Nakajima and J Mitsuda, CORROSION/2000.
- PM Scott, Research Topical Symposium at CORROSION/96, 1996.
- DS Morton, SA Attanasio and MA Ando, 10th Environmental Degradation Conference, August 2001.
- WJ Mills and CM Brown, Bechtel report B-T-3435, March 2002.
- S Le Hong, JM Boursier, C Amzallag and J Daret, 10th Environmental Degradation Conference, August 2001.
- G Economy, RJ Jacko and FW Pement, *Corrosion*, 43, 1987.
- T Cassagne, B Fleury, F Vaillant, O de Bouvier & P Combrade, 8th Environmental Degradation Conference, August 1997.
- W Bamford and J Foster, EPRI Report MRP-21, June 2000.
- SA Attanasio, DS Morton, MA Ando, NF Panayotou & CD Thompson, 10th Environmental Degradation Conference, August 2001.

688

LOCKHEED MARTIN

Appendix - Measured SCCGR Data (Not Normalized)

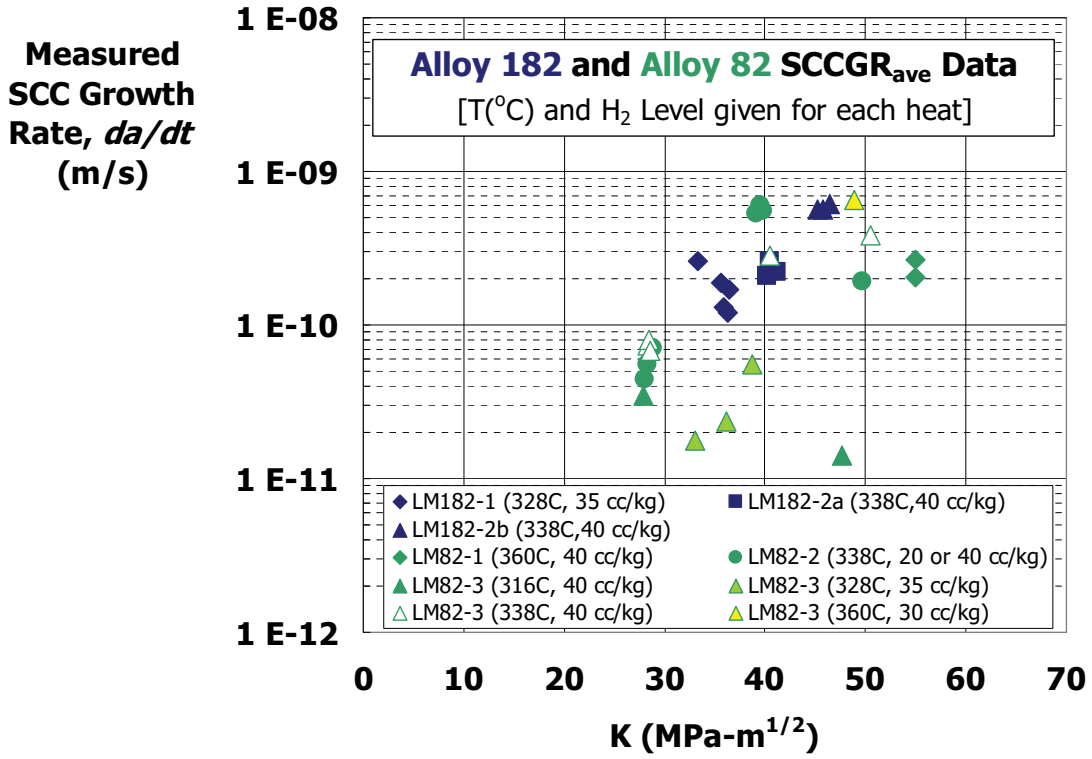

- TS orientation (all data)
- K is reported as the average K value during a test
- No unload-reload cycles
- LM (Lockheed Martin) heats 182-2a and -2b have a different yield strength (YS)
  - 454 and 530 MPa, respectively - due to differences in processing
- Room temperature YS for other heats:
  - 182-1: 503 MPa
  - 82-1: 439 MPa
  - 82-2: 465 MPa
  - 82-3: 460 MPa

689

LOCKHEED MARTIN

Appendix - Compare LM Data to Screening Criteria

- All data conform to the following:
  - Single condition tests
  - Data based on post-test destructive examination
  - Careful autoclave chemistry control
  - No periodic unload-reload
- ASTM E647 Specimen Size Criteria
  - 4 data points rejected
- Reject if percent engagement is <50% or if SCC extent < 0.2 mm
  - 14 data points rejected
- Focus on the data that pass the screening criteria

Appendix - Material Composition

Heat	Ni	Cr	Fe	C	Mn	Cu	Si	Co	S	P	Ti	Nb +Ta
LM182-1	Bal	15.0	7.2	0.03	5.9	0.00	0.7	0.03	0.005	N/A	0.5	2.0
LM182-2	68.7	15.1	7.0	0.02	6.0	0.00	0.8	0.03	0.005	0.01	0.5	1.9
LM82-1	73.4	17.5	1.7	0.047	3.14	0.05	0.26	0.04	0.005	N/A	0.17	3.64
LM82-2	73.5	19.0	1.46	0.045	2.80	0.05	0.12	0.04	0.001	0.013	0.30	2.32
LM82-3	71.5	20.6	1.27	0.045	2.81	0.31	0.14	0.04	0.002	0.012	0.35	2.44

691

Influence of temperature on Primary Water Stress Corrosion Cracking of Alloy 600 Weld Metals

Yoshito Nishikawa, Nobuo Totsuka and Koji Arioka

Institute of Nuclear Safety System, Inc.

Background

- PWSCC were found in Alloy 182 in PWR nuclear power plants.
- There are some studies on Alloys 82 and 182. But a few studies about influence of temperature and susceptibility of heat affected zone (HAZ).

694

Purpose

- To clarify the difference of the susceptibility on PWSCC between Alloys 82 and 132 (modified metal of 182).
- To clarify the difference of the susceptibility on PWSCC between weld metal and HAZ.

Chemical Compositions and Mechanical Properties of Weld Metals and Base Metal

Composition (wt%)	C	Si	Mn	P	S	Ni	Cr	Fe	Cu	Nb
82	0.017	0.26	2.54	0.006	0.001	72.9	17.95	3.72	0.01	1.93
132	0.030	0.30	2.10	0.009	0.002	71.5	15.40	8.50	0.01	1.88
600 (Base Metal)	0.030	0.27	0.29	0.010	0.001	72.9	16.20	-	0.05	-
182	≤ 0.10	≤ 1.0	5.0~ 9.5	≤ 0.03	≤ 0.015	≥ 59.0	13.0~ 17.0	≤ 10.0	≤ 0.50	1.0~ 2.5

Mechanical Properties	0.2% YS (N/mm^2)	TS (N/mm^2)	Elongation Rate (%)	Contraction of Area (%)
82	306	625	26.6	20.2
132	291	625	27.3	26.6
600	287	675	43.3	31.8

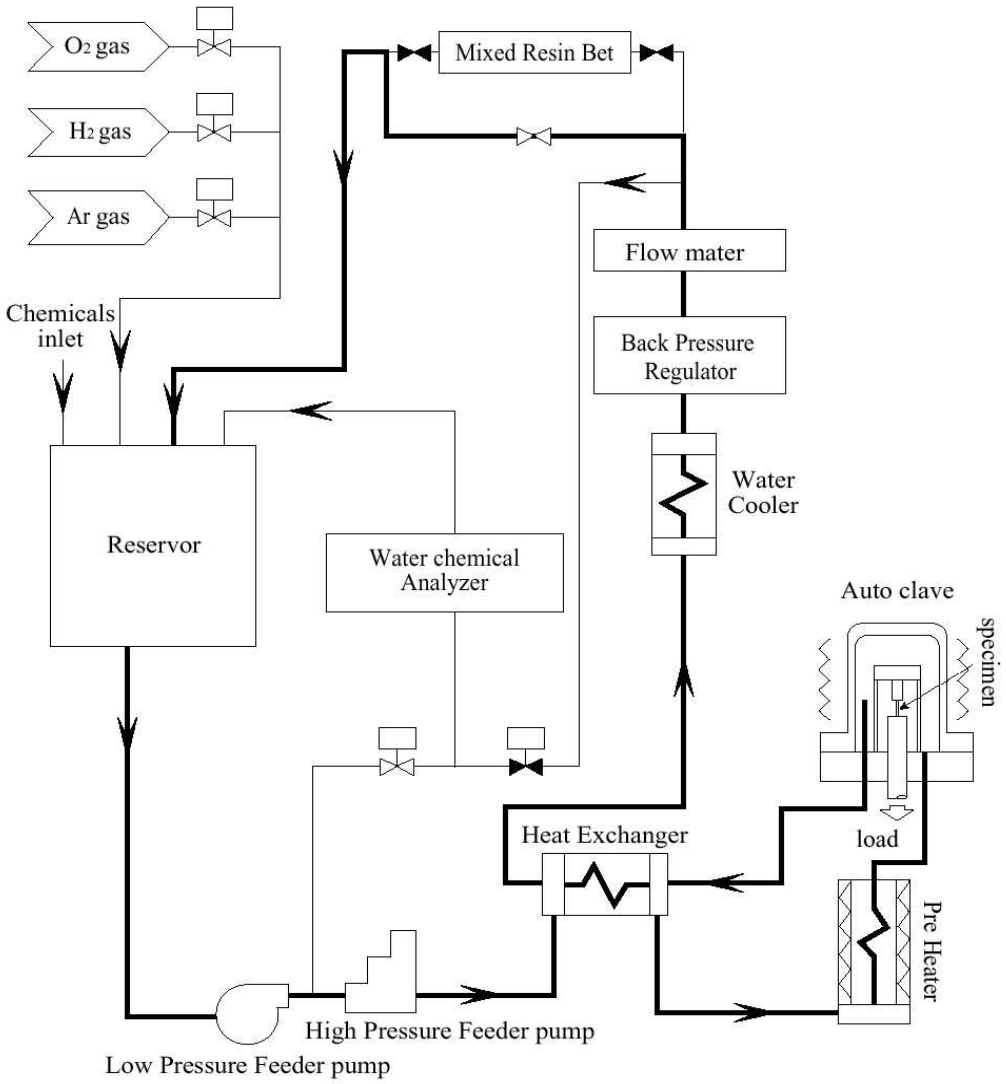

Solution

500 ppm B

2 ppm Li

2.75 ppm H_2

Temperature

360 ~ 330 °C

Strain Rate

5×10^{-7} /s

as 20 mm gauge length

969

Test System and Environment

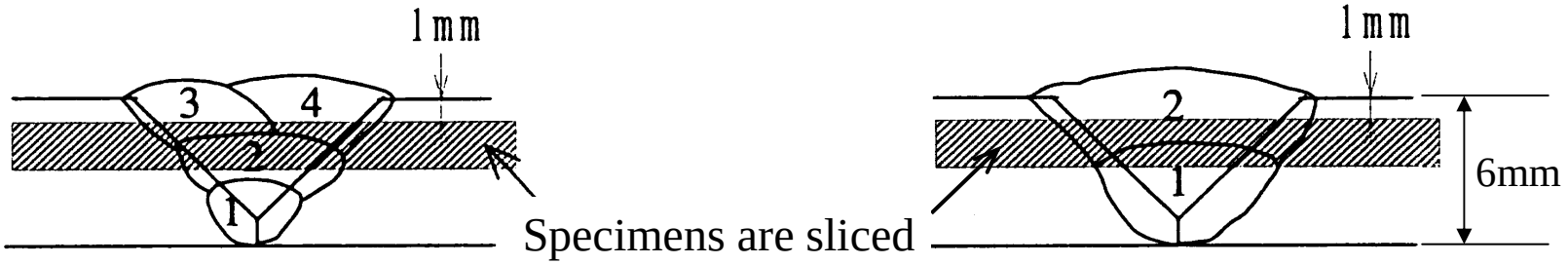

Path of 82 (TIG)

Path of 132 (SMAW)

697

Welding heat

about 10 kJ/cm (both TIG and SMAW)

Welding conditions

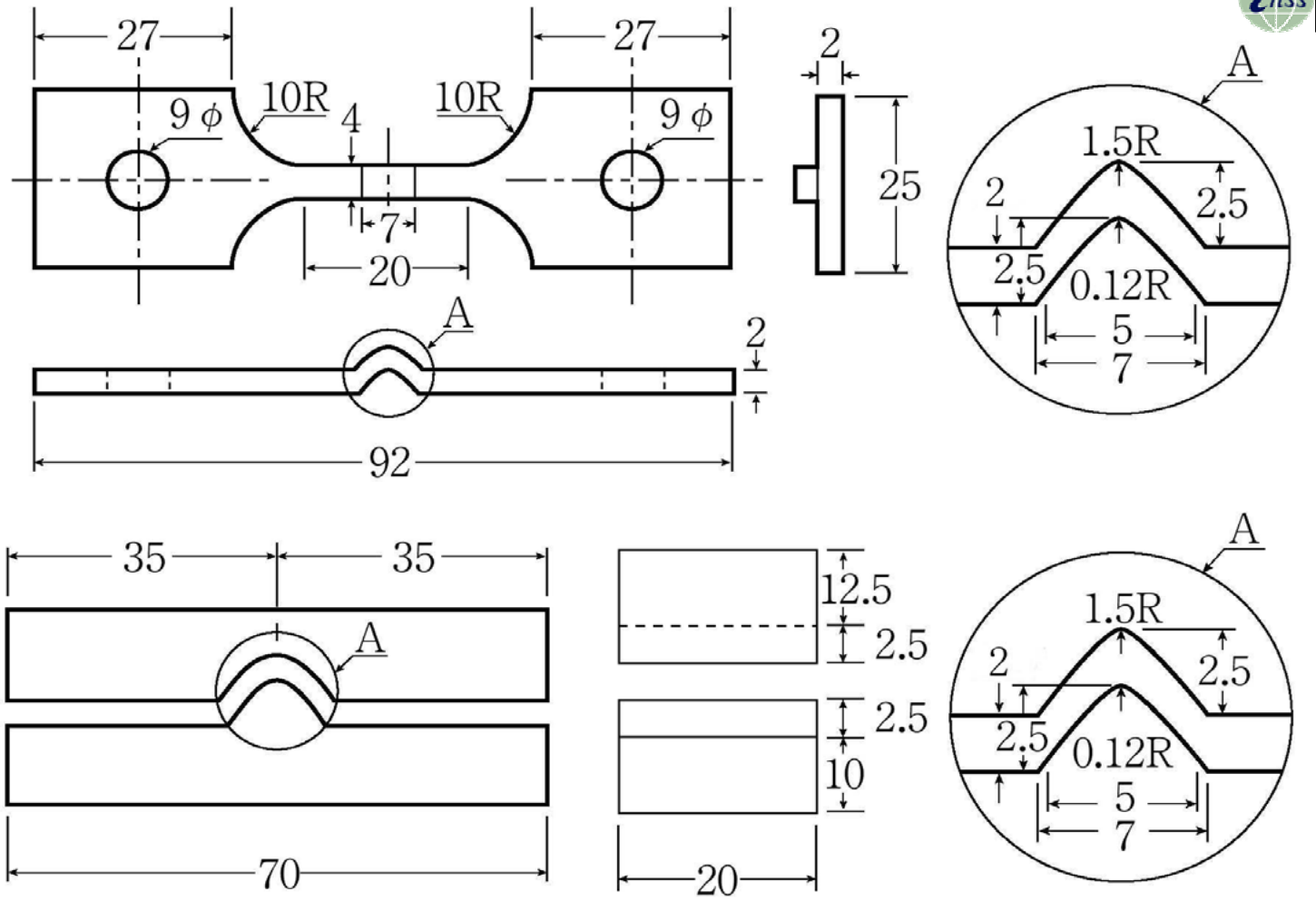

Specimens Used in the Accelerated SSRT Method

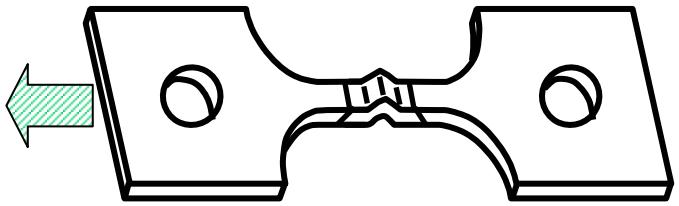

Extend at constant strain rate

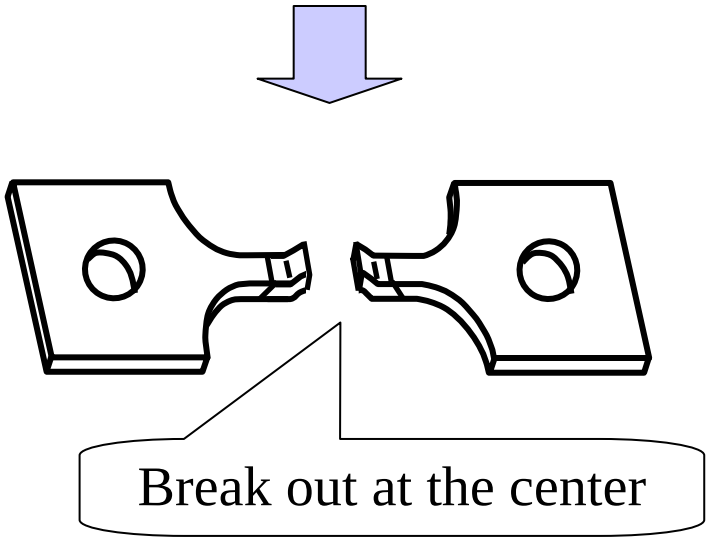

PWSCC

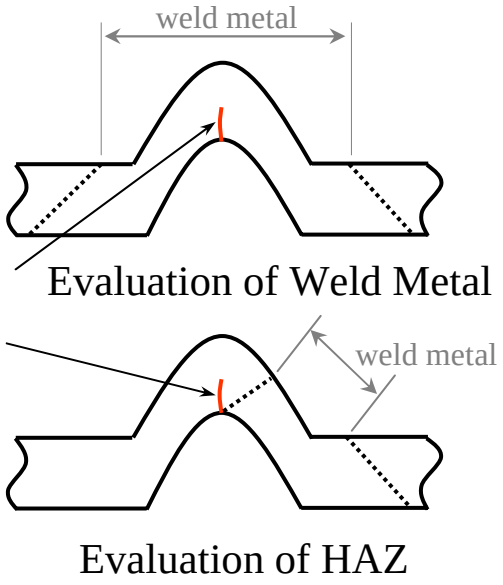

669

Specimen with hump

700

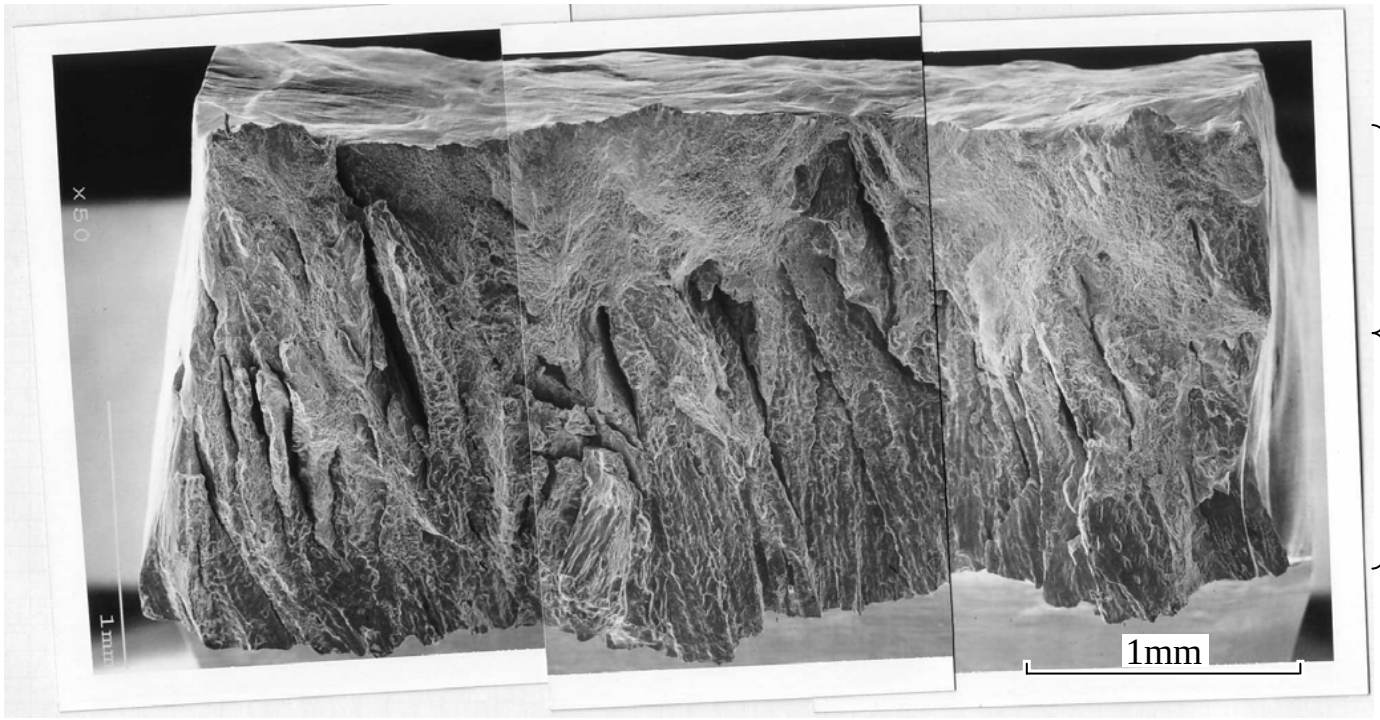

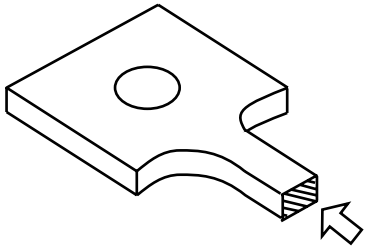

Temperature : 360 °C
Strain Rate : $5\times10^{-7}s^{-1}$
Time to Failure: 67.4 hr
SCC% : 52.6 %

SEM photo of alloy 82

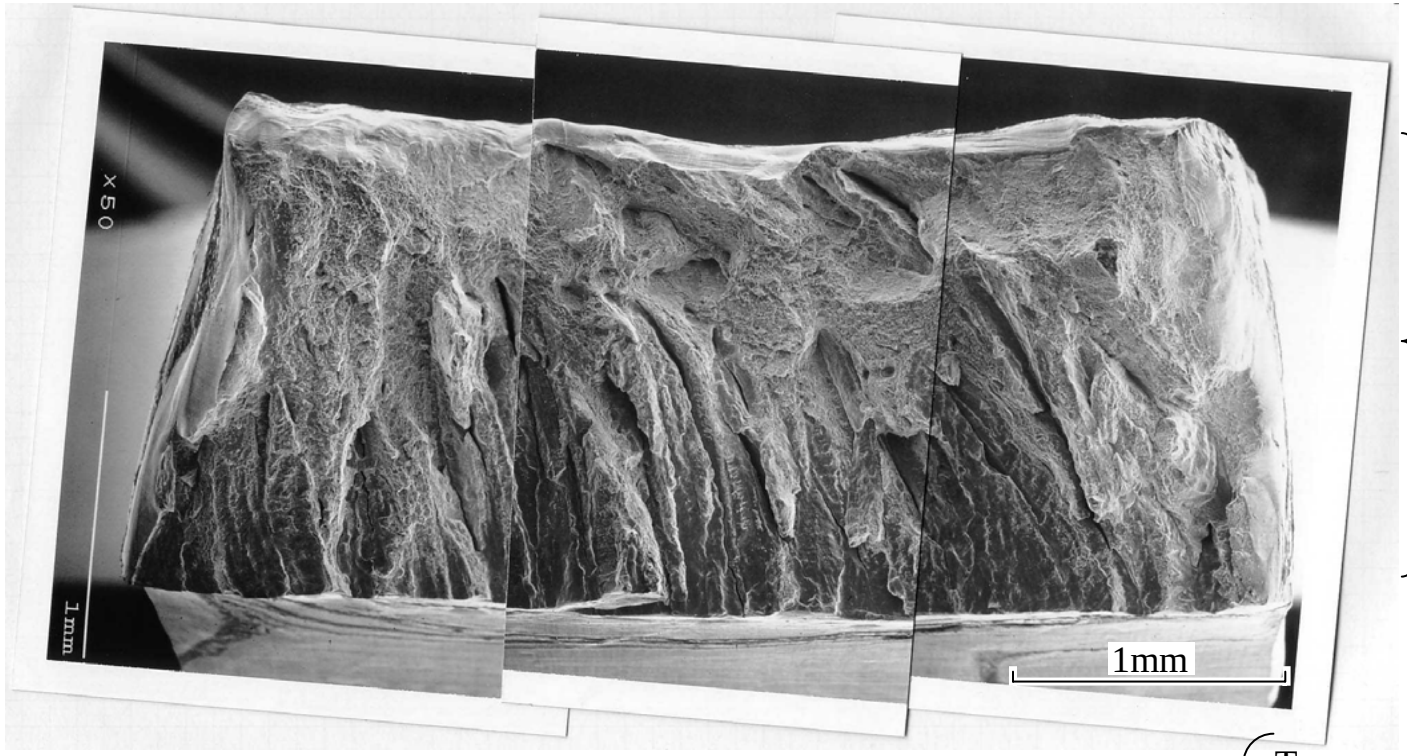

Ductile

Dendritic

Temperature : 360 °C
Strain Rate : $5\times10^{-7}s^{-1}$
Time to Failure: 73.6 hr
SCC% : 33.0 %

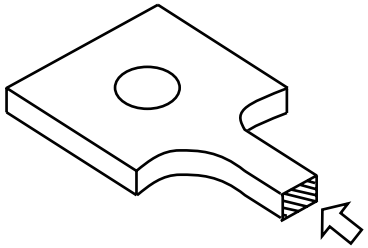

SEM photo of alloy 132

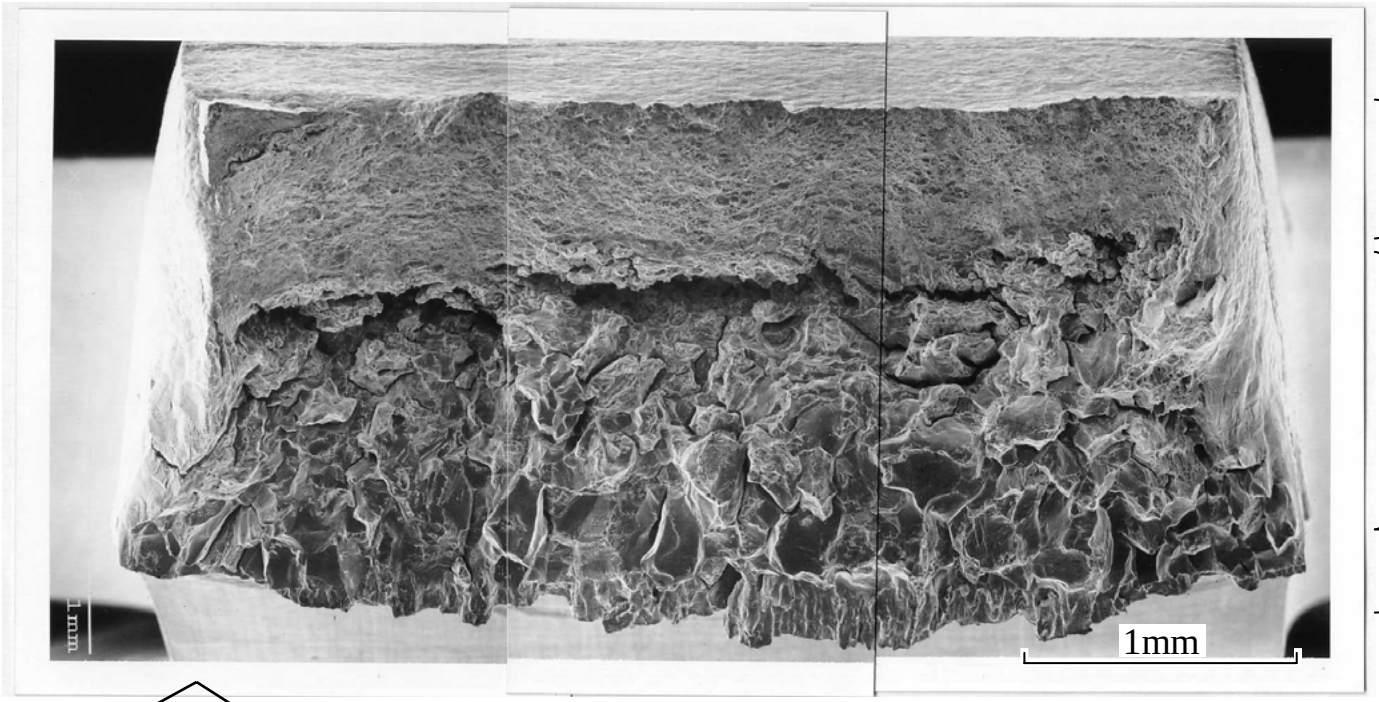

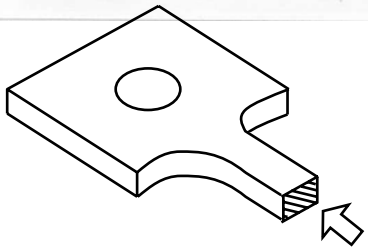

Temperature : 360 °C
Strain Rate : $5\times10^{-7}s^{-1}$
Time to Failure: 64.3 hr
SCC% : 55.9 %

SEM photo of HAZ welded by alloy 82

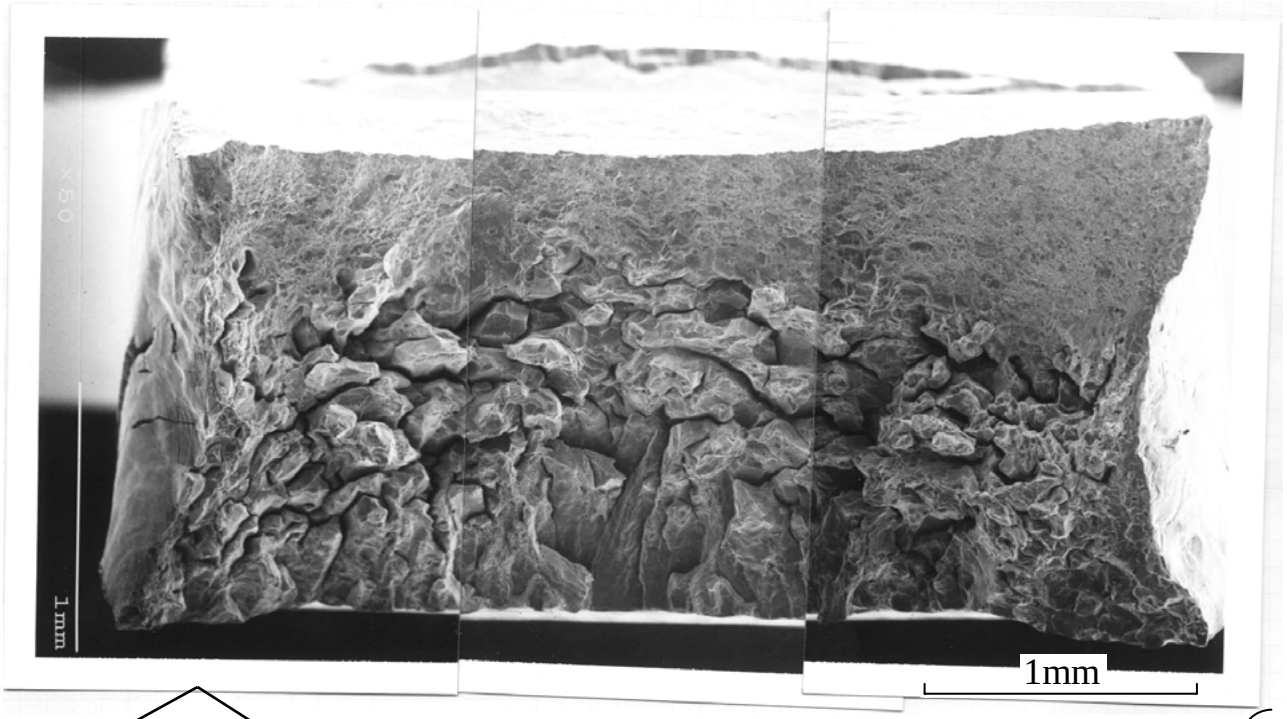

Ductile

Intergranular Cracking

Dendritic

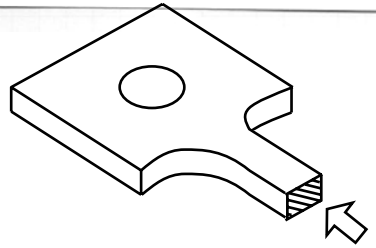

Temperature : 360 °C
Strain Rate : $5\times10^{-7}s^{-1}$
Time to Failure: 82.3 hr
SCC% : 61.8 %

SEM photo of HAZ welded by alloy 132

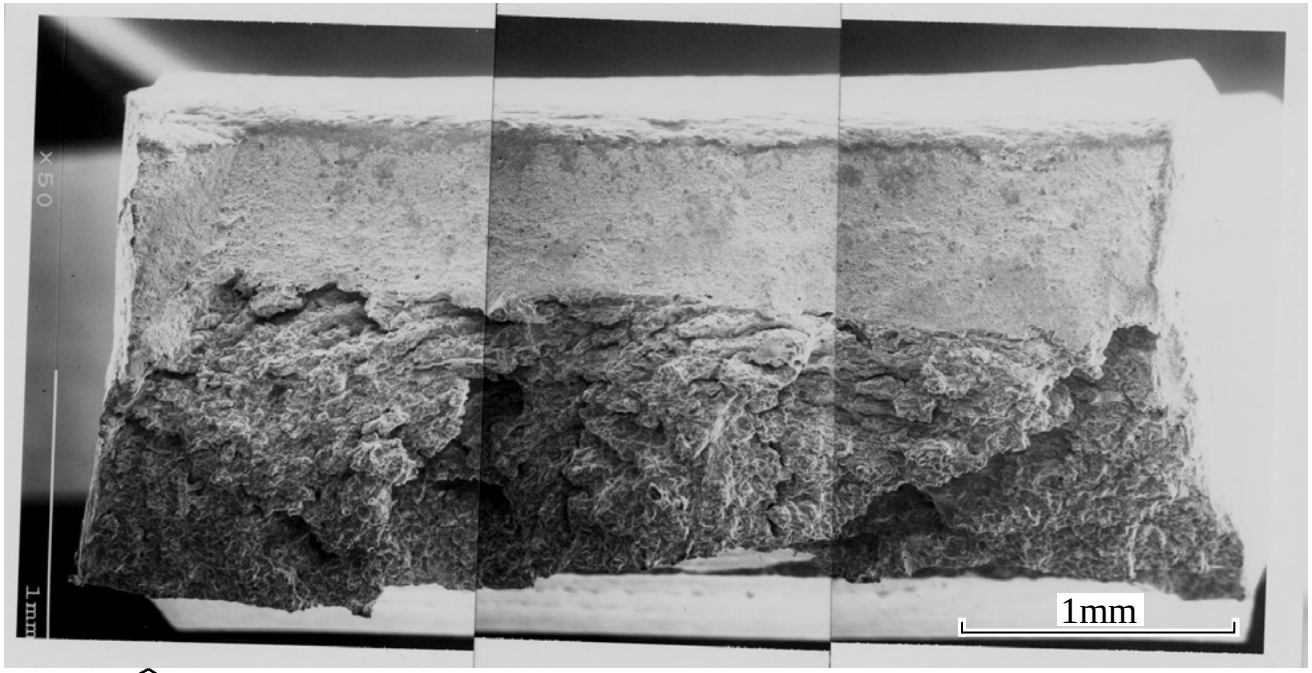

Ductile

Intergranular Cracking

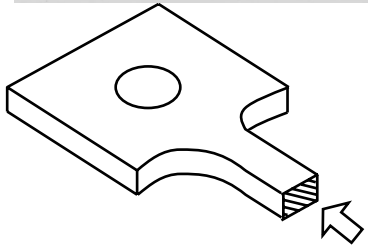

Temperature : 360 °C
Strain Rate : $5\times10^{-7}s^{-1}$
Time to Failure: 101.9 hr
SCC% : 60.8 %

SEM photo of alloy 600 base metal

Crack Growth Rate (v)
= Plate Thickness × SCC % / Time to failure

$$\mathbf{Ea = - R \ln(v_1 / v_0) / (1/T_1 - 1/T_0)}$$

where

Ea : Apparent activation energy

R : Gas constant = 8.3145×10^{-3} kJ/(mol·K)
= 1.9862×10^{-3} kcal/(mol·K)

T_0 , T_1 : Absolute temperature

v_0 : Rate at temperature T_0

v_1 : Rate at temperature T_1

Calculation of Apparent Activation Energy by Arrhenius' Equation

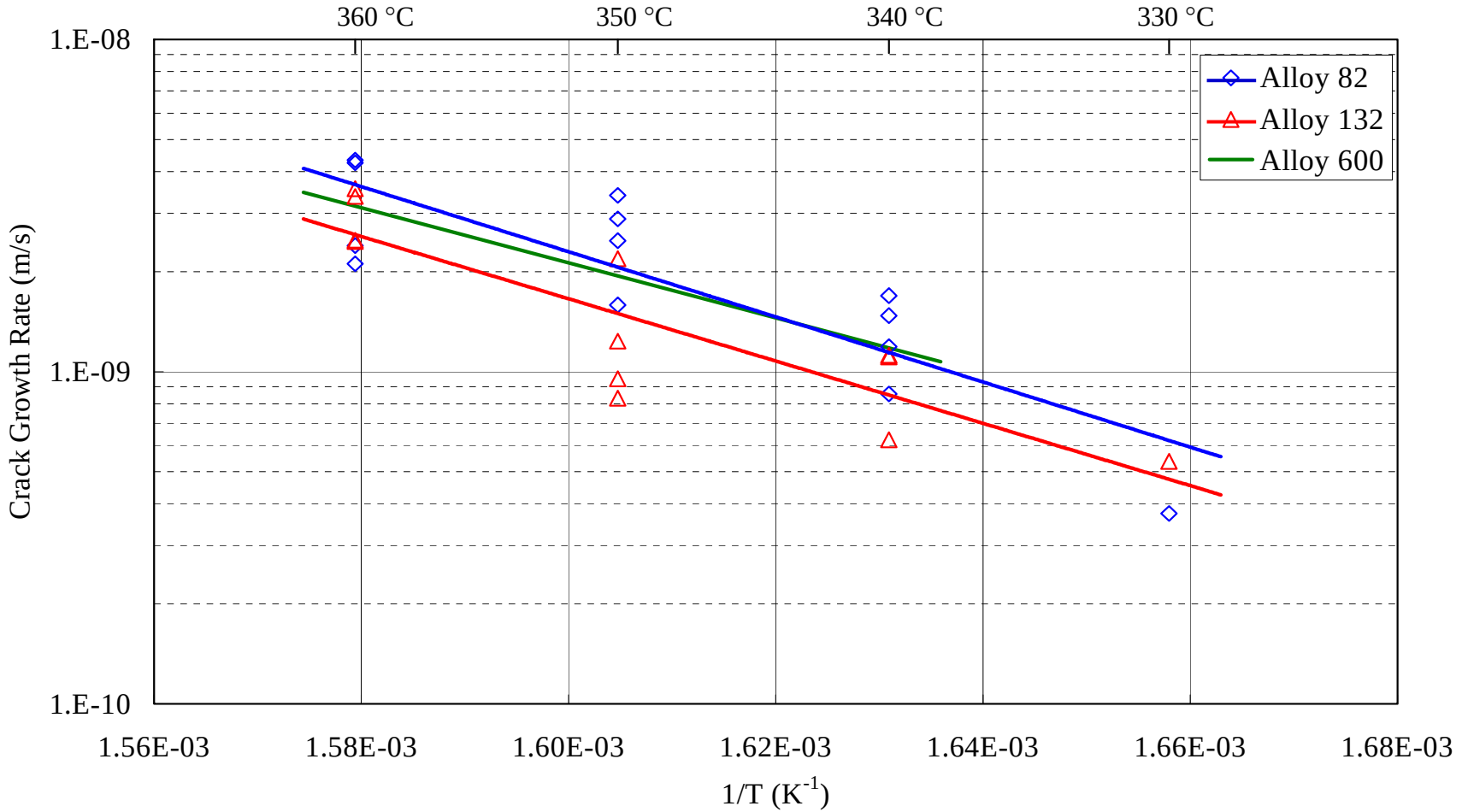

706

Relationship between Temperature and Crack Growth Rate of Weld Metal in SSRT

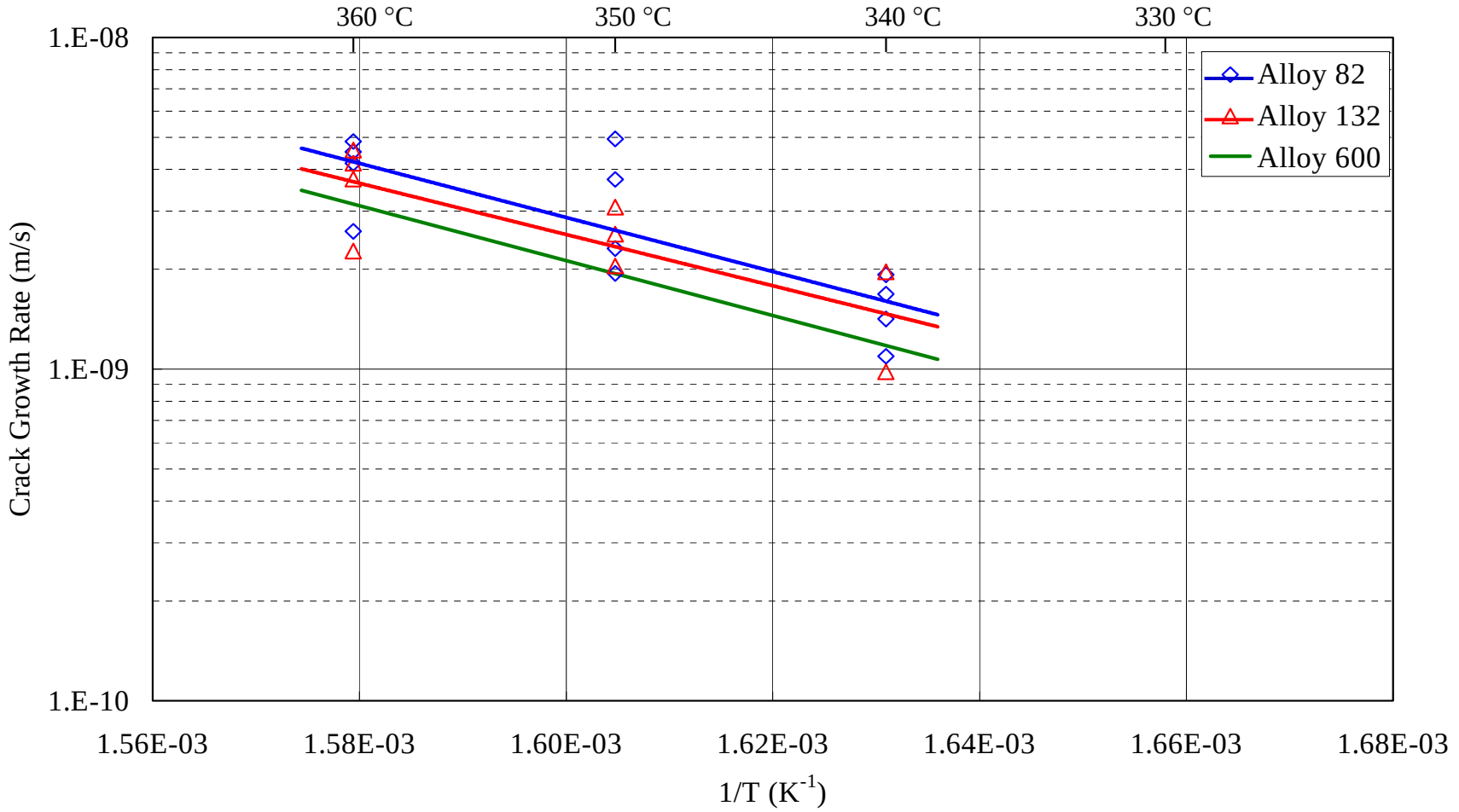

Relationship between Temperature and Crack Growth Rate of HAZ in SSRT

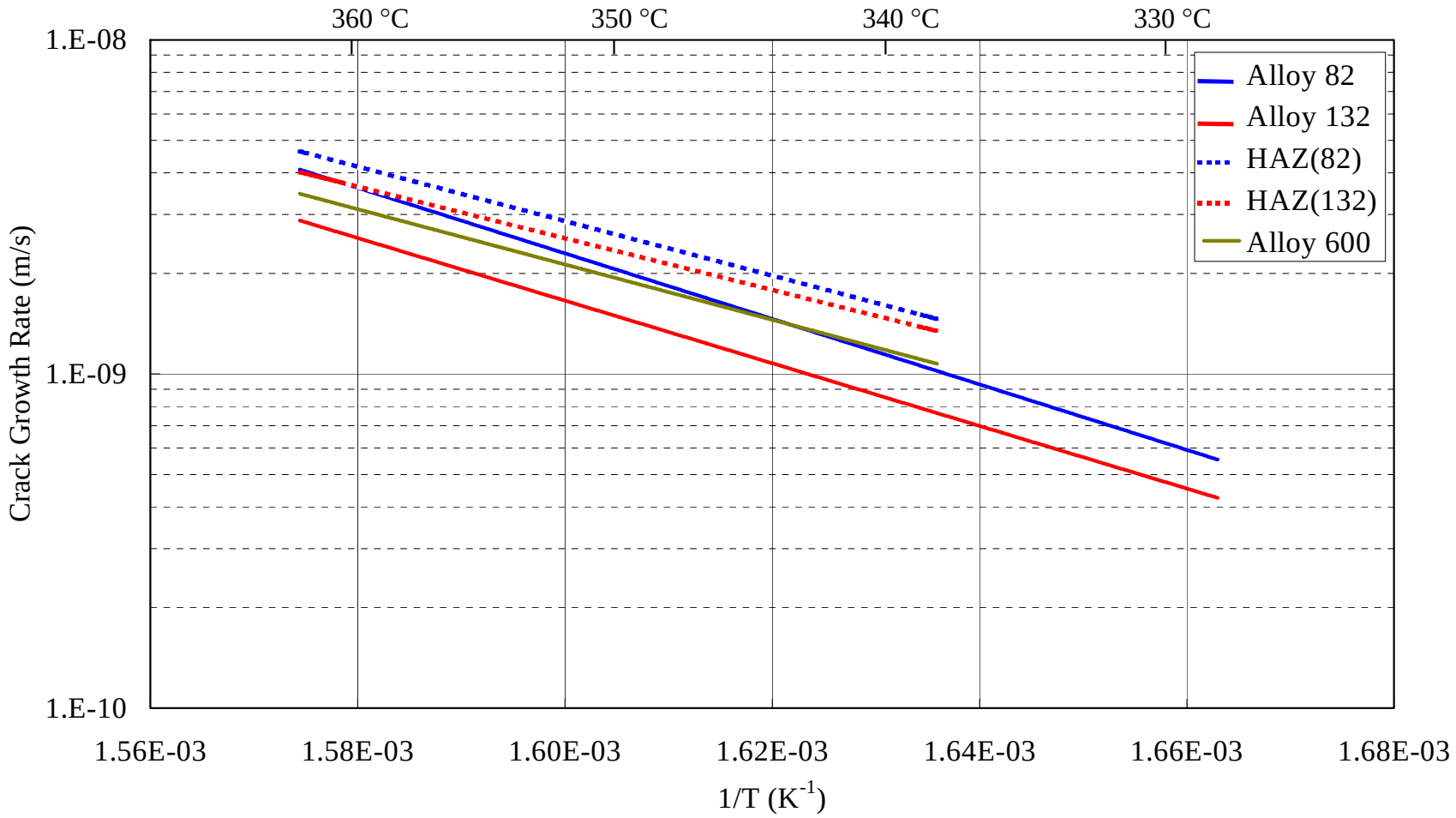

708

Relationship between Weld Metal, HAZ and Base Metal in SSRT

Results

Alloy	Weld Metal or HAZ	Apparent Activation Energy
82	Weld Metal	188 kJ/mol (45 kcal/mol)
132		179 kJ/mol (43 kcal/mol)
82	Heat Affected Zone	156 kJ/mol (37 kcal/mol)
132		148 kJ/mol (35 kcal/mol)

Alloy 600 Base Metal	167kJ/mol (40 kcal/mol)

Conclusions

- The effects of temperature on PWSCC are similar between Alloys 82 and 132.

- The apparent activation energy of weld metal is a little higher than that of heat affected zone (HAZ). It seems that PWSCC on weld metal is more rarely than on heat affected zone at lower temperature.

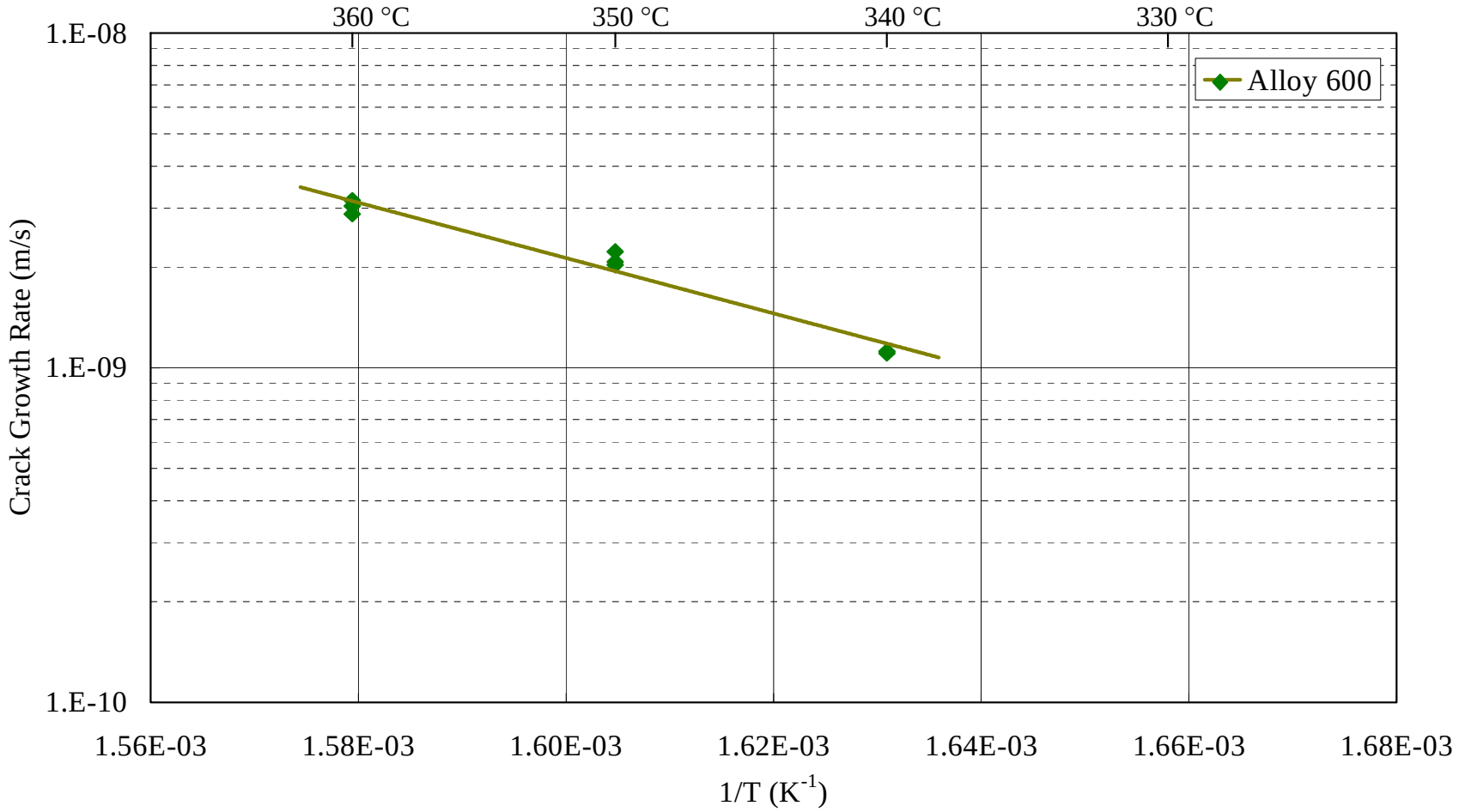

Crack Growth Rate and its approximately curve of Alloy 600 base metal

Evaluation of Scattering

Alloy	Weld Metal or HAZ	Deviations*	total
82	Weld Metal	1.43	1.44
132		1.38	
82	Heat Affected Zone	1.37	
132		1.33	
600	Base Metal	1.20	

* Deviations: Index numbers of standard deviations of logarithms of deviance of each crack growth rate from the approximated curve

FRI

Experimental and Numerical Approaches for Characterizing the Crack Growth Behavior of Alloy 600 in PWR Primary Water, and Lifetime Predictions for Welded Structures

Tetsuo Shoji, Zhanpeng Lu and Qunjia Peng

Fracture Research Institute
Tohoku University
Sendai 980-8579, JAPAN

Outline (1)

- Introduction
- Literature Survey

  -Existing Crack Growth Data and Significant Parameters
- FRI Generalized Crack Growth Rate Formulation
- Numerical Analysis
  - K dependence
  - Effects of yield strength
  - Effects of dK/dt

Outline (2)

- Prediction of Crack Growth Behavior in Weld Residual Stress Field
  - -Core Shroud Cracking
  - -VHP behavior
- Disposition of Flaws
- Conclusions
- Acknowledgements

715

Introduction (1)

- More concerns on PWSCC of alloy 600 and weld metals such as 182 in PWR Vessel Penetrations.
- Need Quantitative Evaluation of the remaining lifetime of the vessel penetration (VP) in PWR
- Need fully understanding of the crack growth behavior of Ni-based alloys from a view point of Disposition of Flaw.

716

Introduction (2)

- Special emphasis should placed on the K dependence of crack growth rate as a function of metallurgical variables, mechanical properties, temperature and dK/dt.

- Therefore, multiple factors, such as material, environmental, and mechanical are involved in EAC processes and their synergy effects are complex.

- Prediction of nickel base alloy components in real PWR plants based on PWSCC mechanism and CGR modeling is highly demanded

717

Literature Survey(1)

-Existing CGR Data-Laboratories & Plants

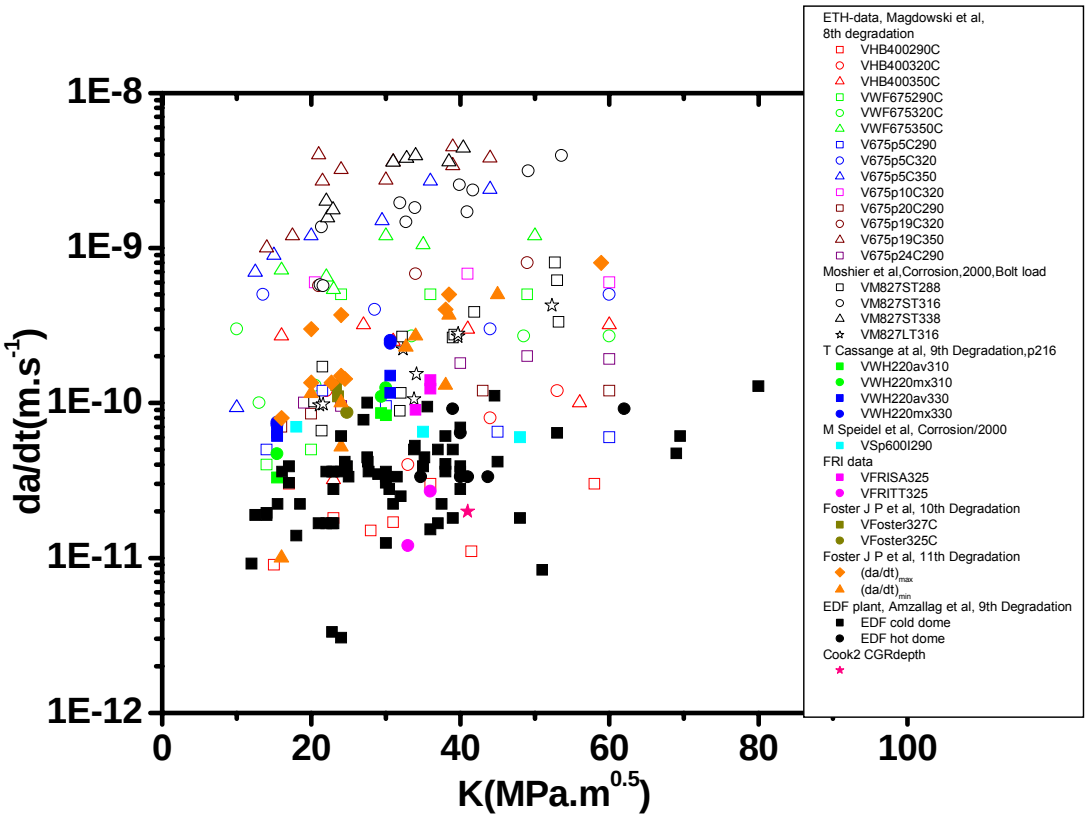

CGRs of Alloy 600 in PWR environments

- Lab. data:

-thick plate material

-fracture mechanics specimen

- Plant data:
  EDF & Cook 2

>Huge scatter of the data in da/dt vs K

718

Literature Survey(2)
-Significant Parameters for CGR

- Material Chemistry and Microstructure

  -Carbide content and distribution
  (Grain boundary carbides improve SCC resistance)
  -Fraction of Coincidence Site Lattice Boundaries (CSLB)
  (High CSLBs-low IGSCC susceptibility)

- Temperature effects

  CGR increase follows Arrhenius law
  ~180kJ/mol for component failure time(including initiation)
  ~130kJ/mol for crack growth rate

- DH effects

  ~da/dt(max) near the Ni/NiO equilibrium potential line

Literature Survey(3)
-Significant Parameters for CGR

- K effects

  -CGR plateau region at high K level(ETH data, EDF data, et c.)

  -CGR monotonically increase-(Westinghouse data, EDF data, etc.)

Most CGR models are based on K effect

- YS effects

  High YS from material chemistry or cold/warm rolling

  -significantly raise CGR

In empirical equations, a coefficient is used to introduce CW effect

- Loading and dK/dt effects

  -Loading mode effect

  -dK/dt effect for weldments with residual stress/strain

etc.,

720

FRI Generalized CGR formulation (5)

-CTSR formulation - Gao & Hwang's equation

- Gao and Hwang's definition of work hardening exponent, n,

$$\varepsilon = \begin{cases} \left(\frac{\sigma}{E}\right) & \text{for} \quad \sigma \le \sigma_y \\ \left(\frac{\sigma}{E}\right) + c\cdot(\sigma - \sigma_y)^n & \text{for} \quad \sigma > \sigma_y \end{cases}$$

- Gao & Huang's equation for the crack tip strain of a growing crack for constant K and da/dt.

$$\varepsilon_{ct} = \beta\left(\frac{\sigma_y}{E}\right)\left[\ln\left(\frac{A}{r}\right)\right]^{\frac{n}{n-1}} \qquad \varepsilon_{ct} = \beta\left(\frac{\sigma_y}{E}\right)\left\{\ln\left[\left(\frac{\lambda}{r}\right)\left(\frac{K}{\sigma_y}\right)^2\right]\right\}^{\frac{n}{n-1}}$$

Derived under the condition of plain strain and small scale yield

721

FRI Generalized CGR formulation (6)

-CTSR formulation - Validity Confirmed by 3D-FEM

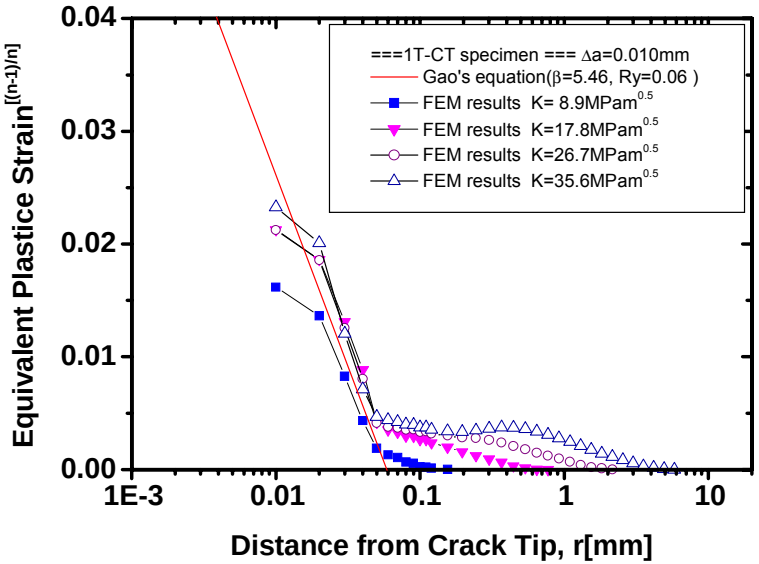

Equivalent plastic strain distribution at crack tip under constant load conditions, n (Gao's definition) is 10.

- 3D-FEM results match well with the theoretical calculation at different values of stress intensity factor, K.
- Although Gao's equation was derived for a steady growing crack under quasi-static loading (constant K), the 3D-FEM analyses indicate that Gao's equation may still be applicable even under the loading conditions without constant crack growth and/or constant K.

FRI Generalized CGR formulation (9)

-Shoji's model based on Slip/Oxidation mechanism

- FRI theoretical CGR formulation, based on the crack tip reaction kinetics and the theoretical CTSR formulation

$$\frac{da}{dt}=[\frac{M\cdot i_0}{z\cdot\rho\cdot F\cdot(1-m)}](\frac{t_0}{\varepsilon_f})^m\left\{\beta\cdot(\frac{\sigma_y}{E})\cdot(\frac{n}{n-1})\cdot[2\cdot\frac{\dot{K}}{K}+\frac{\dot{a}}{r}]\cdot\left\{\ln[\lambda\cdot\frac{(\frac{K}{\sigma_y})^2}{r}]\right\}^{\frac{1}{n-1}}\right\}^m$$

- *A unique expression for CGR as a function of K- combining a mechanism of crack growth with the mechanics of a crack tip stress/strain field.*
- *Synergistic terms among the material parameters, mechanical properties, electrochemical properties and crack tip mechanics in terms of K and dK/dt*

723

FRI Generalized CGR Formulation (10)

-CGR equation

A generalized CGR formulation can be obtained by combining the general oxidation mechanism and the theoretical CTSR equation,

$$\frac{da}{dt} = \kappa_a \cdot \left\{ \beta \cdot \left(\frac{\sigma_y}{E}\right) \cdot \left(\frac{n}{n-1}\right) \cdot \left[2 \cdot \frac{\dot{K}}{K} + \frac{\dot{a}}{r}\right] \cdot \left\{ \ln\left[\lambda \cdot \frac{\left(\frac{K}{\sigma_y}\right)^2}{r}\right] \right\}^{\frac{1}{n-1}} \right\}^m$$

where κ_a is a crack tip oxidation rate constant, which is a function of local material chemistry, local environmental chemistry, transient interfacial rate kinetic law, and the stress/strain state.

724

FRI Generalized CGR Formulation (12)

-Possible Accelerated CGR testing based on mechanism (1) YS& κ_a effect

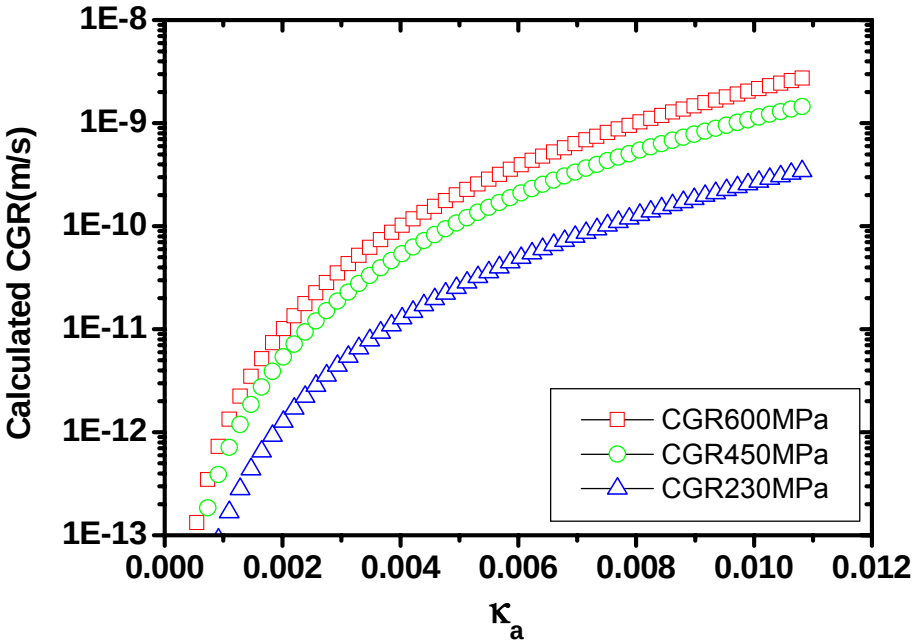

Sensitivity analysis of YS effect at different κ_a levels (m= constant)

- **At each YS level, CGR increases with increasing of κ_a value**
- **A non-linear relationship between CGR and κ_a**
- **CGR increases with YS**

FRI Generalized CGR Formulation (13)

-Possible Accelerated CGR testing based on mechanism (2) YS & m effect

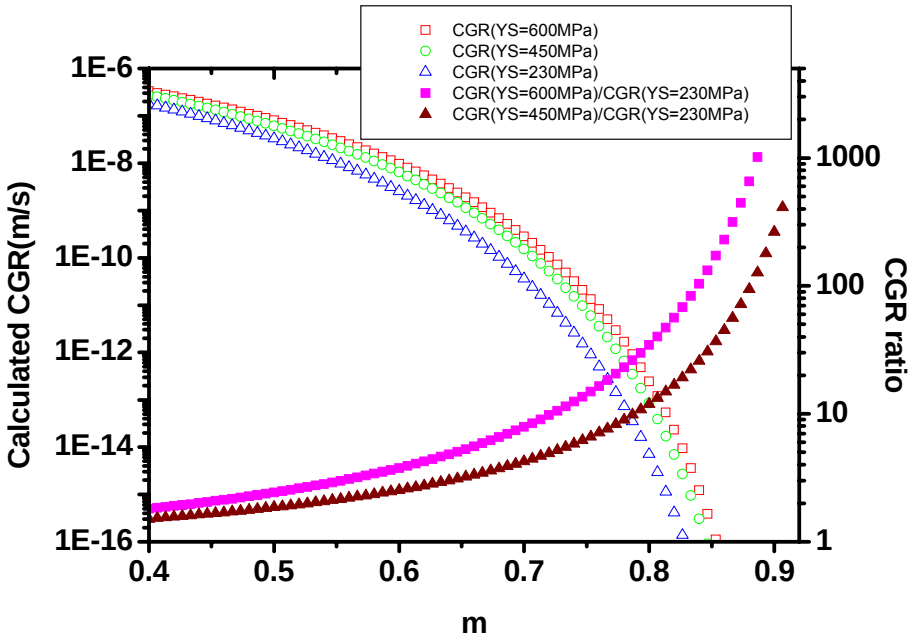

Sensitivity analysis of the effect of YS on CGR for different values of m (κ_a =constant)

CGR ratio= CGR(YS)/CGR(230MPa)

- CGR decreases with an increase of m
- Effect of YS increases with an increasing m,

-implying that the effect of YS is more significant for materials with a faster repassivation (or fast film recovery) process

726

FRI Generalized CGR Formulation (14)

- Possible Accelerated CGR testing (3)YS & κ_a & m effect

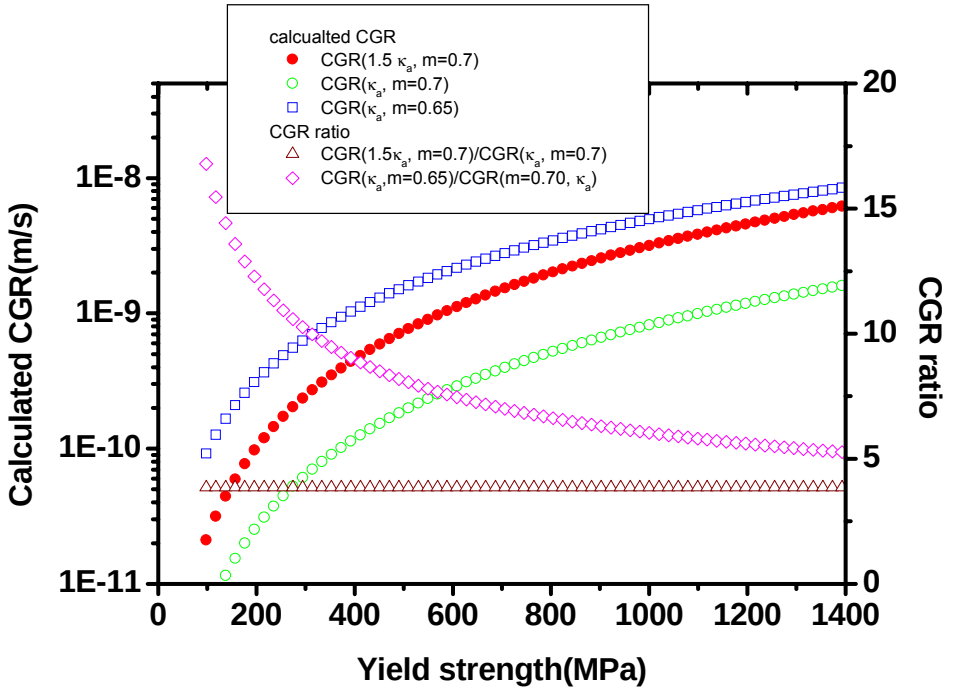

- The enhancement factor by decreasing m is less with an increase of YS.

-CGR enhancement by decreasing *m* (slower film recovery process) could be more significant for materials of lower YSs

FRI Generalized CGR Formulation (16)

- Possible Accelerated CGR testing based on mechanism (5) K&dK/dt effect

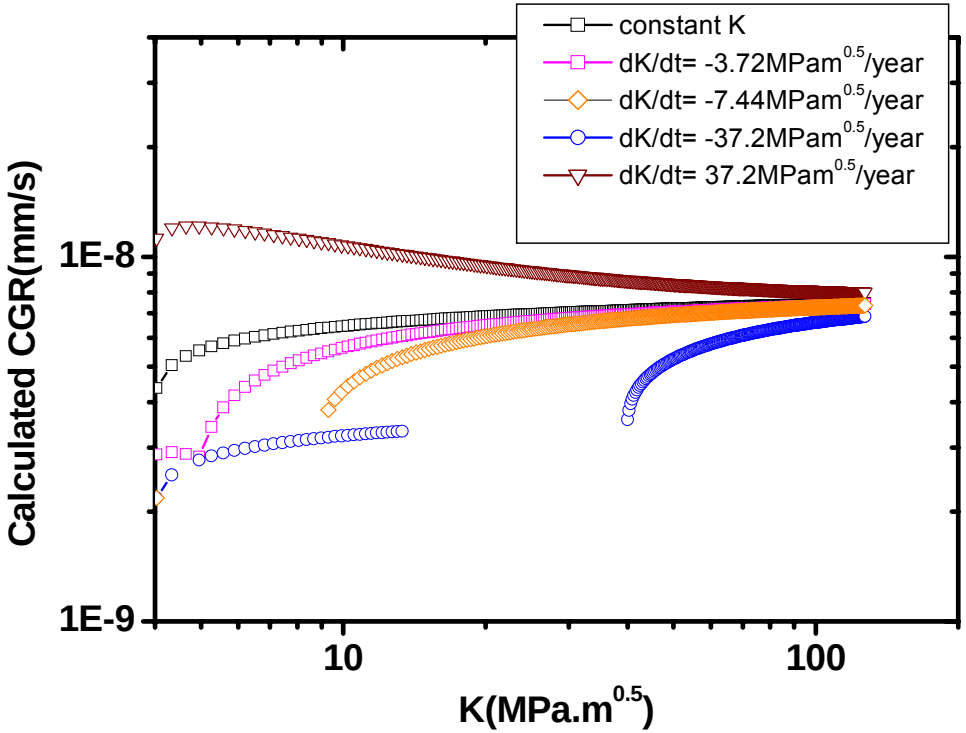

n=9
m=0.5
YS=200MPa
Different dK/dt

- Significant effect of dK/dt on CGR
- Negative dK/dt results in lower CGR and higher threshold
- CGR testing at higher dK/dt accelerates CGR-specimen design

Numerical Analysis of experimental CGR(1)
-K dependence - Moderate K effect

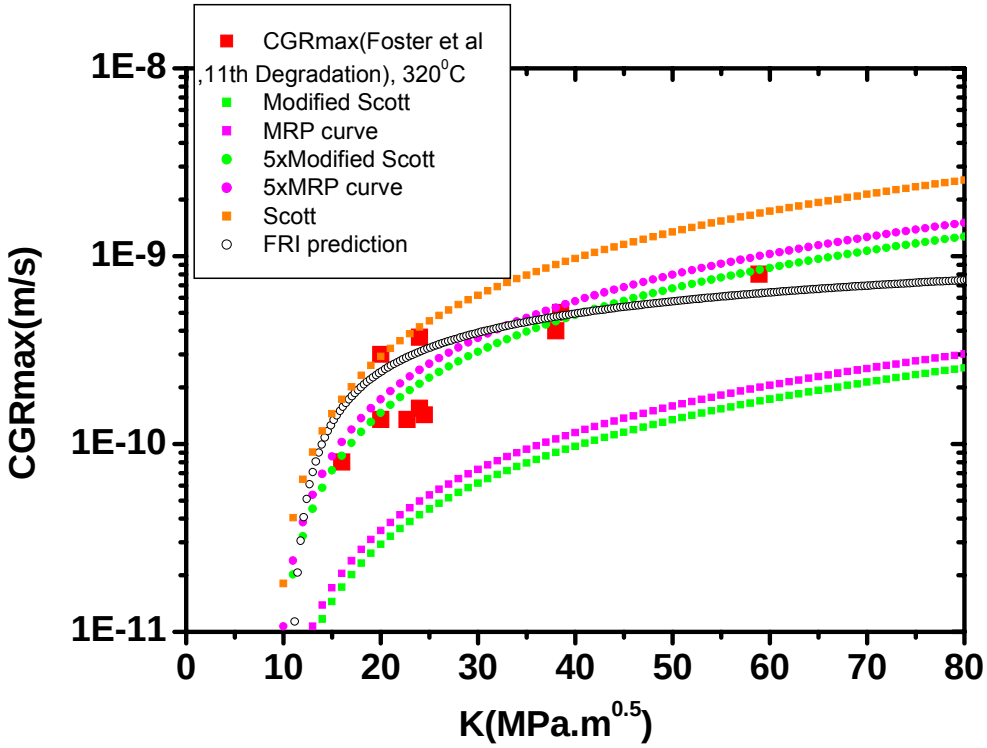

Alloy 600, heat 69
Material of low YS,
YS=274MPa
n=3

Parameter used in the model:
m=0.77

- FRI prediction on the material with YS=274MPa
- Comparison with modified Scott model & MRP model.

Numerical Analysis of experimental CGR(4) -YS effect (1)

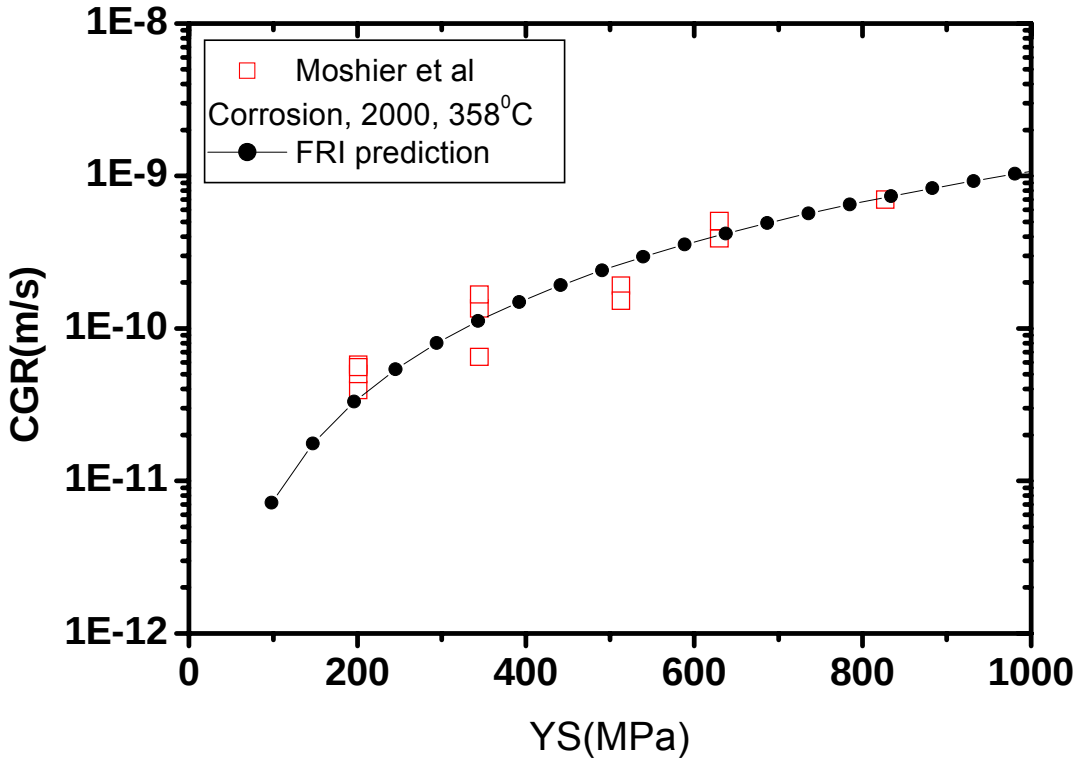

Parameters used in the model: m=0.70 and n=6

The effect of YS on CGR can be predicted by FRI generalized model

Numerical Analysis of experimental CGR(5)
-YS effect (2) YS & T effect

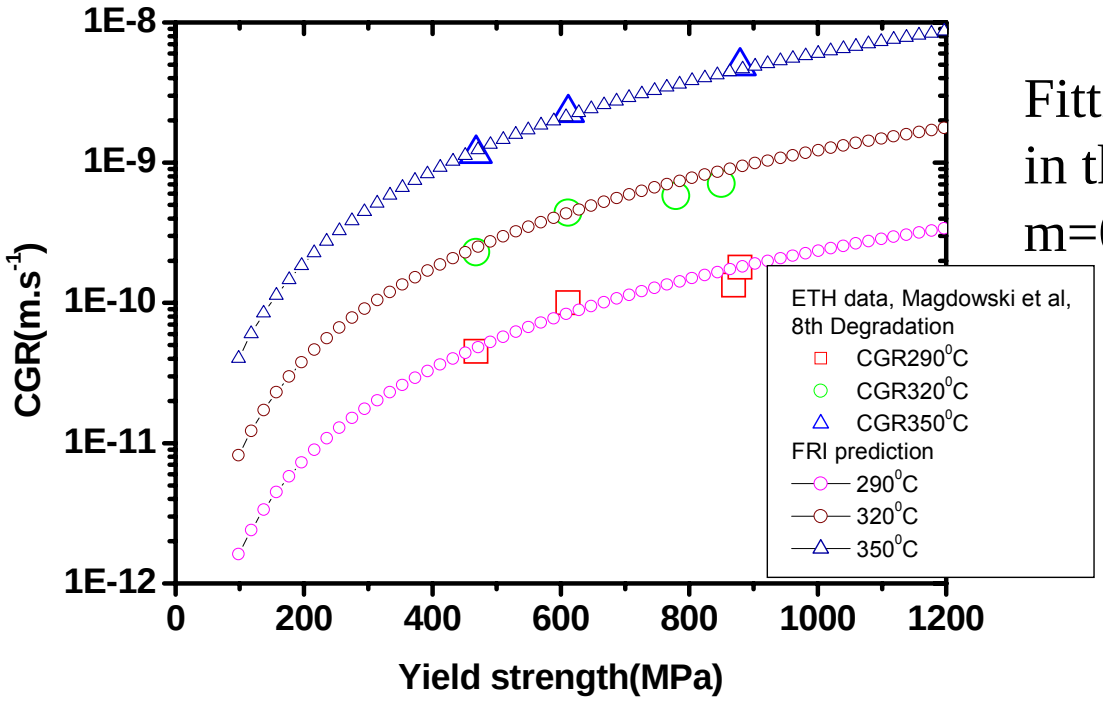

Fitting parameters in the model: m=0.70 and n=6

- Again, effect of YS can be formulated with the FRI generalized model
- CGRs at different can be calculated by only changing values of κ_a

Numerical Analysis of experimental CGR(7)
-dK/dt effect

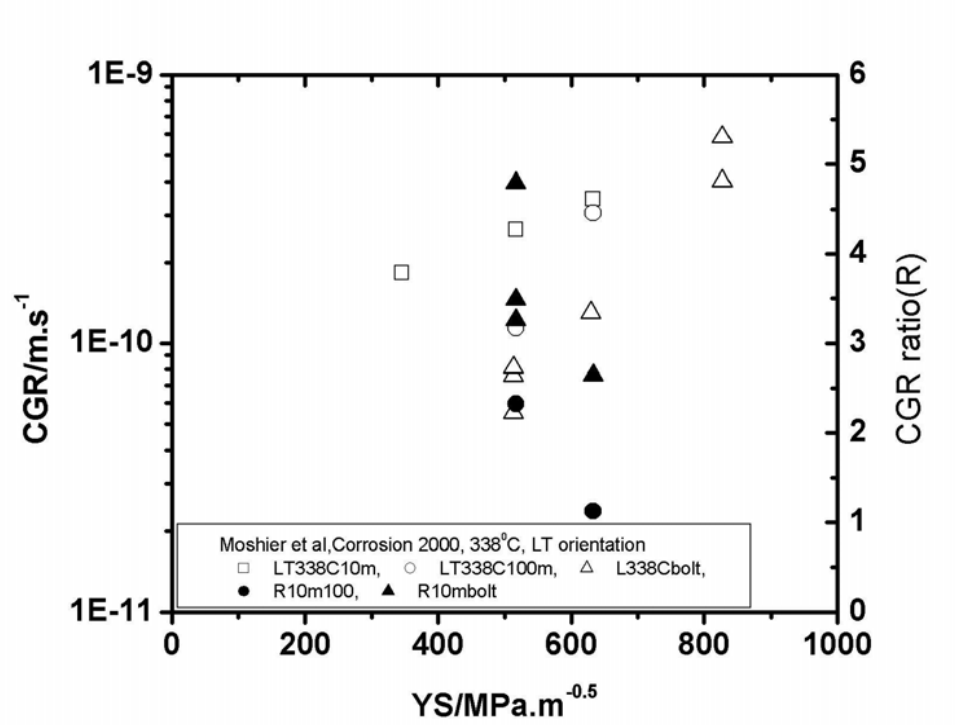

- CGR(bolt)<CGR(active load) in this data set, can be explained by the sensitivity analysis of dK/dt effect by FRI mode

Prediction of CGR in Weld Residual Stress Field(1)
-Core Shroud Cracking(1)Residual Stress distribution

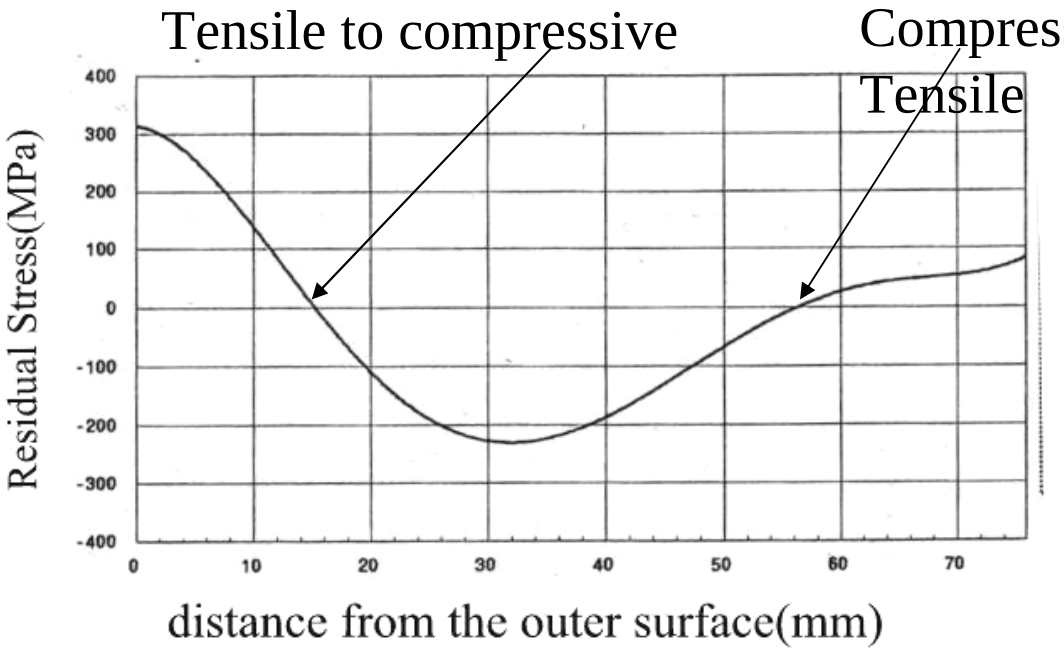

Distribution of the axial residual stress in H6a in a BWR core Shroud

- The residual stress changes from tensile to compressive or vise versa at certain depths of the weldment

Prediction of CGR in Weld Residual Stress Field(2)

-Core Shroud Cracking(2) K distribution

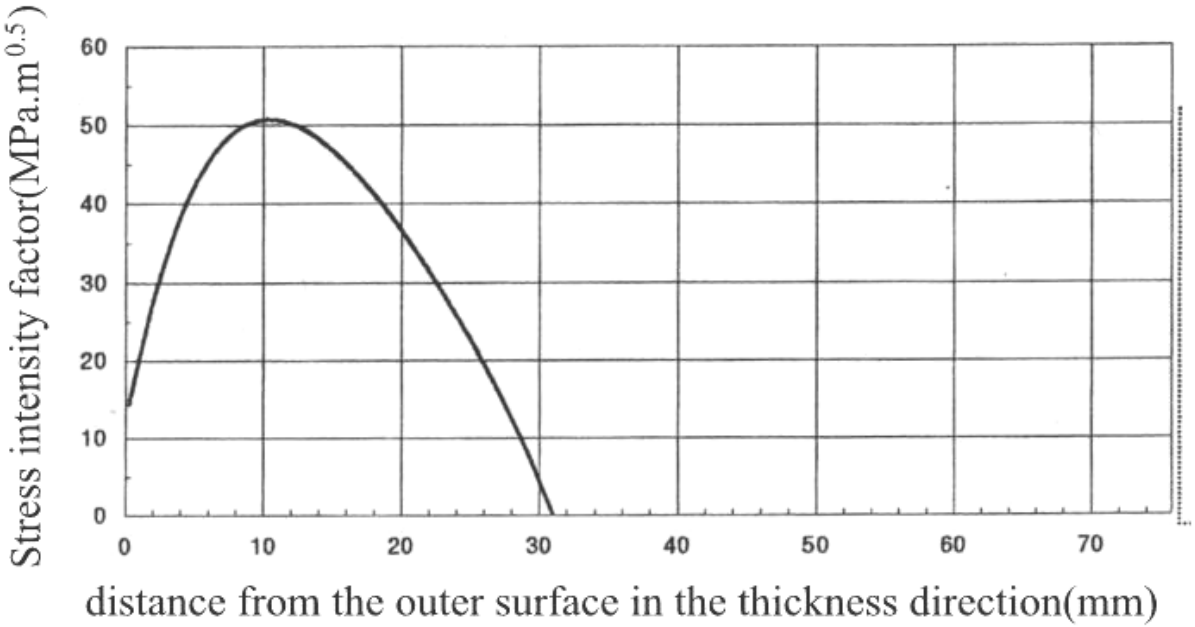

Estimated distribution of K in H6a in a BWR Core Shroud

- K increases to a maximum value and then decreases in the through-thickness direction of the weldment.

Prediction of CGR in Weld Residual Stress Field(4)

-Core Shroud Cracking (4) Crack depth prediction

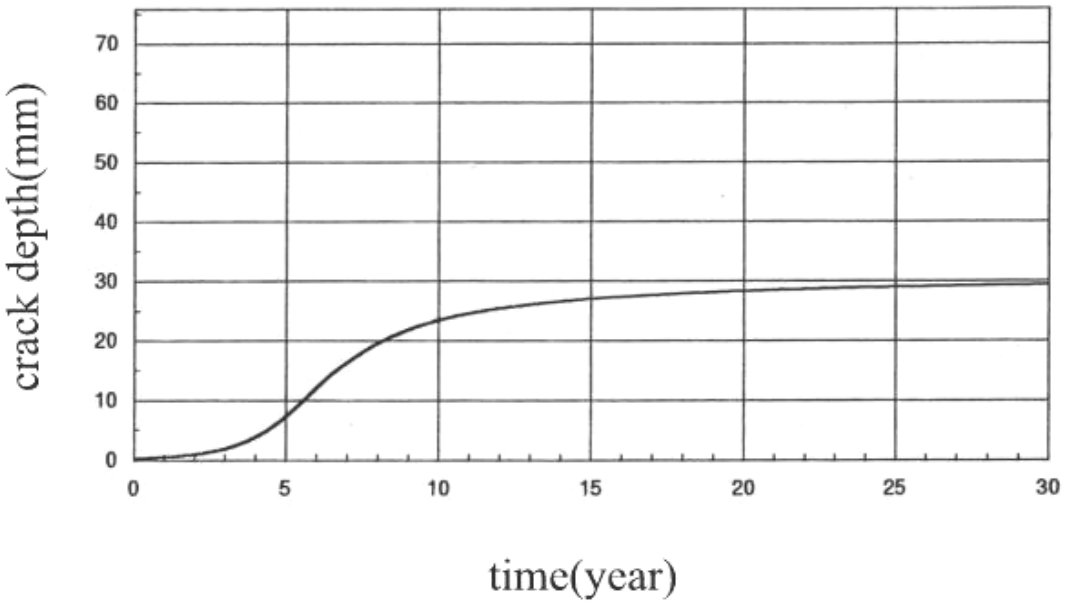

Relationship between the crack depth and time

- High crack growth rate is expected for the period of 4-9years
- After ca. 9 years, CGR decreases with time

Prediction of CGR in Weld Residual Stress Field (6)

-Details of a PWR VHP & an Inside-reactor Instrument tube

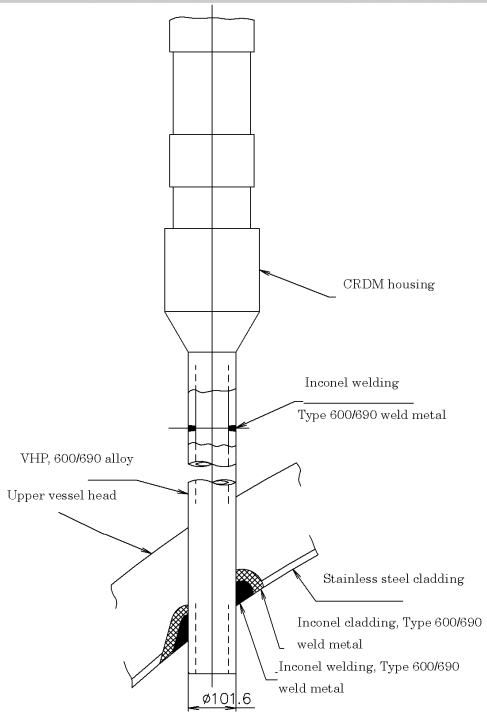

Structure of the VHP

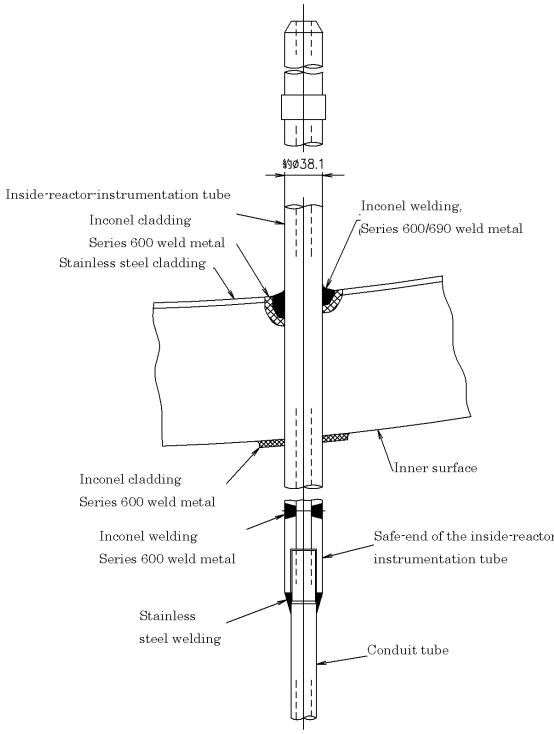

Structure of the inside-reactor-instrumentation tube

Illustration of a PWR VHP(left) and an inside-reactor instrument tube(right)

Prediction of CGR in Weld Residual Stress Field (7)

-PWR VHP(3) Crack growth behavior of PWR VHPs

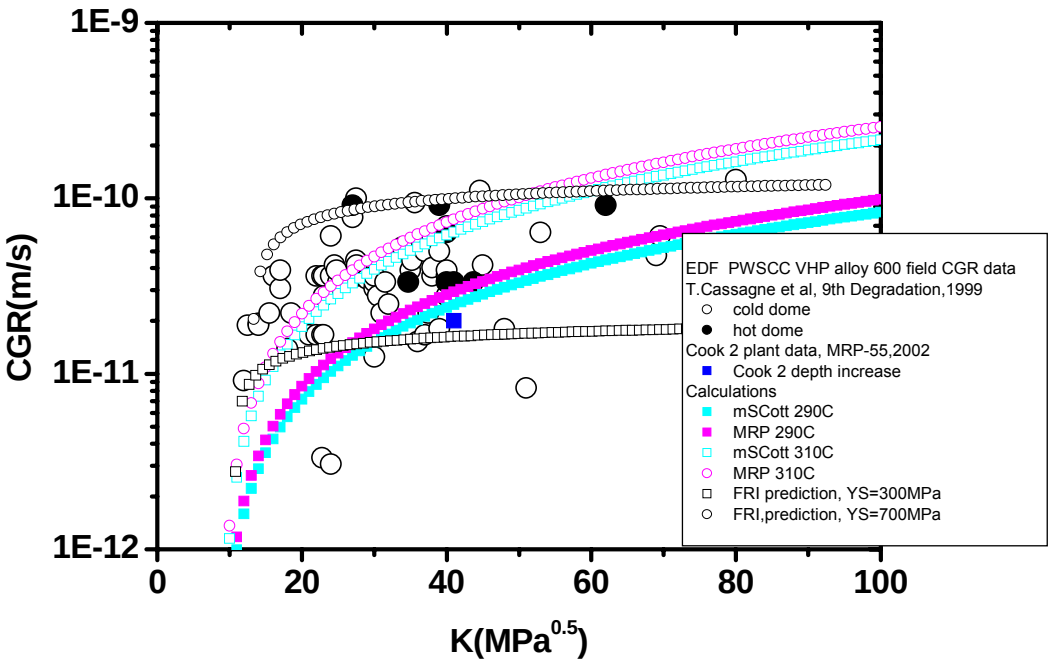

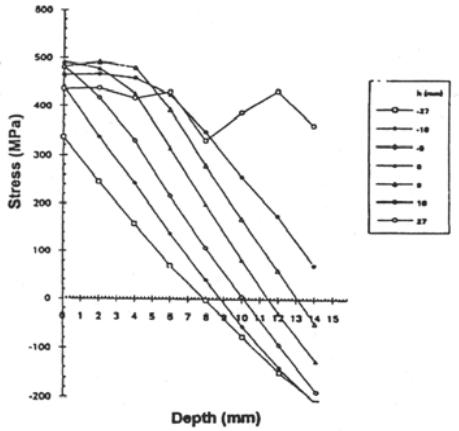

Weld Residual stress analysis of a PWR VHP (EDF data)

CGR prediction of Plant CGRs(from EDF & MRP) due to variations of YS may partly explain the scattered CGR data in the CGR-K diagram

Disposition of flaws (6)

- PWR environments (5) FRI generalized CGR model

-CGR is very sensitive to YS and this effect could be one of the factor of the scattered CGR in the data base.

-The shape of the CGR-K curve is important for developing the disposition line. **Variability in strain hardening ability may contribute to different types of CGR-K relationship**.

-Time variation of K(dK/dt) with crack growth can significantly affect the CGR of structural materials either in BWR or in PWR

Disposition of flaws (7)

- PWR environments (6) FRI generalized CGR model

-**This dK/dt variation** with crack growth can be more important in crack growth under the real plant condition where crack grows **in welded component**.

-**Loading condition and residual stress/stain analysis** is necessary for the crack growth rate formulation and for lifetime prediction of NPP components, especially for weldments.

FRI Generalized CGR Formulation

A generalized CGR formulation can be obtained by combining the general oxidation mechanism and the theoretical CTSR equation,

$$\frac{da}{dt} = \kappa_a \cdot \left\{ \beta \cdot \left(\frac{\sigma_y}{E}\right) \cdot \left(\frac{n}{n-1}\right) \cdot \left[2 \cdot \frac{\dot{K}}{K} + \frac{\dot{a}}{r}\right] \cdot \left\{ \ln\left[\lambda \cdot \frac{\left(\frac{K}{\sigma_y}\right)^2}{r}\right] \right\}^{\frac{1}{n-1}} \right\}^m$$

where κ_a is a crack tip oxidation rate constant, which is a function of local material chemistry, local environmental chemistry, transient interfacial rate kinetic law, and the stress/strain state.

Conclusions (1)

- FRI Model and CGR formulation can predict experimental and field CGR data with a good agreement, taking into account the effects of K, yield strength, strain hardening, temperature and dK/dt on CGRs

- Based upon the FRI model, CGR should have K dependence in the form of $\{\ln K\}^{m/n-1}$ in principle where m is oxidation kinetic parameter and n strain hardening coefficient.

741

Conclusions (2)

- The significance of K, yield strength and strain hardening coefficient on CGR was demonstrated by numerical analysis.

- Particularly, numerical calculation showed that CGR under negative dK/dt condition can be much lower than those obtained under constant K or positive dK/dt condition.

742

Conclusions (3)

- The effect of dK/dt on CGR can be critical in lifetime prediction of NPP welded components such as VHPs and BMIs in PWR

- Experimental verification of the crack growth behavior under the condition of positive and negative dK/dt would be highly recommended for better lifetime prediction of NPP welded components. Disposition line for flaw evaluation may take into account of these effects on CGR

743

Hydrogen Assisted Fracture Model Predictions for Alloy 600 PWSCC

Sensitivities of Crack Growth Rate to Applied Stress Intensity Factor, Temperature, Carbon Concentration, Yield Stress and Crack Growth Orientation and coolant-borne hydrogen

745

M. M. Hall, Jr., W. C. Moshier and D. J. Paraventi

Conference on Vessel Head Penetration
Inspection, Cracking, Repairs

Sponsored by the US NRC and ANL
September 29 – October 2, 2003
Gaithersburg, MD, USA

OUTLINE

- SCC Variables
- HAF Model Concepts and Equation Development
- Experimental
- SCC Data
- Comparisons to Model

Variables Potentially Affecting NiCrFe Alloy PWSCC CGR*

- Alloy and Corrosion Film Composition and Structure
  - chromium and carbon concentrations, carbide morphology and distribution, grain size (Alloy X-750)
  - cold work (yield stress, strain hardening, strain rate sensitivity)
  - crack growth orientation for cold worked material
- Crack Tip Environment
  - $[H^+] = 10^{-pH}$
  - hydrogen over potential $\eta = E - E_r$ where E_r is the reversible H_2 / H^+ potential determined by coolant-borne hydrogen, DH_2
  - temperature
  - other ionic species
- Stress Intensity Factor

* Variables in red are currently included in HAF Model

747

Hydrogen Assisted Fracture (HAF) Model*
- Concepts -

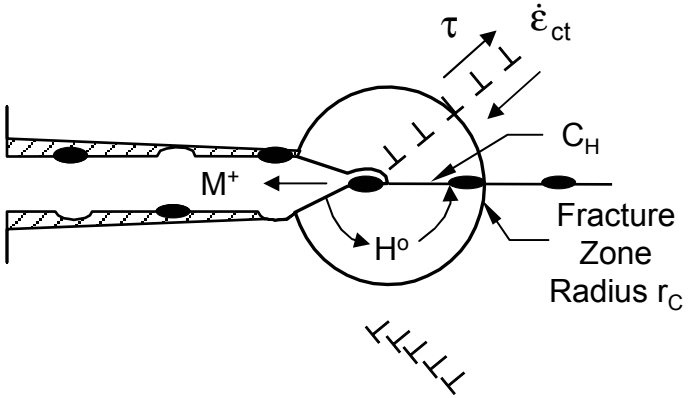

$$\dot{a} = \frac{r_c\,\dot{\varepsilon}_{ct}}{\varepsilon_f} = \frac{r_c\,\dot{\varepsilon}_{ct}}{\varepsilon_{fo}}\left(\frac{c_{gb}}{c_o}\right)^{\frac{1}{2}}$$

- Hydrogen evolves at crack tip due to cathodic reduction of water
- Hydrogen absorbs, permeates, diffusively segregates and is trapped at grain boundaries
- Cracks advance due to hydrogen-assisted-creep fracture of hydrogen embrittled grain boundaries
- Rate limiting step potentially may be any of the hydrogen and crack tip strain rate processes

*M. M. Hall, Jr. and D. M. Symons, "Hydrogen Assisted Creep Fracture Model for Low Potential Stress Corrosion Cracking of Ni-Cr-Fe Alloys", Chemistry and Electrochemistry of Stress Corrosion Cracking: A Symposium Honoring the Contributions of R. W. Staehle, R. H. Jones, Ed. TMS, 2001, 447 - 466.

HAF Model Equations

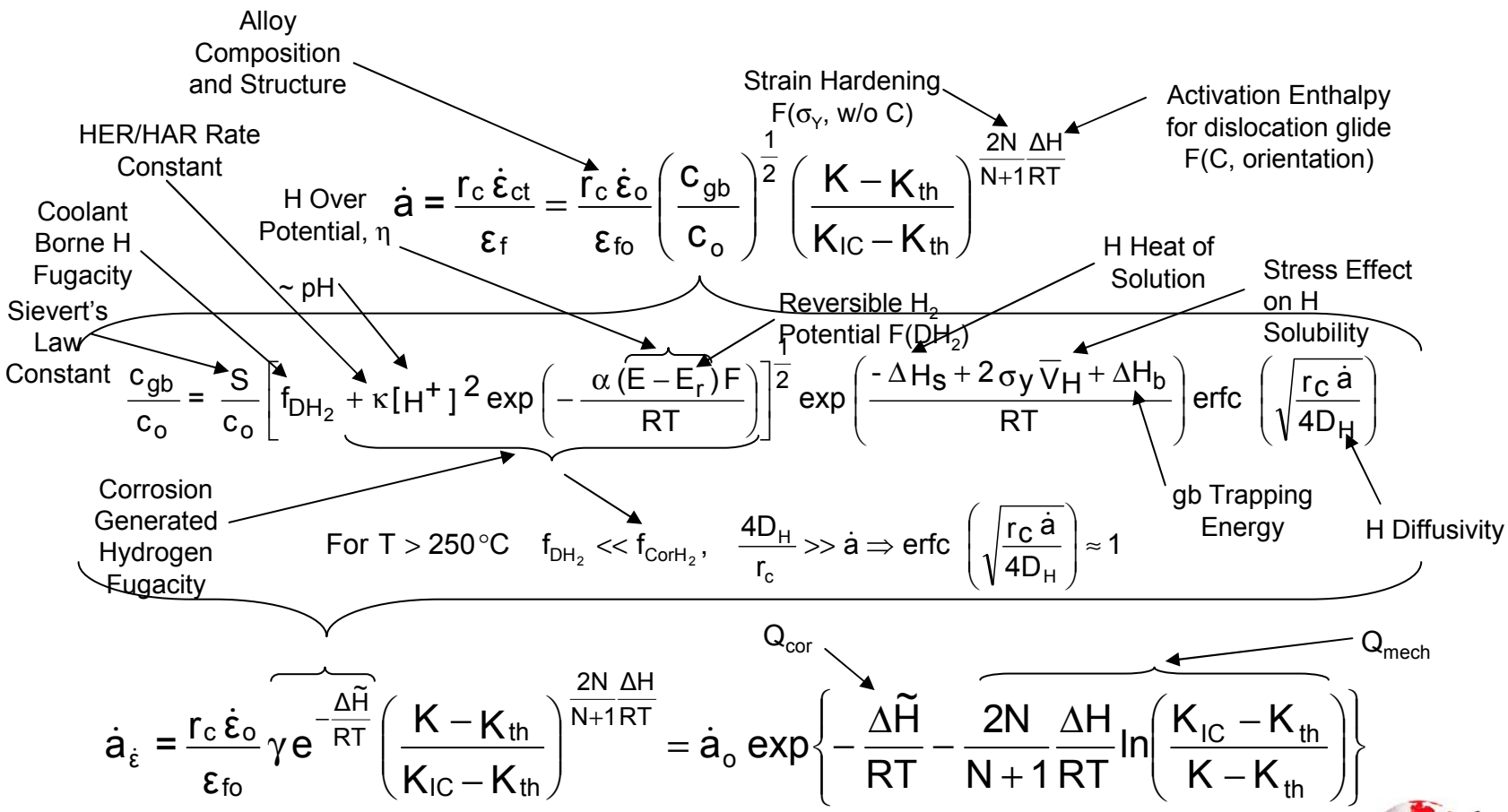

$$\dot{a} = \frac{r_c \dot{\varepsilon}_{ct}}{\varepsilon_f} = \frac{r_c \dot{\varepsilon}_o}{\varepsilon_{fo}} \left(\frac{c_{gb}}{c_o} \right)^{\frac{1}{2}} \left(\frac{K - K_{th}}{K_{IC} - K_{th}} \right)^{\frac{2N}{N+1}\frac{\Delta H}{RT}}$$

$$\frac{c_{gb}}{c_o} = \frac{S}{c_o} \left[f_{DH_2} + \kappa [H^+]^2 \exp\left(-\frac{\alpha (E - E_r) F}{RT} \right) \right]^{\frac{1}{2}} \exp\left(\frac{-\Delta H_s + 2\sigma_y \bar{V}_H + \Delta H_b}{RT} \right) \operatorname{erfc}\left(\sqrt{\frac{r_c \dot{a}}{4 D_H}} \right)$$

For $T > 250\,^{\circ}C$ $\quad f_{DH_2} << f_{CorH_2}$, $\quad \frac{4D_H}{r_c} >> \dot{a} \Rightarrow \operatorname{erfc}\left(\sqrt{\frac{r_c \dot{a}}{4 D_H}} \right) \approx 1$

$$\dot{a}_{\dot{\varepsilon}} = \frac{r_c \dot{\varepsilon}_o}{\varepsilon_{fo}} \gamma e^{-\frac{\Delta \tilde{H}}{RT}} \left(\frac{K - K_{th}}{K_{IC} - K_{th}} \right)^{\frac{2N}{N+1}\frac{\Delta H}{RT}} = \dot{a}_o \exp\left\{ -\frac{\Delta \tilde{H}}{RT} - \frac{2N}{N+1}\frac{\Delta H}{RT} \ln\left(\frac{K_{IC} - K_{th}}{K - K_{th}} \right) \right\}$$

Modeling Dynamic Strain Aging Effects* on Alloy 600 Crack Growth Rate

Mobile ⊥ x o Interaction Energy

Drag-free Activation Energy

$$\dot{a}_{\varepsilon} = \dot{a}_o e^{-\frac{\Delta\tilde{H}}{RT}} \left(\frac{K - K_{th}}{K_{IC} - K_{th}} \right)^{\frac{2N}{N+1}\frac{\Delta H}{RT}}$$

Activation Enthalpy for dislocation glide F(C, orientation)

$$\Delta H = \Delta H^o(C) + U(\bar{n}) = \Delta H^o \left\{ 1 - \alpha \exp\left[-\beta \left(\ln\left(\frac{T}{T_o} \right) \right)^2 \right] \right\} \cong \Delta H^o \left| 1 - \frac{T}{T_o} \right|$$

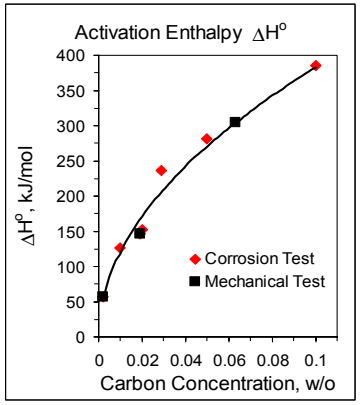

Interaction Strength Factor $F(\sigma_Y, C) \cong 1$ for σ_Y = 826 MPa and 0.063 w/o C

Temperature @ Which Dislocation Wait Time = Solute Diffusion Time

$$T_o \approx \frac{U(\bar{n})/R}{\ln(1/C)}$$

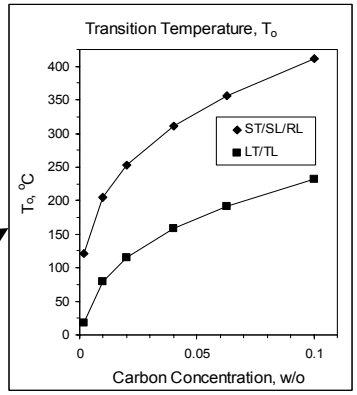

*M. M. Hall and D. M. Symons, "Constitutive Deformation Model for Analysis of Stress Corrosion Crack Tip Strain-Rates in Ni-Cr-Fe Alloy 600", International Conference on Hydrogen Effects on Material Behavior and Corrosion Deformation Interactions, R. Jones, N. Moody, A. Thompson, T. Magnin, R. Ricker and G. Was, Ed., TMS, 2002

Linearized HAF Model Equations

Better Suited for Data Analysis

$$\ln \dot{a} = A_o - A_1 \frac{T_o}{T} \pm A_2 \frac{T_o}{T} \ln K_R \mp A_2 \ln K_R; \quad \pm \Rightarrow \text{orientation}$$

$$A_o = \ln \dot{a}_o \quad A_1 = \frac{\Delta \tilde{H}}{RT_o} \quad A_2 = \frac{2N}{N+1} \frac{\Delta H^o}{RT_o} \quad K_R = \frac{K - K_{th}}{K_{IC} - K_{th}}$$

751

Experimental
Bettis Data

- Alloy 600 plate given HTA – 1100°C/3600s/FC
- 0.063 w/o Carbon
- Extensive gb decoration with carbides
- 0% – 28% CW (YS 187 MPa – 826 MPa)
- 50 cc/kg dissolved hydrogen
- Conventional FM specimens and test methods
- LT and ST crack growth orientations

SCC Test Conditions

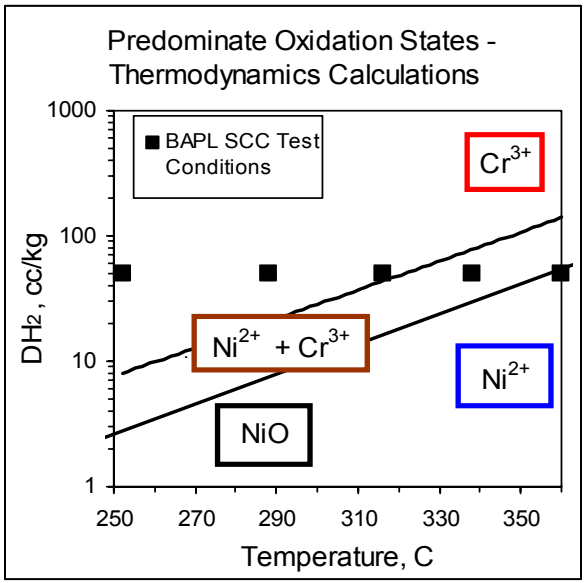

- SCC tests conducted at 252° C to 360° C at or on the Ni side of the Ni - NiO phase field boundary

Crack Growth Orientations for Plate and Bar

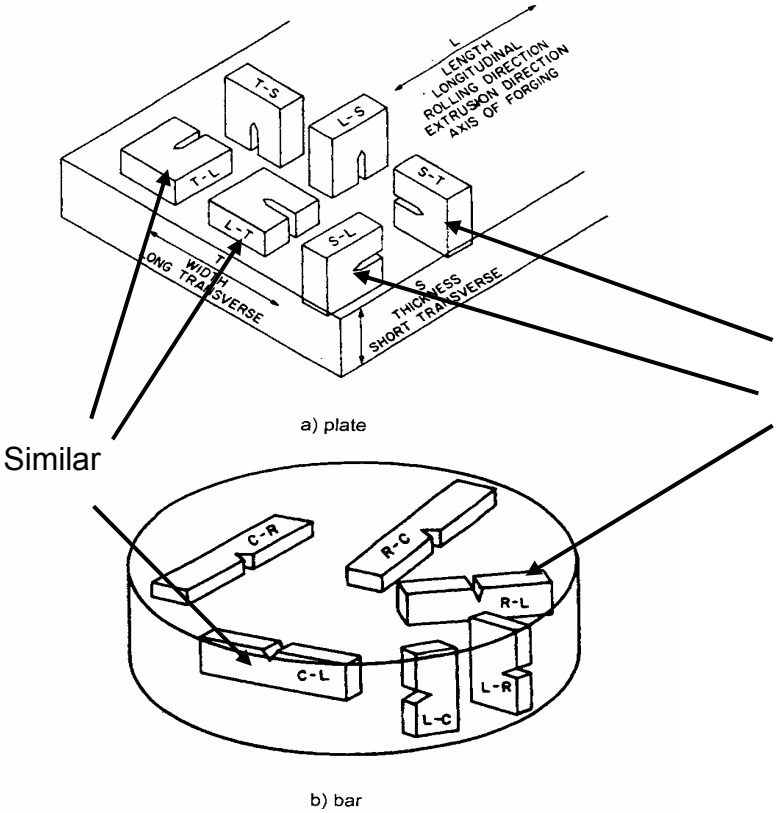

LT / TL / CL Similar Orientations

ST / SL / RL Similar Orientations

ST / LT orientation CGR data – single heat of Alloy 600

RL / CL orientation CGR data – different heats of Alloy 600

Stress Intensity Factor Exponent m
Depends on Temperature and RT Yield Stress

Data Due to Moshier and Paraventi

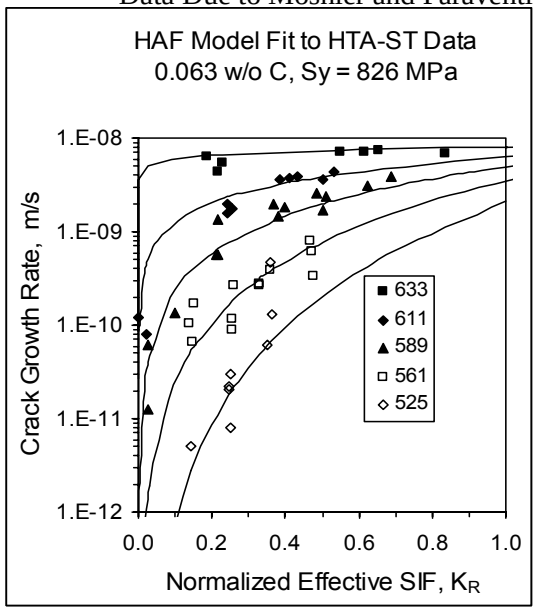

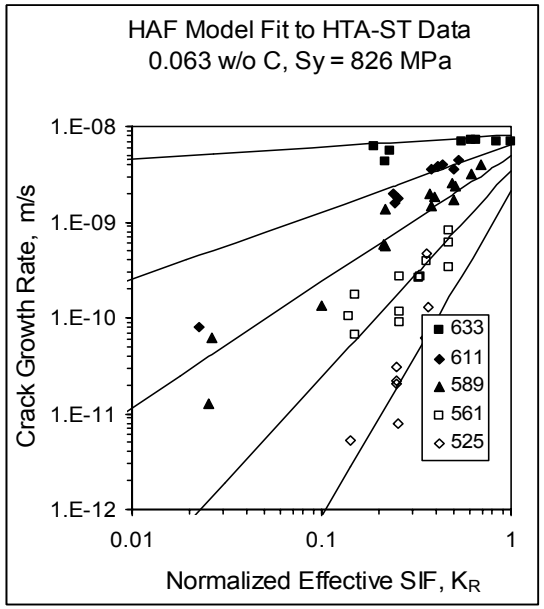

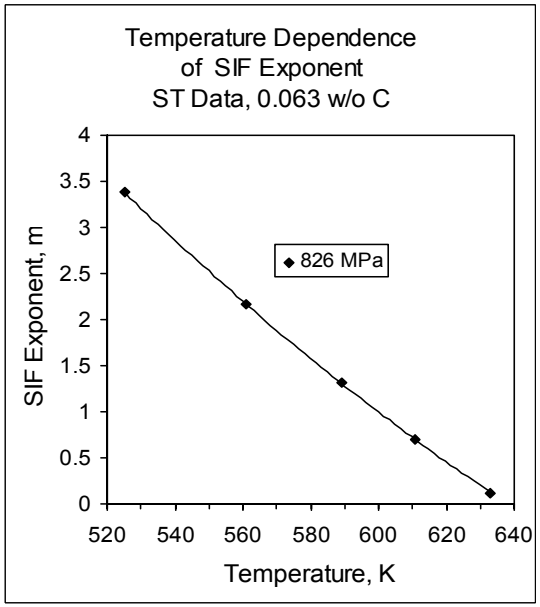

$$K_R \equiv \frac{K - K_{th}}{K_c - K_{th}} \qquad m \equiv \left.\frac{\partial \ln \dot{a}}{\partial \ln K_R}\right|_{T,\eta} \cong \frac{2N}{N+1}\frac{\Delta H^o}{RT}\left(1 - \frac{T}{T_o}\right); \quad T < T_o$$

ST orientation m value decreases with increasing temperature

LT Crack Growth Orientation Unlike ST

Data Due to Moshier and

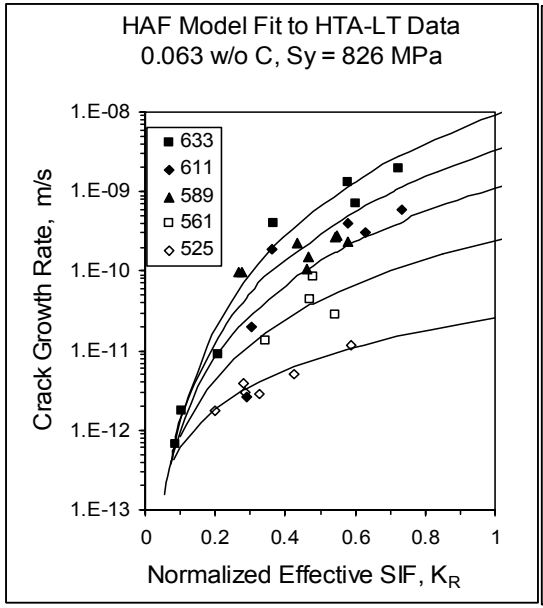

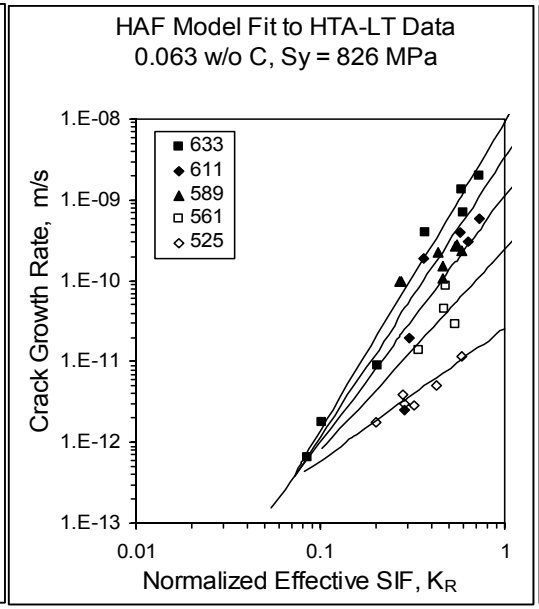

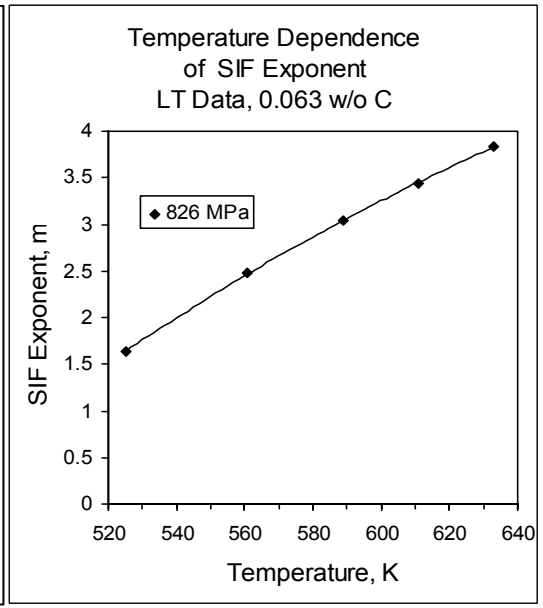

$$K_R \equiv \frac{K - K_{th}}{K_c - K_{th}}$$

$$m \equiv \left.\frac{\partial \ln \dot{a}}{\partial \ln K_R}\right|_{T,\eta} = \frac{2N}{N+1}\frac{\Delta H^o}{RT}\left(\frac{T}{T_o} - 1\right); \quad T > T_o$$

LT orientation m *increases* with increasing temperature

RL Crack Growth Orientation Similar to ST

Data due to Speidel and Magdowski

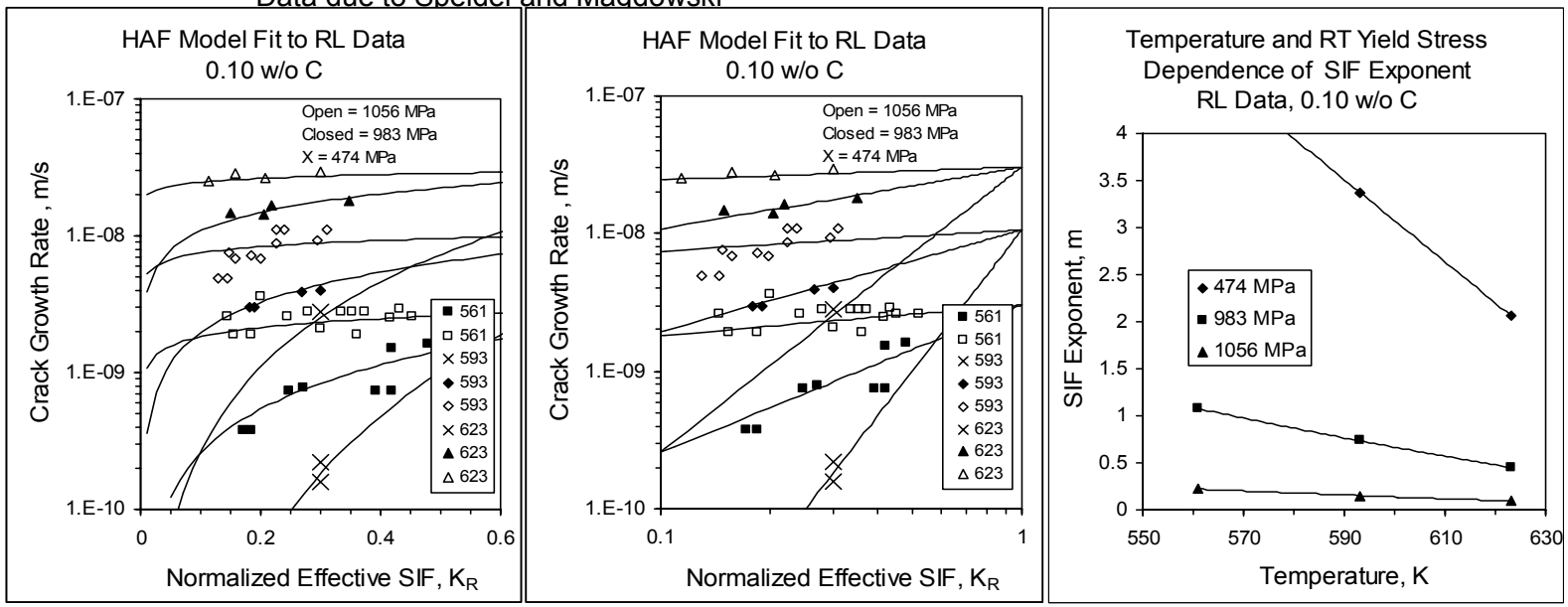

$$K_R \equiv \frac{K - K_{th}}{K_c - K_{th}}$$

$$m \equiv \left.\frac{\partial \ln \dot{a}}{\partial \ln K_R}\right|_{T,\eta} \cong \frac{2N}{N+1}\frac{\Delta H^o}{RT}\left(1 - \frac{T}{T_o}\right); \quad T < T_o$$

RL orientation m decreases with increasing temperature and RT yield stress (pre-strain or CW)

CL Crack Growth Orientation Similar to LT

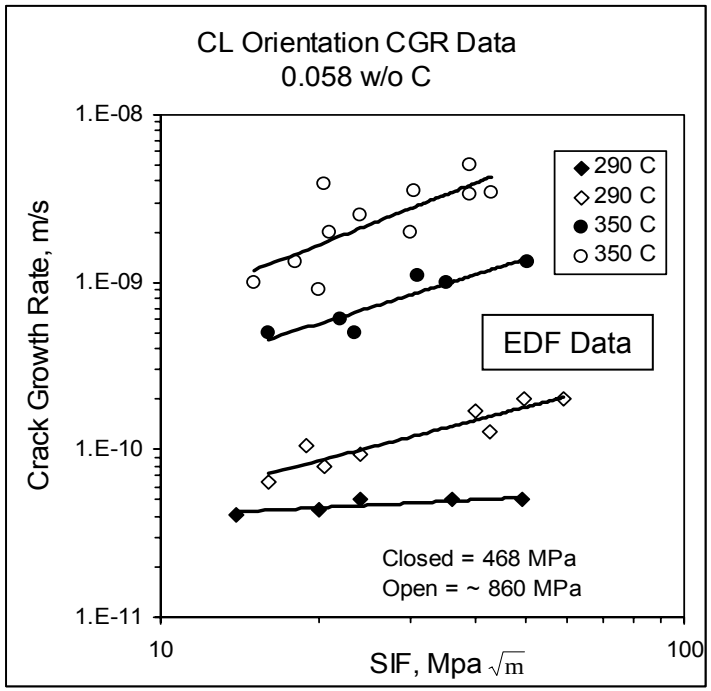

CL orientation m increases with increasing temperature and RT yield stress (pre-strain or CW)

ST Orientation Apparent Activation Energy Q is Decreasing Function of Stress Intensity Factor

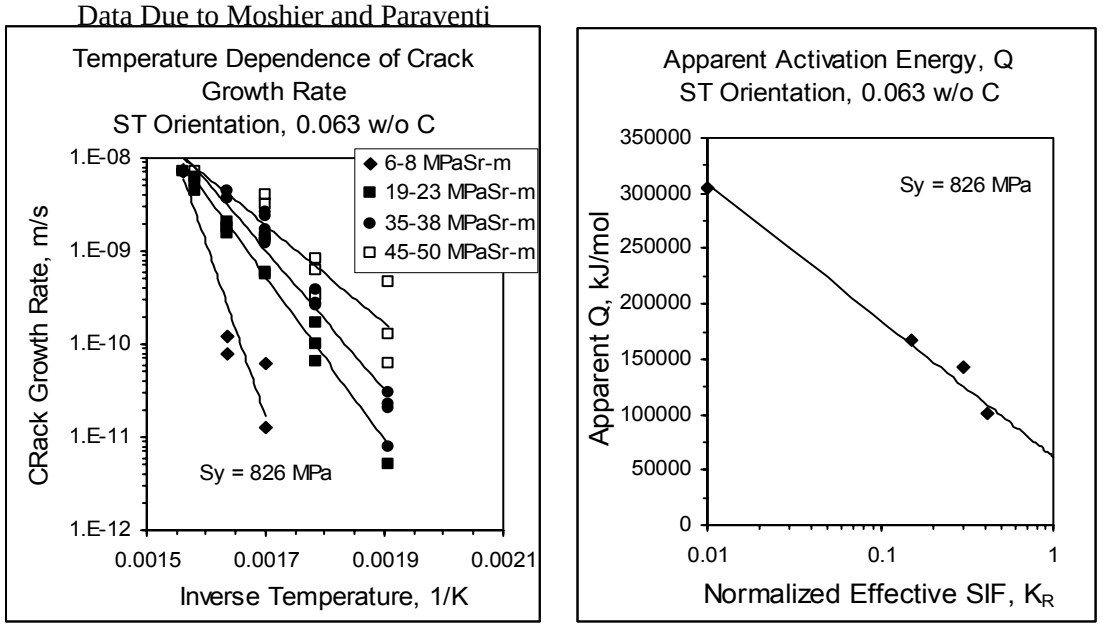

$$Q \equiv -R\frac{\partial \ln \dot{a}}{\partial (1/T)}\bigg|_{K_R,\eta} = \Delta\tilde{H} - \frac{2N}{N+1}\Delta H^{o}\ln\left(\frac{K - K_{th}}{K_c - K_{th}}\right)$$

Apparent activation energy Q decreases with increasing Applied Stress Intensity Factor, K

RL Orientation Apparent Activation Energy Q is Decreasing Function of RT Yield Stress

Data due to Speidel and Magdowski

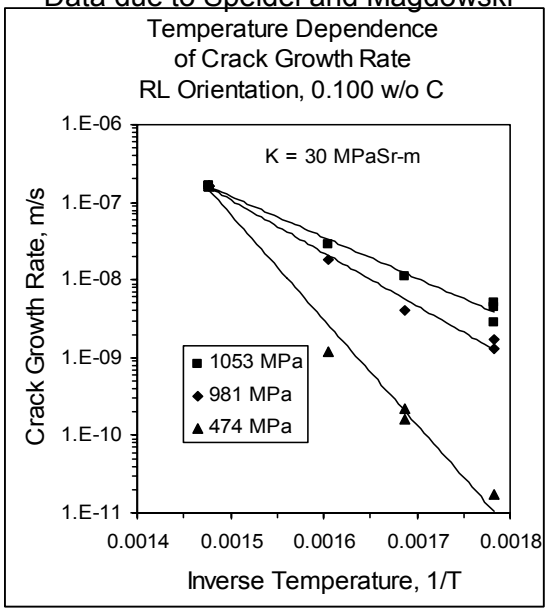

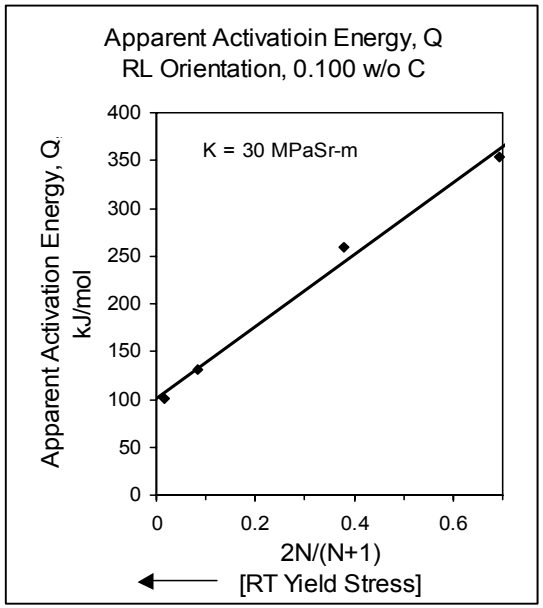

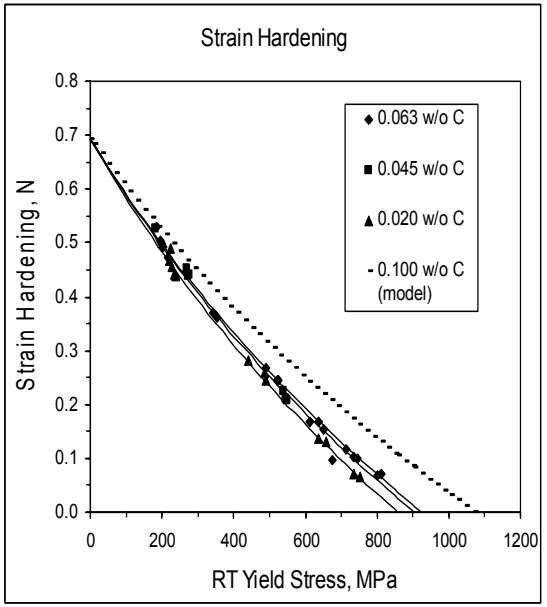

$$Q \equiv -R\left.\frac{\partial \ln \dot{a}}{\partial (1/T)}\right|_{K_R,\eta} = \Delta\tilde{H} - \frac{2N}{N+1}\Delta H^{o} \ln\left(\frac{K - K_{th}}{K_c - K_{th}}\right)$$

$$N = \ln\left(\frac{2}{1 - \sigma_y / \sigma_s}\right)$$

Apparent activation energy Q decreases with increasing RT yield stress (decreasing strain hardening)

LT Orientation Apparent Activation Energy Q Also is Decreasing Function of RT Yield Stress

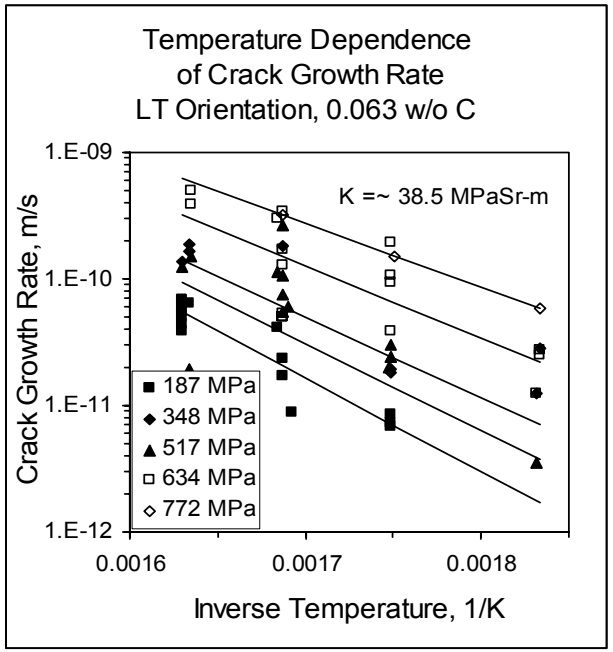

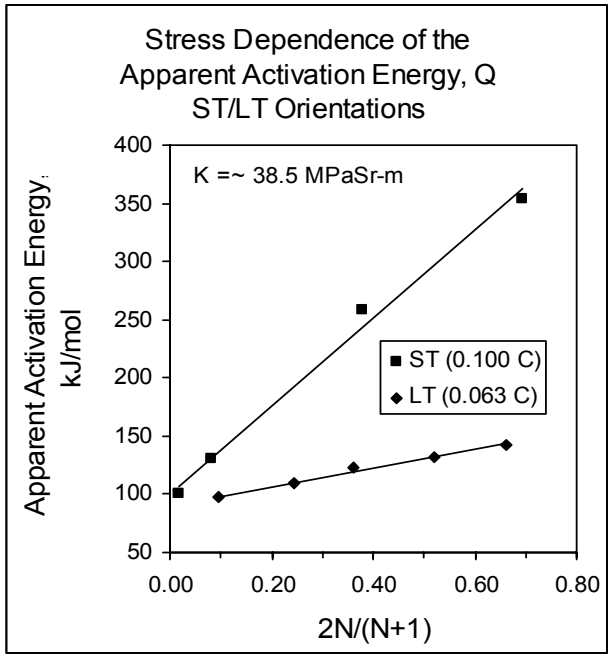

$$Q \equiv -R\left.\frac{\partial \ln \dot{a}}{\partial (1/T)}\right|_{K_R,\eta} = \Delta\tilde{H} - \frac{2N}{N+1}\Delta H^{o} \ln\left(\frac{K - K_{th}}{K_c - K_{th}}\right)$$

LT orientation Q decreases with increasing RT YS (decreasing N) but at a lesser rate than for ST orientation

Reality Checks

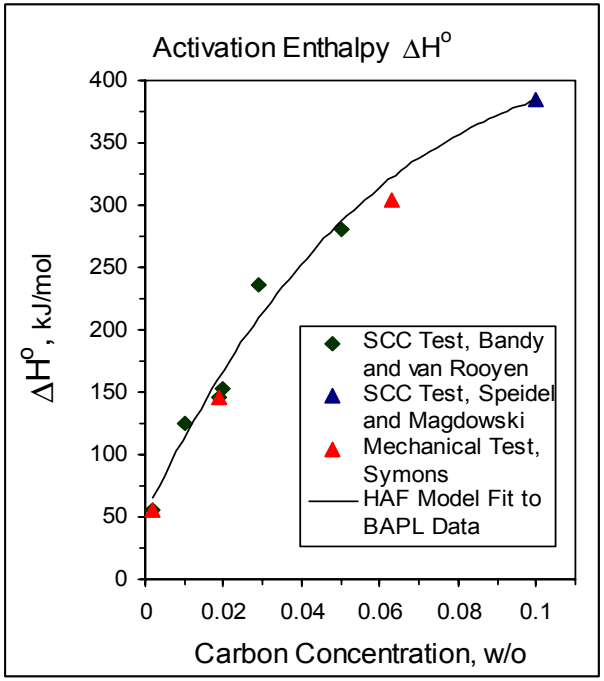

- Model fitting parameters must fall within physical bounds
- Parameter values, e.g, ΔH^o, obtained by fitting models to SCC data should be consistent with data obtained by separate effects tests

Conclusions

- A600 PWSCC is a complex function of the SCC variables
- To capture this complexity requires comprehensive data sets obtained on single heats of Alloy 600
- Physical models help in sorting out complex behaviors and provide higher confidence disposition curves

763

QUESTIONS?

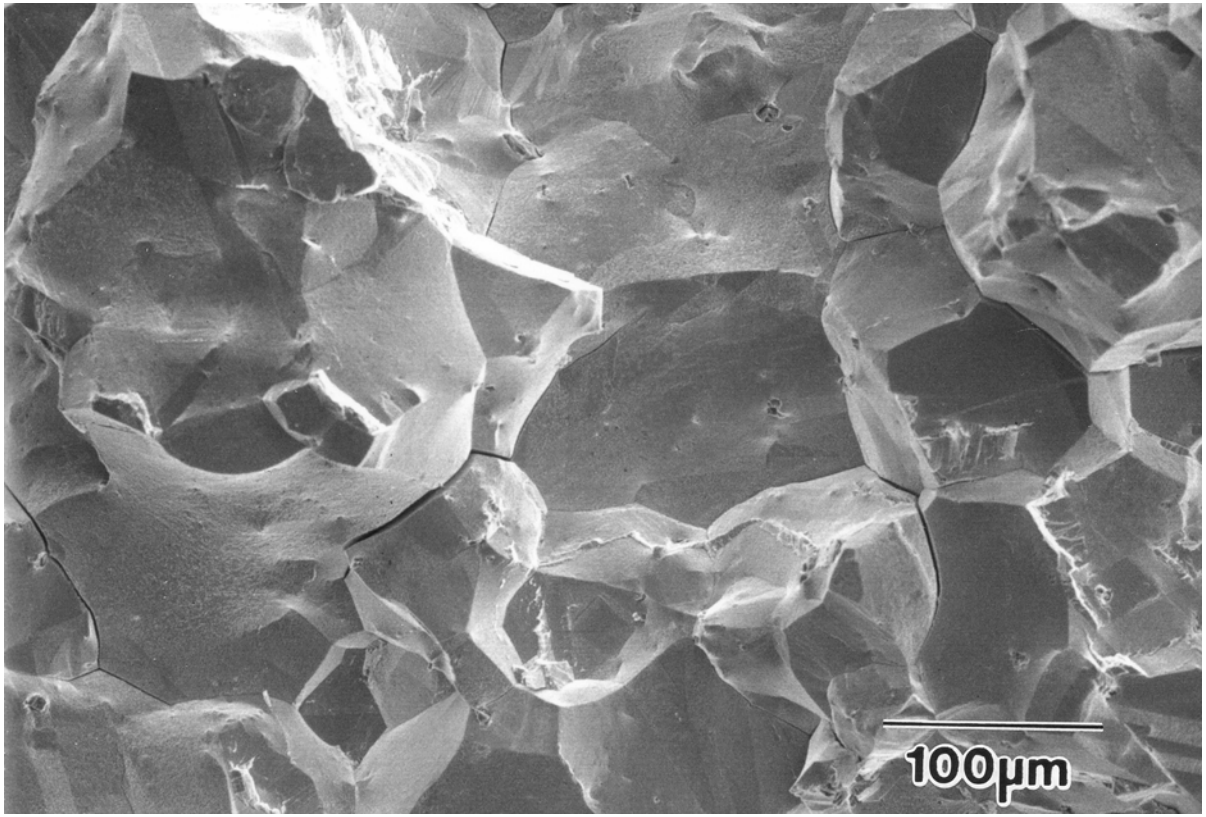

Orientation Dependence of CGR Established by Transition Temperature T_o

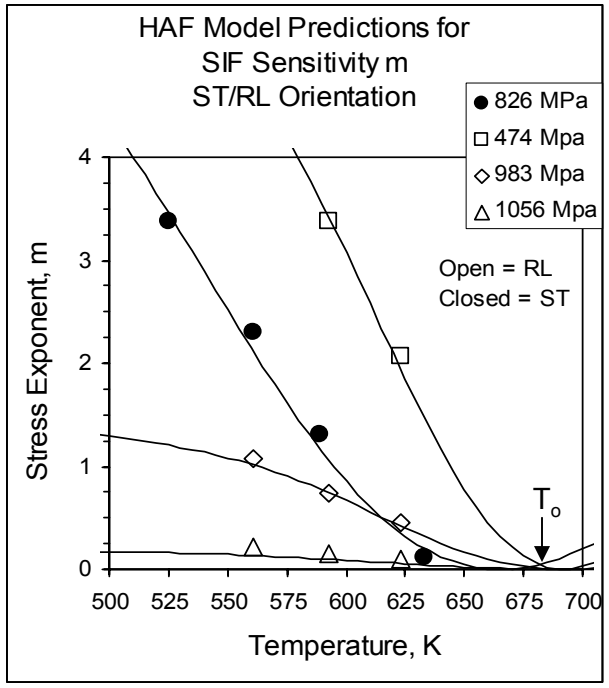

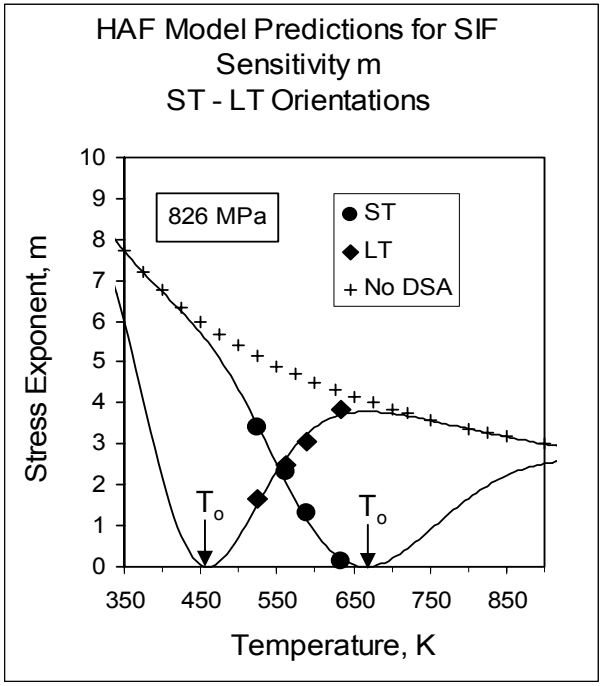

$$m = \frac{2N}{N+1}\frac{\Delta H^o(C) + U(\bar{n})}{RT} = \frac{2N}{N+1}\frac{\Delta H^o}{RT}\left\{1 - \alpha \exp\left[-\beta\left(\ln\left(\frac{T}{T_o}\right)\right)^2\right]\right\}$$

Modeling Coolant Borne Hydrogen Effects on Alloy 600 Crack Growth Rate

DH_2 establishes E_{rev} (H_2 / H^+)

Large DH_2 results in no Ni corrosion and no H_2(cor)

Anode : $Ni + H2O = NiO + 2H^+ + 2e^-$

Cathode : $H^+ + e^- = H^o$; $2H^o \Leftrightarrow H_2(cor)$

$$f_{H_2(cor)} = \kappa[H^+]^2 \exp\left(-\frac{\alpha \eta F}{RT}\right) \propto i_c$$

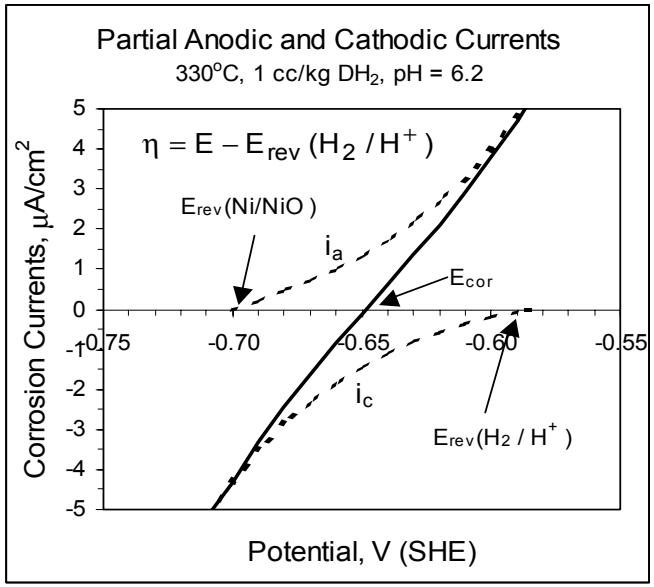

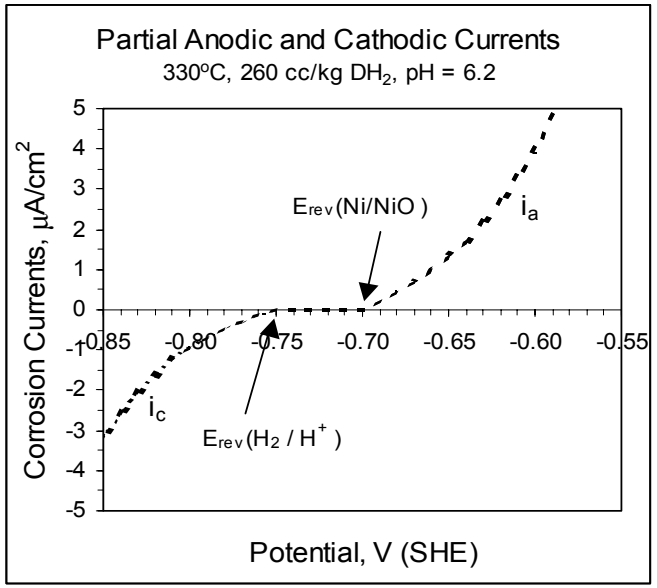

SCC Growth Rate of Nickel Based Alloy 132 Weld Metal

September 29- October 2, 2003
US NRC Conference on
Vessel Penetration Inspection, Cracking and Repairs

T.Yonezawa*, K.Tsutsumi, H.Kanasaki*, K.Yoshimoto*, Y.Nomura*, S.Asada****

***Takasago R & D Center, Mitsubishi Heavy Industries, LTD.**
****Kobe Shipyard & Machinery Works,**
Mitsubishi Heavy Industries, LTD.

MITSUBISHI HEAVY INDUSTRIES, LTD.
TAKASAGO R&D CENTER

CONTENTS

1. INTRODUCTION
2. EXPERIMENTAL PROCEDURES
3. RESULTS
4. DISCUSSIONS
5. SUMMARY

MITSUBISHI HEAVY INDUSTRIES, LTD.
TAKASAGO R&D CENTER

CONTENTS

769

INTRODUCTION

MITSUBISHI HEAVY INDUSTRIES, LTD. TAKASAGO R&D CENTER

- **In Japan, maintenance guide rule as ASME Sec.XI for allowable SCC flaw size is not established except austenitic stainless steels for BWRs.**
- **In order to complete data base for the maintenance guide rule for allowable SCC flaw size, the Japanese national project on SCCGR measurement test program on the Alloy 600 and its weld metals of Ni based alloys for PWRs and BWRs has been started from April 2000.**
- **Before starting this project, MHI has checked the propriety and applicability of periodic unloading method for PWSCC GR measurement test.**

INTRODUCTION (Contd.)

MITSUBISHI HEAVY INDUSTRIES, LTD. TAKASAGO R&D CENTER

- **In western PWR plants, Alloy 182 is used for SMAW to Alloy 600. In Japanese PWR plants, Alloy 132 was used for different welding method (:alternating current as welding electric current) as the SMAW and consideration of resistance of hot cracking.**

INTRODUCTION (Contd.)

MITSUBISHI HEAVY INDUSTRIES, LTD. TAKASAGO R&D CENTER

Japanese Status on Welding Materials for RV Nozzles

Table Difference of Welding Materials between Japan & Western Countries

	Japanese PWRs	Western PWRs
Welding Materials	Alloys 132 and 82	Alloys 182 and 82
Yield Strength of Base Metal (MPa)	200～350	300～500
Surface Finishing	Polished by Buff	Grinded

Alloy 132 : 70Ni-15Cr-9Fe-1Mn-2.5Nb

182 : 67Ni-15Cr-8Fe-7Mn-1.8Nb-0.5Ti

82 : 71Ni-20Cr-2Fe-3Mn-2.5Nb-0.5Ti

PWSCC CGR is affected by the material properties

INTRODUCTION (Contd.)

MITSUBISHI HEAVY INDUSTRIES, LTD. TAKASAGO R&D CENTER

The effect of Cr content on PWSCC susceptibility of Alloy 600.

- The PWSCC susceptibility of Alloy 600 decreases with increasing of Cr content.
- Alloy 132, 182 ; 15Cr
  82 ; 20Cr

⬇

- The stress corrosion cracking resistance of Alloy 82 may be higher than that of Alloy 132 and 182.

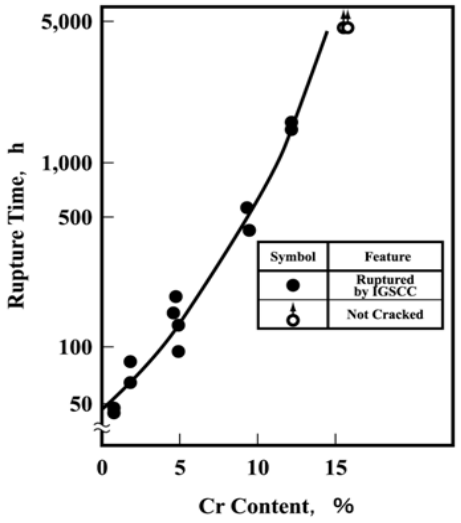

Fig 6. Effect of Cr content on the stress corrosion cracking resistance of solution annealed Ni base-Cr-Fe alloys in 360℃ high temperature water using by constant load stress corrosion cracking test (applied stress is 2.4 × 0.2% Proof stress)

INTRODUCTION (Contd.)

MITSUBISHI HEAVY INDUSTRIES, LTD. TAKASAGO R&D CENTER

The effect of Nb content on PWSCC susceptibility of Alloy 600.

- Nb and Ti addition increase PWSCC susceptibility of Alloy600, due to suppressing of IG carbides precipitation.

- Alloy 132 ; 2.5Nb
  182 ; 1.8Nb-0.5Ti
  82 ; 2.5Nb-0.5Ti

- The susceptibility of Alloy 132 may be same as that of Alloy 182.

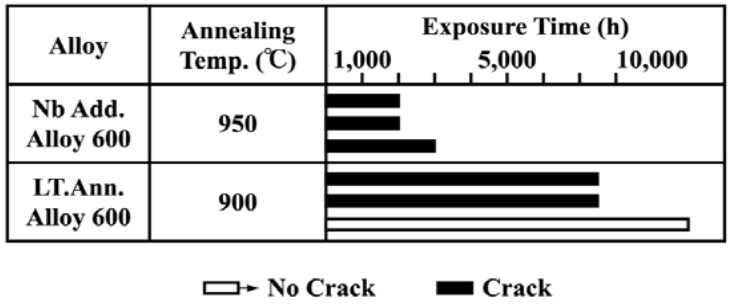

Fig7. Effect of Nb addition on the sress corrosion cracking resistance of annealed Alloy 600 in 360℃ high temperature water, using by prestrained U bent specimen.

INTRODUCTION (Contd.)

MITSUBISHI HEAVY INDUSTRIES, LTD. TAKASAGO R&D CENTER

- **In western PWR plants, Alloy 182 is used for SMAW to Alloy 600. In Japanese PWR plants, Alloy 132 was used for different welding method (:alternating current as welding electric current) as the SMAW and consideration of resistance of hot cracking.**

- **In this study, we tested the PWSCC growth rate of Alloys 132 and 82 welded.**

OBJECTIVES

MITSUBISHI HEAVY INDUSTRIES, LTD. TAKASAGO R&D CENTER

- **To compared the PWSCC growth rates of Alloys 132 and 82 with literature data on Alloy 182.**

- **To recommend PWSCC GR measurement test techniques. (The propriety and applicability of periodic unloading method for PWSCC GR measurement test.)**

MITSUBISHI HEAVY INDUSTRIES, LTD.
TAKASAGO R&D CENTER

CONTENTS

1. INTRODUCTION
2. EXPERIMENTAL PROCEDURES
3. RESULTS
4. DISCUSSIONS
5. SUMMARY

EXPERIMENTAL PROCEDURES

MITSUBISHI HEAVY INDUSTRIES, LTD. TAKASAGO R&D CENTER

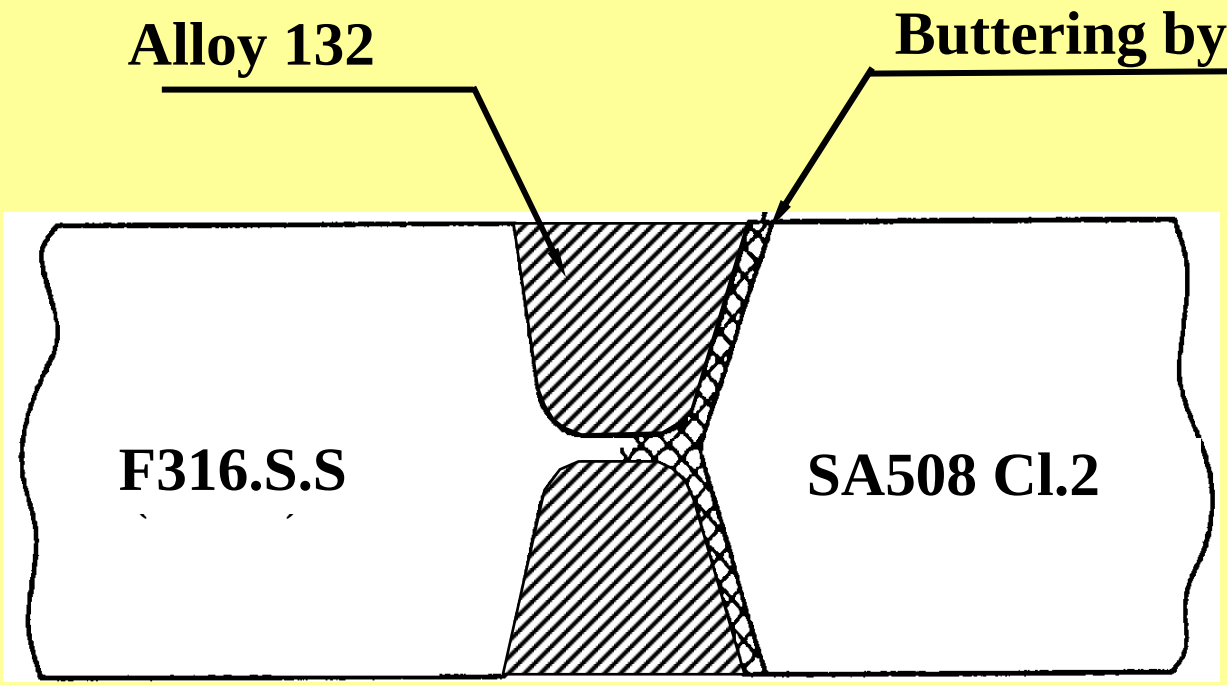

Figure Welding joint configuration of dissimilar metal arc welding model by Alloy 132

EXPERIMENTAL PROCEDURES

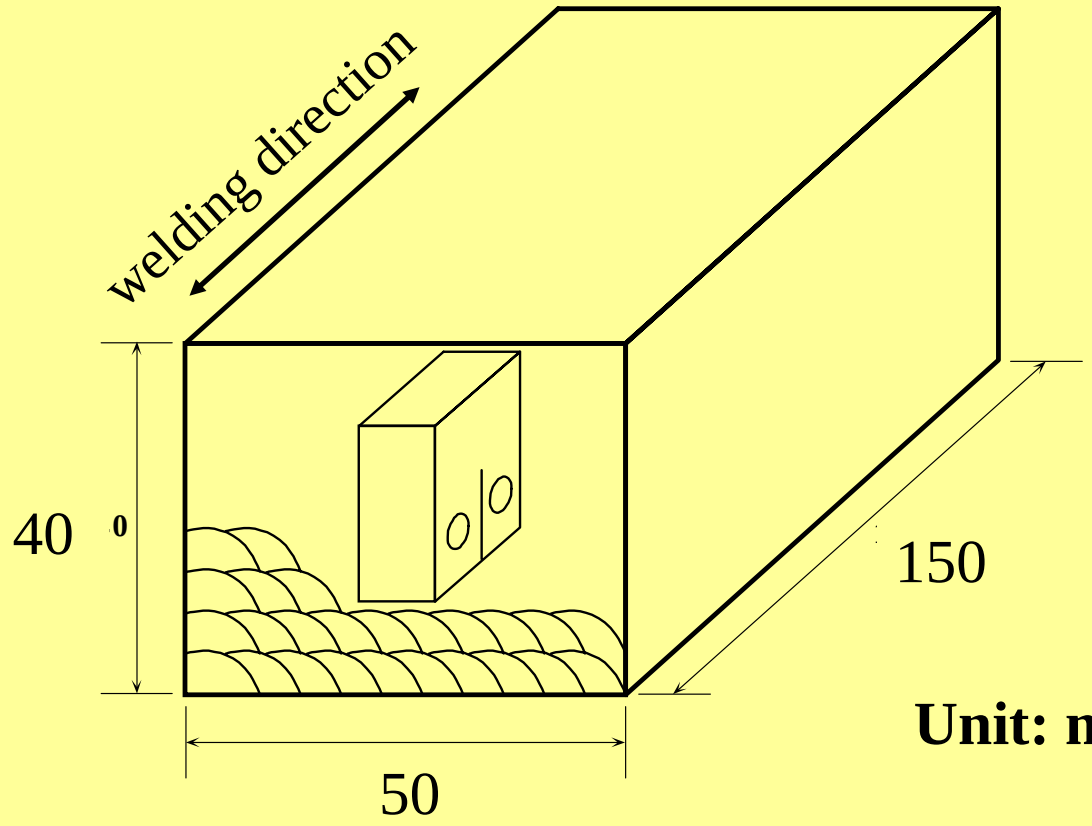

Figure Machining orientation of CT specimens from deposited metal model of TIG welding by Alloy 82

EXPERIMENTAL PROCEDURES

MITSUBISHI HEAVY INDUSTRIES, LTD.
TAKASAGO R&D CENTER

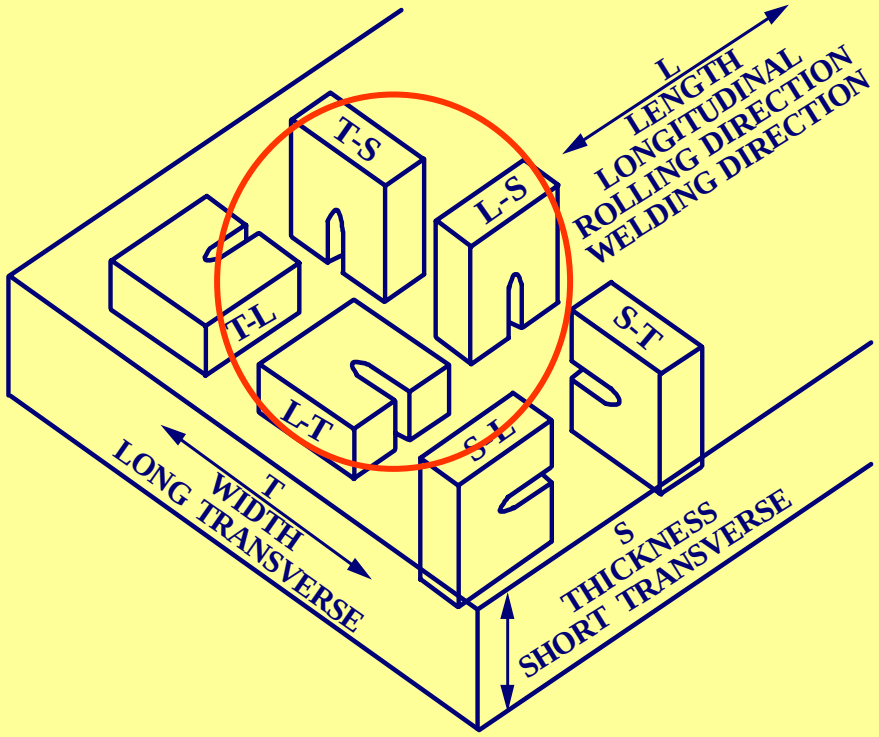

Test Specimens

- 1/2T CT
- Specimen Orientation
  TS, LS, LT
- The pre-crack length about 1mm
- K_I values
  20, 35, 60 MPa $\sqrt{m}$

Figure Terminology used for orientation of cracks in the test specimens with respect to the weld

EXPERIMENTAL PROCEDURES

MITSUBISHI HEAVY INDUSTRIES, LTD. TAKASAGO R&D CENTER

Testing Environment

Temperature	**; 325°C**
H_3BO_3	**; 1800 ppm as Boron**
LiOH	**; 3.5 ppm as Lithium**
DH_2	**; 30cc/kg STP H_2O**
DO_2	**; <5ppb**
Autoclave	**; refreshed type**

781

EXPERIMENTAL PROCEDURES

MITSUBISHI HEAVY INDUSTRIES, LTD. TAKASAGO R&D CENTER

The periodic unloading conditions for Alloys 132 and 82, to evaluate the effect of the periodic unloading condition on the CGRs of weld metals.

(1) Trapezoidal wave 1 : R = 0.7, holding time : 360 seconds (0.1 hours)
(2) Trapezoidal wave 2 : R = 0.7, holding time : 1,080 seconds (0.3 hours)
(3) Trapezoidal wave 3 : R = 0.7, holding time : 9,000 seconds (2.5 hours)
(4) Constant loading

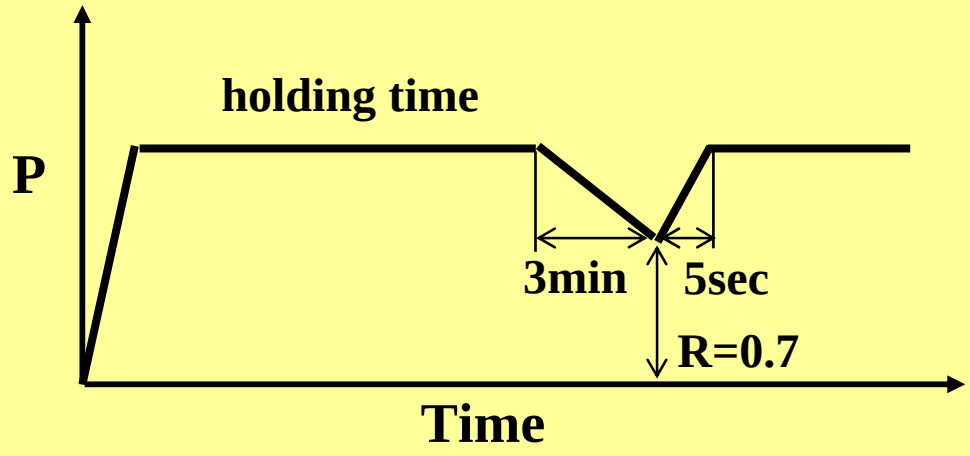

Figure Trapezoidal Wave form

EXPERIMENTAL PROCEDURES

MITSUBISHI HEAVY INDUSTRIES, LTD. TAKASAGO R&D CENTER

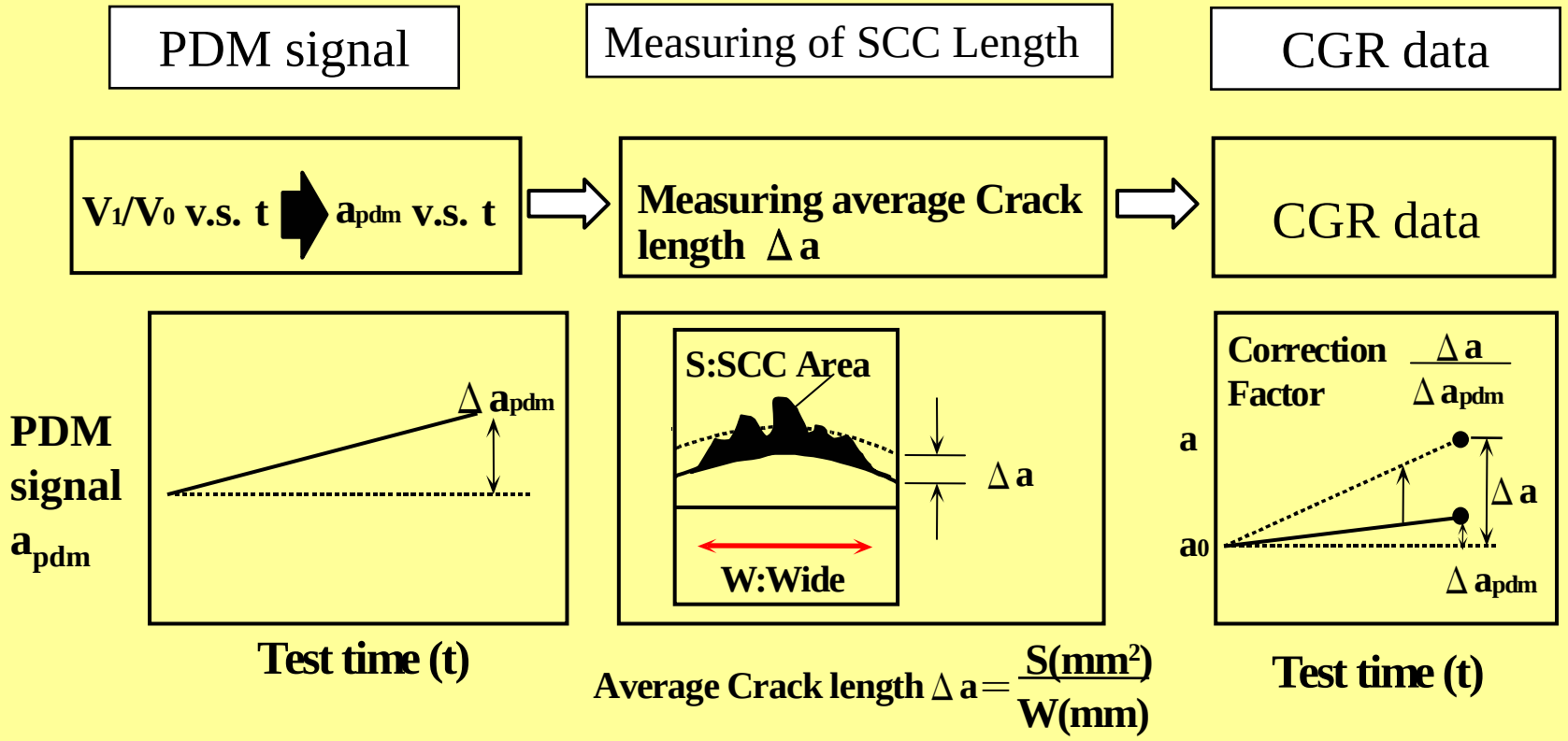

Figure CGR evaluation method

MITSUBISHI HEAVY INDUSTRIES, LTD.
TAKASAGO R&D CENTER

CONTENTS

RESULTS (Effect of K value)

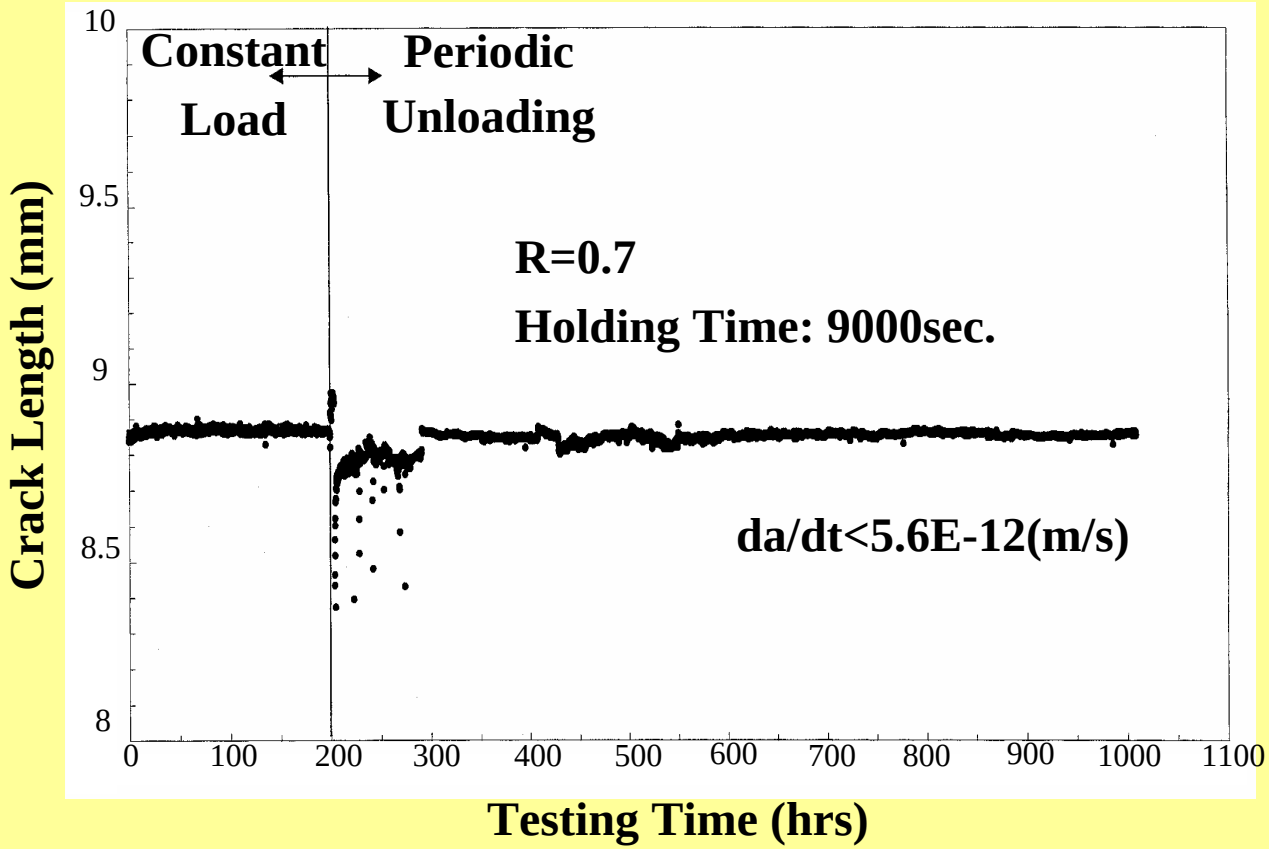

Alloy 132,

K_I values :20 MPa√m,

TS orientation

Figure CGR on-line monitoring results

RESULTS (Effect of K value)

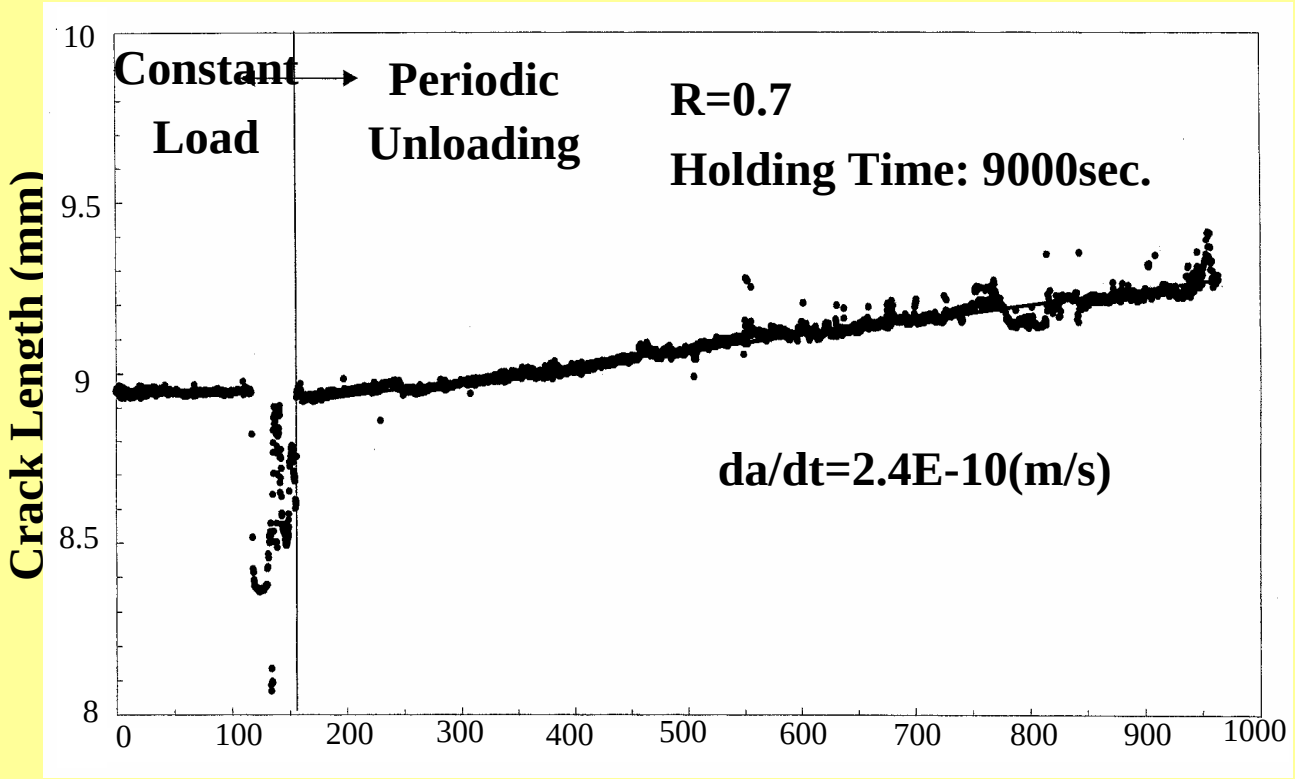

Alloy 132,

K_I values :35MPa√m,

TS orientation

Figure CGR on-line monitoring results

RESULTS (Fractography)

MITSUBISHI HEAVY INDUSTRIES, LTD. TAKASAGO R&D CENTER

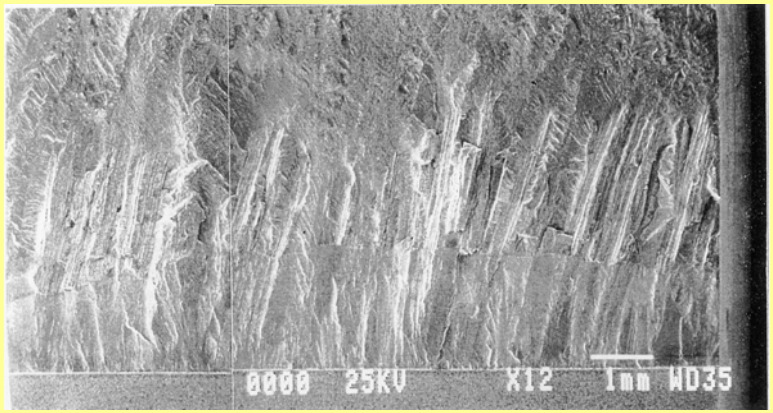

SEM

- The crack front of these inter-dendritic PWSCC was not uniform and the area of no ID PWSCC initiation zone was also observed at the fatigue pre-crack tip.
- The crack propagation path was inter-dentrite and parallel direction for dendrite.

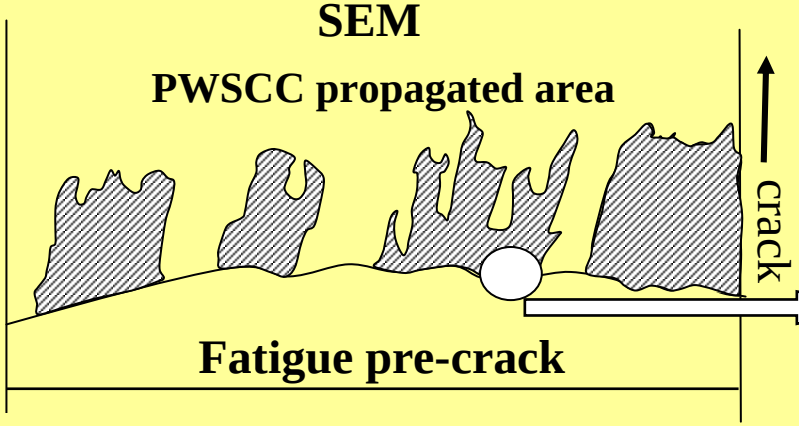

Inter-dentrite

Figure Fractography of TS specimen after SCC test

RESULTS (Fractography)

MITSUBISHI HEAVY INDUSTRIES, LTD. TAKASAGO R&D CENTER

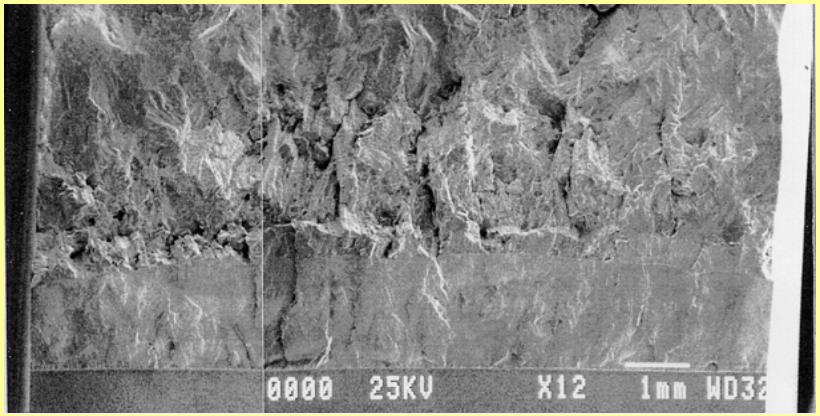

- The crack front of these inter-dendritic PWSCC was complicated and not uniform.
- The crack propagation path was inter-dentrite and perpendicular direction for dendrite.

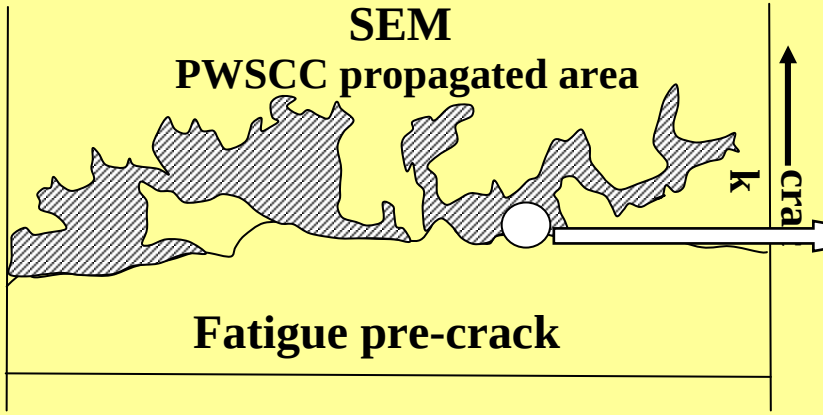

Inter-dentrite

Figure Fractography of LT specimen after SCC test

RESULTS (CGR of Alloys 132, 82 and 182)

MITSUBISHI HEAVY INDUSTRIES, LTD. TAKASAGO R&D CENTER

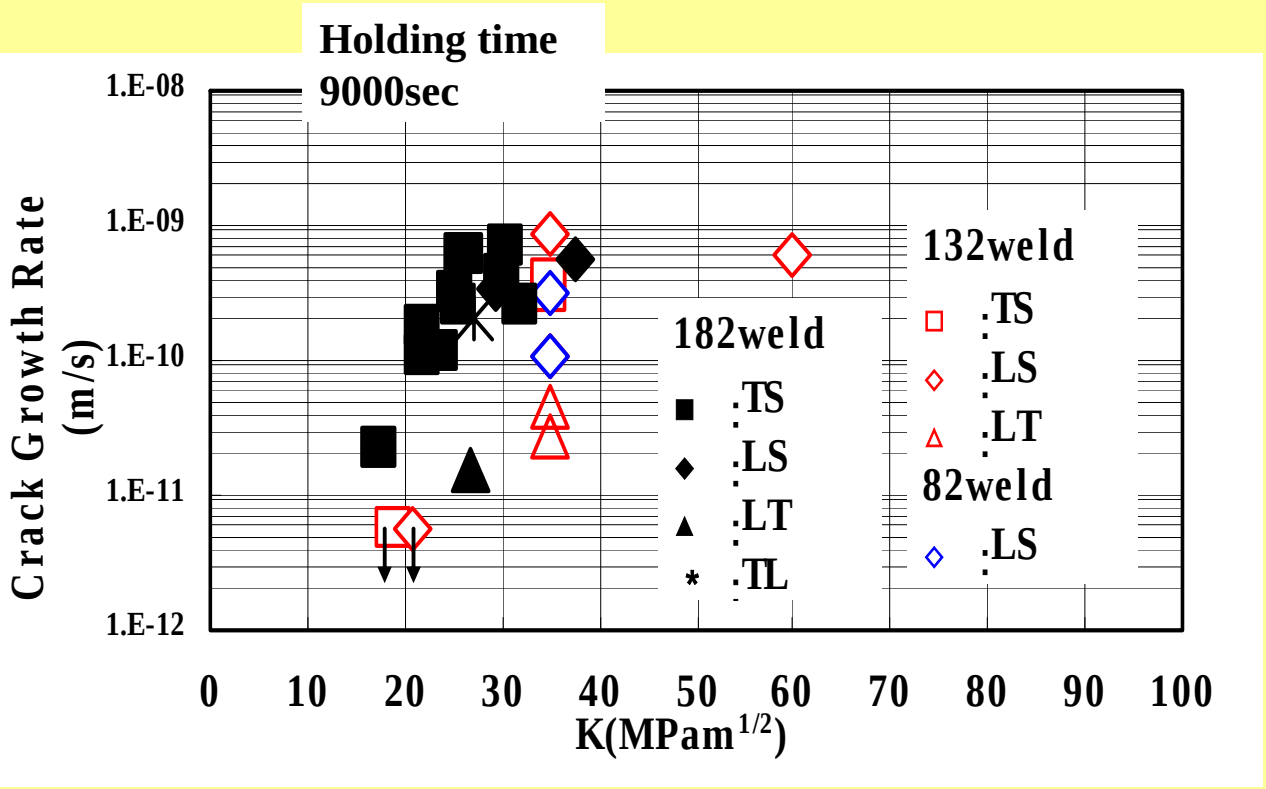

PWSCC CGRs

1) Alloy 132 ≥ Alloy 82
2) LS, TS > LT
3) LS nearly equal to TS

Figure Comparison between CGR of Alloys 132, 82 and 182 weld metal

RESULTS (CGR of Alloys 132,82 and 182)

MITSUBISHI HEAVY INDUSTRIES, LTD. TAKASAGO R&D CENTER

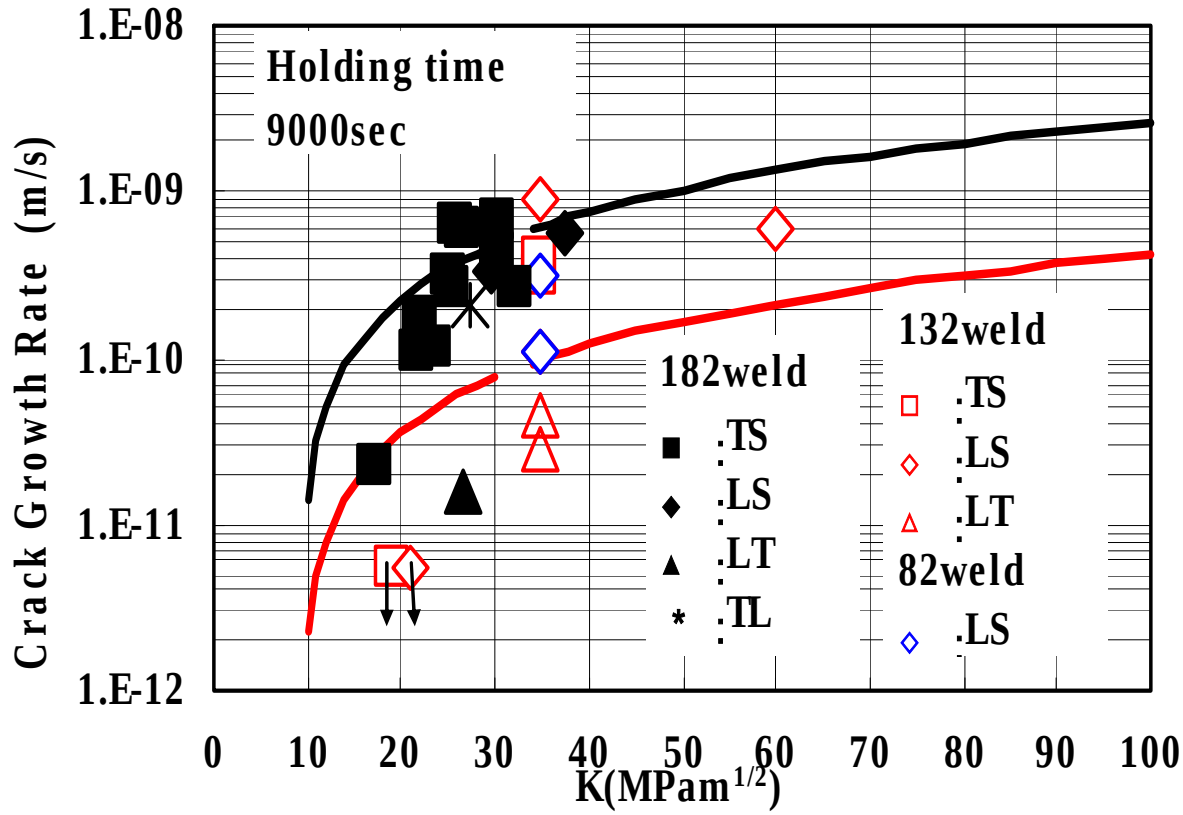

182 weld(325°C)
W.Banford

Alloy 600 (325°C)
P.Scott

PWSCC GRs

Alloy 182

≒ Alloy132

> Alloy600

Figure Comparison between CGR of Alloys 132, 82 and 182 weld metal

MITSUBISHI HEAVY INDUSTRIES, LTD. TAKASAGO R&D CENTER

CONTENTS

1. INTRODUCTION
2. EXPERIMENTAL PROCEDURES
3. RESULTS
4. DISCUSSIONS

“the effect of periodic unloading on the CGR”.

(1) Maintaining of the straight crack front

(2) The effect of the holding time on acceleration of the SCC GR

(3) Reducing SCC incubation time

5. SUMMARY

DISCUSSIONS

MITSUBISHI HEAVY INDUSTRIES, LTD. TAKASAGO R&D CENTER

1. Maintaining of the straight crack front

The straight crack front was not gained for the specimens of the Alloy 132 under constant loading in spite of periodic unloading.

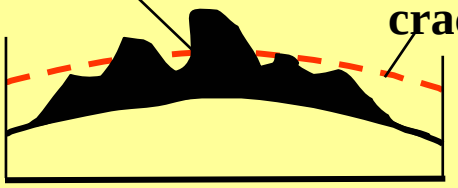

The PWSCC susceptibility is affected by the Metal. Condi. of the G.B. And the Metal. Condi. of G.B. for W.M. is very complicated.

The periodic unloading method has not to be applicable for the ID PWSCC GR measurement of Ni based W. M., to maintain the straight crack front.

DISCUSSIONS

MITSUBISHI HEAVY INDUSTRIES, LTD. TAKASAGO R&D CENTER

2. The effect of holding time on acceleration of the SCC GR

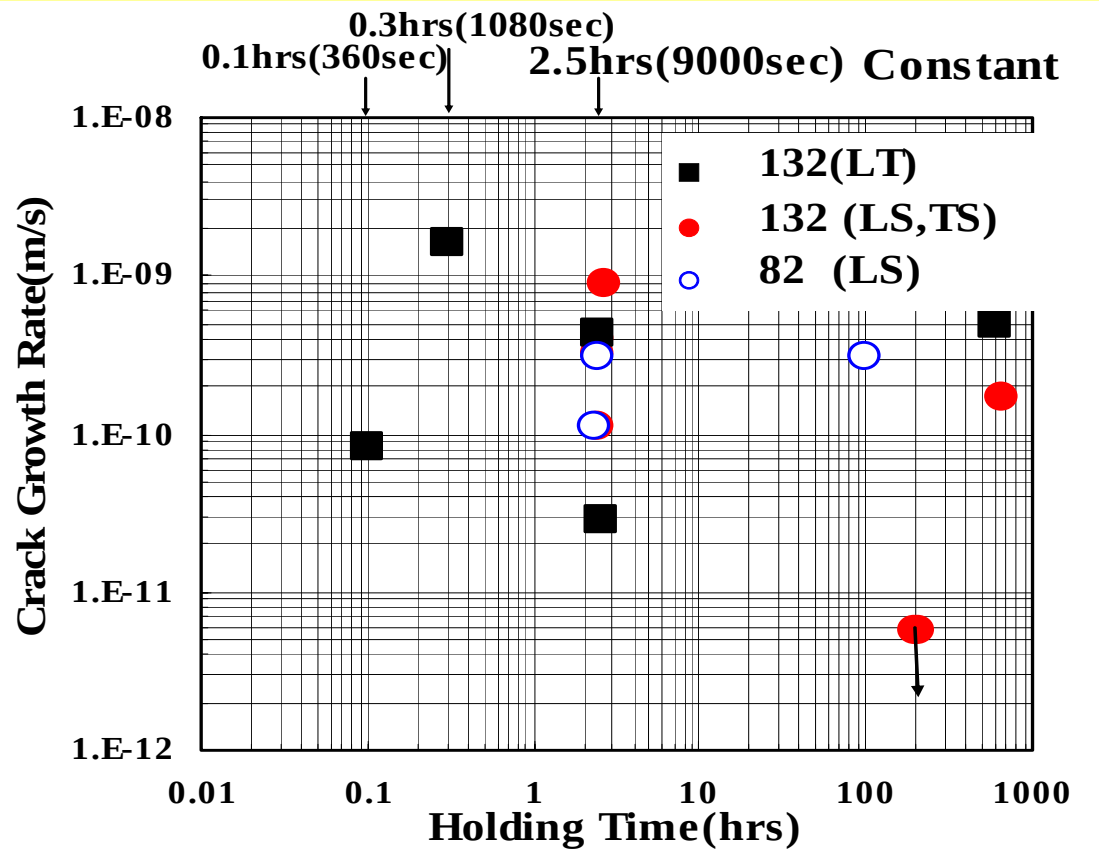

K=35MPa√m
325°C
B/Li:1800/3.5ppm
DO<0.005ppm
DH=30cc/kg H_2O

Figure The effect of holding time for cyclic loading on CGRs

DISCUSSIONS

MITSUBISHI HEAVY INDUSTRIES, LTD. TAKASAGO R&D CENTER

2. The effect of holding time on acceleration of the SCC GR

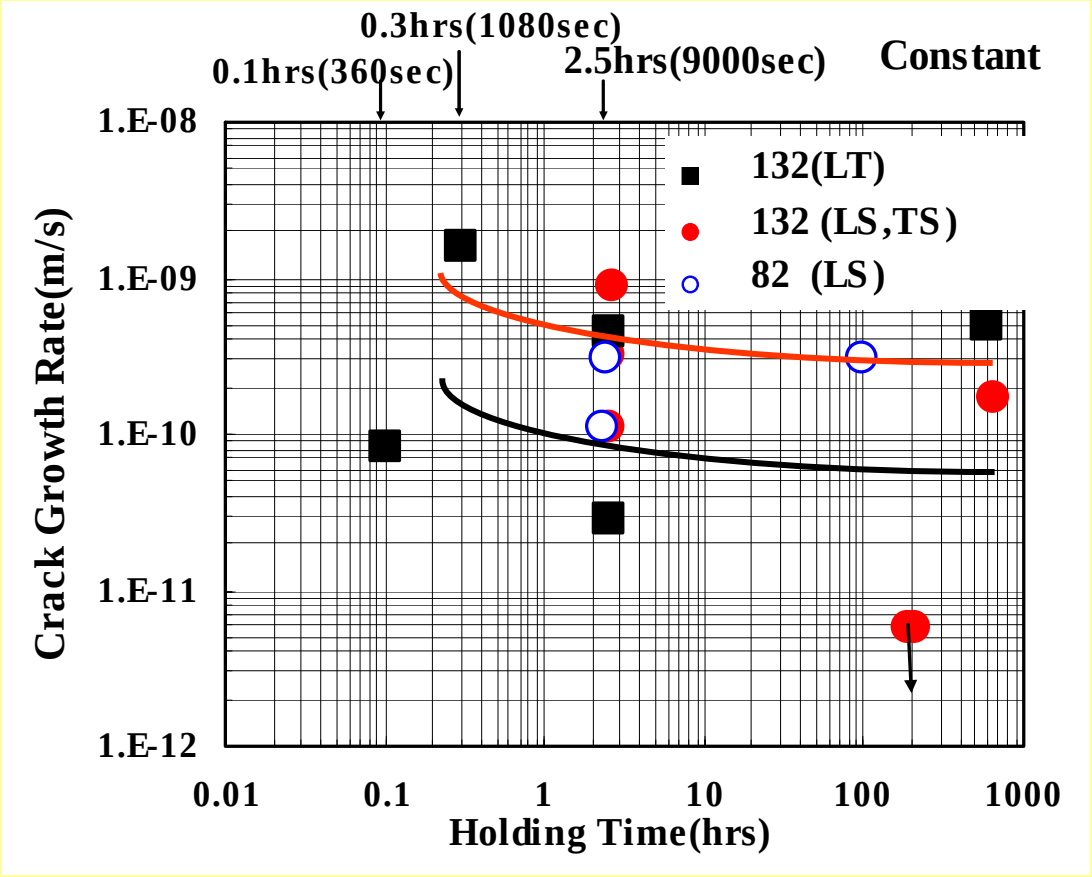

K=35MPa√m
325°C
B/Li:1800/3.5ppm
DO<0.005ppm
DH=30cc/kg H_2O

Figure The effect of holding time for cyclic loading on CGRs

DISCUSSIONS

MITSUBISHI HEAVY INDUSTRIES, LTD. TAKASAGO R&D CENTER

3. Reducing SCC incubation time

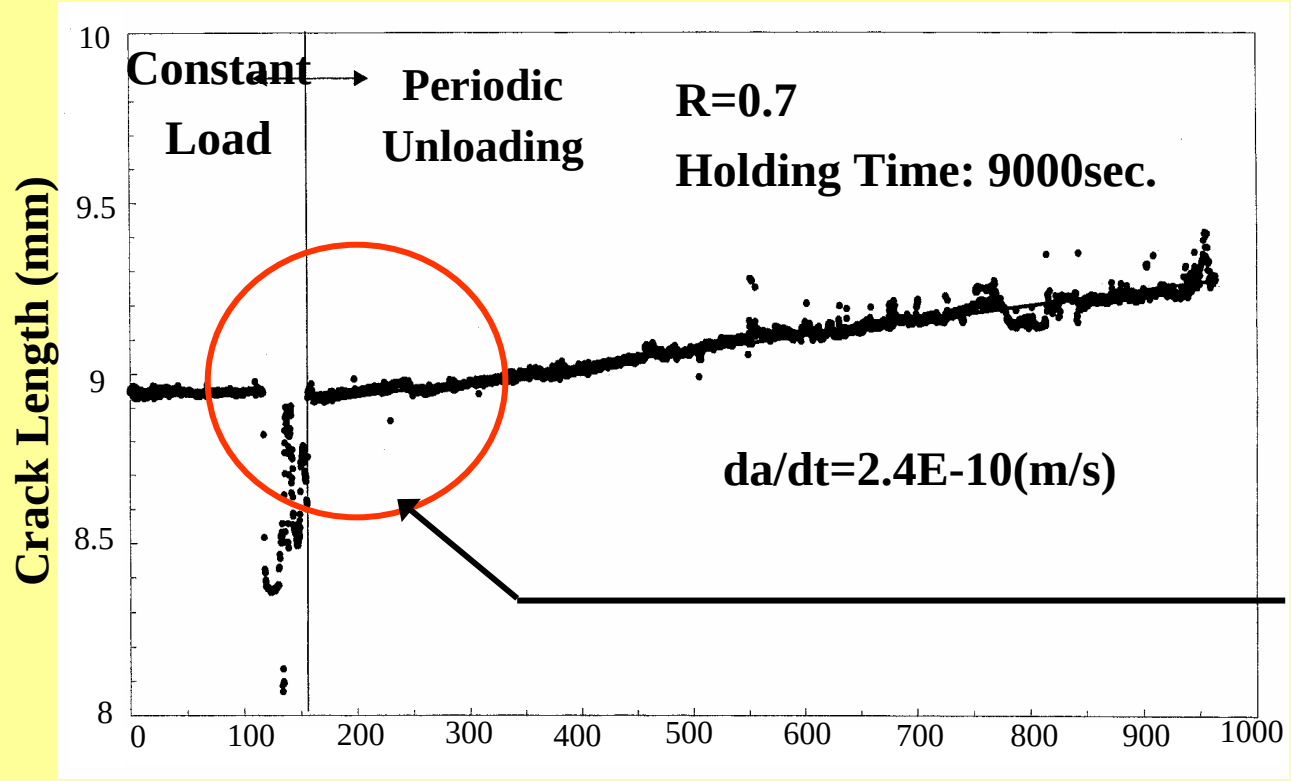

Remarkably changed

The recommended holding times will vary for different materials and specimen orientations.

DISCUSSIONS

MITSUBISHI HEAVY INDUSTRIES, LTD. TAKASAGO R&D CENTER

3. Reducing SCC incubation time

•**Periodic unloading is recommended for producing the ID pre-crack for the PWSCC GR measurement test. But, the effect of periodic unloading on the real PWSCC GR is not always well known.**

•**The ID PWSCC GR measurement test should be conducted under constant loading or trapezoidal wave with a sufficiently long holding time to eliminate the influence of fatigue.**

MITSUBISHI HEAVY INDUSTRIES, LTD.
TAKASAGO R&D CENTER

CONTENTS

797

SUMMARY

MITSUBISHI HEAVY INDUSTRIES, LTD. TAKASAGO R&D CENTER

(1) The PWSCC GR of Alloy 132 in this study was not larger than that of Alloy 182 reported in the literature.

(1) The PWSCC was propagated along the dendrite, CGRs of the TS and LS specimens were about 3 to 10 times larger than that of the LT specimen.

(1) The crack front of PWSCC on the fracture surface of specimens was not uniform, even under P.U.

(1) P.U. is recommended for producing the ID pre-crack for the PWSCC GR measurement test. The ID PWSCC GR measurement test should be conducted under C.L. or trapezoidal wave with sufficiently long holding time to eliminate the effect of fatigue.

LOCKHEED MARTIN

The Stress Corrosion Crack Growth Rate of Alloy 600 Heat Affected Zones Exposed to High Purity Water

George A. Young, Nathan Lewis, and David S. Morton

Lockheed Martin Corporation
P.O. Box 1072
Schenectady, NY 12301-1072

LOCKHEED MARTIN

Main Points

- Need to consider SCCGR of HAZ independently of base metal (and weld metal)
- Data presented here likely not worst case
- Other nickel-base alloys (*e.g.* A690) likely show increased susceptibility to PWSCC in the HAZ

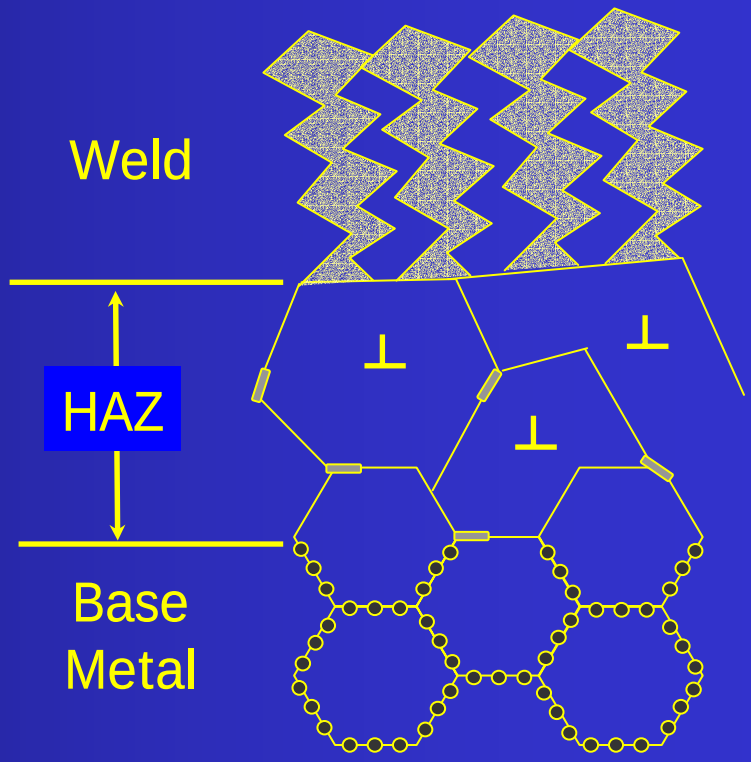

LOCKHEED MARTIN

Background

- **Vessel head penetration SCC in three locations**
  - From A600 penetration ID to OD
  - In E-182 weld metal
  - Near the interface of the A600 penetration and the J-groove weld - ***is this SCC in the HAZ?***

- **Primary water stress corrosion crack growth rate of A600 and its weld metals are well studied - what about the A600 heat affected zone (HAZ)?**

801

LOCKHEED MARTIN

Machine 1.0 CT Specimens from EN82H/A600 HAZ, no PWHT

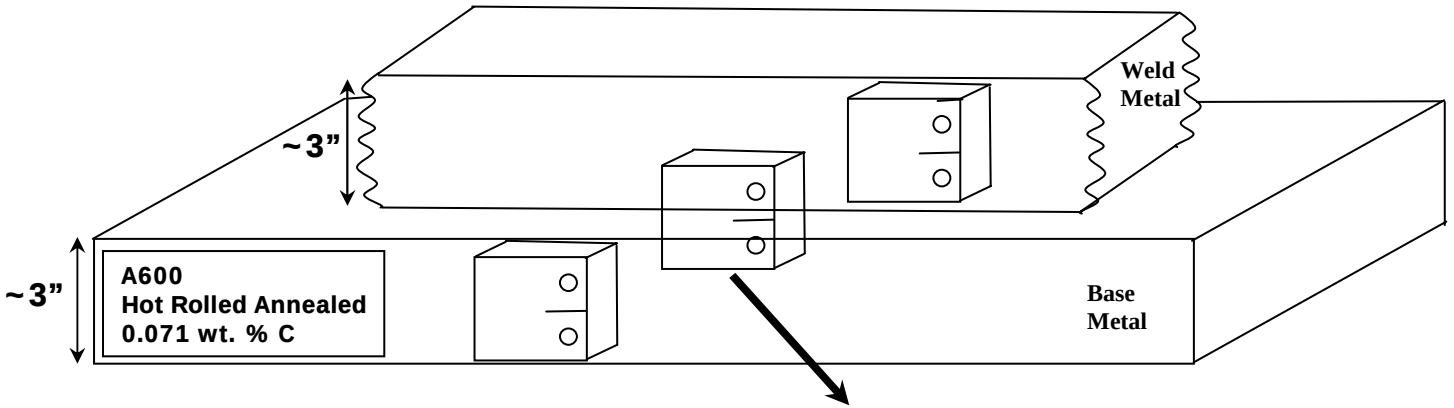

GTAW weld buildup of EN82H

Mill Annealed A600 plate

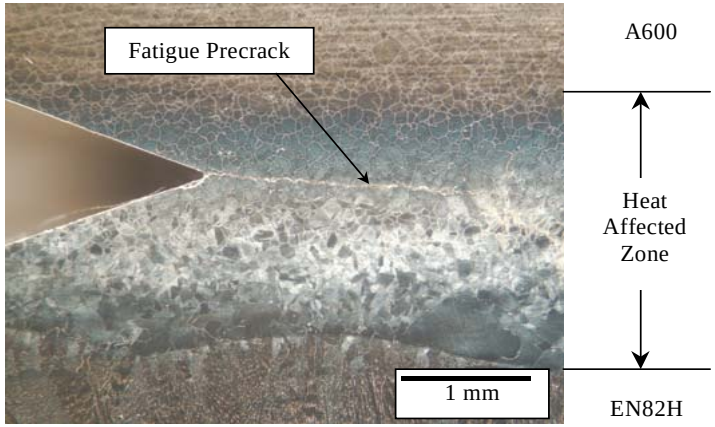

LOCKHEED MARTIN

Notch and precrack entirely in the HAZ

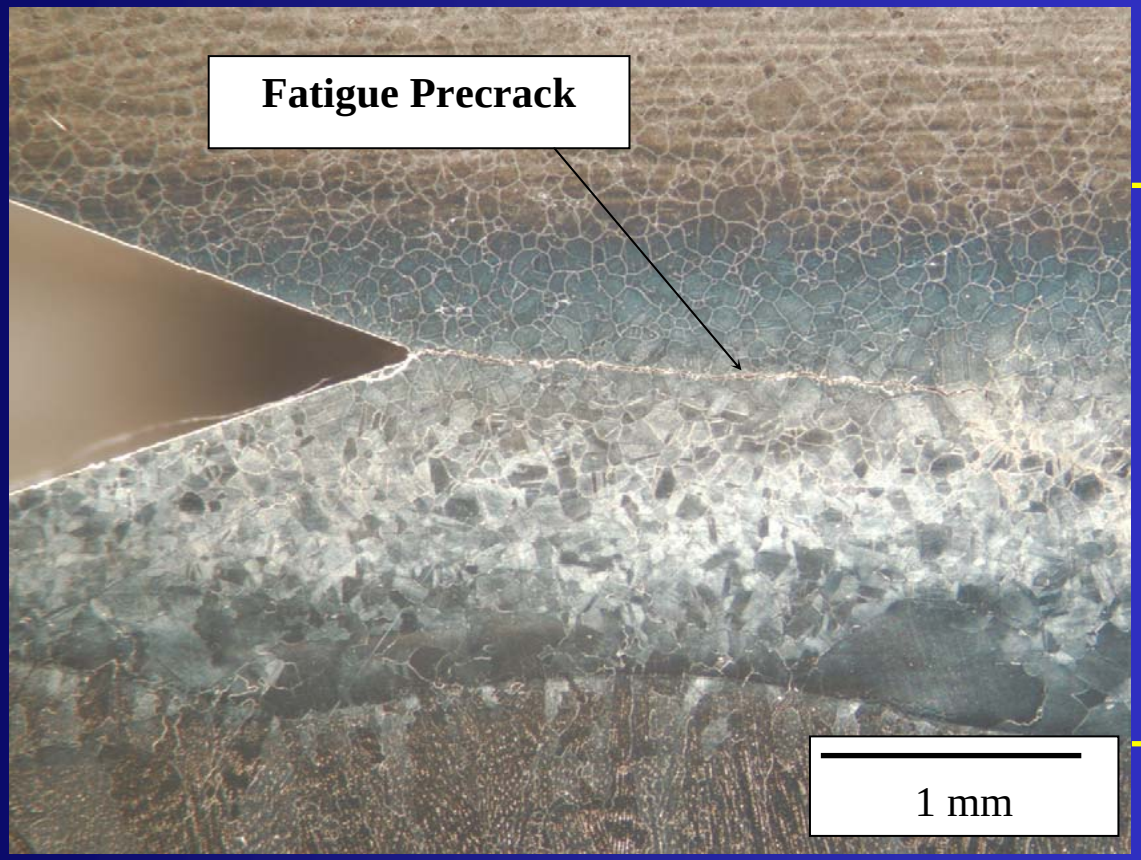

LOCKHEED MARTIN

Testing Goals and Conditions

- **Determine temperature dependence (Q_{SCCGR})**
  - Constant electrochemical potential
- **Determine effect of coolant H_2 around Ni / NiO**
- **"Constant" K (constant load)**
- **Each sample destructively examined post test**

Temperature (^oF / ^oC)	Hydrogen (scc/kg)	Approximate ΔECP from Ni/NiO (mV)	Initial Stress Intensity Factor (ksi$\sqrt{in}$)
600 / 316	9	+2	40
640 / 338	1	-41	40
	18	+6	40
	120	+56	40
680 / 360	30	+6	40

LOCKHEED MARTIN

Results

- **SCC occurred entirely in the A600 HAZ**

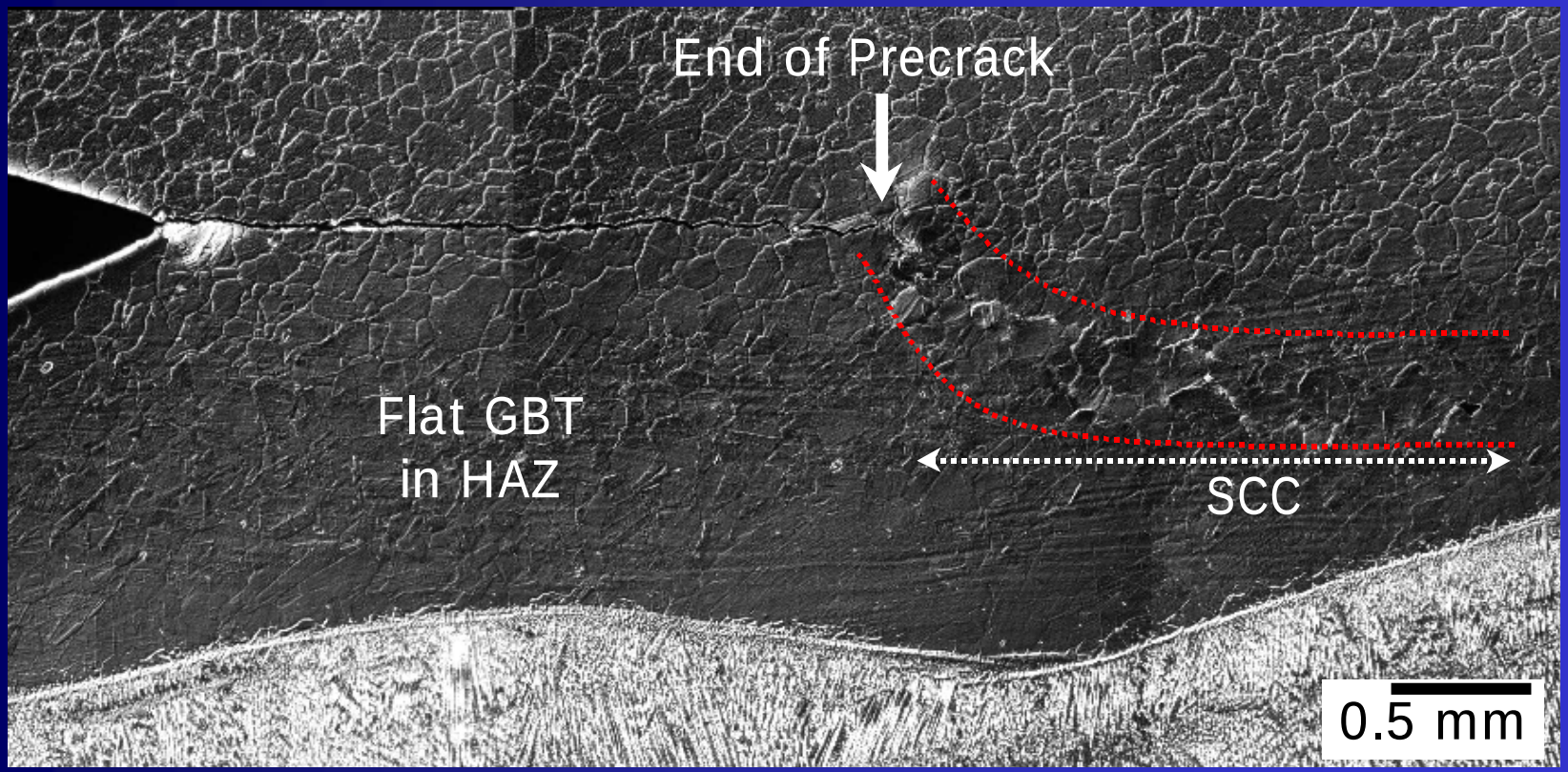

805

LOCKHEED MARTIN

Branched IGSCC in the A600 HAZ

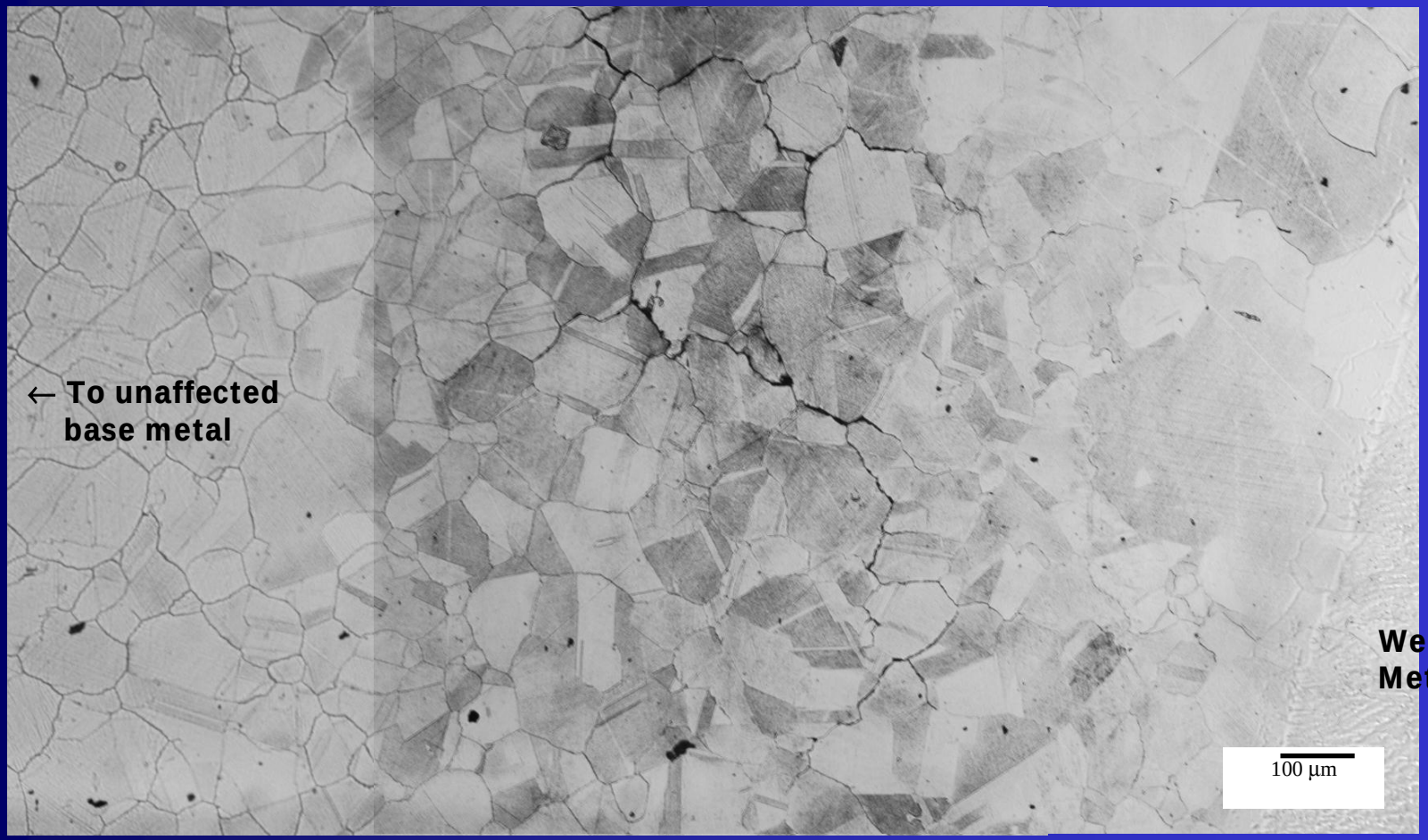

808

LOCKHEED MARTIN

The A600 HAZ displayed ~30X faster crack growth rates than the base metal

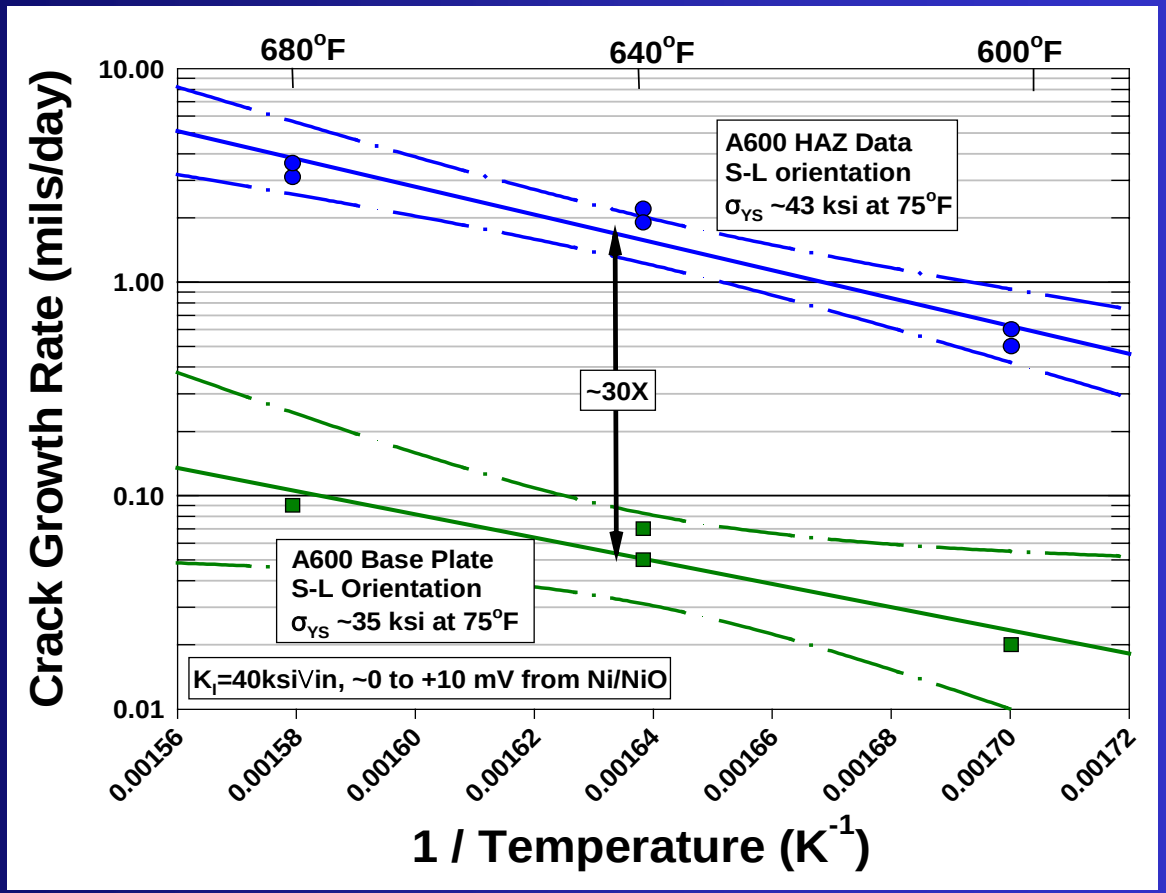

807

LOCKHEED MARTIN

The *Q* for the HAZ is ~ 125kJ/mol

within experimental error of unaffected base metal

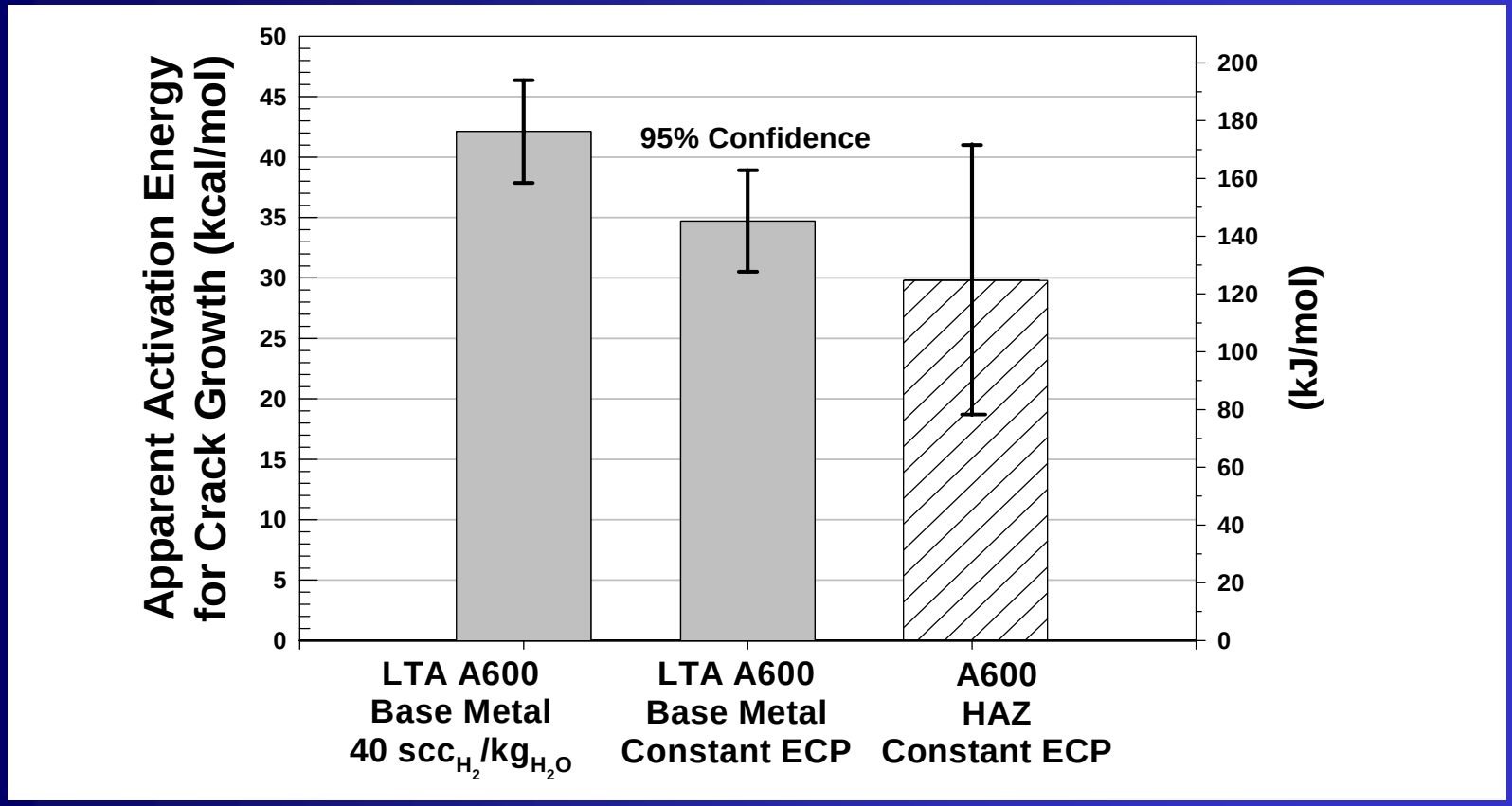

808

- Need to consider ΔECP when determining the apparent activation energy, *Q*, for crack growth
- Conduct tests at constant ΔECP or well into Ni metal stability for 'true' *Q*

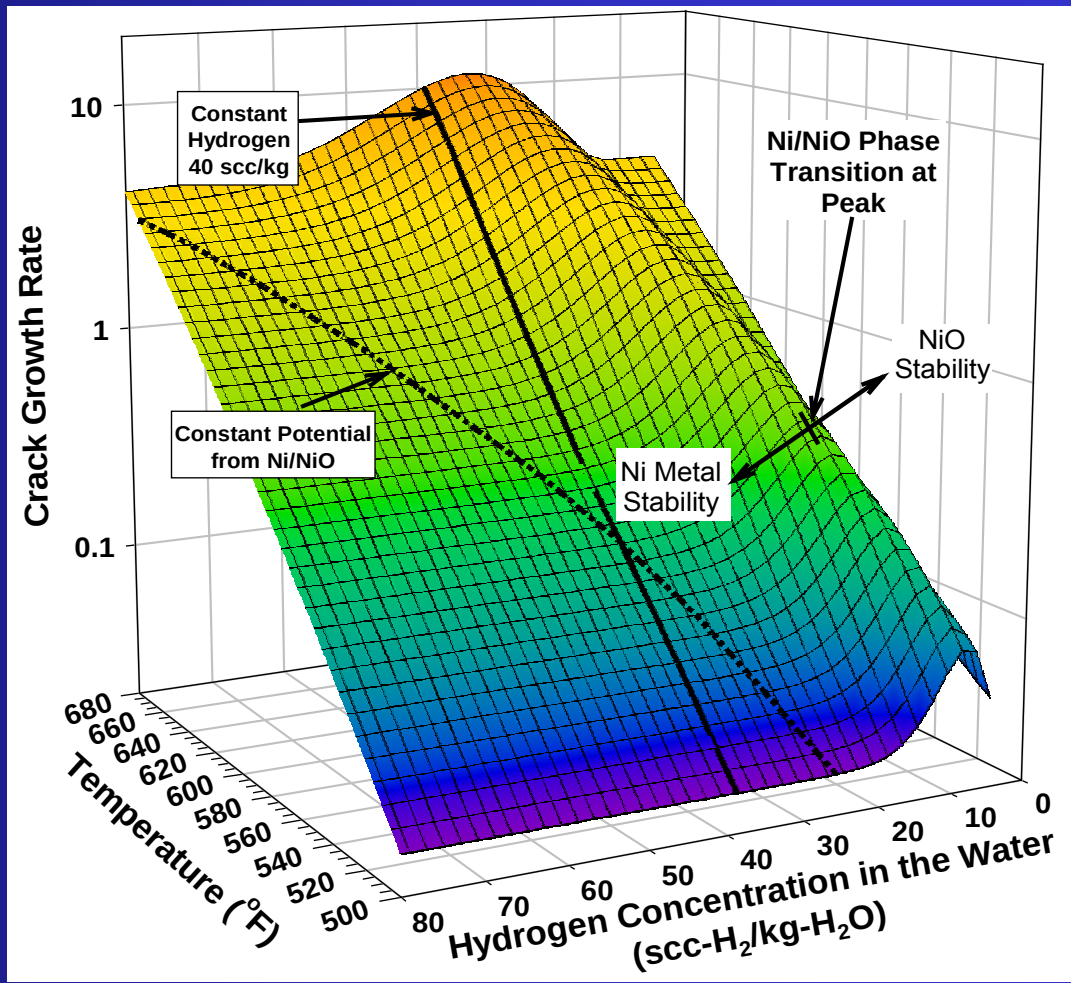

See Morton *et al.*, in 10th Env. Deg. Conf. NACE 2001

LOCKHEED MARTIN

The 'coolant hydrogen effect' for the HAZ is nearly identical the base metal (~2.8X)

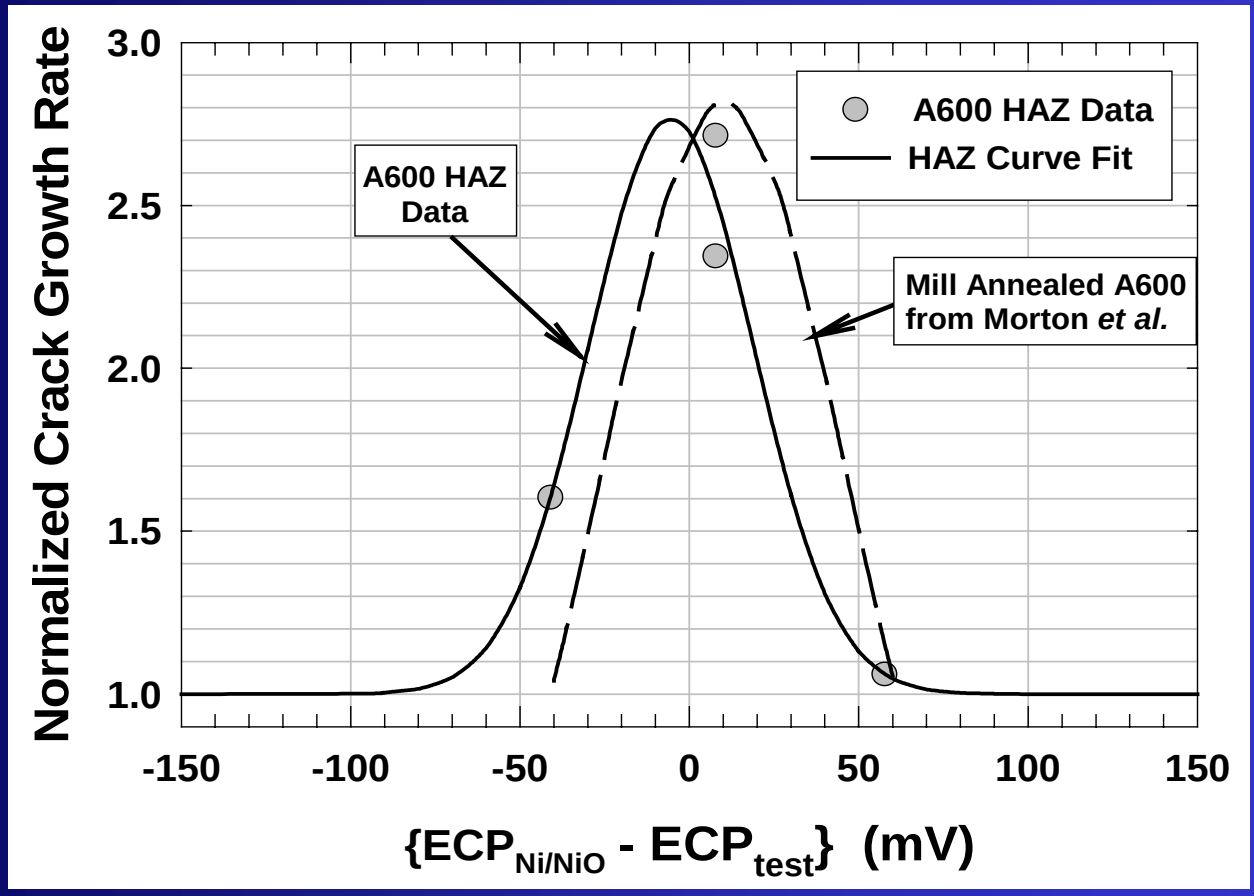

LOCKHEED MARTIN

Why does the A600 HAZ SCC at fast rates?

→ Fewer grain boundary Cr-rich carbides

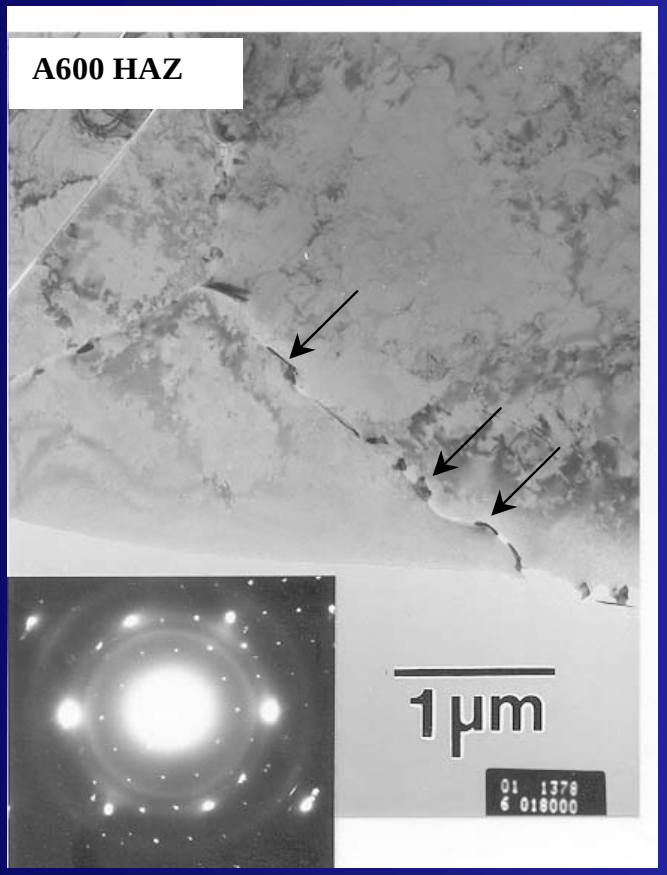

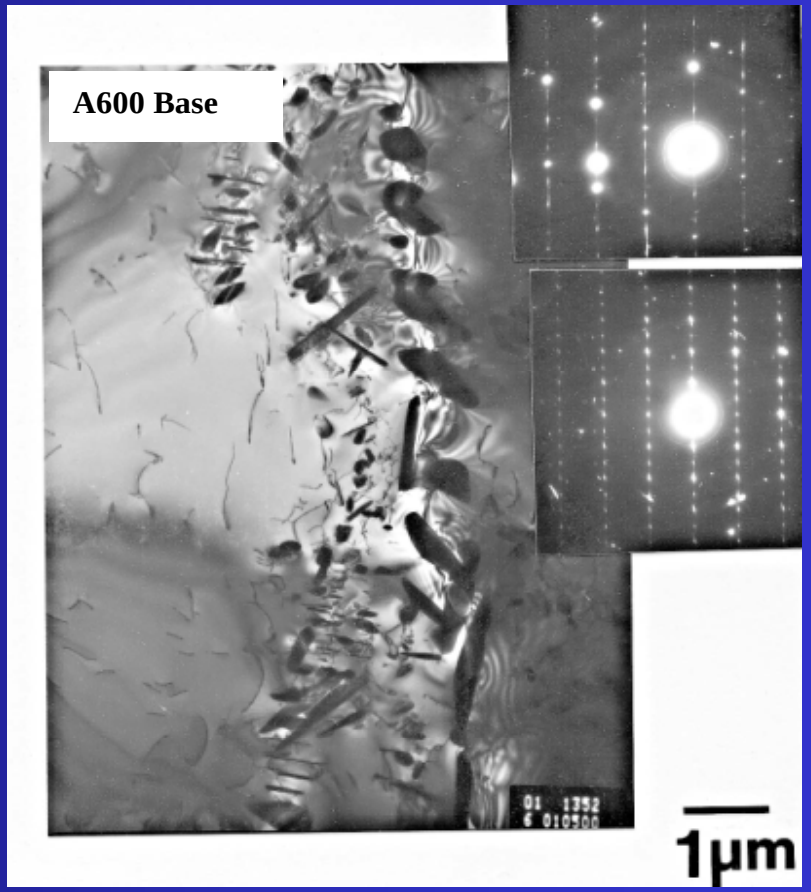

LOCKHEED MARTIN

(1) Microhardness
(2) Strain Quantification via EBSD
(3) Strain Mapping via EBSD

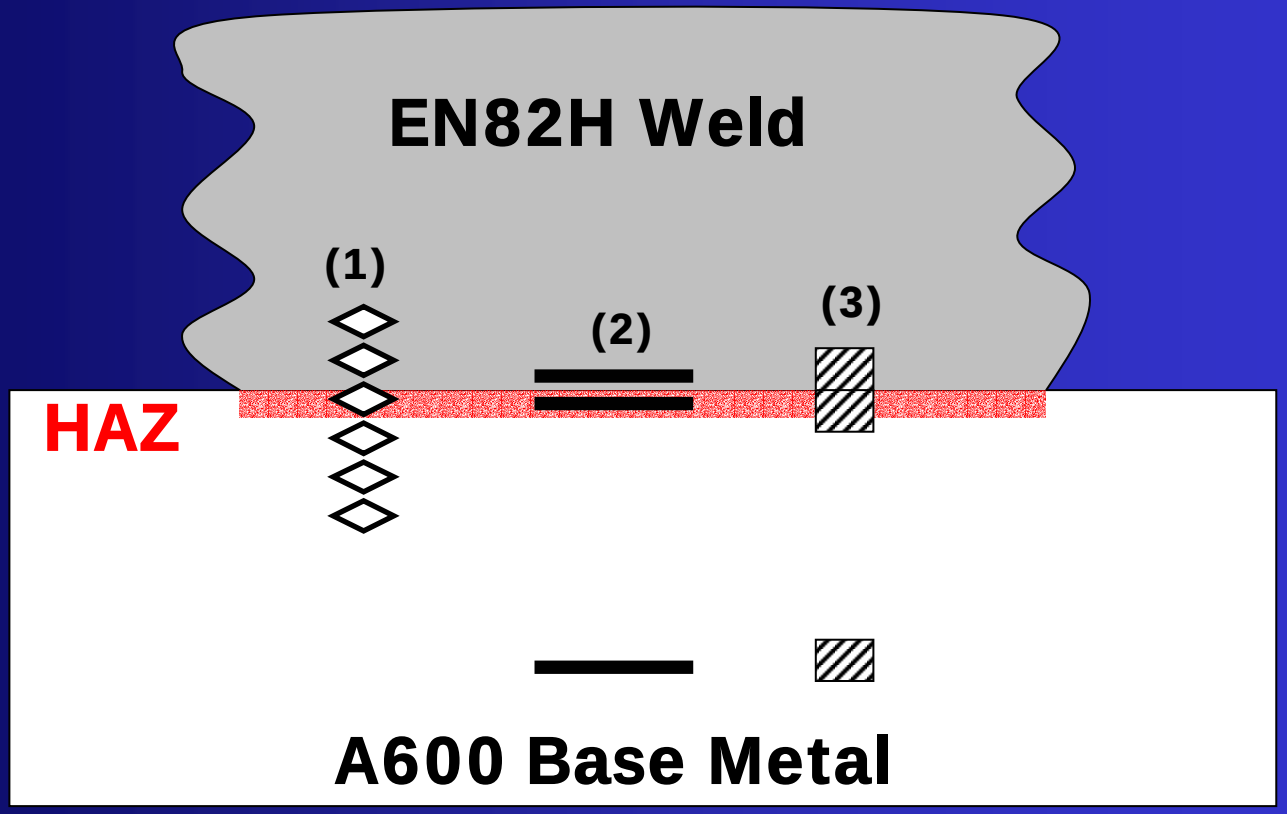

LOCKHEED MARTIN

The HAZ shows increased hardness relative to the unaffected base metal

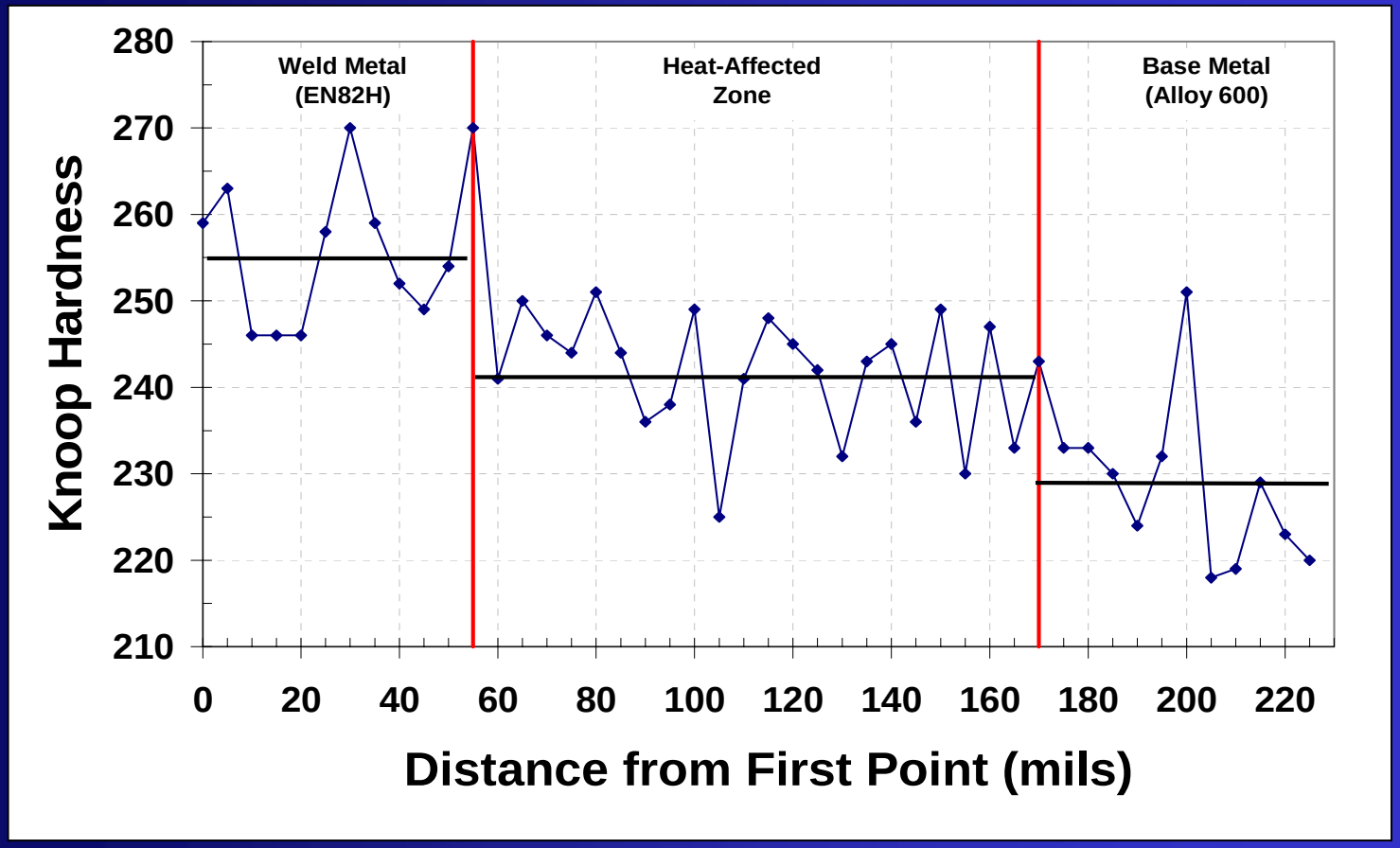

LOCKHEED MARTIN

Why does the A600 HAZ SCC at fast rates?
→ increased plastic strain (~6%) in the HAZ

Far from Weld ⟵ A600 HAZ ⟶ EN82H GTA Weld

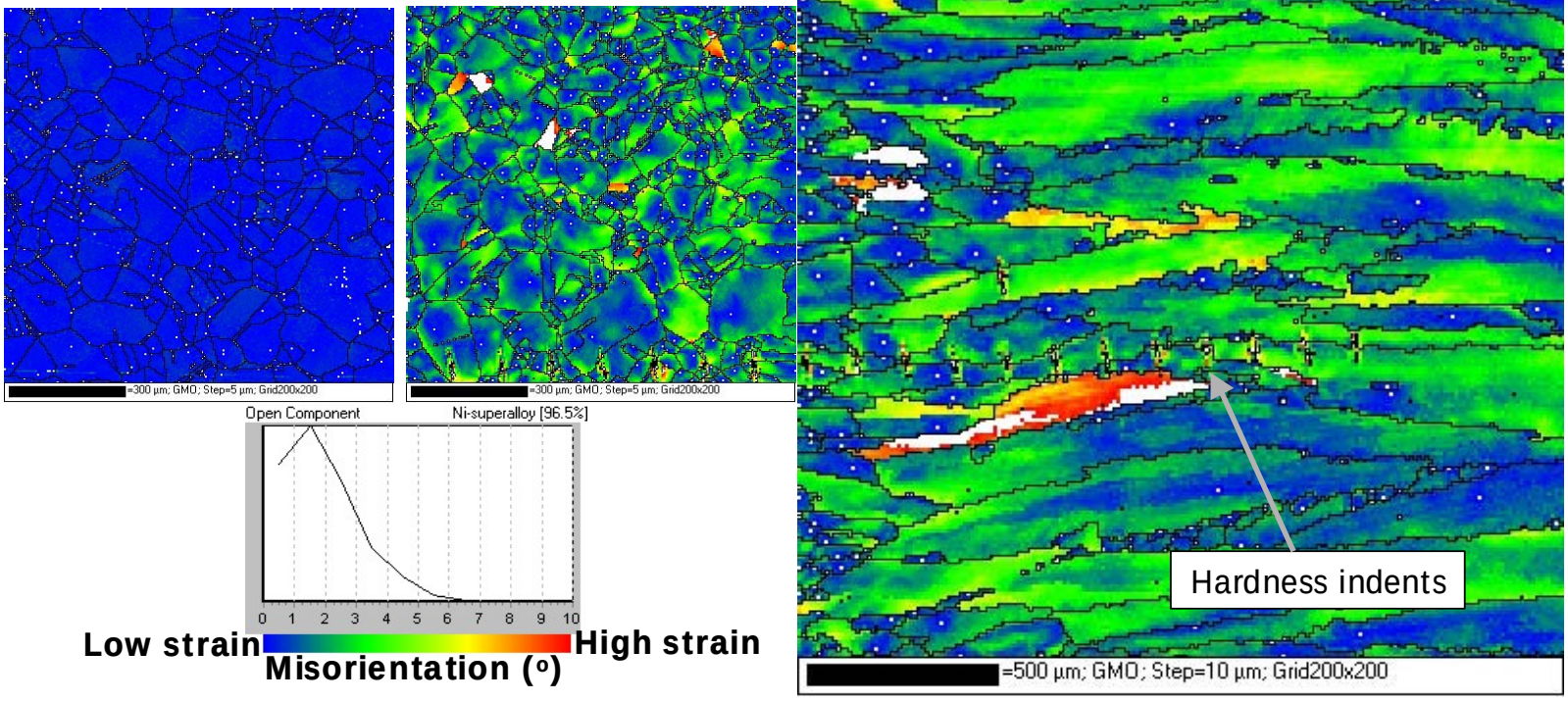

LOCKHEED MARTIN

Discussion

- **The HAZ tested was from a very PWSCC resistant base plate (well annealed, good microstructure). Other heats may show significantly different crack growth rates.**

- **The HAZ tested was low constraint (~6% ε). Higher constraint welds may contain higher plastic strains (~15% ε ?) and exhibit faster crack growth rates.**

  See Young *et al.* in 6th International Conference on Trends in Welding Research, ASM, 15 April 2002, pp. 912-917.

LOCKHEED MARTIN

Discussion

- **Other nickel-base alloys which rely on grain boundary Cr-rich precipitates for PWSCC resistance (*e.g.* A690) may show increased susceptibility to PWSCC in the HAZ.**

- **Post weld heat treatment / bead tempering may help recover PWSCC resistance but ...**
  - plastic strain may promote intra vs. intergranular carbide precipitation
  - may need significantly longer PWHT times (or higher T) than are typical

LOCKHEED MARTIN

Conclusions

- **Need to consider PWSCC of the HAZ separately from the base metal and weld metal.**
- **The susceptibility of the HAZ is due to:**
  - Loss of grain boundary Cr_7C_3 carbides
  - (Less grain boundary Cr depletion)
  - Residual plastic strain from welding
- **The temperature dependence of the A600 HAZ SCC is very similar to unaffected base metal**

A600 HAZ	125 kJ/mol ± 47 kJ/mol	$\|_{95\%}$
'Typical' A600 base metal	145 kJ/mol ± 18 kJ/mol	$\|_{95\%}$

LOCKHEED MARTIN

Conclusions

- The 'coolant hydrogen effect' in the A600 HAZ is ~2.8X, similar to the unaffected base metal
- The A600 HAZ studied is likely not the worst case HAZ
- Other nickel-base alloys which rely on grain boundary Cr-rich precipitates for PWSCC resistance (*e.g.* A690) may show increased susceptibility to PWSCC in the HAZ.

In-situ Raman Spectroscopic Study on Alloy 600 CRDM Nozzle Material and Its Implications

Ji Hyun Kim, Il Soon Hwang
Department of Nuclear Engineering, Seoul National University
and
Tae Ryong Kim
Korea Electric Power Research Institute
Republic of Korea

Conference on Vessel Penetration Inspection, Cracking and Repairs
2003. 9. 29 ~ 10. 2
Gaithersburg. MD, U.S.A.

Outlines

- 1. Introduction
- 2. Rationale and Approach
- 3. In-situ Raman Spectroscopy
- 4. Results
- 5. Ni/NiO Equilibrium & Implication to PWSCC
- 6. Conclusions

820

1. Introduction: PWSCC

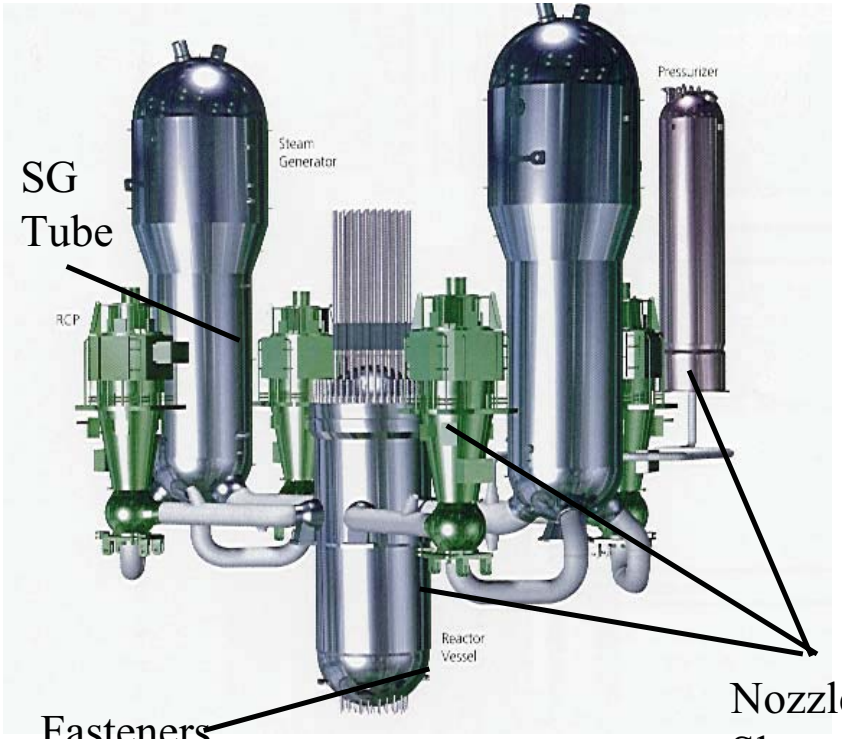

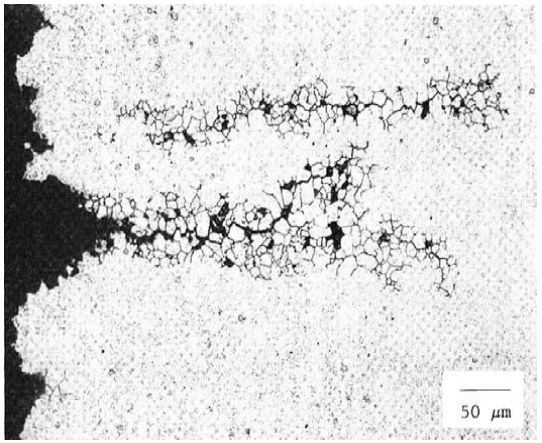

821

1. Introduction: PWSCC

- No general agreement on the mechanism of PWSCC
- It is conceivable that the damage to the alloy substrate is related with the integrity of surface oxide film

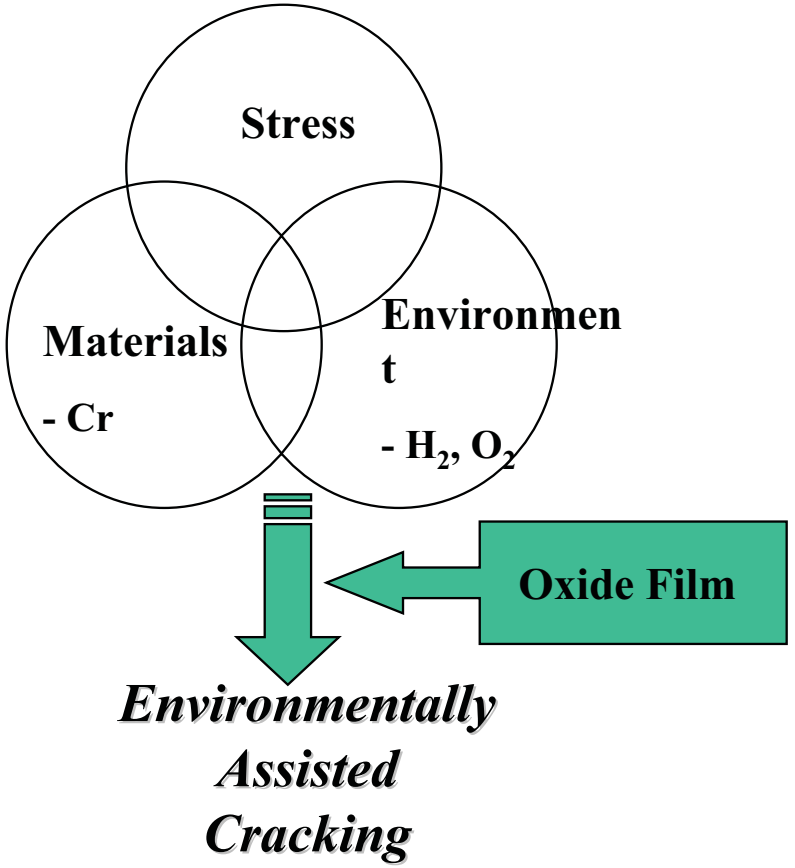

1. Introduction: PWSCC

Influence of [H_2] on PWSCC initiation

(G. Airey. '80)

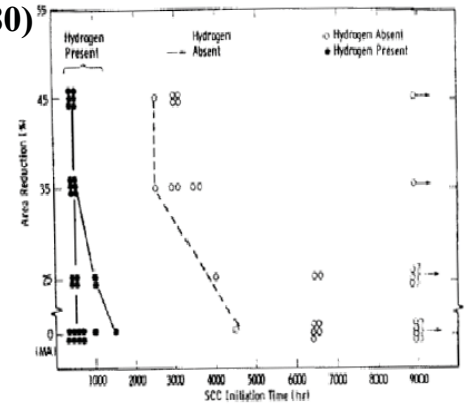

(T. Cassagne et al. '93)

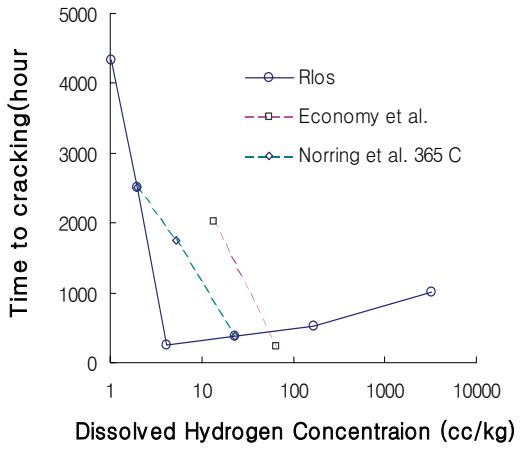

Influence of [H_2] on PWSCC

(T. Cassagne et al. '93)

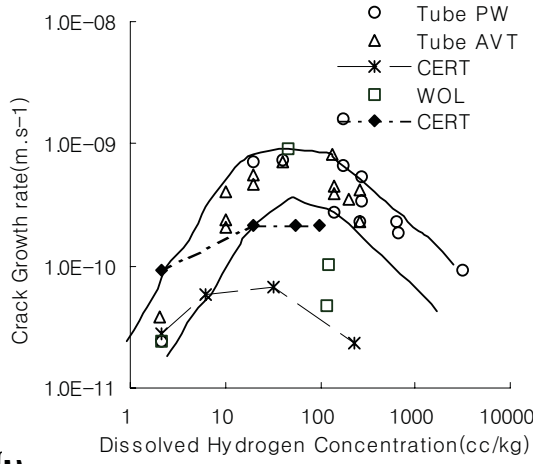

(D. Caron '06)

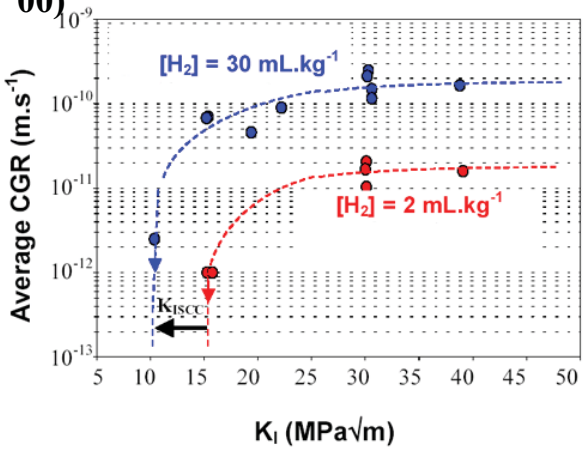

1. Introduction: PWSCC

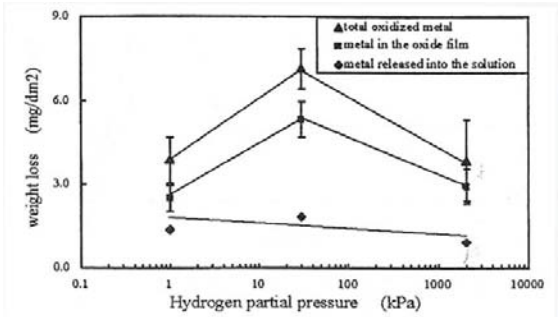

Figure 7: Weight measurements of oxidized metal on alloy 600

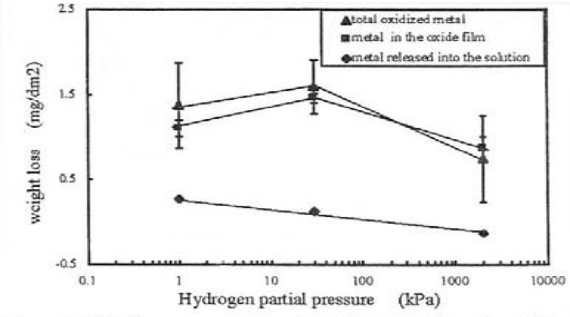

Figure 8: Weight measurements of oxidized metal on alloy 690

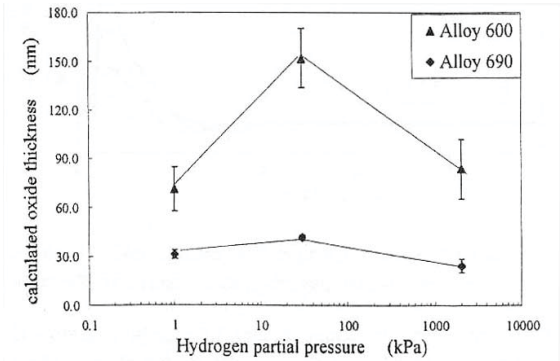

Figure 9: thickness of the oxide layers calculated from the weight measurements (assuming an oxide density of 5)

H_2 overpressure (kPa)	<1	30	2000
Alloy 600 -Weight measurement -X-ray diffraction	60nm 80nm	150nm 175nm	90nm 60nm
Alloy 690 - Weight measurement	30nm	40nm	25nm

(C. Soustelle et al. '99)

- Total amount of oxidized metal(oxide+dissolved cations) as well as oxide thickness are maximum at the intermediate hydrogen overpressure.

824

2. Rationale and approach

- **The characterization of the oxide film of alloy 600 under PWR primary water conditions**
  - **one of key elements for understanding how the oxide film behaves in the cracking process.**
- **In-situ study can give potentially a clearer picture of the corrosion mechanism**
  - **Removal of the material from the corrosion environment can result in modification of the oxide film structure and chemistry.**
- **In-situ oxide study in high temperature water**
  - **for pure metals and alloys in <u>air-saturated</u> or <u>BWR</u> water**
  - **by T. Devine et al. and J. Maslar et al.**

⇨ ***Need in-situ information on oxide film of alloy 600 in <u>PWR</u> environment***

825

2. Rationale and approach

- **Characterization of oxide structure and chemistry under various PWR environments by in-situ experimental method**
  - **Ex-situ reference oxide powder experiment**
  - **In-situ experiment at various PWR conditions**

  - **Ni/NiO domain on ECP-T coordinate**
  - **Comparison with thermochemical calculations on Ni/NiO**

  - **Oxide structure examination**
  - **Comparison of oxide chemistry with earlier ex-situ results**

826

3. In-situ Raman Spectroscopy

- **Raman spectroscopy**
  - **the measurement of the wavelength and intensity of inelastically scattered light from molecules by irradiating a sample with the monochromatic radiation from a laser.**
  - **Performed by collecting the light that is inelastically scattered by the sample.**

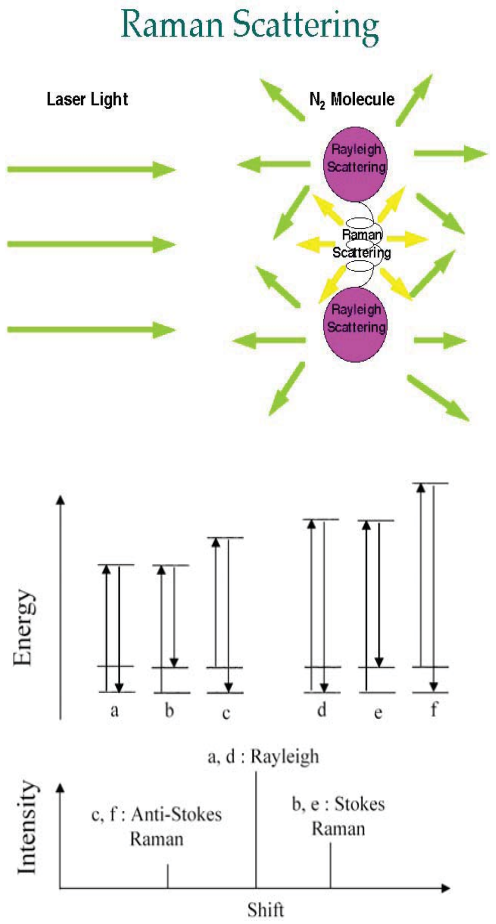

827

3. In-situ Raman Spectroscopy

Material

- **Alloy 600 : hot forged, SA at 1050°C for 2hrs and water cooled**

Elem.	C	Mn	Fe	S	Si	Cu	Ni	Cr	Al	Ti	Nb	P	B	N
Comp.	0.06	0.26	8.31	0.001	0.3	0.12	75.12	15.25	0.16	0.36	0.04	0.009	0.002	0.001

Water environment

- **PWR primary water chemistry**
  - ✓ **Deionized and deaerated water : DO_2 < 10 ppb (inlet)**
  - ✓ **Boron: 1,000 ppm, Lithium : 2 ppm**
- **Hydrogen gas injection**
  - ✓ **Pure hydrogen gas of 0.7 atm overpressure : ~ 30 cm^3(STP)/kg**
  - ✓ **5% hydrogen & 95 % He of 0.6 atm overpressure : ~ 1 cm^3(STP)/kg**
- **Temperature : 250 ~ 350 ℃**
- **Pressure : 180 atm**

828

3. In-situ Raman Spectroscopy

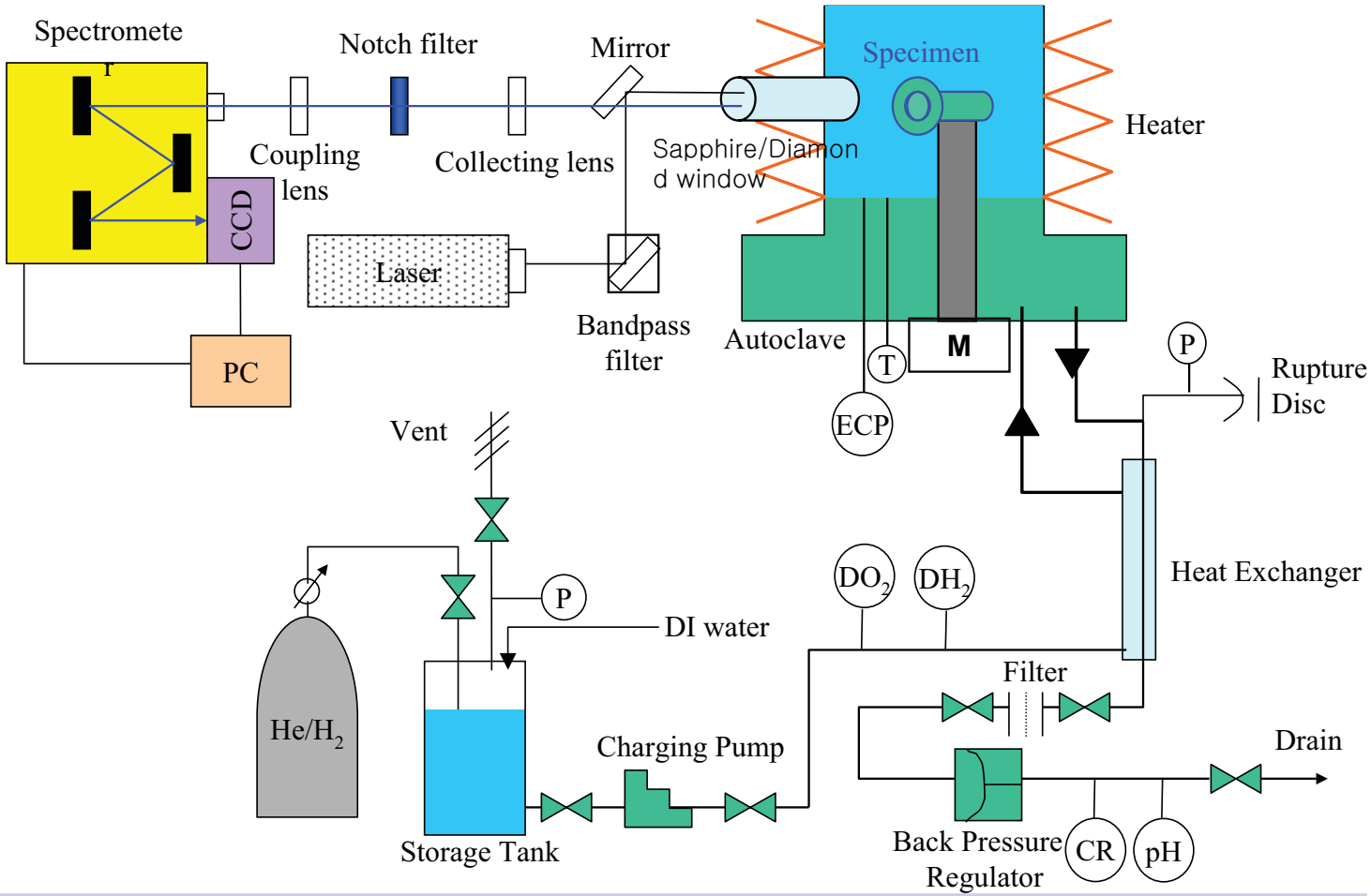

3. In-situ Raman Spectroscopy

➢ Bird's-eye view of Raman system

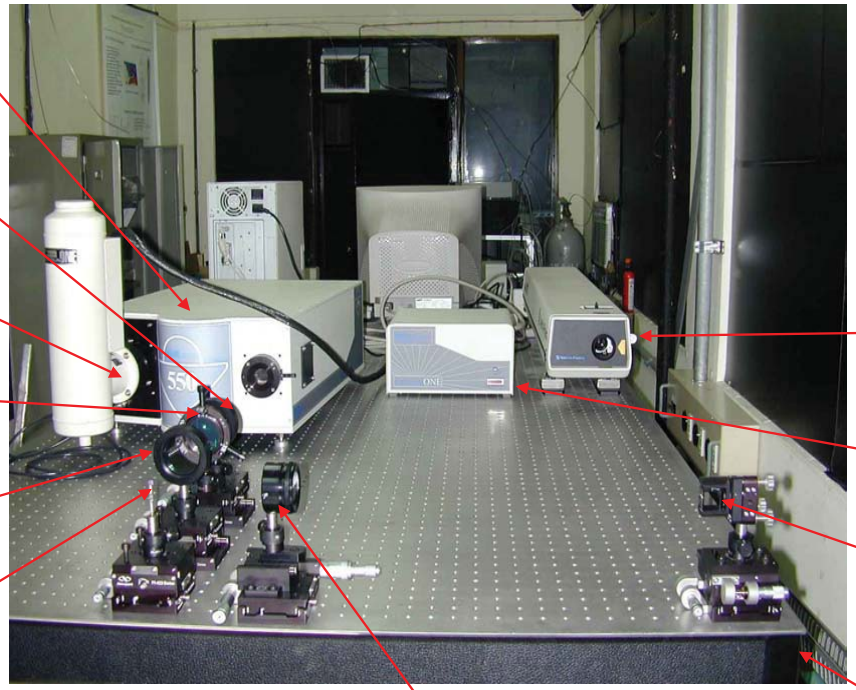

3. In-situ Raman Spectroscopy

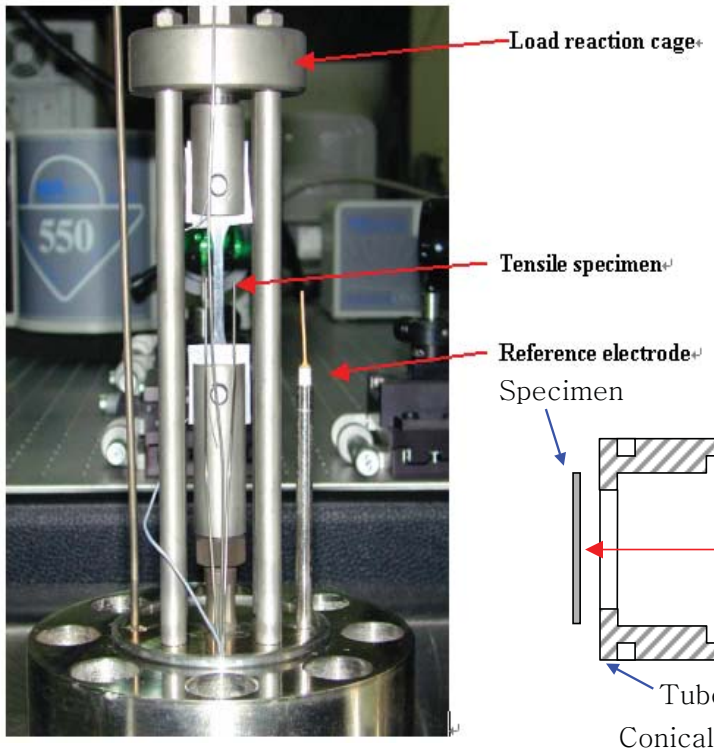

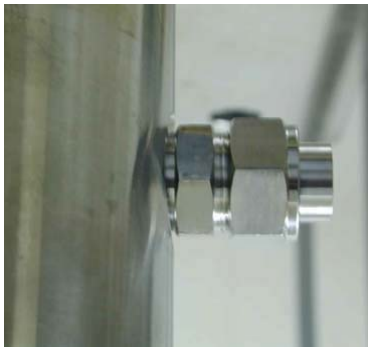

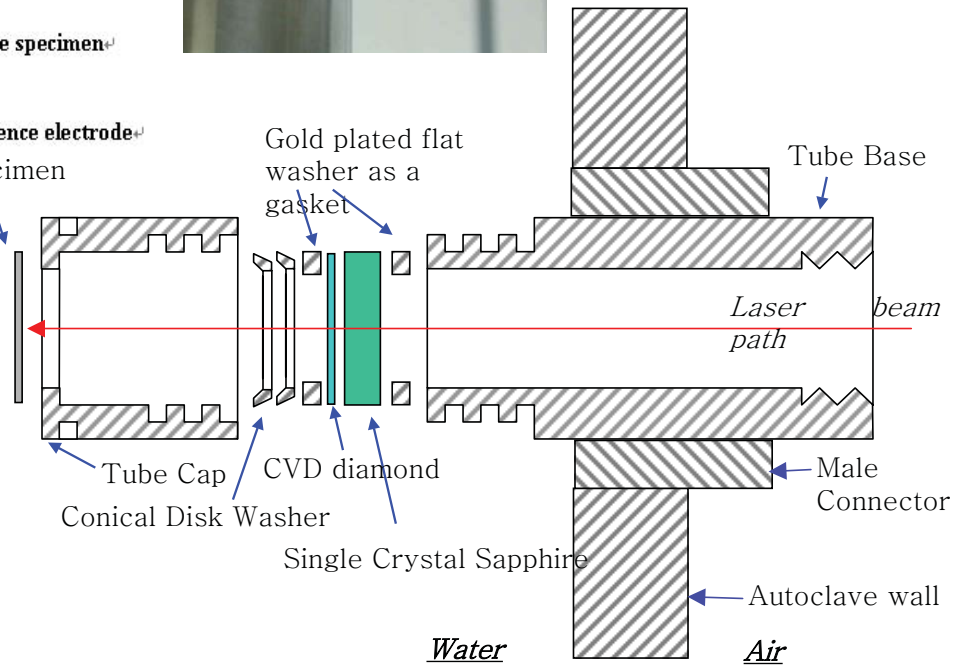

831

3. In-situ Raman Spectroscopy

- **Reference Raman spectra measurement in air**
  - **NiO**
  - **$NiFe_2O_4$**
  - **Cr_2O_3**
  - **$NiCr_2O_4$**

- **In-situ Raman spectra measurement**
  - **Dissolved hydrogen concentration variation**
  - **Temperature variation**

832

4. Results : Reference Powder in Air at RT

➢ **NiO**

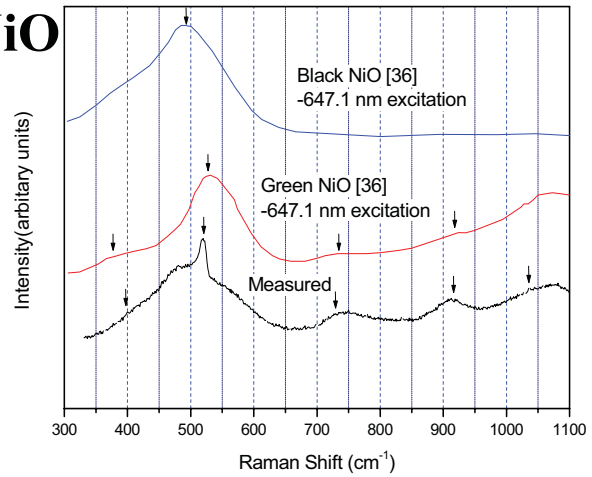

➢ **$NiFe_2O_4$**

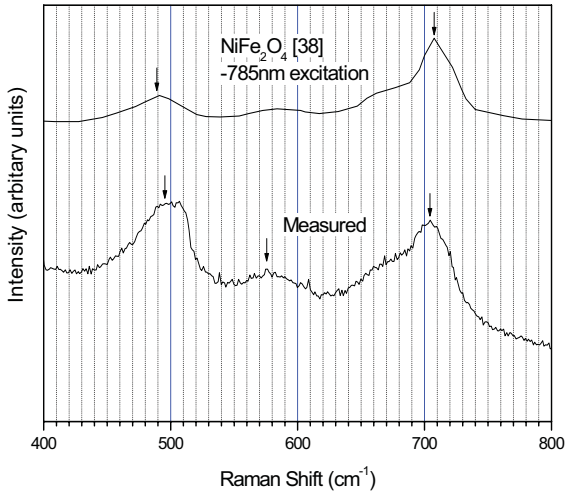

➢ **Cr_2O_3**

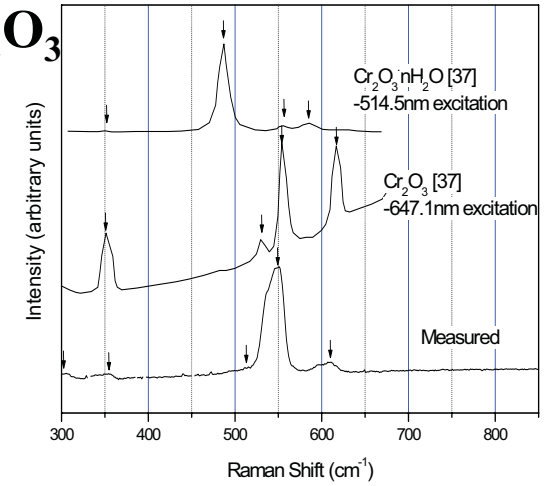

➢ **$NiCr_2O_4$**

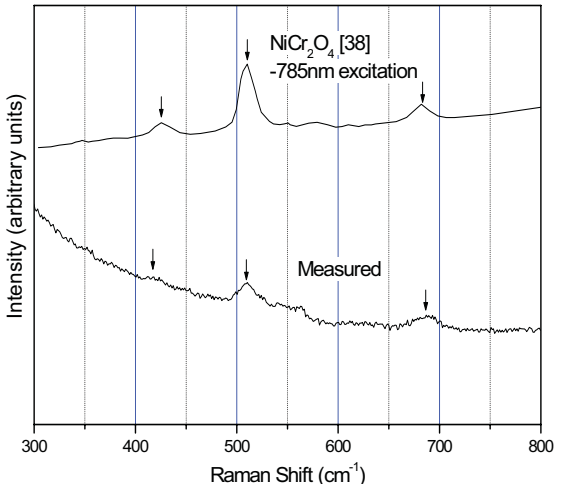

4. Results in PWR conditions

- **Temperature and alloy 600 exposure time prior to in-situ Raman spectra measurements**

Temperature (℃)	Total exposure time prior to first measurement at temperature (h)	Hold time at each temperature prior to first measurement (h)
250	28	2
290	33.5	3
320	42	7
350-I	47.5	3.5
350-II	69.5	20.5

834

4. Results in PWR conditions

➢ In-situ Raman Spectra with DH_2=30cc/kg

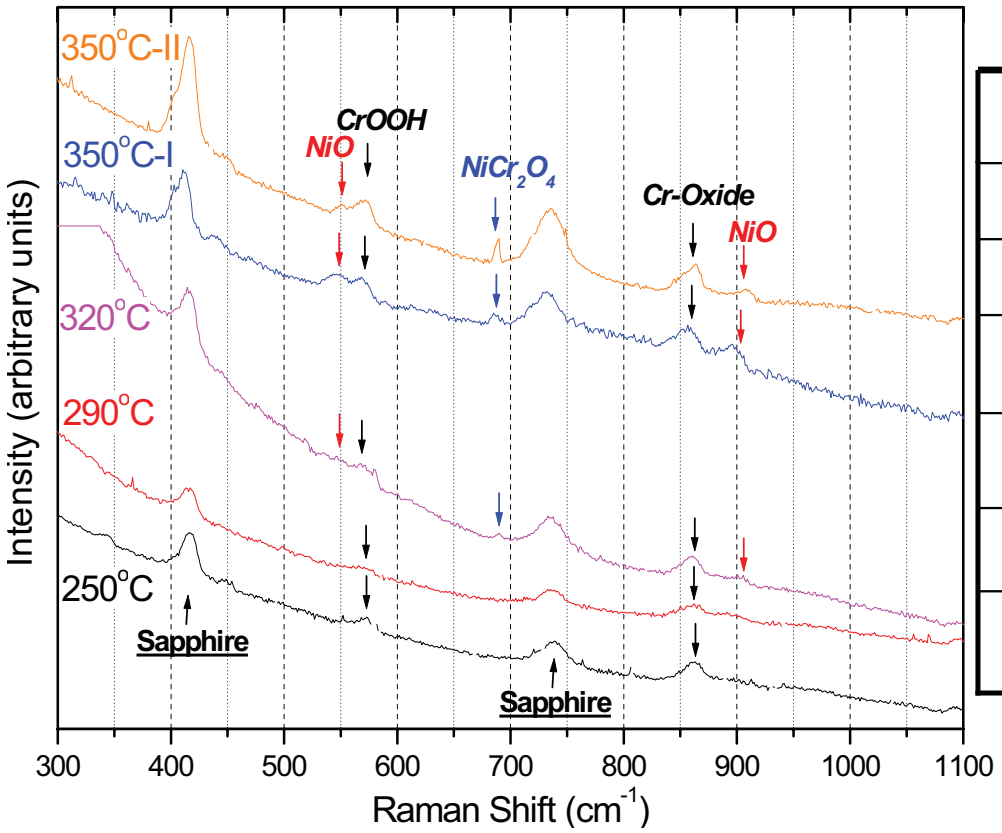

Species	Peaks
$NiCr_2O_4$	430 510 682
CrOOH	ca. 546-587
Cr^{III}/Cr^{VI} oxide	340-350 840-880
$NiFe_2O_4$	570 704
NiO	550 910
Sapphire	417 751

4. Results in PWR conditions

➢ In-situ Raman Spectra with DH_2=1cc/kg

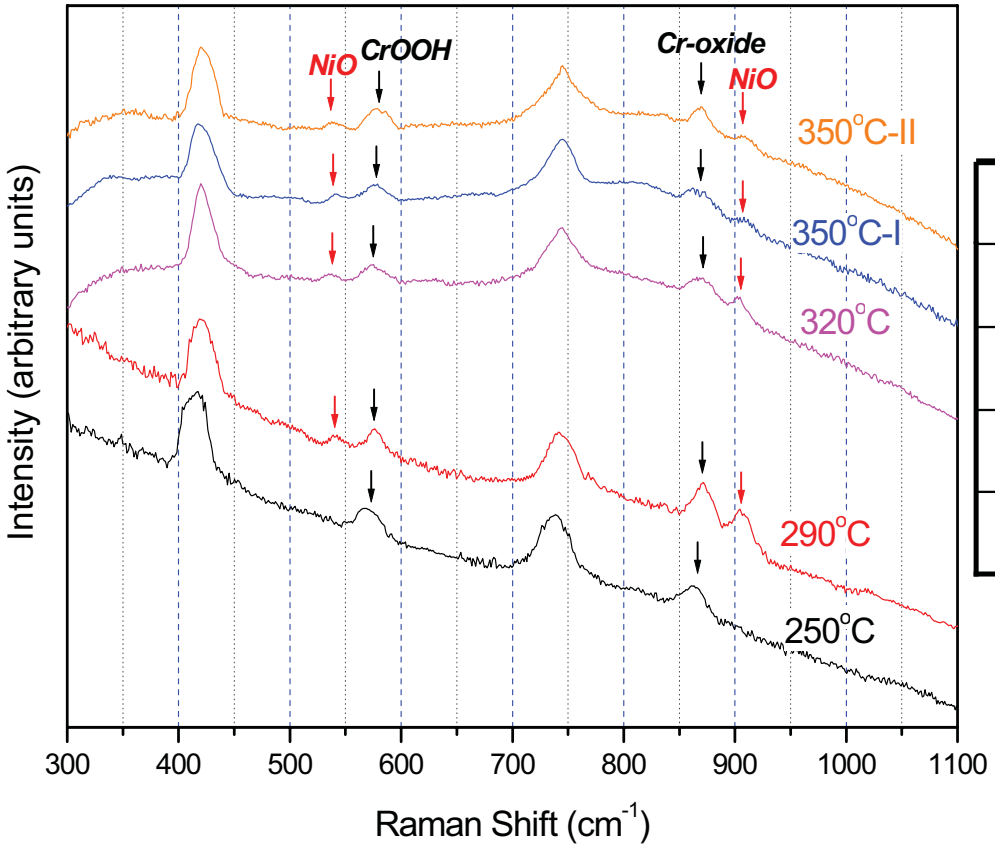

Species	Peaks
CrOOH	ca. 546-587
Cr^{III}/Cr^{VI} oxide	340-350 840-880
NiO	550 910
$NiCr_2O_4$	430 510 682

4. Results in PWR conditions

Change of dissolved hydrogen concentration

1cc/kg -> 30cc/kg

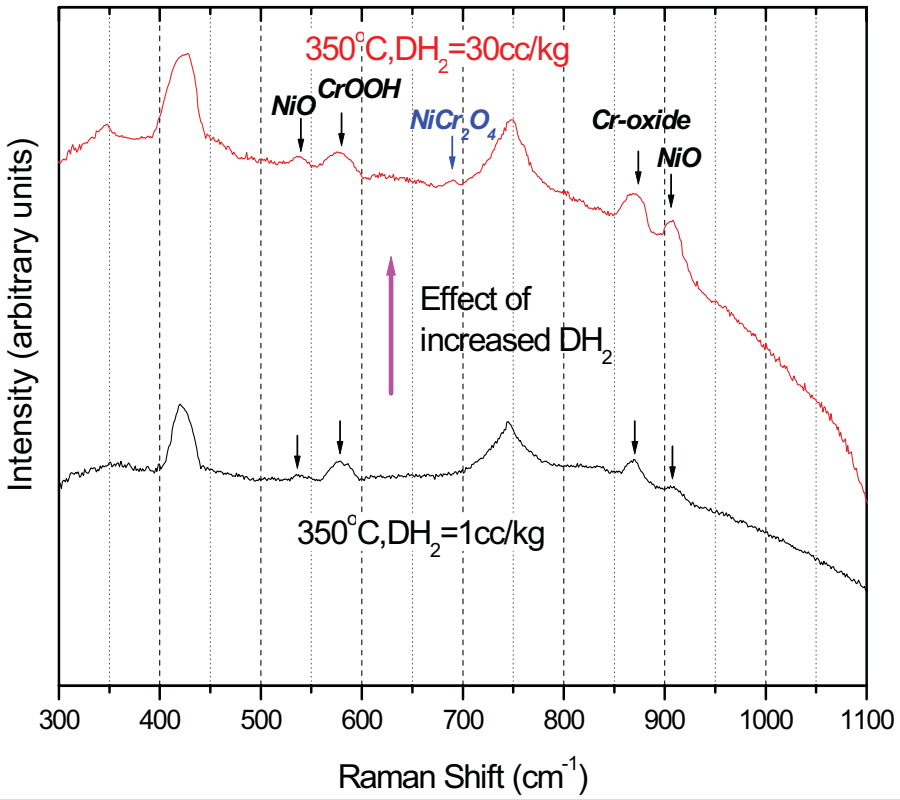

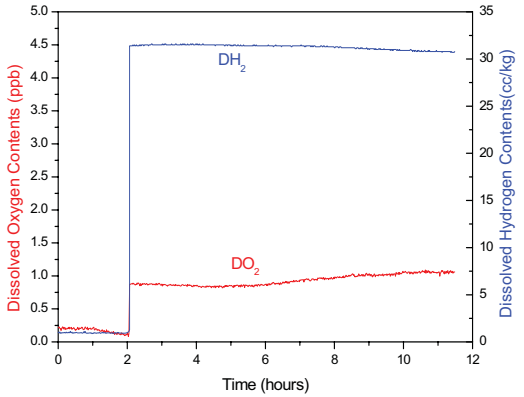

Species	Peaks
CrOOH	ca. 546-587
Cr^{III}/Cr^{VI} oxide	340-350 840-880
NiO	550 910
$NiCr_2O_4$	510 682

4. Results: in-situ vs. ex-situ

- **After cool-down to room temp. and exposure to air**
  - **No remarkable change in Raman spectrum**
  - **lower of Cr-oxide peak(~870cm^{-1}) : absence of borate**

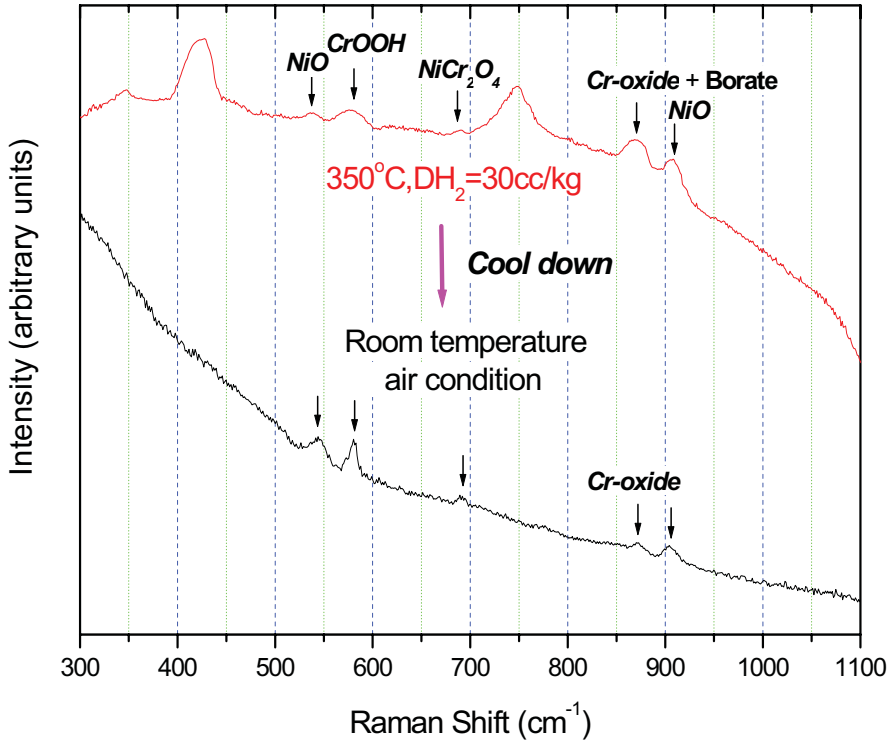

4. Results: in-situ vs. ex-situ

➢ Comparison with past work

	In-situ (This work)	Soustelle et al.	Caron	Nakagawa et al.
Method	In-situ Raman	GDOS+EDS	XPS	Synchrotron XRD + TEM
T (°C)	350	360	330	320
Exposure time (hrs)	71	300	1869	1000
Oxide(s) at high DH_2	CrOOH, Cr-Oxide, NiO +$NiCr_2O_4$	Compact layer ($NiCr_2O_4$) + Precipitates ($NiFe_2O_4$)	$NiCr_2O_4$	(Ni+Cr-rich) oxide + Ppt. ($NiFe_2O_4$)
Oxide(s) at low DH_2	CrOOH, Cr-Oxide, NiO	Compact layer ($NiCr_2O_4$)	NiO	NiO

839

4. Results: in-situ vs. ex-situ

- $NiFe_2O_4$ detected at high DH_2 condition in ex-situ studies could not be observed in-situ at above 290℃. Suppression of precipitate layers in this work is attributed as the cause for the difference. But FE-SEM post-examination of oxide showed scarcity of precipitates on film.
- CrOOH that was not detected in the past was observed by Raman.
- NiO, Cr_2O_3, $NiCr_2O_4$ were observed in agreement with results of earlier ex-situ studies.

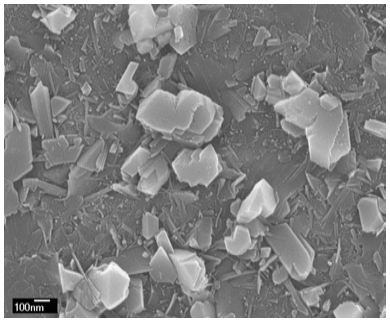

FE-SEM micrograph

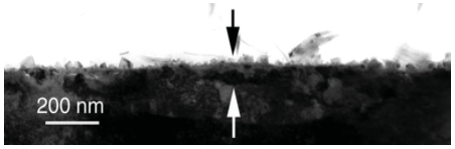

TEM micrograph

840

5. Ni/NiO equilibrium: measured & predicted

- **Regular solution theory**
  - **Enthalpy of mixing**
    - ✓ Hertzman & Sundman (1985)
    - ✓ Use binary interaction coefficients to describe the enthalpy of mixing and extrapolation of high temperature (> 1100 K) thermodynamic data
  - **Standard Gibbs energy of formation of austenitic Ni-Cr-Fe solid solution**

$$\Delta_f G_T^o(alloy) = \sum_i^3 x_i \Delta_f G_T^o(i, fcc) + RT \sum_i^3 x_i \ln x_i + {}^E G_T^o + {}^{mag} G_T^o$$

where $\Delta_f G_T^o(alloy)$ = standard Gibbs energy of formation of the alloy

$\Delta_f G_T^o(i, fcc)$ = standard Gibbs energy of formation of component i in the fcc structure of alloy

${}^E G_T^o$ = excess Gibbs energy

${}^{mag} G_T^o$ = standard Gibbs energy due to magnetic ordering

- **Chemical thermodynamic data**
  - Room temperature data: standard literature source and HSC database
  - HT data by Criss-Cobble, HKF relation and extrapolation procedure
  - Data for chromium hydrolysis species : Ziemniak (1998)
  - Data for nickel and iron hydrolysis species : Tremaine et al. (1980)

841

5. Ni/NiO equilibrium: measured & predicted

➢ DH2 vs. T and Comaprision with Earlier Work

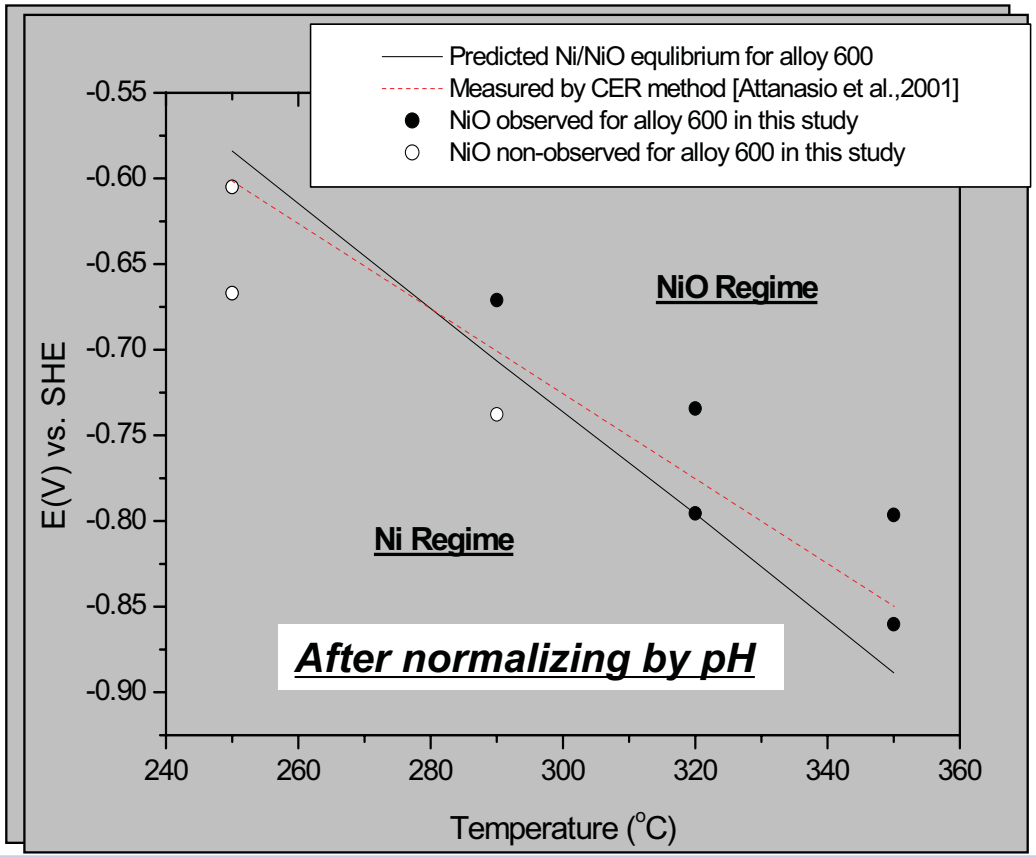

842

5. Ni/NiO equilibrium: Implication to PWSCC

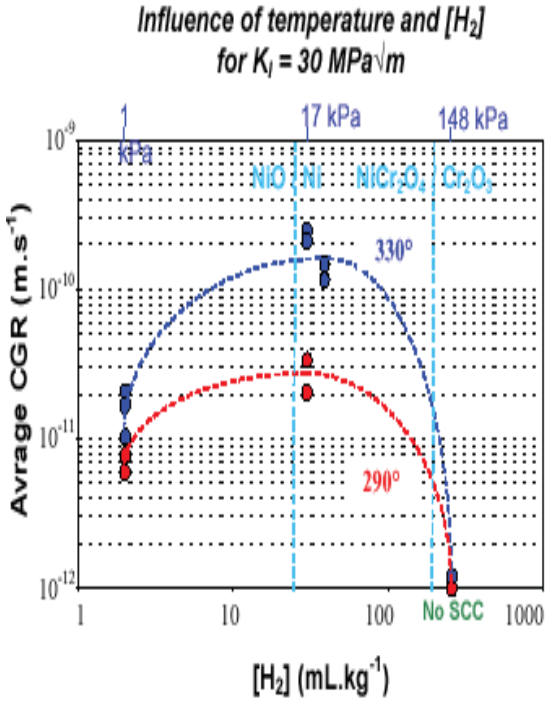

(T. Cassagne et al. '97 @ 330C)

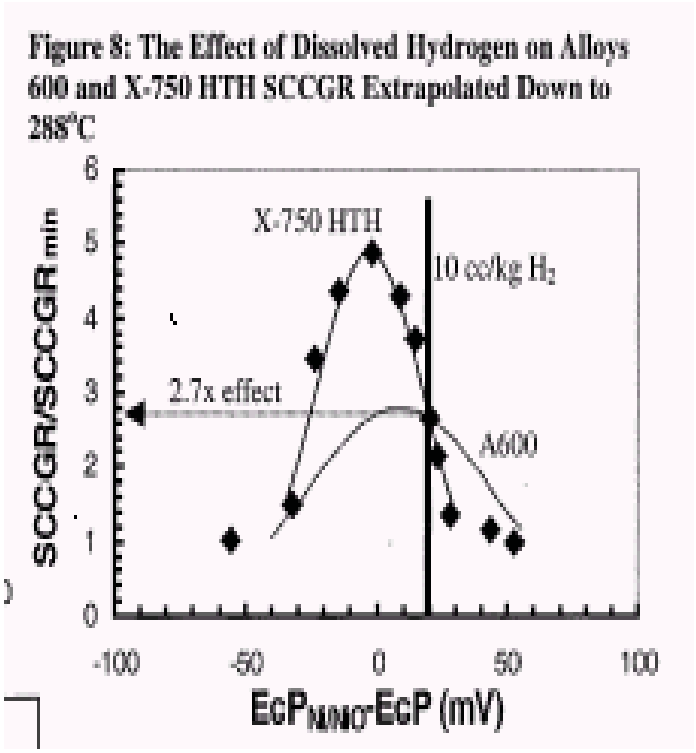

(S. Attanasio et al., '01 @ 288C)

5. Ni/NiO equilibrium: Implication to PWSCC

Accelerated corrosion due to Tetragonal/Monoclinic phase transition of ZrO2

New Hypothesis on PWSCC
Redox alteration of Ni/NiO may enhance film-percolation and PWSCC

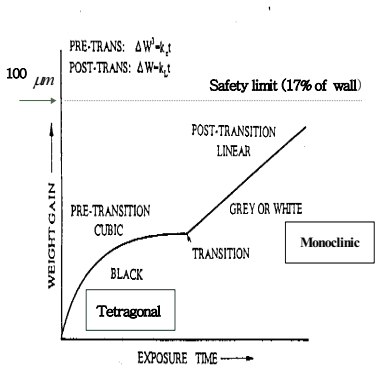

Oxidation behavior of zirconium alloys in nuclear power plants [Edward Hillner, 1977]

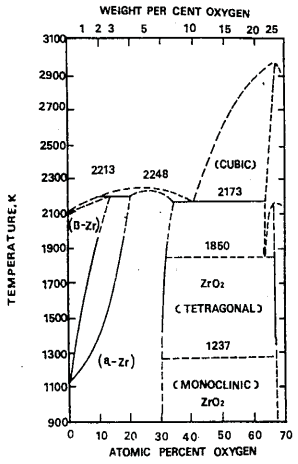

Phase diagram of Zirconium oxide [F. Garzarolli,1991]

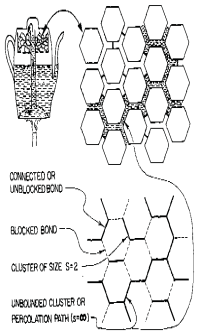

Percolation model of a flow through a porous medium that is modeled as a network of interconnected channels..

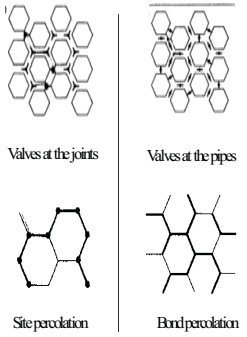

Plumbing analogy for the distinction Between site percolation and bond percolation

Nuclear Materials Laboratory 5

Nuclear Materials Laboratory 16

844

5. Ni/NiO equilibrium: Implication to PWSCC

Implication to Mitigation Effort

- Tighter DH2 Control at PWR
  - DH2 controlled by cover gas pressure in CVCS
  - H2 pressure may vary with time(0~50 cc/kg?)

- Systematic investigation on DH2 effect
  - Initiation and crack growth rate study as function of DH2, temperature and stress
  - Explore alternate DH2 levels;
    - either lower or higher than now (30 cc/kg H2O)

845

6. Conclusions

- In-situ Raman spectroscopy system was developed to obtain needed information on oxide films on Alloy 600 in in PWR water conditions .
- Some unique observations were made, compared with earlier ex-situ results;
  - CrOOH phase, undetected by ex-situ methods, was observed under most conditions.
  - $NiFe_2O_4$ usually found in precipitate layer was not observed, conceivably due to the suppression of precipitate layers in this work.
- NiO, Cr_2O_3 and $NiCr_2O_4$ phases were observed, in reasonable agreement with ex-situ results.

6. Conclusions

- **Ni/NiO equilibrium was determined as function of dissolved hydrogen concentration and temperature.**
  - **Comparison of observed results with thermodynamic predictions showed a good agreement on Ni/NiO equilibrium at the temperature range from 250 to 350 degree C.**
  - **A good agreement was found between in-situ Raman results and those from contact electrical resistance (CER) measurements on Ni/NiO equilibrium.**

- **Fluctuation in DH2 in PWR may cause Ni/NiO alternation and accelerate PWSCC**
  - **Stable DH2 control at PWR is suggested**
  - **Systematic study is needed for lower/higher DH2 control for mitigation.**

847

Analysis of Alloy 600 Stress Corrosion Cracking with an Artificial Neural Network.

M.J. Pattison, S. Belsito, S. Banerjee

MetaHeuristics LLC, Santa Barbara, CA 93105

W.H. Cullen

Nuclear Regulatory Commission, Rockville, MD 20852

Contents

1. Available models
2. Approach taken – why neural networks?
3. ANN model developed
4. Results and comparison with data
5. Relative importance of variables

Existing Models

Scott (1991) model:

$$CGR = 2.8\times10^{-11}(K-9)^{1.16}$$

Ford (1987), Ford et al. (1997)

$$CGR = 7.8\times10^{-3}n^{3.6}\left(4.1\times10^{-14}K^{4}\right)^{n}$$

Model temperature dependence as:

$$CGR \sim \exp\left(-E/kT\right)$$

Principal Variables

- Applied stress
- Temperature
- Solution chemistry
  - Impurities and additives, e.g. lithium, boron, sulphates
  - pH
  - Dissolved gases: hydrogen, oxygen
- Alloy properties
  - Composition
  - Grain size
  - Cold/hot work - affects structure and yield strength
  - Grain carbide coverage
  - Carbides present

Diagram of Neural Network

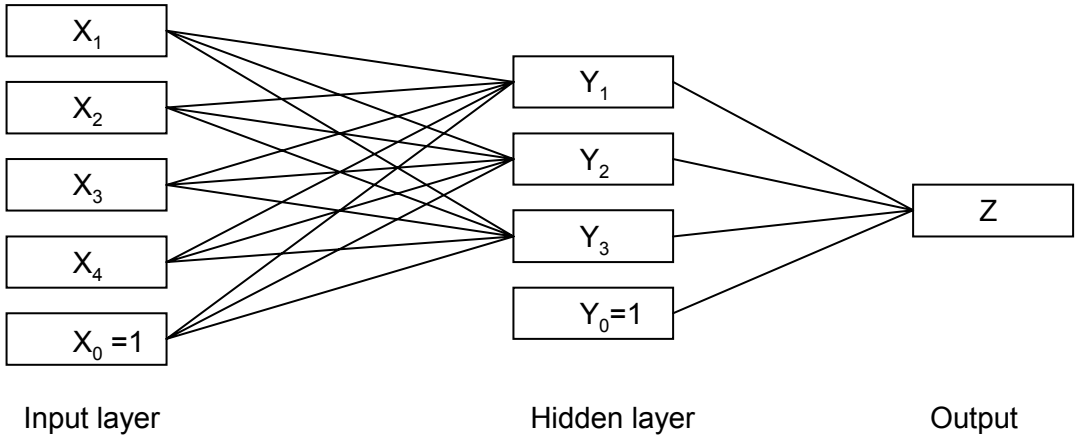

$$\mathrm{Y}_j = f\left(w_{0\,j} + \sum_{i=1}^{i=m} w_{ij} X_i \right)$$

$$f(x) = \tanh(x)$$

$$\mathrm{Z} = f\left(w_0^h + \sum_{i=1}^{j=n} w_j^h Y_i \right)$$

Training of Neural Network

Objective: Calculate weights, **w**, so as to minimise the energy function:

$$e(\mathbf{w}, \mathbf{x}, m) = \sum_{k=1}^{n} \left(z - z_p \right)^2$$

The MetaSolve algorithm uses a novel, computationally efficient, iterative approach using ODEs to determine the weights

Verification of Solution

- Danger of overtraining – with sufficient hidden nodes, the neural net can fit the data to any degree of accuracy
- With an overtrained net, data used for training can be reproduced well, but poor performance will be obtained for other data
- Usual to split the database into two parts – one for training and one for testing

Validation of Model

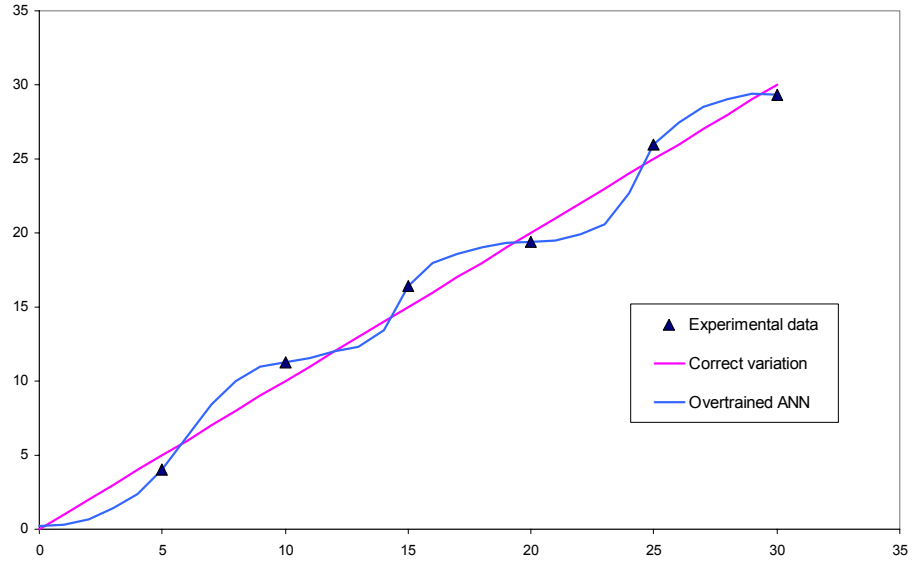

- Overtraining can happen if too many nodes used for number of data
- Split database to check for this:
  - 75% for training, 25% for testing

Database Available

- ~200 experimental measurements of crack growth rates (CGRs)
- Data cover a wide range of applied stress, temperature, and water chemistries
- Number of different specimens used
- Conditions similar to those in a PWR
- Split database 75% for training, 25 for testing

Network Derived

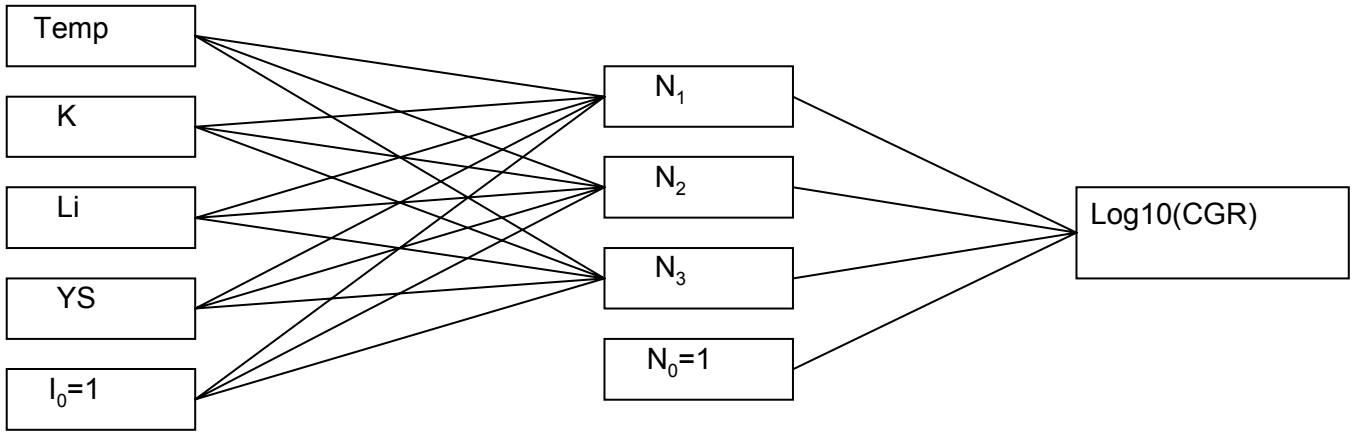

	Node 0	Node 1	Node 2	Node 3
Temperature		-0.19699	-0.27891	-0.2595
Stress		-0.26174	-1.948	-0.39729
Li conc.		-0.07173	2.20143	-0.07249
Yield strength		0.91762	-2.62216	1.57788
I0		-1.34723	-1.59432	-1.38374
Log10(CGR)	-11.364	-0.83189	5.31381	-5.89371

Comparison of Measured and Predicted Data

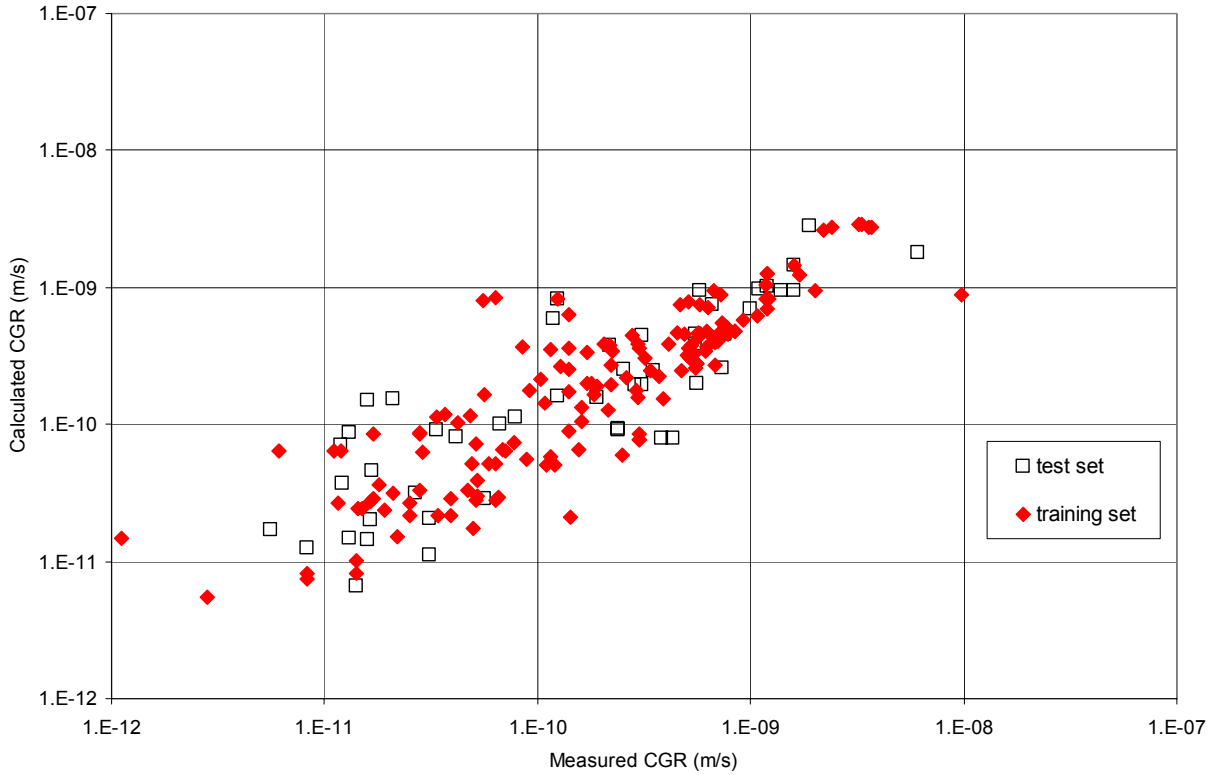

CGR vs. Applied Stress

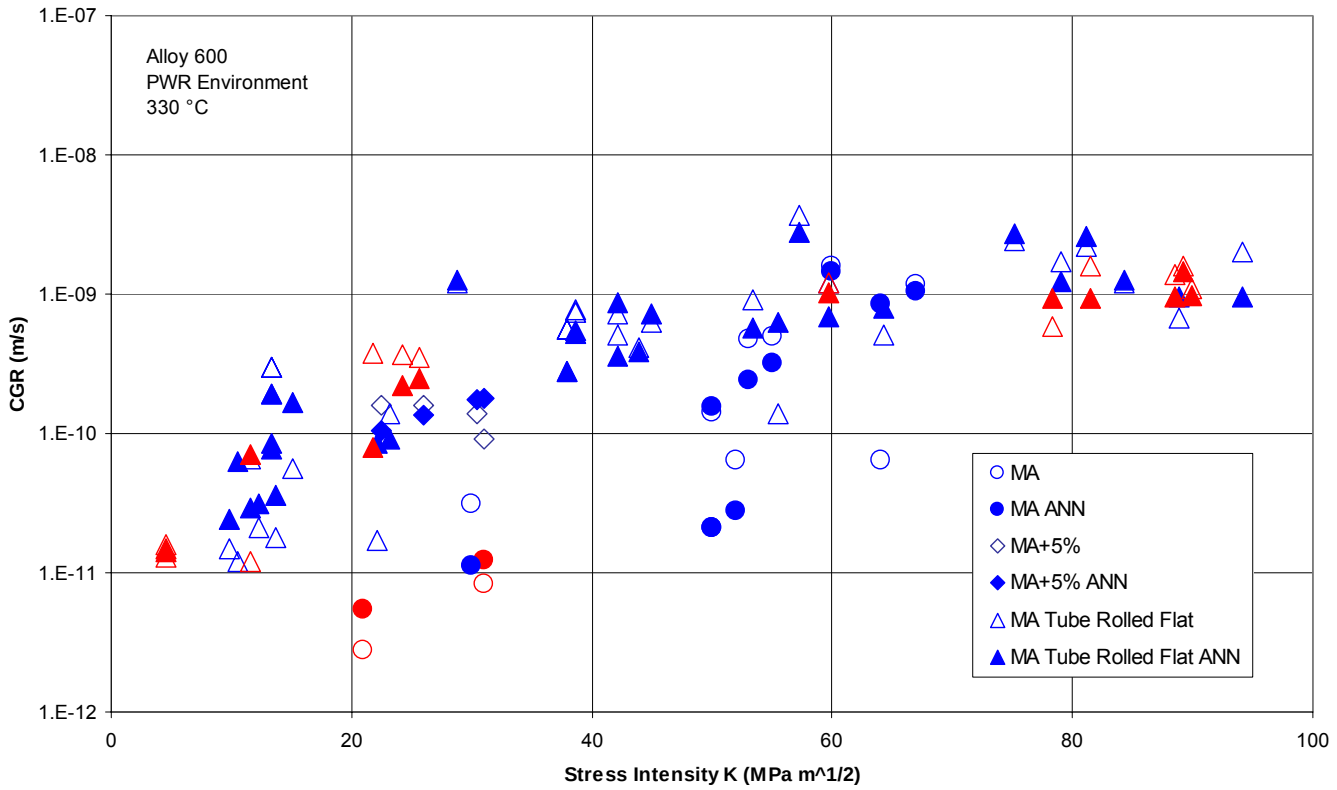

CGR vs. Temperature

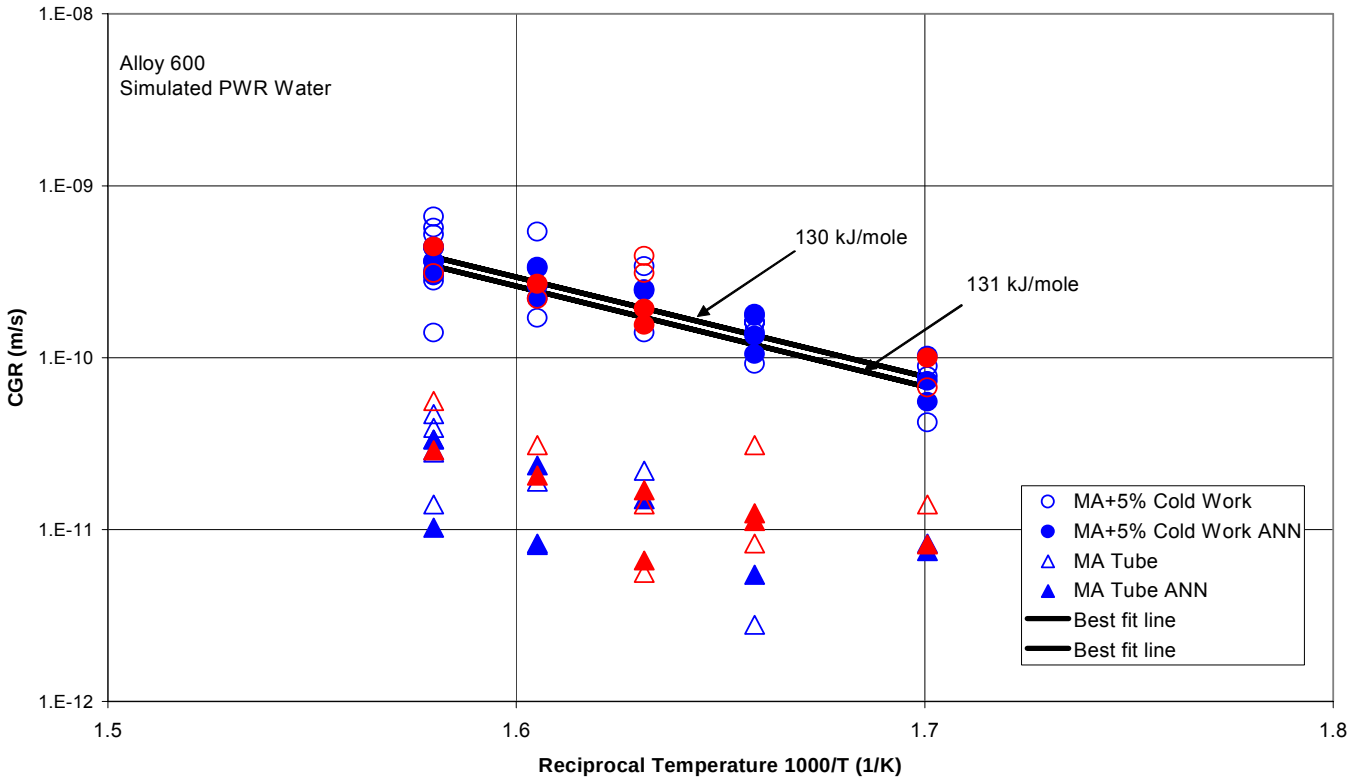

Comparison with Correlations - 330°C

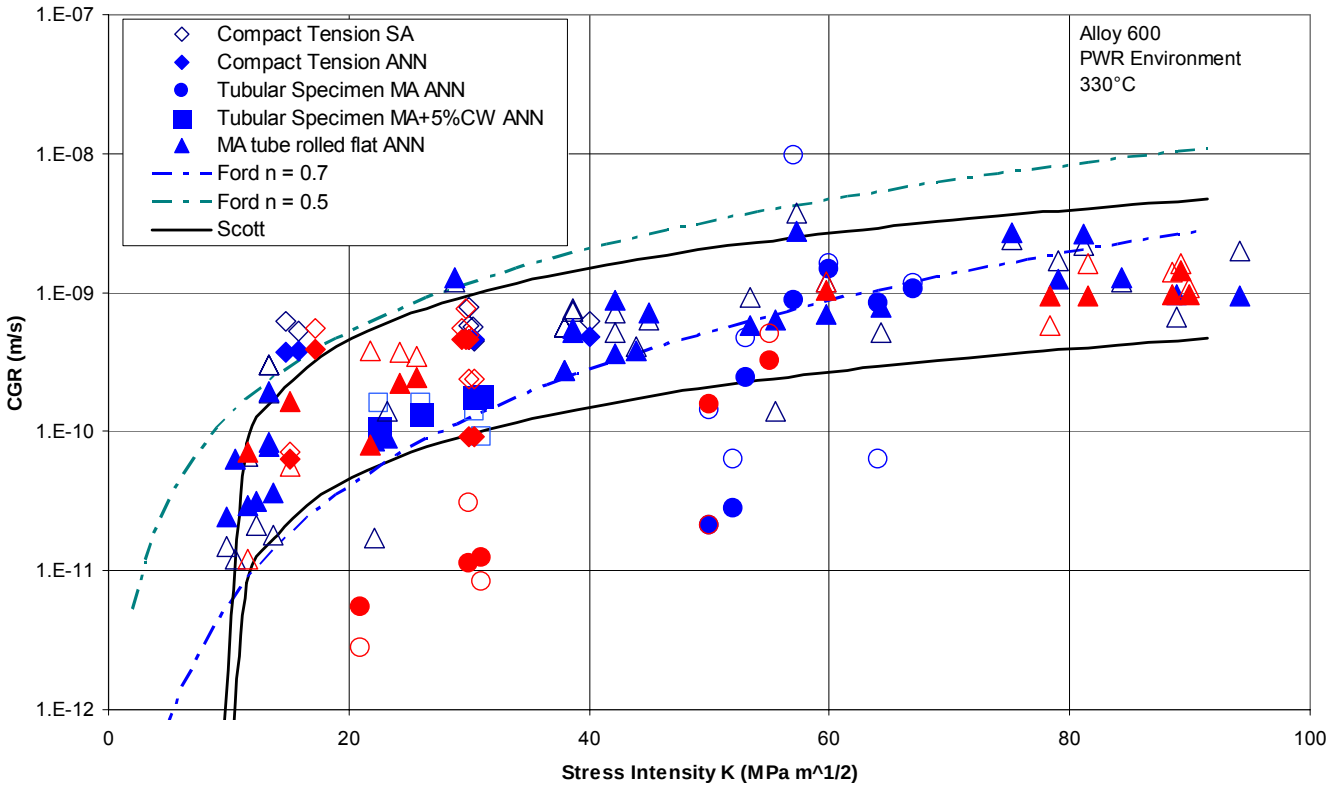

Comparison with Correlations - 350°C

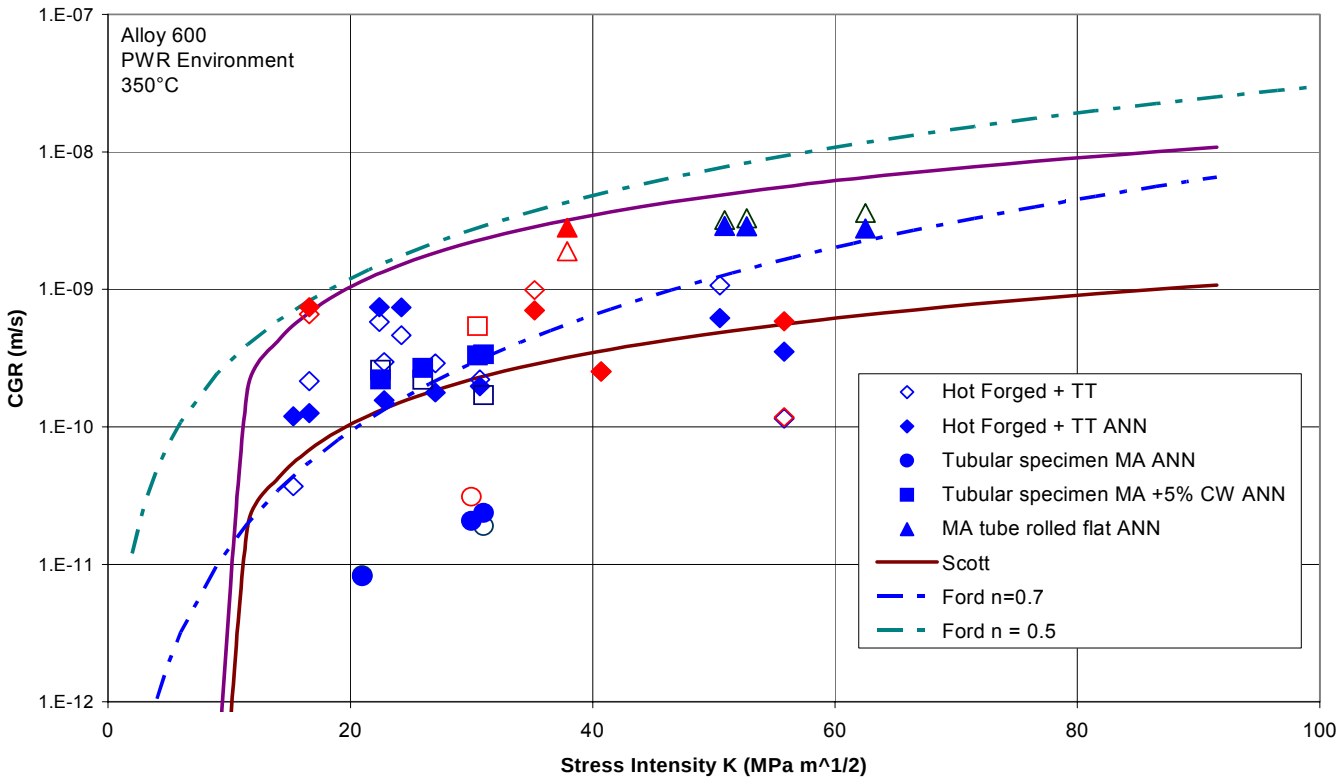

Variation of CGR with Stress for Different Temperatures

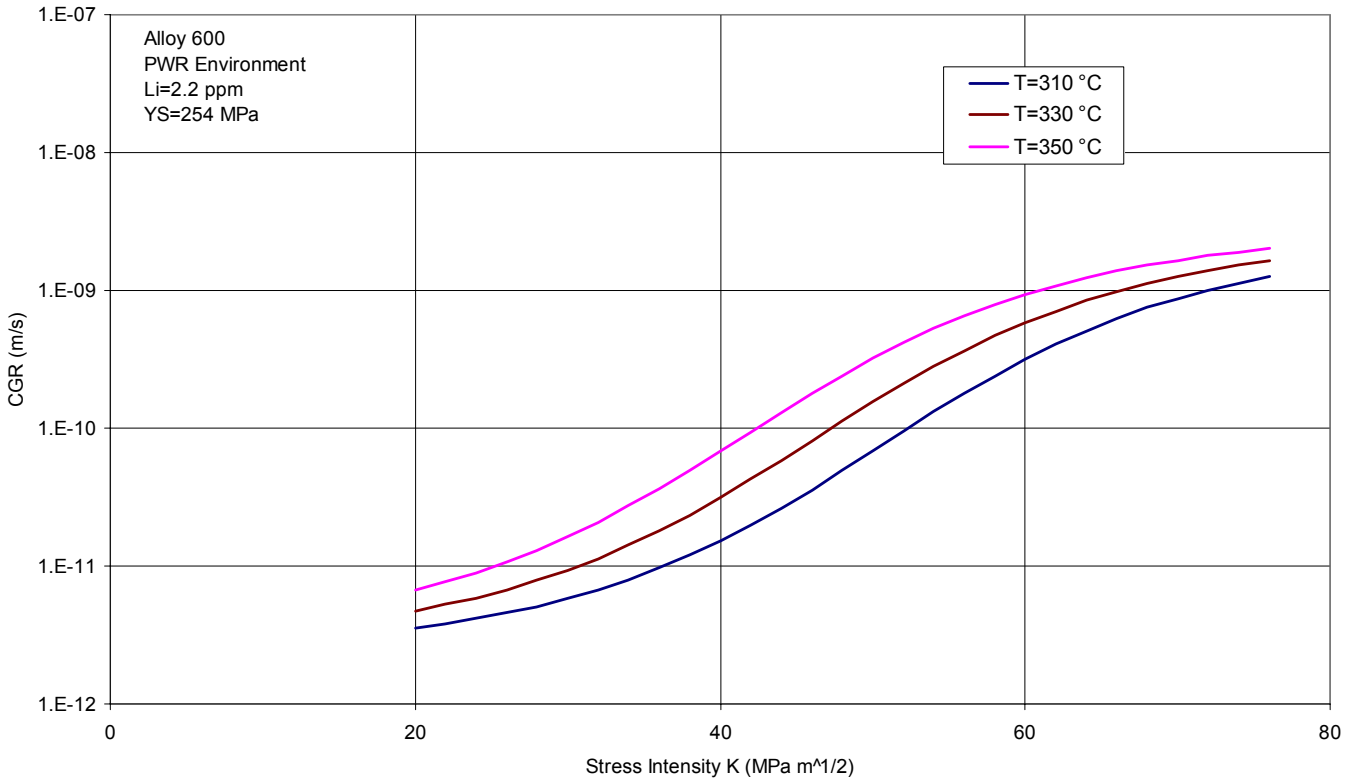

Variation of CGR with Temperature for Different Yield Strengths

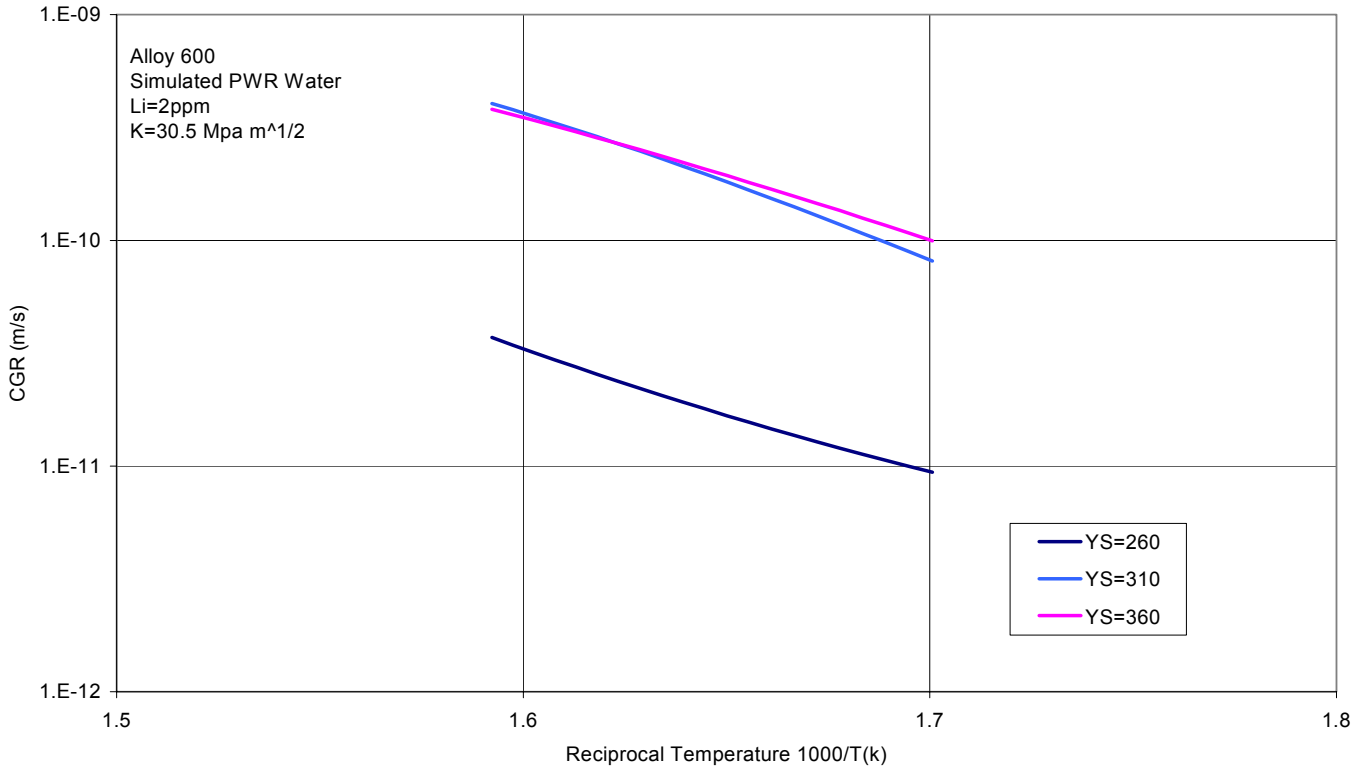

Relative Effect of Variables

Parameter	Variation [decades]	Range	Direction	Notes
Temperature	0.5 (factor of 3)	310 – 350˚C	CGR decreases with temperature	Few data were available for lower temperatures. An activation energy of 130kJ/mol predicts a variation of about 0.75 decades over this range.
Lithium concn.	1 (factor of 10)	0-10 ppm	CGR increases with Li concn.	Most records in database had a conc. of ~2ppm. Comprehensive data for a range of concns. were only available for specimens with a yield strength of ~500 MPa
Applied stress	1 to 2.5 (factor of 10 to 300)	20–60MPam^{½}	CGR increases with applied stress	The CGR was much more sensitive to this parameter for specimens with a low yield strength
Yield strength	1.5 (factor of 30)	200-500MPa	CGR increases with yield strength	Yield strength correlates strongly with amount of cold work

A BNFL Group Company

BNFL

Westinghouse

CONFERENCE ON VESSEL HEAD PENETRATION
INSPECTION, CRACKING AND REPAIRS
Gaithersburg, MD – Sept. 29-Oct. 2, 2003

Results of Accelerated SCC Testing of Alloy 82, Alloy 182 and Alloy 52M Weld Metals

R. J. Jacko, R. E. Gold, G. V. Rao,

A. Kroes [Westinghouse Electric] and K. Koyama** [MHI]

BNFL

Westinghouse

Presentation Content

- Background
- Experimental Program and Approach
  - Materials
  - Test Environments
- Results of Corrosion Testing
- Conclusions

Background

- Increased incidences of environmental degradation (PWSCC) of Alloy 600 and the corresponding weld metals have emphasized the need for expanding the corrosion test database.
- The research reported here was conducted to examine:
  - Crack initiation in Alloy 52M (and controls of Alloy 182 and Alloy 600), used for recent weld metal repairs at Ringhals 3 and 4,
  - Crack initiation in Alloy 82 and Alloy 182 weld metal specimens removed from the V.C. Summer RV nozzle safe-end that cracked in service in 2000, and
  - Crack growth rates in the V.C. Summer Alloy 82 and Alloy 182 safe-end weld metals.

870

Overall Test Matrix

MATERIAL	CRACK INITIATION 400°C	CRACK INITIATION 360°C	CGR TESTS 0.5T-CT 325°C
Alloy 82	--	X	X
Alloy 182	X	X	X
Alloy 52M	X	--	--
Alloy 600	X	--	--
Approx. Stress	500 MPa (73 ksi)	500 MPa (73 ksi)	--
Levels	360 MPa (52 ksi)	400 MPa (58 ksi)--	--
Stress Intensity	--	--	20, 35 MPavm

Experimental Program – Crack Initiation Tests

- Four-point bent-beam specimens of Alloy 52M and Alloy 182 weld metal were tested at strains of 0.35 and 1.0 % in a 400°C doped steam environment for periods equivalent to more than forty years at normal operating temperatures.
  - Alloy 600 specimens from archived sections of a CRDM nozzle were included as controls.
- Four-point bent-beam specimens of the V.C. Summer Alloys 82 and 182 weld metals were exposed for 3522 hours in a 360°C (680°F) simulated primary water environment with applied loads equivalent to surface stresses of 400 and 500 MPa.

872

Test Configuration – 400°C Steam Tests
Alloy 52M / Alloy 182 welds – 4 point Bending

Welds for Ringhals 3 and 4 tests are 9 mm thick,
Specimens machined from pre-repair qualification welds

Photos of Alloy 82/182 VC Summer Weld Specimens Accelerated testing in 360°C Primary Water

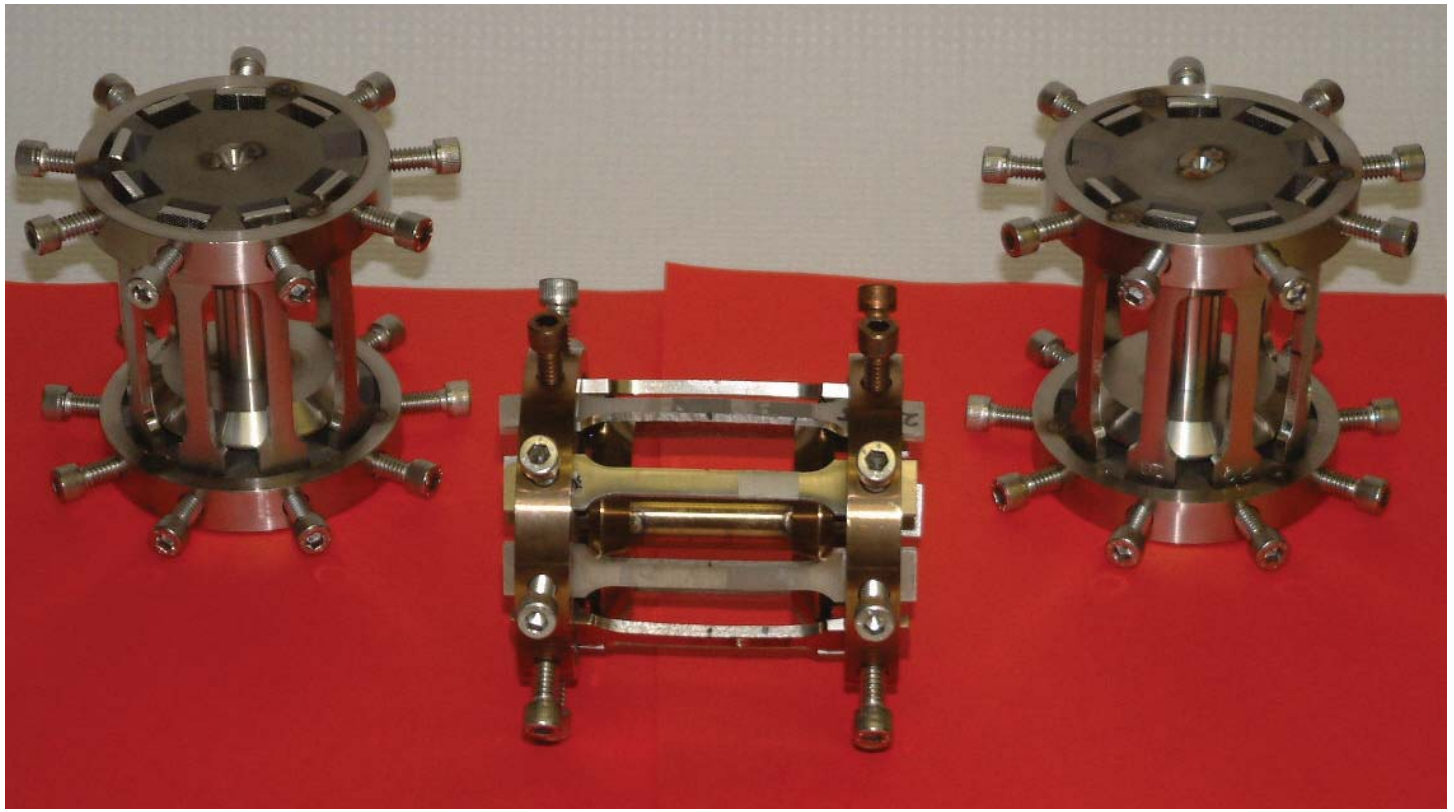

Experimental Program – Crack Growth Rate Tests

- Crack growth rate tests were performed on 0.5T-compact tension specimens of the V.C. Summer Alloy 82 and Alloy 182 weld metals.
- Testing was performed in 325°C (617°F) simulated primary water; 3.5 ppm Li, 1800 ppm B, 32 cm^3 (STP)H_2/kg H_2O.
- Specimens were actively loaded to nominal stress intensities of 20 and 35 MPa$\sqrt{m}$.
- Specimens were periodically unloaded to 0.7 initial load
  - Unloading period 1000 s / 9000 s / or constant load
- Crack growth was monitored using reverse DC potential

875

Crack Initiation Test Results – Alloy 52M, Alloy 182 and Alloy 600 in 400°C Doped Steam

- Alloy 52M is a modified version of Alloy 52 and is used for GTA welding of Alloy 690 [30% Cr compared to 14-16% Cr typical for Alloy 600 and Alloy 182].
- The doped steam-plus-hydrogen environment, containing
  - 30 ppm of F^-, Cl^-, and $SO_4^=$ and
  - 75 kPa of hydrogen in 20 MPa steam,
  - provides an acceleration factor estimated as 195 relative to corrosion at the 322.8°C Ringhals 3 & 4 RV outlet temperature.
- Weld specimen test articles were 180 mm x 40 mm x 9 mm Alloy 600 specimens were 102 mm x 19 mm x 3.8 mm.

876

Crack Initiation Test Results – Alloy 52M, Alloy 182 and Alloy 600 in 400°C Doped Steam (cont'd.)

- The 4-point bent-beam specimens were loaded to either
  - 0.35% strain or
  - 1.0% tensile surface strains;
  - the strains were monitored by strain gages.
- The stresses were "stabilized" by 16 to 19-hour exposures at 400°C, after which the specimens were unloaded and reloaded
- These strains corresponded to residual stresses in the range
  - 320 to 400 MPa [46.4 to 58.0 ksi] for 0.35% strain and
  - 440 to 560 MPa [63.8 to 81.2 ksi] for 1.0% strain.

877

Crack Initiation Test Results – Alloy 52M, Alloy 182 and Alloy 600 in 400°C Doped Steam (cont'd.)

- Interim inspections were performed at intervals varying from 120 hours (early) to 450 hours; at 418 hours, the strains were "verified" by unload-reload.
- After 2051 hours (equiv. to 45.7 efpy), crack initiation was not observed in the Alloy 52M specimens.
- For Alloy 182, cracking occurred in the high-stress specimens after 214 hours [4.8 equiv. efpy], and in the low-stress specimens after 450 hours [10 equiv. efpy].
- Alloy 600 controls cracked only at the high-stress condition in times from 450 to 598 hours [10 to 13.3 equiv. efpy]. This heat of Alloy 600 exhibits generally good resistance to PWSCC.

878

Crack Initiation Test Results – V.C. Summer Alloy 82 and Alloy 182 in 360°C Primary Water

- Specimens were pre-strained to permit testing at 400 and 500 MPa [58.0 and 72.5 ksi] as four-point bent-beams.
- The test environment was 2.0 ppm Li, 500 ppm B and 25-35 cm^3 (STP) H_2/kg water at 360°C (680°F).
- After a total exposure time of 3522 hours, crack initiation was not observed in careful post-test examinations.
- Time equivalent to 5.9 efpy in VC Summer Nozzle
  - Cracking detected at VC Summer after 13.1 efpy in 2000

879

Crack Growth Rate Test Results – V.C. Summer Alloy 82 and Alloy 182 in 325°C Primary Water

- 0.5T-compact tension specimens of the V.C. Summer weld metals were tested at stress intensities of 20 and 35 MPa√m.
- The test environment consisted of 3.5 ppm Li, 1800 ppm B and 30-35 cm^3 (STP) H_2/kg water at 325°C (617°F).
- Specimens were fatigue pre-cracked in air at a stress intensity less than 15 MPa√m.
- Specimens were periodically unloaded to 0.7 initial load.
- Reverse DC potential drop was used to monitor crack growth

880

Crack Growth Rate Test Results – V.C. Summer Alloy 82 & Alloy 182 in 325°C Primary Water (cont'd.)

- Only relatively small differences were observed in the crack growth rates in the Alloy 82 and Alloy 182 specimens.
- The crack growth rates were measured to be between the 75th percentile curve for Alloy 600 (EPRI-MRP) and the curve presently proposed in a preliminary EPRI model for Alloy 182 (PWR MRP-21; TR-1000037).

881

Fractographs – Optical and SEM of 182

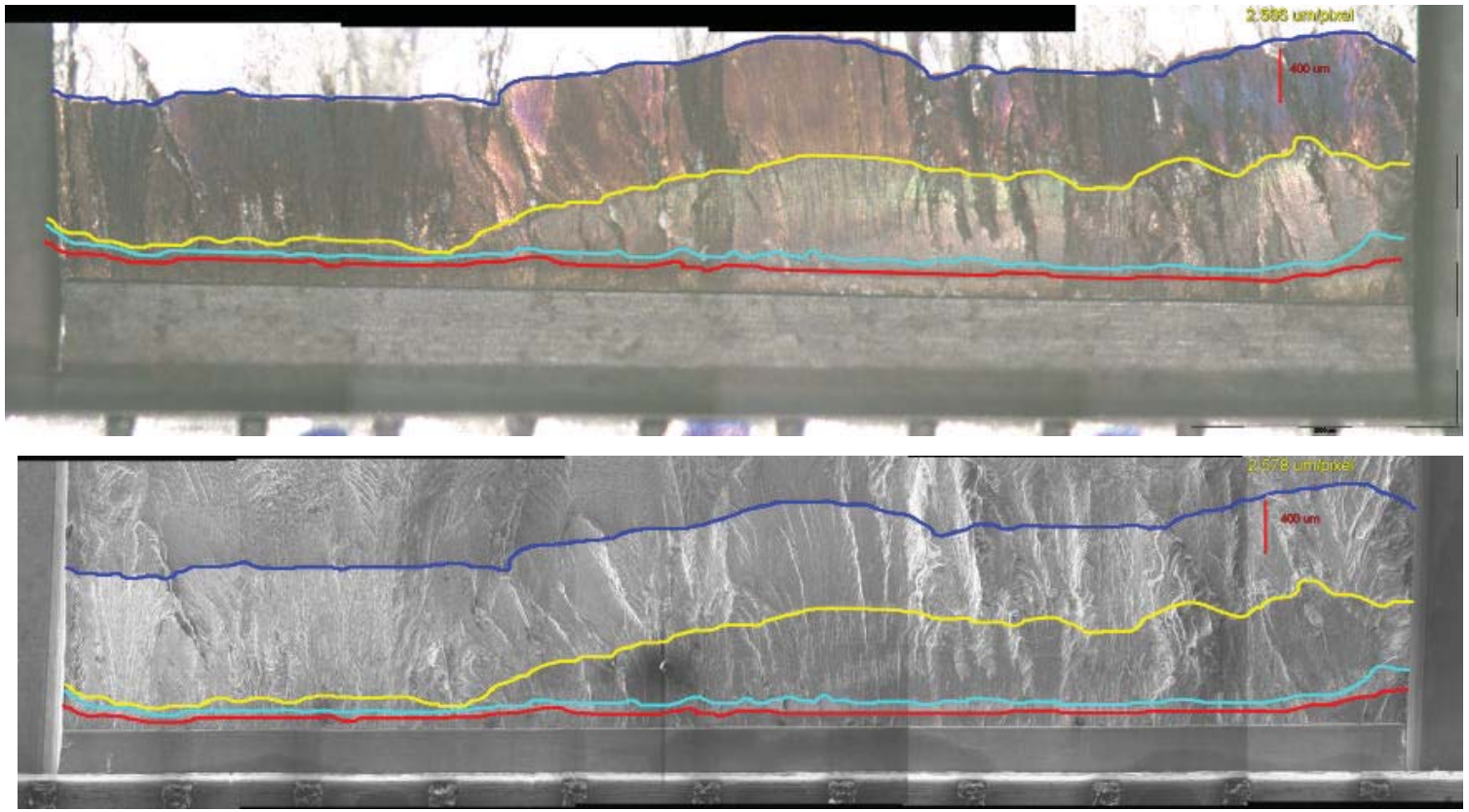

882

Comparison of VC Summer Alloys 82 and 182 Results with EPRI Models

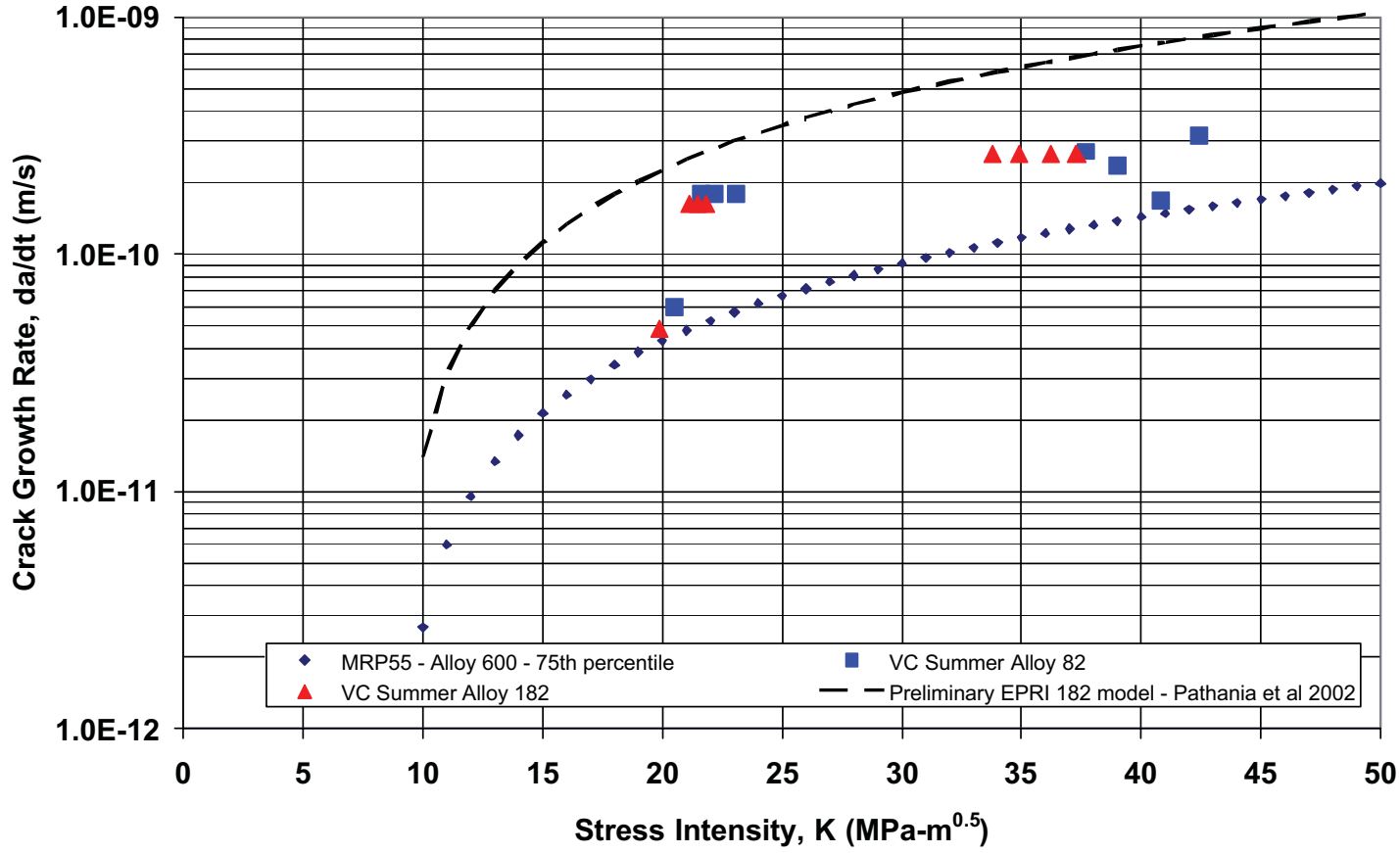

Summary - 400°C Doped Steam Crack Initiation Tests for Ringhals 3 and 4

- Alloy 52M exhibited complete resistance to crack initiation under conditions of high stress (strain)
  - for exposures equivalent to more than 45 years of [322.8°C] operating experience.
- Crack initiation occurred in Alloy 182 and Alloy 600 specimens in shorter periods
  - Alloy 182 equivalent to 5 – 10 efpy
  - Alloy 600 equivalent to 6 – 13 efpy in service.

884

Summary - 360°C Primary Water Initiation Tests VC Summer Weld Material

- V.C. Summer Alloy 82 and Alloy 182 nozzle safe-end weld metal specimens, strain-hardened and stressed to 400 and 500 MPa, resisted crack initiation for 3522 hour exposures in primary water
- Equivalent to > 5 efpy at 320°C (608°F) approximate nozzle outlet temperature].

885

Summary - 325°C Primary Water Growth Rate Tests VC Summer Material

- Crack growth rates measured for Alloy 82 and Alloy 182 RV nozzle safe-end weld metals at stress intensities of 20 and 35 MPa$\sqrt{m}$ were similar
- Growth rates obtained were between the 75th percentile curve for Alloy 600 and a preliminary Alloy 182 curve proposed by EPRI.

886

Conclusions

- Cracking did not initiate in Alloy 52M under extremely aggressive and accelerated test conditions
- Under similar conditions, crack initiation occurred in Alloy 182 weld metal and Alloy 600 CRDM nozzle material
- The V.C. Summer Alloy 82 and Alloy 182 weld metals exhibited fairly good resistance to crack initiation; measured crack growth rates were consistent with the general industry database.

887

888

A BNFL Group Company

BNFL

Westinghouse

A BNFL Group Company

BNFL

Westinghouse

CONFERENCE ON VESSEL HEAD PENETRATION INSPECTION, CRACKING AND REPAIRS
Gaithersburg, MD – Sept. 29-Oct. 2, 2003

Metallurgical Investigation and Root Cause Assessment of the Reactor Vessel Head Penetration Alloy 182/82 J-Groove Weld Cracking in Two Rotterdam Vessels

GUTTI RAO[1], GORAN EMBRING[3], JIM BENNETCH[2], and WAYNE GAHWILLER[1]

[1]Westinghouse Electric Company, Pittsburgh, PA;
[2]Dominion Generation; [3]Vattenfall AB

BNFL

Westinghouse

Objective

- To establish the Mechanism and Root Cause of the CRDM Alloy 182/82 J-Weld Cracking in Rotterdam Vessels

Investigation Centered on J-Groove Weld Indications

- Ringhals 2 CRDM Penetration 62
- North Anna 2 CRDM Penetration 62

892

Summary of Hot Cell Investigations

- Surface Examinations
- Metallographic Examination of the boat Sections
- Fractographic Examination of the freshly opened cracks
- Chemistry Assessment of the weld metal regions and fracture surface by:
  - Energy Dispersive X-Ray Analysis
  - Microprobe Analysis
  - X-Ray Diffraction Analyses Techniques
- Review of the original Fabrication Records
- Mechanistic and Root Cause Assessments

NORTH ANNA 2 - BACKGROUND

- Fall 2001 Outer Surface Inspections of the RV Head revealed Boric Acid Crystals encircling three (Nos. 51, 62 and 63) of the 69 Penetrations
- Subsequent inspection of the Bottom ID Surface of the Vessel Head revealed crack-like indications in the vicinity of the J-Groove weld/butter region of the three penetrations
- An 0.5 inches wide, 2 inch long boat sample, circumferentially positioned in the butter region of the weld and containing the affected region, was removed for investigation
- Hot Cell investigation was conducted at Westinghouse Pittsburgh Laboratories

NORTH ANNA BOAT SAMPLE

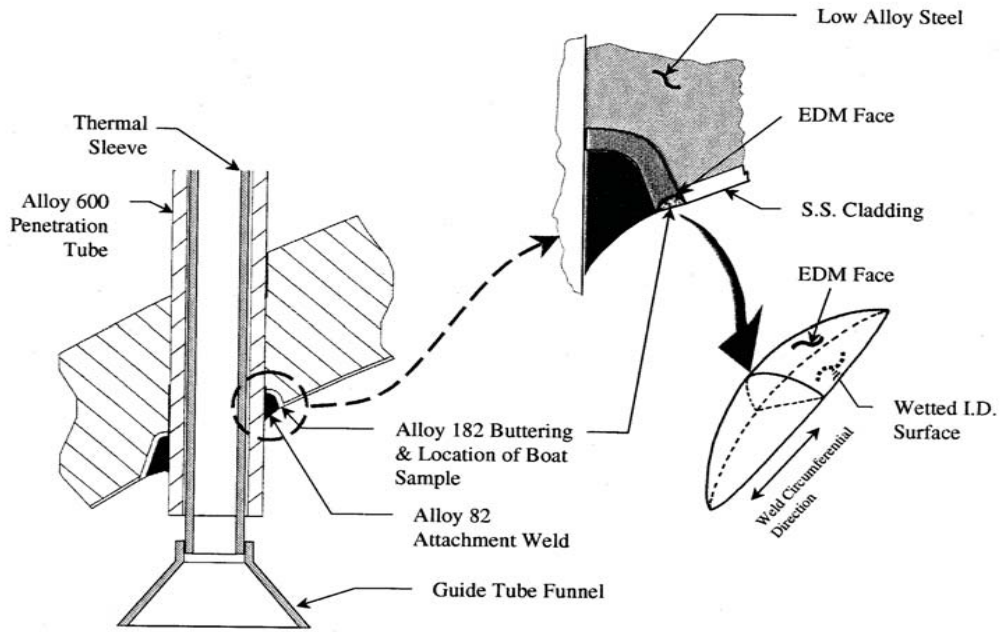

Schematic Representation of the Boat Sample Location in North Anna 2 Reactor Vessel Head Penetration J-Groove Weld

SUMMARY OF NORTH ANNA 2 BOAT SAMPLE

- Examinations confirmed extensive hot cracking in the buttering adjacent to the low alloy steel and stainless steel interfaces
- Few of the hot cracks extended to the wetted ID surface of the buttering
- The propensity of hot cracking in the buttering decreased as we moved away from low alloy steel interface

968

NORTH ANNA 2 BOAT SAMPLE

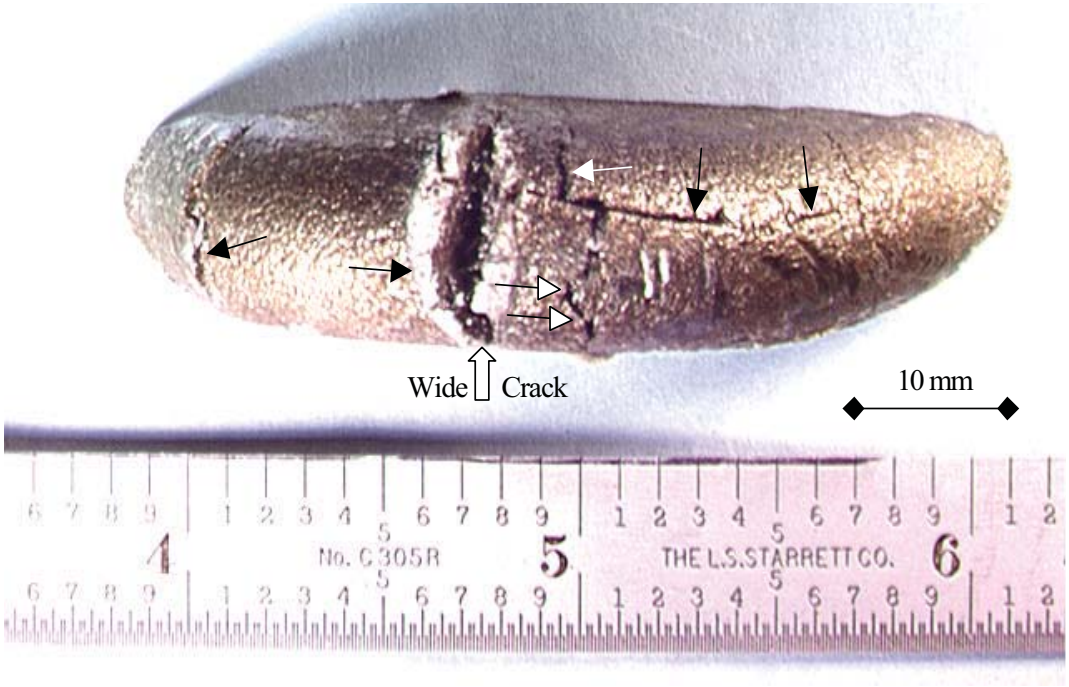

Illustration of the EDM Cut Face
North Anna 2 Boat

NORTH ANNA 2 BOAT SAMPLE

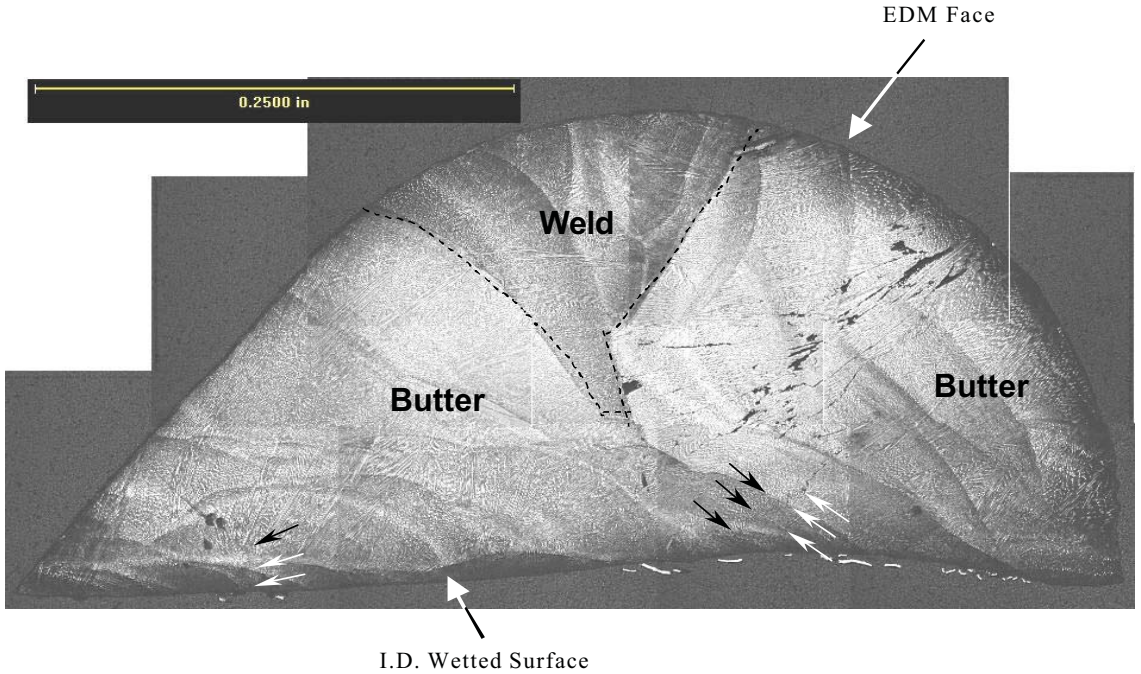

Metallography with Identified Butter and Weld Regions
By EDAX Analysis, North Anna 2 Boat

898

NORTH ANNA 2 BOAT SAMPLE

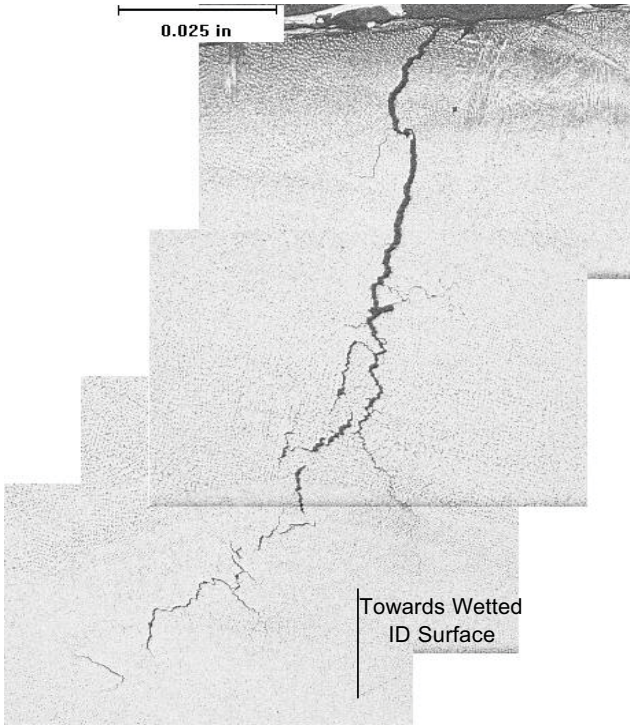

Axial Section of North Anna 2 Boat, Showing PWSCC Crack Progressing from EDM Cut Fact to the Wetted ID Face of RVH

668

RINGHALS 2 - BACKGROUND

- 1993 outage inspections revealed a 7-inch (18 cm) long circumferentially-oriented surface indication in the J-weld of Penetration No. 62
- Investigations centered on:
  - Two small boats – 1 inch diameter and 0.1 inch thick
  - Two large boats – 2.75 inches long, 0.8 inch deep
- Hot Cell investigations were conducted at:
  - Studsvik Laboratory in Sweden
  - Westinghouse Laboratories in Pittsburgh, USA

900

SUMMARY OF RINGHALS 2 BOAT SAMPLES

- Evidence of 0.02 inch-wide crack between low alloy steel and Alloy 182 buttering running along the entire boat length
- The crack was arrested and blunted as it extended into the Type 309 stainless steel cladding
- The crack appeared wider at the EDM cut face and it narrowed down as it approached cladding
- Incomplete wetting (fusion) of the first layer of buttering resulting in “lack of fusion” defects at the interface
- Significant carbide precipitation in the fusion zone
- The interconnected microfissures provided access of primary water to the weld interface and contributed to:
  - Microscopic wastage of low alloy steel interface
  - Secondary crack extension of the weld defects by PWSCC

901

RINGHALS 2 BOAT SAMPLE

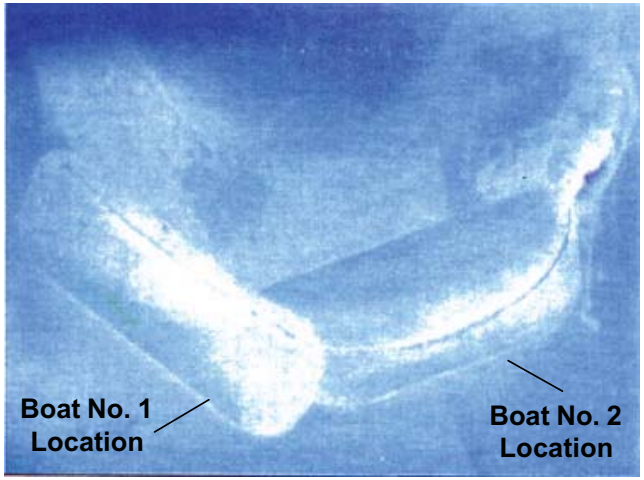

Before PT

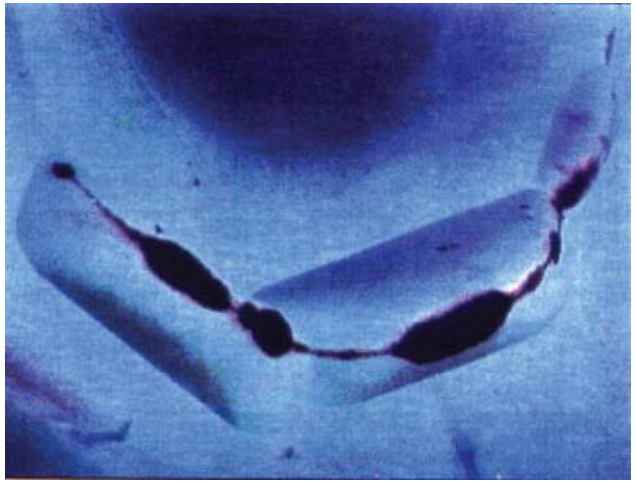

PT Results

Appearance of Crack at the Bottom of Divots
(Ringhals 2 Penetration 62)

902

RINGHALS 2 BOAT SAMPLE

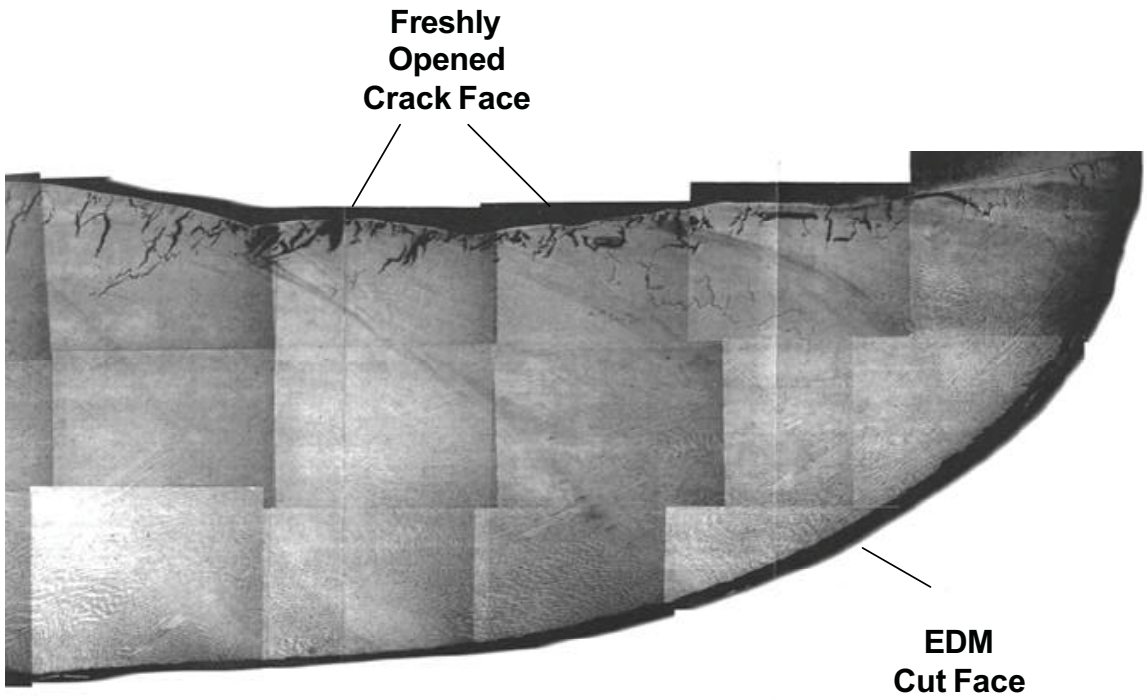

Cracking Morphology in the Butter at the Nozzle Interface (Large Boat 1)

903

RINGHALS 2 BOAT SAMPLE

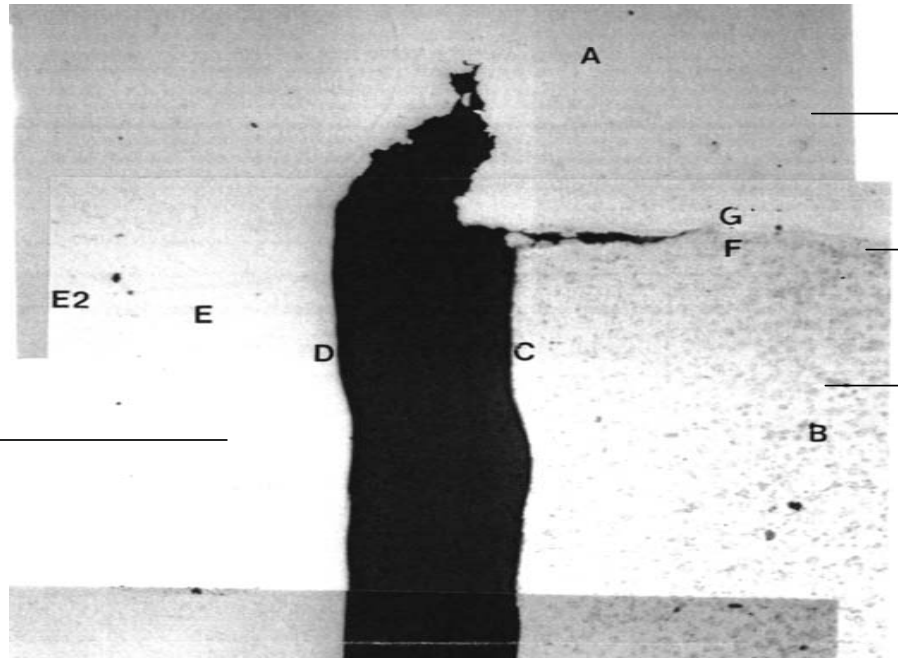

Crack Termination at the Cladding

RINGHALS 2 BOAT SAMPLE

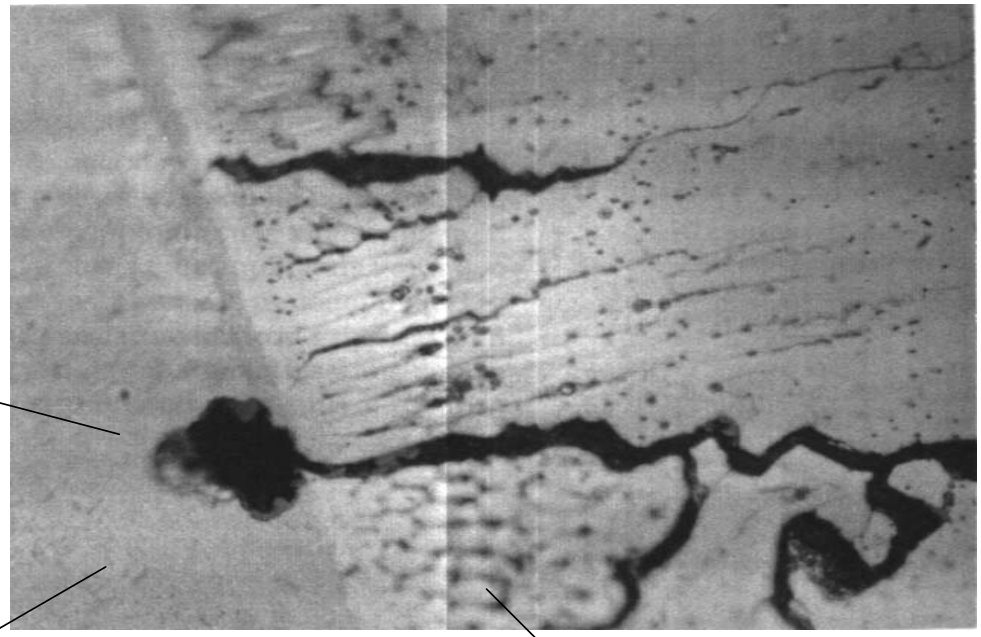

Evidence of Carbon Steel Wastage at the Butter Interface

905

ROOT CAUSE CONSIDERATIONS AND POSTULATED MECHANISM

- The J-Weld preparation by Air Arc Gouging Technique left an oxide layer and carbon residue on the low alloy steel surface
- Inadequate cleaning prior to welding left oxide, carbon and moisture on the surface
- The surface condition contributed to a non-wetting and lack of fusion bonding during the deposition of the first layer of buttering at the low alloy steel interface

906

ROOT CAUSE CONSIDERATIONS AND POSTULATED MECHANISM (continued)

- Attempt to repair this during subsequent depositions was unsuccessful, leaving presence of heavy carbides, slag inclusions and poor bonding at the interface
- A thin initial layer of buttering and non-uniform temperatures may have led to the de-bonding of the weld interface under the influence of thermal stresses even while the top (ID surface) layers of the weld metal were being deposited
- The movement of the crack faces and the crevice condition of the crack created a strain field at the crack tip during the fusion of the top layers of the weld inducing microfissures due to hot cracking of the weld metal

907

RINGHALS 2 BOAT SAMPLE

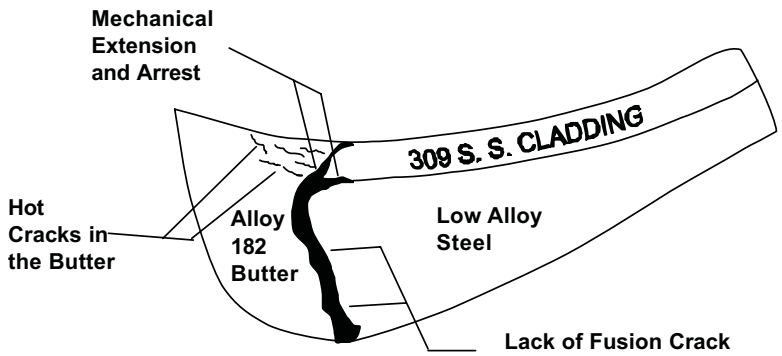

Ringhals 2 Boat Sample (Transverse Section)

808

CONCLUSIONS

- North Anna and Ringhals Boat Samples showed similar characteristics
- The investigation results of the CRDM Penetration cracking at Ringhals 2 and North Anna 2 units supports that the observed cracking originated from the original fabrication of the J-Weld buttering
- The microfissuring of the final layers of weld metal buttering occurred by a “hot cracking” mechanism. Excessive strains caused by the occurrence of a sub-surface larger lack-of-fusion crack at the weld metal to low alloy steel interface most likely contributed to the cracking in the Ringhals weld.

606

CONCLUSIONS (continued)

- The occurrence of the main crack at the weld interface and the microfissuring of the weld metal are both caused by the inadequate surface preparation of the J-Groove prior to the welding and/or weld repair
- The root cause of the cracking in the Ringhals and North Anna vessels examined here is believed to be lack of fusion at the Low Alloy Steel Interface
- Primary water accessed to the area of lack of fusion through exposed hot cracks at the wetted surface provided potential for additional cracking by PWSCC

910

A BNFL Group Company

BNFL

Westinghouse

French Regulatory Experience and Views on Nickel-Base Alloys PWSCC Prevention & Treatment

by

Guy TURLUER, Gérard CATTIAUX, Bernard MONNOT

(IRSN/DES, Fontenay-aux-Roses, France)

Institute for Radiological Protection & Nuclear Safety *

Department of Safety Evaluation

and

David EMOND , Jacques REUCHET, Philippe CHARTIER,

(DGSNR/BCCN, Dijon, France)

General Directorate for Nuclear Safety and Radiological Protection **

Nuclear Steam Supply System Inspectorate

* http:/www.irsn.fr/ guy.turluer@irsn.fr , fax: + 33 1 47 46 10 14

** http:/www.asn.gouv.fr/ david.emond@asn.minefi.gouv.fr , fax: + 33 3 80 29 40 88

French Nuclear Safety Bodies Presentation Outline

- Context & objectives of a presentation by French Nuclear Safety Bodies
- Specific features of French nuclear organizations and practices
- An all PWR fleet prone to « generic effects » illustrated by the Inconel Zones

- Features , Principles and Evolution of French Regulatory Rules
- Specific Features of Alloy 600 PWSCC
- « Inconel Zones Review », A Proactive Approach to maintenance vs PWSCC
  - background
  - objectives
- Treatment of Inconel Zones
- Use of PWSCC initiation models (Interest and limitations)
- Involvement of ASN / IRSN in the implementation and follow-up of a comprehensive In Service Inspection (ISI) Program
- Status of Vessel Head Inspection and Replacement
- Status and Prospects for Bottom Vessel Head Penetrations in France

- Future Prospects and Investigation Needs
- French Nuclear Safety Authority (ASN) & IRSN CONCLUSIONS

Context & Purpose of the IRSN/DGSNR Presentation in this Conference
Presentation of the French Nuclear Safety Organizations & their role

EDF the French sole Nuclear Operator in France, in the first place, responsible for the Nuclear Safety of a fleet of 58 PWRs: It has:

- **A large expertise in terms of R/D, failed components investigation capabilities,**
- **International activities and is an active EPRI member,**
- **Structured and comprehensive maintenance programs and central support staffs to anticipate problems and instruct an important experience feedback,**
- **Units and staffs devoted to manage safety, set doctrines & audit their implementation.**
- **been PROACTIVE with regard to the Inconel vessel penetrations since 1991**

The vigilance and positions of the French Safety Bodies may have played a crucial role in the early strategies and steady follow up of the Inconel Saga.

Hence the objectives of the IRSN/DGSNR (ASN) presentations:

- **Recall the main specific aspects of the French situation vs. the Inconel zones,**
- **Recall the main regulatory features and their evolutions in France,**
- **Present the « PROACTIVE Inconel Zones » return of experience », as perceived by the Safety Bodies from the technical and regulatory stand point,**
- **Explain the reasons for the technical and regulatory positions of DGSNR/IRSN on the now 13 years old « Inconel Zones Review » in France,**
- Bring some Testimony in the USA, in the wake of the « Davis Besse Lessons Learned Issue »

Specific features of French Nuclear Organizations & Practices

- One Nuclear Power Operator of a fleet of 58 PWRs — EDF
- One Power Reactor Manufacturer — Framatome-ANP
- One Scientific Organization in charge of Nuclear R&D — CEA
- One Regulatory Body for Nuclear Safety & Rad Protection — (ASN) ⇔ DGSNR
  - Central Staff (150 members) + regional offices (100 members) ….
- One Body for Nuclear Safety and Radiological Protection, (staff 1500) — IRSN
  - performing Research mainly in accident studies, radiological protection…
  - & Technical Support to DGSNR, (staff : 350), some specialists following Materials, Components, NDE, R&D issues, with some limited confirmatory or exploratory Research

- **No License Renewal in FRANCE,**
- **Importance of Decennial Complete Visits for: (DCV = 10 yearly outage)**
  - Comprehensive Components Condition Investigations, Repairs , Replacements
  - and for Safety Reassessment, & Implementation of Safety improvements
- **Decennial Complete Visits (DCV)** including regulatory hydro test for primary circuit
  - CP 0 (900 MWe) Second DCV, nearing Third (BUGEY 3 CRDM Leak at 1st DCV)
  - CP1-CP2 (900 MWe) first DCV, some Second DCV
  - P4-P'4 (1300 MWe) first DCV
  - Latest French Design N4 series (4 Units) , commissioned in 1996-99

An All PWR Fleet of 58 Reactors, where Alloys 600/182-82 extensively used

- An important all PWR fleet (63 GWe- 80 % of French electricity)
- Standardized in 4 PWR series constructed and commissioned in a crash program,
- Sensitivity to generic effects,
- Advantage for the return of experience.

Some differences with the use of alloys 600, 600 TT, 690 , Stainless Steel within the series

SERIES	Loops/MWe	N° of units	Date of Commission	Main Specific initial features, as commissioned
CPO	3 /900	6	1977-79	Hot Plenum, Bugey 3 (1978)
CP1-CP2	3 /900	28	1981-87	Cold Plenum, Blayais 1, (1981) some SG tubing in 6OO TT
P4 –P'4	4 /1300	20	1984-93	Hot Plenum, Alloy 600 TT for SG Alloy 600 for PZR nozzles, Cat. 2 (1987)
N4	4 /1450	4	1996-99	Alloy 690 for SG, CRDM (4 units) Alloy 690 for BMI (2 units) 3 last Units with Vessel/Primary loop Alloy /82 DMW (600°C stress relieved)

Specific Features of Nickel base Alloys PWSCC

PWSCC may be considered as a major contributor to degradation & aging in PWRs, particularly difficult to assess since:

- **The degradation mechanisms are not yet fully established neither understood,**
- **Characterized by incubation times (crack initiation) which can be very long,** ex: **Fessenheim 2** CRDM first incipient penetration crack detected after some **130 000 h.**, to be compared to some units like **Cattenom (30 000 h.) or Blayais (80 000 h).**
- **Inconel PWSCC crack initiation times t_i are not only governed in a deterministic manner** by various parameters difficult to assess , quantify, and weigh, i. e. :
  - **Actual Wall Temperature and temperature dependence (activation energy)**
  - **Bulk and Surface Residual + Operational Stresses (σ) $\Rightarrow$ $1/t_i \alpha . \sigma^n$, n= 4±?**
  - **Material composition (C content) & microstructure (grain boundary Chromium Carbide relative coverage) and other metallurgical unknowns,**
- **Inconel PWSCC crack initiation times are also governed by stochastic processes** and characterized by a large scatter (large distribution of time to initiation for identically stressed carefully controlled identical Inconel specimen even in the laboratory tests,
- **Stress Assessment :** actual **residual stress** fields, **bulk**, **surface**, **static** and some **dynamic operation cycling or transients** may strongly govern in a complex manner both Crack Initiation (CI) & Crack Propagation Rates (CGR).

Features, Principles and Evolution of French Regulatory Rules to Ensure Integrity of the Main Primary Circuit *(1/3)*

Evolution of French Regulatory Practices:

- **Ministerial order 1974 :** concerning the Main Primary Circuit **(manufacturing and operation),**
- **Ministerial order 1999 : concerning the surveillance in operation for Main Primary and Secondary Circuits,**
- **RCCM code (last edition June 2000),**
  (Rules for Conception, Construction of PWR Mechanical components):
  compiled by EDF (utility) and Framatome (designer/manufacturer);
- **RSEM code (first edition 1997) :**
  - **Rules of Surveillance in Operation for PWR Mechanical components, compiled by EDF**
  - **and accepted by French Safety Authority (ASN)**
- **Regulatory decisions since 2000: ASN may write and publish decisions (web site),**
  - **with requests about important technical problems,**
  - **for example the decision for Inconel Zones (IZ) in March 2001.**

Features, Principles of French Regulatory Rules to Ensure Integrity of the Main Primary Circuit (*continued, 2/3*)

- **Preclude (avoid and prevent leak) any leak in the main primary circuit**
- **Make sure that no flaws would lead to a leak during operation**
- **Methodology pertaining to the so called « Sensitive Zones »(SZ)**
  - **Search for possible degradations through:**
    - **Design files (Stress analysis reports),**
    - **Fabrication files (repairs, deviation from procedures),**
    - **Complex loads such as mixing fluids, possible synergetic effects of cyclic loads on SCC,**
  - **Sensitivity analysis ⇒ zones ranking regarding their sensitivity to some likely degradation mechanisms (such as corrosion, SCC, Fatigue, Corrosion-fatigue..),**
  - **⇒ Determination of Sensitive Zones (SZ),**
  - **In SZ, knowledge and characterization of the Degradation mechanism(s) anticipated,**
  - **In SZ, determination of flaw critical size (with security margins),**
- **Methodology for In Service Program (ISI)**
  - **Definition of an ISI program as preventive, and capable to detect flaws prior to reaching critical size,**

Features, Principles of French Regulatory Rules to Ensure Integrity of the Main Primary Circuit (*continued 3/3*)

- **Coverage of Inconel Zones Families would be possibly achieved by inspection of several precursor SZ among all the SZs:**
  - **Precursor should be truly representative of SZ (i.e..: same degradation mechanism), provided it is truly demonstrated as a forerunner for initiation,**
    and exhibits a faster degradation propagation rate (CGR),
  - **⇒ requires the definition of extension rules in ISI program.**
- **Methodology of NDE qualification:**
  - **Ensure flaw detection before reaching critical size,**
  - **⇒ choice of NDE method & performances and a qualification process,**
  - **In SZ ⇒ flaw detection demonstration:**
    - **When flaws have already been detected in components,**
      ⇒ »specific» qualification,
    - **When flaws are « feared » but not yet detected,**
      ⇒ »general» qualification,
  - **In Non SZ ⇒ only a description of methods performances is required,**
  - **For each NDE method, the nature, the objective & NDE intervals should be specified.**

INCONEL ZONE REVIEW for the French FLEET of 58 PWRs
(Background which entailed a Strong PROACTIVE PROJECT)

- 1959, by CORIOU et. al. in CEA/Saclay first Laboratory Discovery of Alloy 600 propensity to crack by SCC in PURE WATER at 350 °C,
- 1959-1975, confirmation of Alloy 600 SCC in Pure & in nominal Primary Water (hence the acronym PWSCC, PW for Pure or Primary Water), then ⇒
- Alloy 600 and Nickel base alloys prone to PWSCC in nominal Primary Water (hydrogenated HT water ⇒ places Ni base alloys in the unfavorable SCC susceptibility range close to Ni/NiO transition).
  - ⇒ Generic problem on highly stressed Nickel base alloy components,
  - ⇒ Hence a source of primary components failures and primary water leaks for which anticipation methodologies may be limited*.
- In 1989, in addition to many SG tubing problems, 2 fast PWSCC degradations could occur in France within the first fuel cycle on 1300 MWe units (Nogent 1)
  - Circumferential through wall Cracking on new alloy 600TT, SG tubing on top of TS,
  - Leaks on PZR instrumentation nozzles of 1300 MWe units (made from alloy 600).
- 1989, Initiation of the "Inconel Zones Review" by EDF & Framatome, at the "strong request of ASN, i.e. more than 1 year before the Bugey 3 CRDM leak.

* refer to :« ***status of alloy 600 components degradation by PWSCC in France; incentives & limitations of life predictions as viewed by a Nuclear Safety Body*** » , by G. TURLUER, IPSN/DES/SAMS, Fontenay-aux Roses, France,Proc. of Intern. Symposium on Plant Aging & Life Prediction of Corrodible Structures , May 15-18, 1995, Sapporo, Japan

PROACTIVE « Inconel Zones Review » in France: Objectives and Tasks

- Review for all « Inconel Zones (IZ) Potential PWSCC Occurrence,
- Assess all IZ fitness for service,
- Develop NDE inspections techniques & tooling,
- Implement NDE Program for the most PWSCC prone IZ,
- Justify the IZ Review by a comprehensive R&D Program,
- Refine an empirical PWSCC initiation model for ranking purposes,
- Verify the postulated IZ, time to cracking by a sufficiently large NDE program:
  - Either full scale, (100 %)
  - Or on significant sampling rate,
- Perform a Safety assessment for each IZ, postulating worse consequences:
  - From Leaks, which, in many instances of un-sustained leak, may lead to dry boric acid/salts deposits, with no measurable general corrosion, BUT:
    - small concealed low leak rates may entail penetration OD SCC (Bugey 3, Occonee)
    - to higher leak rates ⇒ corrosion/flow accelerated corrosion to low alloy steel,
  - From a possible Break, including Control rod ejection.
- Prepare for mitigation techniques, including repair or replacement

Use of PWSCC Initiation deterministic (empirical) Models as a Predictive Tool for PWSCC Occurrence in Plants ?

- **Crude Temperature/time models(?), ignoring paramount effects of stress, metallurgical factors, & batch to batch variations, are irrelevant, (misleading?)**
- **More sophisticated models such as those developed in France,**
  either expressed in terms of relative sensitivity of Inconel Zones or estimated time to initiation :
  - **Need a sufficient validation with NDE findings in the field,**
  - **Then may be used with caution for ranking purposes (precursor determination),**
  - **CANNOT be used to predict the time to macroscopic crack initiation (ti) for a given component, since :**
    - **Intrinsic material sensitivity to PWSCC can only be qualitatively estimated,**
    - **Effective Stress, including surface CW, residual Surface Stress due to assembly, machining, grinding or final surface finish (Sigma to the power 4 ± x) cannot be estimated everywhere exactly on as fabricated components,**
    - **Uncertainty brackets cannot easily be estimated (in terms of index or time ti).**
- **IRSN & DGSNR accepted only the empirical models only for**
  - **comparing and integrating Inconel zones data,**
  - **Ranking purposes to set inspections priorities,**
- **IRSN/DGSNR did not accept any absolute time to initiation prediction of the kind «no cracking anticipated before 30years of operation » for a given zone,**
- **Hence the request to proceed to NDE at least on a sampling basis**

Implementation of a comprehensive In Service Inspection (ISI) Program IRSN & ASN involvements (1/2)

Vessel Head CRDM Penetrations

Needs
- Detect, localize cracks
- Identify & size them

Determine field CGR

NDE Development
- NDE qualification:
- Remote Video inspect.
- Dye Penetrant ,
- Eddy Current (EC)
- UT

NDE Implementation
- focus on Max, not only on mean crack depth & CGR
- Devise an adapted NDE program as a function of previous NDE (results)
- Plan a timely V.H. replacement Program
- In situ CGR evaluation from O to max CGR

Safety Bodies involvement at all stages to follow up the dossiers and give advice on

- ☞ methods qualifications, performance assessment,
- ☞ NDE program definition and scope,
- ☞ CGR field data (kinetics and crack profile evolutions) assessment
- ☞ NDE results evaluation,
- ☞ Annual validation of the maintenance program (surveillance, RVH replacement)

IRSN recommendations ⇒ to ASN acceptation, requests &, if need be, ASN decisions

Inplementation of a comprehensive In Service Inspection (ISI) Program IRSN & ASN involvments (2/2)

Other Inconel Zones :
R.V. Bottom Mounted Instrument (BMI) Penetrations
Local Vessel under clad defect repairs with Inconel 182

Nuclear Safety Bodies examine

- ☞ **Maintenance & NDE doctrines, including the analysis of possible «Inconel Zones» degradation, potentially prone to PWSCC or to other types of degradations,**
- ☞ **NDE objectives definition files (*technical requirements*,..)**
- ☞ **Methods qualification results (performances,..)**
- ☞ **Procedures,**
- ☞ **NDE Results,**
- ☞ **NDE « maintenance » programs,**
- ☞ **Miscellaneous : Mitigation and repair files, ..**

IRSN specialists issue recommandations to ASN leading either to EDF proposal acceptation or to further requests or possible ASN decisions*. *(*Published on ASN web site)*

Status of Vessel Head Penetration Inspection and Replacement (as of 07/03)

- **After 12 years of Inconel Zone Policy implementation in France:**
  - **42 vessel heads replaced,** out of 54 units initially fitted with alloy 600 CRDM

    ⇒ **46 units** in operation **with alloy 690 CRDM & vent penetrations,**
- **On 11 out of 42 retired VH, CRDM J groove welds have been inspected in details, by remote high resolution video inspection**
  - **No PWSCC crack initiations were ever found**
- **3 replacement vessel heads with penetrations in alloy 690 have been successfully inspected after some 10 years of operation,**
- **Vessel head replacement planning for the future would normally depend on regular NDE results, on remaining un-replaced VH,**
- **but in many instances, replacement is made by anticipation,**
- Would the VH replacement planning in France be affected by the sudden surge of urgent vessel replacement needs in the USA ?

Present Status of the Inconel Zone Treatment in France (as of 07/03)

- Focus on Reactor bottom head penetrations (BMI) assessment and inspection
  - Normally, BMI are stress relieved with the vessel (600 °C), after welding into the vessel,
  - Some repaired or straightened penetrations after the in shop vessel stress relief,

- So far, 12 units successfully inspected for BMI penetrations integrity, (including Bugey 3 inspected 3 times).

Schematic representation of BMI zones ⇒ inspected by NDE

  - 1 search zone for OD cracks
  - 2 search of interfacial defects
  - 3 search zone for ID cracks

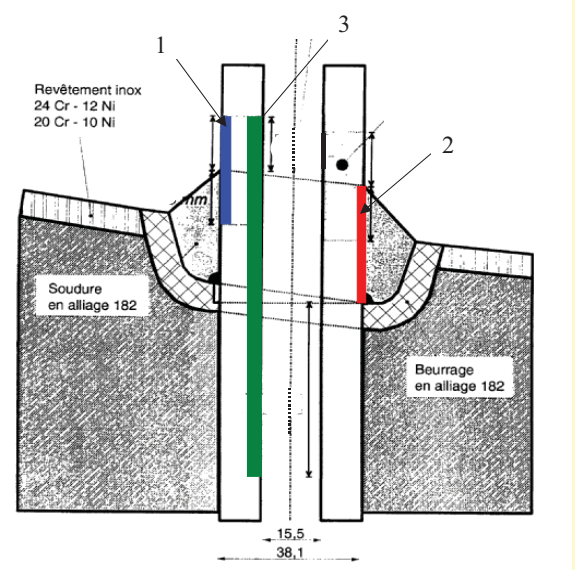

- Steam Generator Partition Plate and its welded zones: (in progress),
- Other zones …(in progress).

Future Prospects and Needs (to better analyze World Wide Experience)

- Focus in the future On Weld Metal Behavior, in the Field & Lab,
- Need to better assess initiation & CGR dependence on Temperature,
- Provide enough accurate data on:
  - Actual IZ wall temperature
  - Account for variations of PWSCC Sensitivity of Inconel components as a function of process, & fabrication variables & metallurgical state,
  - Improve the evaluation of residual AND Operational Stresses,
  - Take into account the final surface state resulting from machining, grinding, or other surface finish,
  - NDE performances and resolution,
- Express and use CGR in terms of maximum rate, or CGR brackets and not only by « mean values »,
- Take into account possible synergistic effects of various forms of mechanical stresses or strains other than residual ones (ex. low f cyclic ripple or load transients),
- Last but not least, review & refine crack initiation anticipation methodology, in order to mitigate early enough leak consequences.

ASN/IRSN French Experience: CONCLUSIONS (1/2)

- **PRECLUDING LEAKAGE: Successful strategy,**

  since Bugey 3, no other CRDM leak

- Importance of regulatory hydro-test at 1.2 times the design pressure

  as an in depth defense measure, with «bare metal Surface access» for leak detection,

  not as an « NDE method of detecting flaws »,

- **Recourse to extensive ISI,**
  - First 100% to assess the whole fleet condition with regard to PWSCC for CRDM penetrations,
  - Then flexible re-inspection schedule for PWSCC affected un-replaced vessel heads,
  - NDE inspection & re-inspection of BMI on an oriented sampling basis,

    with a priority to units comprising repaired or straightened up BMI after vessel stress relief treatment,
  - ASN allowed maintaining some medium size PWSCC cracks for «in the field CGR» assessment by UT.

930

ASN/IRSN French Experience: CONCLUSIONS (2/2)

- **Considerable R&D by EDF and Framatome to constitute & improve:**
  - **Crack initiation data base from Lab & Field NDE detection,**
  - **Propagation data bases : Max CGR derived from Lab & Field,**
  - **Comparisons should be made with international data ,**
    ⇒ looking for clear, fair & «CONSERVATIVE SCREENING CRITERIA»
  - **reported regularly to ASN & IRSN,**
- **Timely replacement of the most PWSCC affected vessel heads**
- **Only 3 young units (N4) with stress relieved alloy 82 DMW on Vessel/Primary loops junctions,**
  Now in France, no Inconel parts linked to the Pressurizer,
- **Now, continued focus on BMI & other Inconel Zones,**
- **Interest to follow up closely worldwide experience feedback**
  for weld materials where PWSCC initiation and propagation were observed,
  since weld cracking by PWSCC hardly experienced in France. Why?
- **So far, so good.., in France, but .. let us keep vigilance as plants age!**
  One example of precaution : 3 full NDE inspections of replacement Vessel Heads with Inconel 690 penetrations after some 10 years of operation.